Universiteit
Leiden
The Netherlands

Discovery of minor histocompatibility antigens as targets for immunotherapy

Pont, M.J.

Citation
Pont, M. J. (2016, June 7). *Discovery of minor histocompatibility antigens as targets for immunotherapy*. Retrieved from https://hdl.handle.net/1887/39949

Version:	Not Applicable (or Unknown)
License:	Licence agreement concerning inclusion of doctoral thesis in the Institutional Repository of the University of Leiden
Downloaded from:	https://hdl.handle.net/1887/39949

Note: To cite this publication please use the final published version (if applicable).

Cover Page

Universiteit Leiden

The handle http://hdl.handle.net/1887/39949 holds various files of this Leiden University dissertation.

Author: Pont, M.J.
Title: Discovery of minor histocompatibility antigens as targets for immunotherapy
Issue Date: 2016-06-07

DISCOVERY OF MINOR HISTOCOMPATIBILITY ANTIGENS AS TARGETS FOR IMMUNOTHERAPY

Margot Pont

Discovery of minor histocompatibility antigens as targets for immunotherapy
© 2016 Margot Pont Amsterdam

Cover image: Kristian Bolk, Mt. Rainier National Park rainforest
Layout: Margot Pont, based on design by Liset Westera
Printing: Ipskamp, Enschede, The Netherlands

ISBN: 978-94-028-0175-0

The research described in this thesis was performed at the Department of Hematology of the Leiden University Medical Center in Leiden, the Netherlands and was financially supported by the Dutch Cancer Society (UL 2010-4748).

Printing of this thesis was financially supported by Boehringer Ingelheim, Chipsoft, Greiner Bio-One and BD Biosciences.

Discovery of minor histocompatibility antigens as targets for immunotherapy

Proefschrift

ter verkrijging van
de graad van Doctor aan de Universiteit Leiden,
op gezag van Rector Magnificus prof.mr. C.J.J.M. Stolker,
volgens besluit van het College voor Promoties
te verdedigen op dinsdag 7 juni 2016
klokke 15:00 uur

door

Margot Jooske Pont

geboren te Leidschendam

in 1986

Promotor:

Prof. dr. J.H.F. Falkenburg

Co-promotor:

Dr. M. Griffioen

Promotiecommissie:

Prof. dr. S.H. van der Burg

Prof. dr. T.C. de Gruijl, VU Medisch Centrum, Amsterdam

Dr. T. Mutis, VU Medisch Centrum, Amsterdam

wees niet bang voor al te grote dromen
ga als je het zeker weet, en als je aarzelt wacht
hoe ijdel zijn de dingen die je je hebt voorgenomen
het mooiste overkomt je, het minste is bedacht

- Freek de Jonge, 'Kijk, Dat Is Freek', 2011

To those who made me who I am

Table of Contents

Chapter 1	General introduction and Aim of the study	**9**
Chapter 2	Microarray gene expression analysis to evaluate cell type specific expression of targets relevant for immunotherapy of hematological malignancies	**29**
Chapter 3	LB-ARHGDIB-1R as novel minor histocompatibility antigen for therapeutic application	**73**
Chapter 4	Minor histocompatibility antigen LB-TTK-1D is encoded by an alternative transcript that is degraded by nonsense mediated decay	**89**
Chapter 5	Integrated whole genome and transcriptome analysis identified a therapeutic minor histocompatibility antigen in a splice variant of *ITGB2*	**107**
Chapter 6	Summary and General discussion	**139**
Appendices	Nederlandse samenvatting	**160**
	Dankwoord	**167**
	Curriculum vitae	**169**
	List of publications	**170**

1

GENERAL INTRODUCTION AND AIM OF THE STUDY

General introduction

Allogeneic hematopoietic stem cell transplantation

Patients with hematological malignancies can be successfully treated with allogeneic hematopoietic stem cell transplantation (alloSCT). In alloSCT, patient hematopoiesis is destroyed and replaced by a new hematopoietic system from a healthy donor. The alloSCT treatment protocol includes pre-transplantation conditioning of the patient with chemotherapy, irradiation and/or immunosuppressive agents. The aim of the conditioning regimen is to eradicate the malignant cells and to suppress the patient immune system to prevent rejection of the donor stem cell engraftment. The donor-derived hematopoietic stem cell graft contains hematopoietic stem and progenitor cells as well as immune cells, including mature B, T and NK cells, and can fully replace the patient lympho-hematopoietic system. Although pre-transplant conditioning regimens aim to reduce tumor burden, outgrowth of residual malignant cells can lead to relapse of the disease. Successful treatment by alloSCT relies on complete eradication of residual malignant cells by donor immune cells as present in the allograft, known as the Graft-versus-Leukemia/Lymphoma (GvL) effect[1-3].

Initial indirect evidence that donor immune cells in the allograft mediate the GvL effect came from studies in which patients with Graft-versus-Host Disease (GvHD) were shown to have a low risk for relapse of their malignancy after alloSCT[4,5]. GvHD is a complication that is characterized by attack of tissues of the patient by donor immune cells in the stem cell graft[6,7]. Large retrospective analysis confirmed a decrease in relapse rate in patients suffering from GvHD after alloSCT as compared to patients without clinically evident GvHD[8]. The beneficial effect on relapse rate was abrogated when T cells were depleted from the allograft to prevent GvHD. In addition, relapse rates are higher in recipients of autologous and syngeneic twin transplants than in patients transplanted with stem cell grafts from other sibling or unrelated donors, demonstrating that GvL and GvHD after alloSCT are caused by alloreactive donor T cells with specific reactivity against patient cells[8-10].

In the early post-transplant period, tissue damage and secretion of inflammatory cytokines caused by the pre-transplant conditioning activate host antigen presenting cells (APC) presenting patient antigens to the donor-derived immune system. In these inflammatory conditions host APCs can efficiently activate donor T cells and the lymphopenic state of the patient stimulates homeostatic proliferation of T cells, thereby often inducing a strong alloreactive immune response that leads to severe GvHD[7,11,12]. To reduce the risk and severity of

GvHD, immunosuppressive drugs such as cyclosporin A, methotrexate and prednisolone can be administered after alloSCT. These immunosuppressive drugs reduce the risk of GvHD, but simultaneously increase the risk of relapse of the malignancy as well as infectious complications. Another approach that has been successfully applied to reduce GvHD is (partial) depletion of T cells from the donor stem cell graft[13-15]. However, also this strategy results in an increased risk of relapse and opportunistic infections.

To re-introduce GvL reactivity and restore anti-viral immunity, donor T cells can be administered after T-cell depleted alloSCT by donor lymphocyte infusions (DLI)[16]. Administration of DLI from 6 months after alloSCT is relatively safe and can be given prophylactically[17] or pre-emptively[18,19]. Late administration of DLI lowers the risk for GvHD, since tissue damage has been restored and APCs of patient origin have been gradually replaced by donor APCs, thus limiting presentation of patient antigens. However, even after delayed administration, DLI can still cause severe side effects in the form of GvHD[20]. Thus, the main challenge for treatment of leukemia with alloSCT and DLI is to evoke an effective GvL response that prevents relapse, while keeping the risk of severe GvHD limited. Relapse risk can be an important factor to determine the treatment protocol of alloSCT and DLI. For example, despite an increased risk of GvHD, DLI is preferably administered early after alloSCT to patients with aggressive malignancies to have a better chance of inducing a strong GvL response that reduces the risk of relapse[21,22].

Minor histocompatibility antigens

To minimize GvHD, patients are preferably transplanted with HLA-matched donors. Selection of the donor is based on genetic identity with the patient for the locus that encodes human leukocyte antigens (HLA) or *major* histocompatibility antigens (MHC) class I and II. HLA class I is expressed on all nucleated cells and presents peptides derived from intracellular proteins on the cell surface to CD8 T cells. Antigen presenting cells can process and present peptides derived from both endogenous and extracellular proteins in HLA class II to CD4 T cells. Genetic disparity between patient and donor outside the MHC locus results in amino acid differences in peptides that are presented by HLA. These polymorphic peptides can be recognized on patient cells by donor T-cells[23,24] and are called minor histocompatibility antigens (MiHA). Most MiHA are encoded by non-synonymous single nucleotide polymorphisms (SNP) and two unrelated individuals differ from each other for ~10,000 non-synonymous SNPs[25,26], giving rise to a large pool of polymorphic peptides that are different between patient and donor and could lead to recognition of patient cells by the donor immune system.

Recognition of MiHA by alloreactive donor T cells can lead to GvL and/or GvHD depending on the tissue distribution of the peptides. Donor T cells recognizing peptides that are expressed on the malignant cells of the patient can lead to GvL. When these peptides are broadly expressed on hematopoietic and non-hematopoietic tissues, donor T cells mediate not only GvL, but also GvHD. After alloSCT, patient hematopoiesis is replaced by a new hematopoietic system from a healthy donor and therefore, donor T cells recognizing MiHA with restricted expression on cells of the hematopoietic system eliminate the malignant cells of the patient, while sparing healthy hematopoietic cells of donor origin. It has previously been proposed that the broad alloreactive response in GvHD might be essential in driving development of GvL reactivity[27]. Marijt et al.[28], however, showed a direct association between emergence of T cells for hematopoiesis-restricted MiHA (HA-1 and HA-2), and disappearance of malignant cells. In one of the patients in this study, induction of high numbers of HA-1 and HA-2 specific T cells coincided with strong GvL, while GvHD was limited (grade I). These studies illustrate that although MiHA-specific T-cell responses often elicit GvHD as well as GvL, these clinical responses can be separated, indicating that MiHA can be exploited to selectively induce GvL after alloSCT without GvHD.

Discovery of MiHA

Over the years, many different methods have been exploited to identify novel MiHA[29,30]. In so-called forward immunology approaches, *in vivo* activated T cells are isolated followed by identification of their specific antigens. For forward approaches aimed at MiHA identification, patients with effective anti-tumor immune responses after alloSCT with an HLA-matched donor are selected for isolation of *in vivo* activated alloreactive T cells. After isolation and *in vitro* culture, the specificity of these T cells and their potential role in GvL and GvHD can be investigated. The intrinsic property of forward approaches is that T cells with undefined specificities are isolated. These strategies can be laborious and large numbers of T-cell clones need to be cultured and screened in order to identify MiHA with hematopoiesis-restricted expression. To increase the efficiency for identification of hematopoiesis-restricted MiHA using forward approaches, T cells can be *in vitro* stimulated with patient leukemic or healthy hematopoietic cells and specifically isolated based on up-regulation of activation marker CD137. Subsequently, in the first round of screening, reactivity against patient fibroblasts can be included to distinguish T-cell clones for broadly-reactive MiHA from T-cell clones recognizing potential hematopoiesis-restricted MiHA. As an alternative strategy that is more focused on direct identification of hematopoiesis-restricted MiHA, reverse immunology approaches emerged in which data from various bio-informatics sources, such as gene expression and

HLA-peptide binding prediction, are combined to select peptide candidates[31-36]. These peptide candidates are then used to search for specific T cells in *in vivo* immune responses after alloSCT or in the naïve T-cell repertoire of healthy individuals. This method allows more direct searching for T cells for a priori selected antigens, but thus far resulted in identification of only a limited number of MiHA.

Initially, MiHA identification in forward approaches was performed by laborious techniques, such as biochemical identification of peptides eluted from HLA-molecules, which has been used to characterize several MiHA, including HA-1 and HA-2[37,38]. cDNA library screening is another method that can be used to identify a MiHA-encoding gene and has also successfully been applied to identify HLA class II-restricted MiHA[39,40]. With the development of whole genome association scanning (WGAs), discovery of MiHA has become more efficient[41-42]. Van Bergen et al.[43] reported the identification of 10 new HLA-class I restricted MiHA using a panel of EBV-LCLs that were SNP-genotyped for 1.1 million SNPs. In WGAs, T-cell recognition of a panel of EBV-LCLs is investigated for association with each individual SNP-genotype. WGAs can be used to identify both HLA-class I and II restricted MiHA[44,45]. Associating SNPs as identified by WGAs may directly produce the MiHA or identify a small genomic region that encodes the MiHA.

For associating SNPs identified by WGAs, the presence of SNP disparity is confirmed by sequencing the gene region of interest for both patient and donor. When SNP disparity has been confirmed, the consequence of the SNP on protein translation is evaluated. Non-synonymous SNPs can directly encode MiHA in the normal open reading frame of the primary gene transcript, while synonymous SNPs encode amino acid differences when the transcript is translated in an alternative reading frame. Therefore, the gene region that encompasses the associating SNP is translated in all three possible forward reading frames and searched for peptides of 9-11 amino acids with predicted binding to the respective HLA-restriction molecule using the algorithm of NetMHC server 3.4[46,47]. According to the algorithm, peptides with predicted binding affinity <500nM and <50nM are classified as weak and strong binders, respectively. Patient (and donor) peptides with predicted HLA binding are then selected, synthesized and tested for T-cell recognition. If the patient variant is recognized by the MiHA-specific T cells, the associating SNP has been confirmed to encode a new MiHA. Associating SNPs can also function as genetic markers for antigen-encoding SNPs that are in linkage disequilibrium with associating SNPs, which have not been captured by the array. For these MiHA, the entire primary gene transcript is sequenced for SNP disparities between patient and donor that can then be evaluated for peptides with predicted HLA binding and T-cell recognition

as described above. Due to genetic linkage in haplotypes, MiHA discovery by WGAs extends far beyond the ~1 million SNPs that are measured by SNP arrays.

Molecular mechanisms of MiHA

Different mechanisms can result in the generation of polymorphic peptides. Most of the HLA-class I-restricted MiHA that are identified to date are encoded by non-synonymous SNPs in coding exons that lead to single amino acid changes translated from primary gene transcripts in the normal reading frame. However, the potential for polymorphic peptides extends far beyond these epitopes to peptides translated in alternative reading frames and peptides encoded by alternative transcripts, thereby greatly increasing the repertoire of different MiHA that can be generated by SNP differences between patient and donor.

HA-1 and HA-2 are examples of MiHA encoded by non-synonymous SNPs in the normal reading frame of the primary gene transcript[37,38]. LB-ECGF-1H[48] and LB-ADIR-1F[49] were the first MiHA that were shown to be translated from the primary gene transcript in an alternative reading frame and also SNPs located in the 5' or 3' untranslated region (UTR) can encode MiHA, as reported for LB-TRIP-10-1EPC[50]. LRH-1 is a MiHA that is translated in an alternative reading frame as a result of an insertion/deletion of a nucleotide (INDEL-variant) and the recognized peptide is encoded by a gene region located downstream from this polymorphism[51]. Another group of MiHA are encoded on the Y-chromosome, the so-called H-Y antigens. H-Y antigens often include multiple amino acid differences from their X-chromosome allelic variants, but they behave in the same way as MiHA encoded by non-synonymous SNPs.

Next to polymorphisms in primary gene transcripts, MiHA can be produced by SNPs that are present in or create alternative transcripts. ACC-6 and ZAPHIR are MiHA that result from alternative splicing[52,53], while PANE1 is generated by a SNP that disrupts a stop codon in an alternative transcript[54]. Even a complete gene can be deleted, rendering the protein as encoded by this gene in the patient entirely polymorphic for the transplanted immune system of the donor. This has been described for *UGT2B17*, a gene that encodes multiple MiHA restricted to HLA-A2, -A29 and -B44[41,55]. An overview of the different molecular mechanisms through which genetic variation can create immune targets is shown in Figure 1. Although examples of MiHA generated by polymorphisms other than non-synonymous SNPs have been described, their frequency is probably underestimated, since MiHA encoded by non-synonymous SNPs are easier to discover by current techniques.

Discovery of MiHA encoded by alternative transcripts may give relevant insight into mechanisms that regulate transcription and translation as well as antigen processing and presentation. Antigenic peptides can be derived from different sources and protein turnover and aberrant translation are relevant factors in processing and presentation of these peptides[56]. Aberrant proteins derived from alternative transcripts or alternative reading frames are examples of defective ribosomal products (DRiPs), which are thought to be a main source of antigenic peptides for T-cell immunosurveillance[57,58]. MiHA derived from alternative transcripts and their specific T cells may therefore function as model antigens to study regulation of transcription, translation and antigen processing and presentation.

Tissue distribution

The tissue distribution of MiHA can be determined to evaluate their role in GvL and GvHD. Ideally, the tissue distribution of MiHA should be analyzed by measuring T-cell recognition of a large variety of (malignant) hematopoietic as well as non-hematopoietic cell types cultured from tissues that are targeted in GvHD. However, primary cells from non-hematopoietic tissues are often difficult to culture and not available in quantities that allow in depth T-cell analysis, which requires expression of the relevant HLA-restriction allele and MiHA-encoding SNP. Therefore, as an efficient and feasible alternative strategy, gene expression can be measured to investigate the tissue distribution of MiHA and estimate their value for therapy.

Thus far, only a limited number of MiHA are encoded by genes with restricted or predominant expression in (malignant) hematopoietic cells, i.e. HB-1H/Y (*HMHB1*)[34,59], HA-2 (*MYO1G*)[37,60], HA-1 (*HMHA1*)[38,61], ACC-1Y/C (*BCL2A1*)[62], LRH-1 (*P2X5*)[51], PANE1 (*CENPM*)[54], ACC-6 (*HMSD*)[53] and UTA2-1 (*KIAA1551*)[63]. With the current repertoire of hematopoiesis-restricted MiHA, only 25% and 40% of recipients of sibling and unrelated donors, respectively, are eligible for T-cell therapies in which one of the therapeutically relevant MiHA is targeted[24]. Therefore, to increase applicability, efficacy and safety of alloSCT, more therapeutic MiHA with favorable population frequencies in common HLA class I alleles are needed.

MiHA as tools to measure GvL and GvHD

Many different alloSCT (and DLI) treatment strategies are currently exploited in various centers leading to significant differences in the occurrence of GvL and GvHD. In many centers patients are transplanted preferably in complete

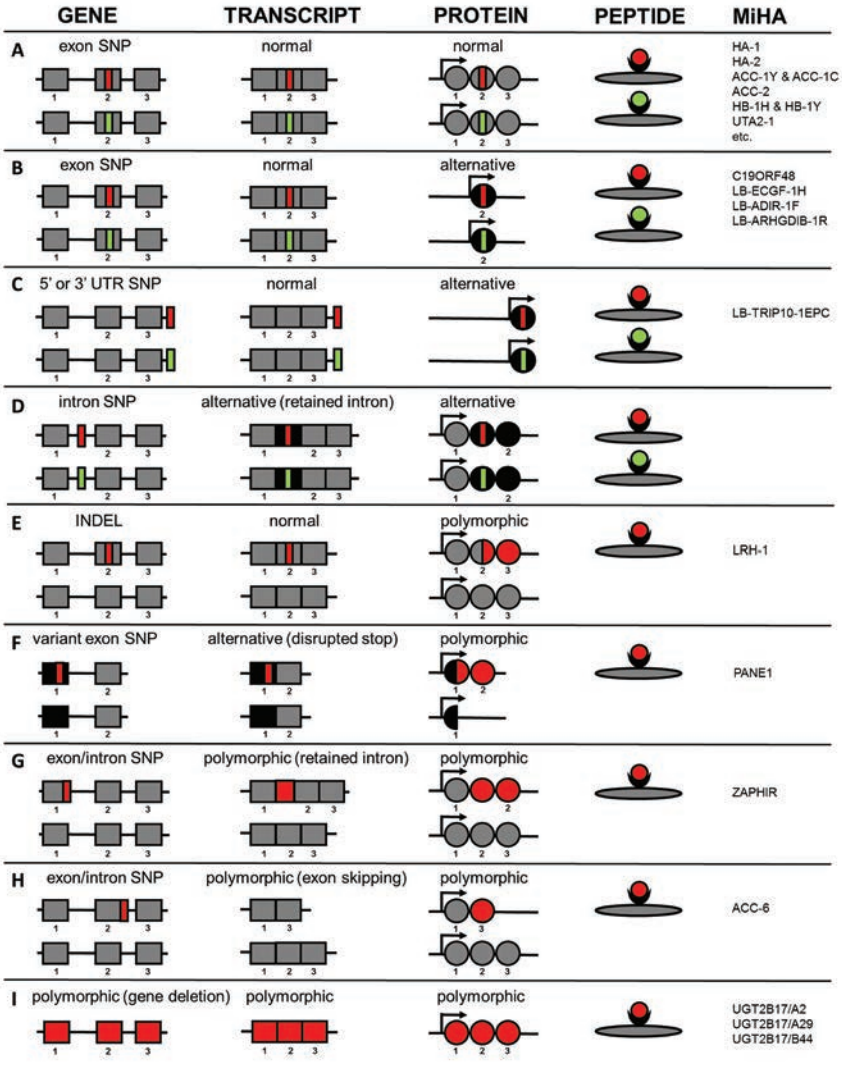

Figure 1: Molecular mechanisms by which genetic variants create MiHA.

Normal DNA, RNA and protein sequences are indicated in gray, whereas alternative sequences are shown in black. Patient and donor sequences are shown in red and green (if allelic variants exist), respectively. Whether the allelic variants are actually presented on the cell surface is also dependent on intracellular processing and presentation mechanisms, which are not taken into consideration in this figure. This figure originates from a review by Griffioen et al.[25].

remission. While long-lasting remissions after alloSCT are indicative of GvL, lack of biomarkers and absence of detectable tumor cells do not allow for evaluation of GvL. Thus, occurrence of GvL responses in the absence of GvHD, which is the most favorable outcome of alloSCT, cannot be monitored and are likely missed when evaluating the efficacy of alloSCT. With the identification of large numbers of MiHA, a toolbox can be generated to screen for immune responses using peptide-MHC (pMHC)-multimers. Screening for MiHA-specific T-cell responses

will reveal specific characteristics of immune responses in GvL and GvHD with respect to specificity, diversity, frequency, and dynamics and thus provide more insight in the biology of GvL and GvHD. Large-scale screening for MiHA-specific T cells may therefore facilitate comparison of *in vivo* immune responses between patients and allow evaluation of different alloSCT treatment strategies.

Studies investigating whether individual MiHA mismatches associate with clinical outcome are hampered by HLA restriction and MiHA allele frequency. Moreover, GvL and GvHD are often mediated by polyclonal immune responses in which multiple MiHA are targeted. In particular the polyclonality of the immune response significantly disturbs analysis of single MiHA, which could explain controversial findings on clinical outcome as for example reported for HA-1[27,64-66]. In contrast, screening for T cells using a large toolbox of MiHA may allow for grouping of patients based on the total number of MiHA that are targeted and the number of MiHA with hematopoiesis-restricted expression *versus* MiHA that are broadly expressed to study their effect on clinical outcome. However, this analysis requires discovery of a large proportion of the entire repertoire of MiHA that are recognized in common HLA alleles. Studies in which female-to-male transplants are screened for T cells recognizing HY antigens[67,68] and their association with clinical outcome may provide a proof of principle. Grouping of patients based on total number of MiHA T-cell responses or number of targeted MiHA with specific tissue distribution patterns can provide the statistical power to assess whether certain types of MiHA mismatches are predictive for clinical outcome. Based on those studies an algorithm may be developed to include or exclude certain MiHA mismatches as a factor in donor selection.

Therapeutic value of MiHA

MiHA are also therapeutically relevant for treatment strategies aimed at augmenting GvL without GvHD. Donor T cells targeting MiHA that are broadly presented on (non-)hematopoietic tissues can be depleted from the stem cell graft or DLI to prevent GvHD, while donor T cells recognizing MiHA with restricted or predominant expression on (malignant) hematopoietic cells can be enriched to selectively induce GvL. Depletion of the majority of T cells targeting broadly expressed MiHA is the rationale behind studies that deplete CD8 T cells from the DLI[69-72], although this also abrogates selective GvL responses induced by hematopoiesis-restricted CD8 T cells. More selective approaches to treat patients with relapsed leukemia after alloSCT are adoptive transfer of *in vitro* induced leukemia-reactive T-cell lines[73], administration of T-cell clones recognizing MiHA on patient hematopoietic cells but not on dermal fibroblasts[74] and cellular therapy with T cells for HA-1[75]. Although these studies support the potential of MiHA-specific T cells to induce GvL upon adoptive transfer, the

results by Warren et al.[74] also indicate that selection of T-cell clones based on lack of *in vitro* reactivity against patient skin fibroblasts is not sufficient to avoid GvHD, since severe toxicity developed as a result of on-target recognition of MiHA in the lung. Thus, in-depth analysis of the tissue distribution is required to accurately estimate the therapeutic potential of MiHA as well as their risk for toxicity. MiHA with therapeutic potential show restricted or predominant expression in cells of the hematopoietic system, since T cells for these MiHA will eliminate the malignant cells of the patient while sparing healthy tissues. A major drawback of *in vitro* generation of MiHA-specific T cells is that long-term *in vitro* culture under stringent GMP conditions is required to obtain sufficient cell numbers for infusion, while this may limit their *in vivo* expansion capacity. Another approach by which long-term *in vitro* culture can be bypassed is adoptive transfer of T cells for hematopoiesis-restricted MiHA directly after isolation from the DLI by pMHC-multimers. Furthermore, T cells can be genetically engineered by T-cell receptor (TCR) gene transfer for hematopoiesis-restricted MiHA to obtain high frequencies of MiHA-specific T-cells[76]. Alternatives to adoptive T-cell transfer include vaccination strategies with donor or patient APC loaded with MiHA peptides, mRNA or DNA[77-79]. In the above-described clinical trials, hematopoiesis-restricted or "therapeutic" MiHA, including newly identified MiHA can be easily employed to selectively induce GvL and reduce GvHD after alloSCT. However, to broaden applicability of MiHA as therapeutic targets to augment GvL after alloSCT without GvHD, more MiHA in different HLA restriction alleles need to be identified.

Aim of the study

To increase effectiveness and safety of alloSCT as treatment modality for hematological malignancies, more MiHA need to be identified for different HLA-restriction alleles. Although MiHA discovery has become more efficient with the implementation of WGAs, MiHA discovery still fails for 20-30% of T-cell clones for which associating SNPs can be successfully identified, but no SNP disparity is present in the primary gene transcript. These MiHA are probably encoded by alternative transcripts and their characterization requires more advanced technologies than WGAs with our standard panel of EBV-LCLs that have been genotyped for 1.1M SNPs. MiHA encoded by alternative transcripts are probably underrepresented in the current collection of known MiHA and discovery of these MiHA is relevant to establish a toolbox to measure T-cell responses in GvL and GvHD after alloSCT and to broaden the repertoire of MiHA that can be used therapeutically.

With the development of WGAs as high-throughput method for MiHA discovery, the need for strategies that allow efficient analysis of the tissue distribution of MiHA increased. The tissue distribution of MiHA is relevant to estimate their role in GvL and GvHD and to separate hematopoiesis-restricted MiHA with potential therapeutic relevance from MiHA that are more broadly expressed on non-hematopoietic tissues. The tissue distribution of MiHA can be determined by measuring T-cell recognition of cell types of different origins, but this analysis is laborious and access to specific tissues is often limited. Therefore, in **chapter 2**, we set out to compose a microarray gene expression database for cell types that are commonly targeted in GvL and GvHD to provide a platform to efficiently establish gene expression patterns. For this purpose, we collected hematological malignancies of different origins as well as healthy (non-) hematopoietic cell samples, validated their cell-type origin and excluded samples that are contaminated with peripheral blood cells. In addition, various non-hematopoietic cells have been cultured in the presence of IFN-γ to allow gene expression analysis under inflammatory conditions and gene expression profiles for various known hematopoiesis-restricted MiHA and B-cell surface antigens have been generated to investigate the value of the microarray gene expression database for evaluation of potential efficacy and toxicity of these antigens as targets for immunotherapy of hematological malignancies.

Using the microarray gene expression database as described in **chapter 2**, we identified LB-ARHGDIB-1R as promising MiHA and therefore aim to characterize this MiHA in detail for its therapeutic relevance in **chapter 3**. We investigated whether LB-ARHGDIB-1R is hematopoiesis-restricted and whether LB-ARHGDIB-1R-specific T cells can recognize and lyse primary leukemic cells, while sparing

skin-derived fibroblasts. In addition, we investigated potential toxicity of LB-ARHGDIB-1R-specific T cells against endothelial cells, in which the *ARHGDIB* gene is expressed at low levels, and studied the *in vivo* immunogenicity of LB-ARHGDIB-1R in MiHA-disparate HLA-B*07:02-positive patient-donor pairs.

To enable discovery of MiHA that are encoded by alternative transcripts, we developed new methods using publicly available whole genome and whole transcriptome data. In **chapter 4**, we aim to identify a MiHA for which multiple associating SNPs were identified in intron regions of the *TTK* gene, but no SNP disparity was found in the primary gene transcript. Using an 'inferred correlation' analysis with publicly available SNP data from the 1000 Genomes Project, we identified LB-TTK-1D and further characterized this MiHA for immunogenicity and tissue distribution by T-cell experiments and quantitative RT-PCR.

In **chapter 5**, we isolated a MiHA-specific T-cell clone from a patient with strong anti-tumor immunity after alloSCT. Similar as in **chapter 4**, the T cells recognized a MiHA for which an associating SNP in an intronic region of the gene was identified, while no SNP disparity was present in the normal *ITGB2* gene transcript. To investigate whether the MiHA could be encoded by an alternative transcript, we searched for alternative *ITGB2* transcripts in publicly available whole transcriptome data and identified LB-ITGB2-1 as novel MiHA that is encoded by an alternative transcript. The tissue distribution of the alternative transcript has been studied by T-cell recognition and quantitative RT-PCR and the cytolytic potential of LB-ITGB2-1-specific T cells has been studied in chromium-release and clonogenic progenitor assays.

In **chapter 6**, we summarize the results on the new MiHA and their gene expression patterns as described in **chapters 2-5**, as well as the identification methods used. We discuss the role of MiHA in GvL and GvHD and the criteria that should be met by MiHA in order to be therapeutically relevant. Furthermore, the added value of whole transcriptome analysis for discovery of these MiHA are discussed as well as the immunological knowledge acquired by studying MiHA as identified by forward strategies.

1

Reference list

1. Appelbaum FR. The current status of hematopoietic cell transplantation. Annu Rev Med. 2003;54:491-512.
2. Wu CJ, Ritz J. Induction of Tumor Immunity Following Allogeneic Stem Cell Transplantation. Advances in Immunology. Vol. Volume 90: Academic Press; 2006:133-173.
3. Falkenburg JH, Warren EH. Graft versus leukemia reactivity after allogeneic stem cell transplantation. Biol Blood Marrow Transplant. 2011;17(1 Suppl):S33-38.
4. Weiden PL, Flournoy N, Sanders JE, Sullivan KM, Thomas ED. Antileukemic effect of graft-versus-host disease contributes to improved survival after allogeneic marrow transplantation. Transplant Proc. 1981;13(1 Pt 1):248-251.
5. Weiden PL, Flournoy N, Thomas ED, et al. Antileukemic effect of graft-versus-host disease in human recipients of allogeneic-marrow grafts. N Engl J Med. 1979;300(19):1068-1073.
6. Gratwohl A, Brand R, Apperley J, et al. Graft-versus-host disease and outcome in HLA-identical sibling transplantations for chronic myeloid leukemia. Blood. 2002;100(12):3877-3886.
7. Ferrara JL, Levine JE, Reddy P, Holler E. Graft-versus-host disease. Lancet. 2009;373(9674):1550-1561.
8. Horowitz MM, Gale RP, Sondel PM, et al. Graft-versus-leukemia reactions after bone marrow transplantation. Blood. 1990;75(3):555-562.
9. Gale RP, Horowitz MM, Ash RC, et al. Identical-twin bone marrow transplants for leukemia. Ann Intern Med. 1994;120(8):646-652.
10. Zittoun RA, Mandelli F, Willemze R, et al. Autologous or allogeneic bone marrow transplantation compared with intensive chemotherapy in acute myelogenous leukemia. European Organization for Research and Treatment of Cancer (EORTC) and the Gruppo Italiano Malattie Ematologiche Maligne dell'Adulto (GIMEMA) Leukemia Cooperative Groups. N Engl J Med. 1995;332(4):217-223.
11. Reddy P, Ferrara JL. Immunobiology of acute graft-versus-host disease. Blood Rev. 2003;17(4):187-194.
12. Shlomchik WD. Graft-versus-host disease. Nat Rev Immunol. 2007;7(5):340-352.
13. Marmont AM, Horowitz MM, Gale RP, et al. T-cell depletion of HLA-identical transplants in leukemia. Blood. 1991;78(8):2120-2130.
14. Barge RM, Starrenburg CW, Falkenburg JH, Fibbe WE, Marijt EW, Willemze R. Long-term follow-up of myeloablative allogeneic stem cell transplantation using Campath "in the bag" as T-cell depletion: the Leiden experience. Bone Marrow Transplant. 2006;37(12):1129-1134.
15. Hobbs GS, Perales MA. Effects of T-Cell Depletion on Allogeneic Hematopoietic Stem Cell Transplantation Outcomes in AML Patients. J Clin Med. 2015;4(3):488-503.
16. Kolb HJ. Graft-versus-leukemia effects of transplantation and donor lymphocytes. Blood. 2008;112(12):4371-4383.
17. Eefting M, Halkes CJ, de Wreede LC, et al. Myeloablative T cell-depleted alloSCT with early sequential prophylactic donor lymphocyte infusion is an efficient and safe post-remission treatment for adult ALL. Bone Marrow Transplant. 2014;49(2):287-291.
18. Schaap N, Schattenberg A, Bar B, Preijers F, van de Wiel van Kemenade E, de Witte T. Induction of graft-versus-leukemia to prevent relapse after partially lymphocyte-depleted allogeneic bone marrow transplantation by pre-emptive donor leukocyte infusions. Leukemia. 2001;15(9):1339-1346.
19. Tomblyn M, Lazarus HM. Donor lymphocyte infusions: the long and winding road: how should it be traveled? Bone Marrow Transplant. 2008;42(9):569-579.
20. Kolb HJ, Schattenberg A, Goldman JM, et al. Graft-versus-leukemia effect of donor lymphocyte transfusions in marrow grafted patients. European Group for Blood and Marrow

Transplantation Working Party Chronic Leukemia [see comments]. Blood. 1995;86(5):2041-2050.

21. Collins RH, Jr., Shpilberg O, Drobyski WR, et al. Donor leukocyte infusions in 140 patients with relapsed malignancy after allogeneic bone marrow transplantation. J Clin Oncol. 1997;15(2):433-444.

22. Eefting M, von dem Borne PA, de Wreede LC, et al. Intentional donor lymphocyte-induced limited acute graft-versus-host disease is essential for long-term survival of relapsed acute myeloid leukemia after allogeneic stem cell transplantation. Haematologica. 2014;99(4):751-758.

23. Falkenburg JH, van de Corput L, Marijt EW, Willemze R. Minor histocompatibility antigens in human stem cell transplantation. Exp Hematol. 2003;31(9):743-751.

24. Warren EH, Zhang XC, Li S, et al. Effect of MHC and non-MHC donor/recipient genetic disparity on the outcome of allogeneic HCT. Blood. 2012;120(14):2796-2806.

25. Griffioen M, van Bergen CAM, Falkenburg JHF. Autosomal minor histocompatibility antigens; How genetic variants create diversity in immune targets. Frontiers in Immunology. 2016;7.

26. Genomes Project C, Abecasis GR, Altshuler D, et al. A map of human genome variation from population-scale sequencing. Nature. 2010;467(7319):1061-1073.

27. Mutis T, Brand R, Gallardo D, et al. Graft-versus-host driven graft-versus-leukemia effect of minor histocompatibility antigen HA-1 in chronic myeloid leukemia patients. Leukemia. 2010;24(7):1388-1392.

28. Marijt WA, Heemskerk MH, Kloosterboer FM, et al. Hematopoiesis-restricted minor histocompatibility antigens HA-1- or HA-2-specific T cells can induce complete remissions of relapsed leukemia. Proc Natl Acad Sci U S A. 2003;100(5):2742-2747.

29. Spierings E. Minor histocompatibility antigens: past, present, and future. Tissue Antigens. 2014;84(4):374-360.

30. Zilberberg J, Feinman R, Korngold R. Strategies for the identification of T cell-recognized tumor antigens in hematological malignancies for improved graft-versus-tumor responses after allogeneic blood and marrow transplantation. Biol Blood Marrow Transplant. 2015;21(6):1000-1007.

31. Hombrink P, Hassan C, Kester MG, et al. Discovery of T cell epitopes implementing HLA-peptidomics into a reverse immunology approach. J Immunol. 2013;190(8):3869-3877.

32. Hombrink P, Hassan C, Kester MG, et al. Identification of Biological Relevant Minor Histocompatibility Antigens within the B-lymphocyte-Derived HLA-Ligandome Using a Reverse Immunology Approach. Clin Cancer Res. 2015;21(9):2177-2186.

33. Mommaas B, Kamp J, Drijfhout JW, et al. Identification of a novel HLA-B60-restricted T cell epitope of the minor histocompatibility antigen HA-1 locus. J Immunol. 2002;169(6):3131-3136.

34. Dolstra H, de Rijke B, Fredrix H, et al. Bi-directional allelic recognition of the human minor histocompatibility antigen HB-1 by cytotoxic T lymphocytes. Eur J Immunol. 2002;32(10):2748-2758.

35. Broen K, Greupink-Draaisma A, Woestenenk R, Schaap N, Brickner AG, Dolstra H. Concurrent detection of circulating minor histocompatibility antigen-specific CD8+ T cells in SCT recipients by combinatorial encoding MHC multimers. PLoS One. 2011;6(6):e21266.

36. Armistead PM, Liang S, Li H, et al. Common minor histocompatibility antigen discovery based upon patient clinical outcomes and genomic data. PLoS One. 2011;6(8):e23217.

37. den Haan JM, Sherman NE, Blokland E, et al. Identification of a graft versus host disease-associated human minor histocompatibility antigen. Science. 1995;268(5216):1476-1480.

38. den Haan JM, Meadows LM, Wang W, et al. The minor histocompatibility

antigen HA-1: a diallelic gene with a single amino acid polymorphism. Science. 1998;279(5353):1054-1057.

39. Griffioen M, van der Meijden ED, Slager EH, et al. Identification of phosphatidylinositol 4-kinase type II beta as HLA class II-restricted target in graft versus leukemia reactivity. Proc Natl Acad Sci U S A. 2008;105(10):3837-3842.

40. Stumpf AN, van der Meijden ED, van Bergen CA, Willemze R, Falkenburg JH, Griffioen M. Identification of 4 new HLA-DR-restricted minor histocompatibility antigens as hematopoietic targets in antitumor immunity. Blood. 2009;114(17):3684-3692.

41. Kamei M, Nannya Y, Torikai H, et al. HapMap scanning of novel human minor histocompatibility antigens. Blood. 2009;113(21):5041-5048.

42. Kawase T, Nannya Y, Torikai H, et al. Identification of human minor histocompatibility antigens based on genetic association with highly parallel genotyping of pooled DNA. Blood. 2008;111(6):3286-3294.

43. Van Bergen CAM, Rutten CE, Van Der Meijden ED, et al. High-throughput characterization of 10 new minor histocompatibility antigens by whole genome association scanning. Cancer Res. 2010;70(22):9073-9083.

44. Spaapen RM, de Kort RA, van den Oudenalder K, et al. Rapid identification of clinical relevant minor histocompatibility antigens via genome-wide zygosity-genotype correlation analysis. Clin Cancer Res. 2009;15(23):7137-7143.

45. Spaapen RM, Lokhorst HM, van den Oudenalder K, et al. Toward targeting B cell cancers with CD4+ CTLs: identification of a CD19-encoded minor histocompatibility antigen using a novel genome-wide analysis. J Exp Med. 2008;205(12):2863-2872.

46. Lundegaard C, Lund O, Nielsen M. Accurate approximation method for prediction of class I MHC affinities for peptides of length 8, 10 and 11 using prediction tools trained on 9mers. Bioinformatics. 2008;24(11):1397-1398.

47. Nielsen M, Lundegaard C, Worning P, et al. Reliable prediction of T-cell epitopes using neural networks with novel sequence representations. Protein Sci. 2003;12(5):1007-1017.

48. Slager EH, Honders MW, van der Meijden ED, et al. Identification of the angiogenic endothelial-cell growth factor-1/thymidine phosphorylase as a potential target for immunotherapy of cancer. Blood. 2006;107(12):4954-4960.

49. van Bergen CA, Kester MG, Jedema I, et al. Multiple myeloma-reactive T cells recognize an activation-induced minor histocompatibility antigen encoded by the ATP-dependent interferon-responsive (ADIR) gene. Blood. 2007;109(9):4089-4096.

50. Griffioen M, Honders MW, van der Meijden ED, et al. Identification of 4 novel HLA-B*40:01 restricted minor histocompatibility antigens and their potential as targets for graft-versus-leukemia reactivity. Haematologica. 2012;97(8):1196-1204.

51. de Rijke B, van Horssen-Zoetbrood A, Beekman JM, et al. A frameshift polymorphism in P2X5 elicits an allogeneic cytotoxic T lymphocyte response associated with remission of chronic myeloid leukemia. J Clin Invest. 2005;115(12):3506-3516.

52. Broen K, Levenga H, Vos J, et al. A polymorphism in the splice donor site of ZNF419 results in the novel renal cell carcinoma-associated minor histocompatibility antigen ZAPHIR. PLoS One. 2011;6(6):e21699.

53. Kawase T, Akatsuka Y, Torikai H, et al. Alternative splicing due to an intronic SNP in HMSD generates a novel minor histocompatibility antigen. Blood. 2007;110(3):1055-1063.

54. Brickner AG, Evans AM, Mito JK, et al. The PANE1 gene encodes a novel human minor histocompatibility antigen that is selectively expressed in B-lymphoid cells and B-CLL. Blood. 2006;107(9):3779-3786.

55. Murata M, Warren EH, Riddell SR. A human minor histocompatibility

antigen resulting from differential expression due to a gene deletion. J Exp Med. 2003;197(10):1279-1289.

56. Bassani-Sternberg M, Pletscher-Frankild S, Jensen LJ, Mann M. Mass Spectrometry of Human Leukocyte Antigen Class I Peptidomes Reveals Strong Effects of Protein Abundance and Turnover on Antigen Presentation. Molecular & Cellular Proteomics. 2015;14(3):658-673.

57. Yewdell JW. Amsterdamming DRiPs. Mol Immunol. 2013;55(2):110-112.

58. Anton LC, Yewdell JW. Translating DRiPs: MHC class I immunosurveillance of pathogens and tumors. J Leukoc Biol. 2014;95(4):551-562.

59. Dolstra H, Fredrix H, Maas F, et al. A human minor histocompatibility antigen specific for B cell acute lymphoblastic leukemia. J Exp Med. 1999;189(2):301-308.

60. Pierce RA, Field ED, Mutis T, et al. The HA-2 minor histocompatibility antigen is derived from a diallelic gene encoding a novel human class I myosin protein. J Immunol. 2001;167(6):3223-3230.

61. Wilke M, Dolstra H, Maas F, et al. Quantification of the HA-1 gene product at the RNA level; relevance for immunotherapy of hematological malignancies. Hematol J. 2003;4(5):315-320.

62. Akatsuka Y, Nishida T, Kondo E, et al. Identification of a polymorphic gene, BCL2A1, encoding two novel hematopoietic lineage-specific minor histocompatibility antigens. J Exp Med. 2003;197(11):1489-1500.

63. Oostvogels R, Minnema MC, van Elk M, et al. Towards effective and safe immunotherapy after allogeneic stem cell transplantation: identification of hematopoietic-specific minor histocompatibility antigen UTA2-1. Leukemia. 2013;27(3):642-649.

64. Goulmy E, Schipper R, Pool J, et al. Mismatches of Minor Histocompatibility Antigens between HLA-Identical Donors and Recipients and the Development of Graft-Versus-Host Disease after Bone Marrow Transplantation. New England Journal of Medicine. 1996;334(5):281-285.

65. Lin M-T, Gooley T, Hansen JA, et al. Absence of statistically significant correlation between disparity for the minor histocompatibility antigen HA-1 and outcome after allogeneic hematopoietic cell transplantation. Blood. 2001;98(10):3172-3173.

66. Tseng L-H, Lin M-T, Hansen JA, et al. Correlation Between Disparity for the Minor Histocompatibility Antigen HA-1 and the Development of Acute Graft-Versus-Host Disease After Allogeneic Marrow Transplantation. Blood. 1999;94(8):2911-2914.

67. Randolph SSB, Gooley TA, Warren EH, Appelbaum FR, Riddell SR. Female donors contribute to a selective graft-versus-leukemia effect in male recipients of HLA-matched, related hematopoietic stem cell transplants. Blood. 2003;103(1):347-352.

68. Gratwohl A, Hermans J, Niederwieser D, van Biezen A, van Houwelingen HC, Apperley J. Female donors influence transplant-related mortality and relapse incidence in male recipients of sibling blood and marrow transplants. Hematology Journal. 2001;2(6):363.

69. Champlin R, Ho W, Gajewski J, et al. Selective depletion of CD8+ T lymphocytes for prevention of graft-versus-host disease after allogeneic bone marrow transplantation. Blood. 1990;76(2):418-423.

70. Klyuchnikov E, Sputtek A, Slesarchuk O, et al. Purification of CD4+ T Cells for Adoptive Immunotherapy after Allogeneic Hematopoietic Stem Cell Transplantation. Biology of Blood and Marrow Transplantation. 2011;17(3):374-383.

71. Meyer RG, Britten CM, Wehler D, et al. Prophylactic transfer of CD8-depleted donor lymphocytes after T-cell–depleted reduced-intensity transplantation. Blood. 2007;109(1):374-382.

72. Baron F, Siquet J, Schaaf-Lafontaine N, et al. Pre-emptive immunotherapy with CD8-depleted donor lymphocytes after CD34-selected allogeneic peripheral blood stem cell transplantation.

Haematologica. 2002;87(1):78-88.

73. Marijt E, Wafelman A, van der Hoorn M, et al. Phase I/II feasibility study evaluating the generation of leukemia-reactive cytotoxic T lymphocyte lines for treatment of patients with relapsed leukemia after allogeneic stem cell transplantation. Haematologica. 2007;92(1):72-80.

74. Warren EH, Fujii N, Akatsuka Y, et al. Therapy of relapsed leukemia after allogeneic hematopoietic cell transplantation with T cells specific for minor histocompatibility antigens. Blood. 2010;115(19):3869-3878.

75. Meij P, Jedema I, van der Hoorn MA, et al. Generation and administration of HA-1-specific T-cell lines for the treatment of patients with relapsed leukemia after allogeneic stem cell transplantation: a pilot study. Haematologica. 2012;97(8):1205-1208.

76. Heemskerk MH, Hoogeboom M, de Paus RA, et al. Redirection of antileukemic reactivity of peripheral T lymphocytes using gene transfer of minor histocompatibility antigen HA-2-specific T-cell receptor complexes expressing a conserved alpha joining region. Blood. 2003;102(10):3530-3540.

77. Hosen N, Maeda T, Hashii Y, et al. Vaccination strategies to improve outcome of hematopoietic stem cell transplant in leukemia patients: early evidence and future prospects. Expert Review of Hematology. 2014;7(5):671-681.

78. Overes IM, Fredrix H, Kester MGD, et al. Efficient Activation of LRH-1–specific CD8+ T-cell Responses From Transplanted Leukemia Patients by Stimulation With P2X5 mRNA-electroporated Dendritic Cells. Journal of Immunotherapy. 2009;32(6):539-551.

79. Rezvani K. Posttransplantation Vaccination: Concepts Today and on the Horizon. ASH Education Program Book. 2011;2011(1):299-304.

2

Plos ONE 2016

MICROARRAY GENE EXPRESSION ANALYSIS TO EVALUATE CELL TYPE SPECIFIC EXPRESSION OF TARGETS RELEVANT FOR IMMUNOTHERAPY OF HEMATOLOGICAL MALIGNANCIES

Margot J. Pont[1], M.W. Honders[1], A.N. Kremer[1,2], C. van Kooten[3], C. Out[4], P.S. Hiemstra[5], H.C. de Boer[6], M.J. Jager[7], E. Schmelzer[8], R.G. Vries[9], A.A. Hinai[10], W.G. Kroes[11], R. Monajemi[12], J.J. Goeman[12,13], S. Böhringer[12], W.A.F. Marijt[1], J.H.F. Falkenburg[1] and M. Griffioen[1]

[1] Department of Hematology, Leiden University Medical Center, Leiden, the Netherlands. [2] Department of Internal Medicine 5, Hematology and Oncology, University Hospital Erlangen, Erlangen, Germany. [3] Department of Nephrology, Leiden University Medical Center, Leiden, the Netherlands. [4] Department of Dermatology, Leiden University Medical Center, Leiden, the Netherlands. [5] Department of Pulmonology, Leiden University Medical Center, Leiden, the Netherlands. [6] Department of Nephrology and the Einthoven Laboratory for Experimental Vascular Medicine, Leiden University Medical Center, Leiden, the Netherlands. [7] Department of Ophthalmology, Leiden University Medical Center, Leiden, The Netherlands. [8] McGowan Institute for Regenerative Medicine, University of Pittsburgh, Pittsburgh, Pennsylvania, US. [9] Hubrecht Institute for Developmental Biology and Stem Cell Research and University Medical Centre Utrecht, Utrecht, the Netherlands. [10] Department of Hematology, Erasmus University Medical Center Cancer Institute, Rotterdam, the Netherlands. [11] Department of Clinical Genetics, Leiden University Medical Center, Leiden, The Netherlands. [12] Department of Medical Statistics and Bioinformatics, Leiden University Medical Center, Leiden, The Netherlands. [13] Radboud Institute for Molecular Life Science, Radboud University Medical Center, Nijmegen, The Netherlands.

2

Cellular immunotherapy has proven to be effective in the treatment of hematological cancers by donor lymphocyte infusion after allogeneic hematopoietic stem cell transplantation and more recently by targeted therapy with chimeric antigen or T-cell receptor-engineered T cells. However, dependent on the tissue distribution of the antigens that are targeted, anti-tumor responses can be accompanied by undesired side effects. Therefore, detailed tissue distribution analysis is essential to estimate potential efficacy and toxicity of candidate targets for immunotherapy of hematological malignancies.

We performed microarray gene expression analysis of hematological malignancies of different origins, healthy hematopoietic cells and various non-hematopoietic cell types from organs that are often targeted in detrimental immune responses after allogeneic stem cell transplantation leading to Graft-versus-Host disease. Non-hematopoietic cells were also cultured in the presence of IFN-γ to analyze gene expression under inflammatory circumstances. Gene expression was investigated by Illumina HT12.0 microarrays and quality control analysis was performed to confirm the cell-type origin and exclude contamination of non-hematopoietic cell samples with peripheral blood cells. Microarray data were validated by quantitative RT-PCR showing strong correlations between both platforms. Detailed gene expression profiles were generated for various minor histocompatibility antigens and B-cell surface antigens to illustrate the value of the microarray dataset to estimate efficacy and toxicity of candidate targets for immunotherapy.

In conclusion, our microarray database provides a relevant platform to analyze and select candidate antigens with hematopoietic (lineage)-restricted expression as potential targets for immunotherapy of hematological cancers.

Introduction

Cellular immunotherapy of hematological cancers has proven very effective. After allogeneic hematopoietic stem cell transplantation (alloSCT), anti-tumor immunity is mediated by donor T cells recognizing the malignant cells of the patient[1]. Another effective approach is targeted therapy by chimeric antigen receptor (CAR) or T-cell receptor (TCR) gene transfer. CAR T-cell therapy specific for CD19 has successfully been used to treat patients with B-cell malignancies[2]. In addition to strong anti-tumor immunity, immunotherapy can cause life-threatening toxicity, i.e. liver or neurological damage as reported after CAR or TCR gene therapy[3,4] or Graft-versus-Host disease (GvHD) after alloSCT[5], due to on-target recognition of healthy organs by the adoptively transferred T cells. Both the efficacy and potential toxicity of immunotherapy is strongly dependent on the tissue distribution of the antigens that are targeted. Thus, gene expression profiles of candidate targets for immunotherapy of hematological cancers need to be carefully examined.

Immunotherapy can be directed against extracellular or intracellular antigens. Specific antibodies or CARs can recognize extracellular antigens that are expressed on the cell surface of malignant cells. These antigens need to be selectively expressed on the tumor or on the lineage from which the tumor originates to limit the risk of toxicity[2,6]. Intracellular antigens can be targeted by specific TCRs when peptides from these proteins are presented by HLA on the cell surface. As such, the repertoire of candidate antigens that can be targeted by TCR-based immunotherapy extends beyond extracellular antigens, but the necessity for tumor- or lineage-restricted expression remains. In the setting of alloSCT, polymorphic antigens with hematopoietic-restricted expression are relevant targets for immunotherapy, since donor T cells recognizing these antigens eliminate the malignant cells of the patient, while sparing healthy hematopoietic cells of donor origin. Polymorphic peptides that are targeted by donor T cells after HLA-matched alloSCT, so-called minor histocompatibility antigens, can be efficiently discovered by whole genome association scanning and minor histocompatibility antigens with hematopoiesis-restricted expression are selected as targets with potential therapeutic relevance[7-11]. Ideally, the tissue distribution of minor histocompatibility antigens is analyzed by measuring T-cell recognition of a large variety of (malignant) hematopoietic and non-hematopoietic cell types cultured from tissues that are targeted in GvHD. However, non-hematopoietic cells are often difficult to culture and not available in quantities that allow in depth T-cell analysis. Therefore, as an alternative, the tissue distribution can be estimated by determining gene expression.

Whole transcriptome analysis can be performed by microarray gene expression or RNA-sequence analysis. Microarray data have become increasingly available over the years in platforms such as Gene Expression Omnibus[12,13]. However, integration of datasets is challenging due to differences in sample handling and technologies. Various integrated and normalized datasets are offered now and allow online analysis of tissue expression. Oncomine is a large platform providing cancer microarray data[14], while BioGPS, among others, allows easy access to Gene Atlas datasets[15]. GeneSapiens[16] provides a bioinformatic analysis of ~10,000 samples including normal human tissues, different cancer types and cell lines. Many samples in these databases represent whole tissues, which are composed of a mix of non-hematopoietic cell types that are often contaminated with peripheral blood cells. Gene expression profiles from these samples are heterogeneous in nature and do not allow accurate identification of hematopoiesis (lineage)-restricted genes. The value of existing datasets with whole tissue samples for estimating the therapeutic relevance and potential toxicity of candidate targets for immunotherapy of hematological malignancies thus remains limited.

AlloSCT and CAR/TCR gene transfer are treatments that can induce inflammation in patients in particular upon development of an effective anti-tumor response[17-19]. Therefore, to estimate potential toxicity, expression of the antigen targeted by immunotherapy needs to be investigated under inflammatory conditions. However, whole tissues or non-hematopoietic cells are generally collected for transcriptome analysis under non-inflammatory conditions and on line databases are therefore of limited use to estimate potential toxicity of immunotherapeutic targets.

In this study, we performed microarray gene expression analysis on hematological malignancies of different origins isolated from bone marrow or peripheral blood based on expression of specific surface markers. We also collected healthy hematopoietic cells and non-hematopoietic cells from organs that are often targeted in GvHD. Non-hematopoietic cells were cultured from tissue specimen or biopsies and various non-hematopoietic cell types were cultured in the presence of IFN-γ to mimic inflammation. Gene expression was investigated by Illumina HT12.0 microarray and quality control analysis confirmed the cell-type origin of the samples and excluded contamination of non-hematopoietic cell samples with peripheral blood cells. We validated gene expression as measured by microarray gene expression analysis by quantitative RT-PCR and investigated gene expression in non-hematopoietic cells under conditions of inflammation. Finally, we illustrated the value of our dataset to estimate efficacy and toxicity of potential targets for immunotherapy of hematological malignancies.

Materials and Methods

Collection of human samples

Malignant and normal hematopoietic cells were isolated from peripheral blood or bone marrow samples and non-hematopoietic cell types were obtained from tissue biopsies or surgically removed specimen obtained from patients or healthy individuals after approval by the Medical Research Ethics Committee and Institutional Review Board of the Leiden University Medical Center (LUMC) and informed consent according to the Declaration of Helsinki. The majority of samples were collected after 2002 and written informed consent was obtained for these samples. Only for leukemic samples collected before 2002, oral informed consent was documented in the patient files by the patient's physician as the only procedure approved by the ethical board.

Isolation and culture of healthy hematopoietic cells

Detailed isolation and culture methods are described in the Supplementary Methods section. Briefly, bone marrow and peripheral blood mononuclear cells (BMMC and PBMC) were isolated by Ficoll-Isopaque separation and cryopreserved. B cells, T cells, monocytes and hematopoietic stem cells were purified by fluorescence-activated cell sorting. Immature DC (imDC) were generated from isolated monocytes and further differentiated into mature DC (matDC). Isolated monocytes were also used to generate M1 and M2 macrophages (MΦ). EBV-transformed B-cell lines (EBV-LCL) and PHA-stimulated T-cell lines (PHA-T) were generated from PBMC as previously described[20,21].

Isolation and characterization of malignant hematopoietic cells

Detailed isolation methods are described in the Supplementary Methods section. In short, flow cytometric analyses were performed on malignant cells, followed by cell sorting based on surface expression of specific markers. Malignant hematopoietic cells included are acute B-lymphoblastic leukemia (ALL) cells, chronic lymphocytic leukemia (CLL) cells, CD34-positive chronic myeloid leukemia (CML) cells, multiple myeloma (MM) cells and acute myeloid leukemia (AML) cells. AML samples were sorted as single cell populations using antibodies for CD33 or as two separate cell populations expressing CD33 in the absence or presence of CD14 to distinguish cells differentiated into the monocytic pathway (CD14pos) from more immature cells (CD14neg). To classify the different malignant samples according to WHO 2008 standards[22], FISH and karyotyping was performed on freshly isolated or cryopreserved cells. For AML

samples, additional analyses were performed to determine *NPM1* mutations and *FLT3* gene internal tandem duplication (*FLT3*-ITD) on genomic DNA and *CEPBA* mutation[23] and *EVI1* overexpression[24,25] on cDNA.

Culture of malignant human cell lines

The human erythroleukemia cell line K562, T-B lymphoblastoid cell line T2, acute myeloid leukemia cell lines AML-193 and THP-1, Burkitt's lymphoma cell line Daudi, acute T cell leukemia cell line Jurkat and the human cervix carcinoma cell line HeLa were obtained from the ATCC. Burkitt's lymphoma cell line Raji was kindly provided by M. Ressing (Dept. of Molecular Cell Biology, LUMC). All cell lines were cultured in IMDM with 10% FCS.

Isolation and culture of non-hematopoietic cells

Fibroblasts, keratinocytes, proximal tubular epithelial cells (PTEC), melanocytes, primary bronchial epithelial cells (PBEC) and human umbilical vein endothelial cells (HUVEC) were derived from tissue biopsies or surgically removed specimen from patients or healthy individuals at the LUMC. Cornea epithelial (Cornea) and stroma cells were harvested from human cadaveric eyes obtained from the EuroCorneabank, (Beverwijk, the Netherlands). Hepatocytes were obtained from Beckton Dickinson (New Jersey, USA) and colon and small intestinal epithelial cells were obtained from epithelial organoid cultures from the Hubrecht Institute for Developmental Biology and Stem Cell Research (University Medical Centre Utrecht, Utrecht, The Netherlands). Bile duct epithelial cells were purchased from ScienCell (Carlsbad, CA, USA). Fibroblasts, keratinocytes, PTEC, melanocytes and HUVEC were also cultured in the presence of IFN-γ (100 IU/ml) for 4 days to mimic inflammation. In addition, two fibroblast samples were cultured with T-cell culture supernatant for 4 days. Isolation and culture of primary cell types from non-hematopoietic tissues was performed as described in the Supplementary Methods section.

Total RNA isolation

Total RNA was isolated with normal and micro scale RNAqueous isolation kits (Ambion, Thermo Fisher Scientific, Waltham, MA, USA) and treated with DNAse I for 30 min at 37°C. RNA clean-up was performed using RNeasy mini kit (Qiagen, Valencia, CA, USA) and the quality of isolated RNA was checked using Agilent RNA 6000 Nano and Pico chips and Agilent Bioanalyzer (Santa Clara, CA, USA). Total RNA was stored at -80°C for gene expression analysis by human HT-12.0 microarrays or quantitative RT-PCR.

Human HT-12.0 microarrays

Total RNA as stored at -80°C was thawed to amplify and biotinylate cRNA using the TotalPrep RNA amplification kit (Ambion) and T7 Oligo(dT) primer for First Strand cDNA synthesis. After preparation, cRNA samples were hybridized onto Human HT-12.0 Version 3 or Version 4 Expression BeadChips (Illumina, San Diego, CA, USA). Hybridization was performed in the hybridization oven for 17 hours at 58°C. Chips were stained with streptavidin-Cy3 and scanned using a Bead Array 500 GX scanner. Raw data were imported into Genome Studio (all Illumina) for gene expression quantification. Microarray gene expression data were analyzed with R 2.15[26]. For this analysis, all samples as measured on Illumina HT-12 chips versions 3 and 4 were combined and merged in one dataset containing all probes as included on both chip versions (n=39,425), of which 28,280 probes (71.7%) are for designated NM transcripts as annotated by RefSeq. Normalization was done in the lumi R package using the variance stabilizing transformation and quantile normalization[27,28]. The data discussed in this publication have been deposited in NCBI's Gene Expression Omnibus[12] and are accessible through GEO Series accession number GSE76340 (http://www.ncbi.nlm.nih.gov/geo/query/acc.cgi?acc=GSE76340). Probe fluorescence is determined as log-transformed value or as 2 to the power of the log-transformed value. In comparisons of gene expression profiles between two sample groups, the average log-transformed values for both groups were subtracted and the fold increase in probe fluorescence was calculated as 2 to the power of this difference ($2^{avg1-avg2}$). Expression profiles could not be determined for all genes that have been described as (non-)hematopoietic lineage specific markers due to probe absence on the Illumina HT12.0 array or inclusion of probes showing overall non-significant fluorescence.

Quantitative RT-PCR

Total RNA as stored at-80°C was thawed to generate cDNA using M-MLV Reverse Transcriptase and Oligo(dT) primer. Quantitative RT-PCR (q-PCR) was performed using predesigned Taqman Gene Expression assays (Table S2) and Universal Master Mix II, no UNG (all Thermo Fisher Scientific, Waltham, MA, USA) and amplification was measured in real-time using LightCycler 480 (Roche, Basel, Switzerland). Data were analyzed using LightCycler 480 software and fit points analyses. Data was normalized using three reference genes: *HMBS* (alias: *PBGD*), *GAPDH* and *ACTB* (alias: *β-actin*). Amplifications started with 10 minutes at 95°C, followed by 45 cycles of 30 seconds for denaturing at 95°C, 30 seconds of annealing at 60°C, and 30 seconds extension at again 60°C. In the regression models, Cp was corrected for a weighted average of Cp values for the three reference genes.

Statistical methods

The predictability of array expression measurements based on RT-PCR measurements was investigated. A quadratic prediction model was built for a set of 24 genes. Measurements of reference genes *HMBS*, *ACTB* and *GAPDH* were available. Missing data was imputed. Data was measured in two batches and genes are corrected against reference genes measured in the same batch. For unsupervised clustering analysis, we estimated the sample relation with hierarchical clustering (average linkage) as provided in the Bioconductor lumi (v2.10.0) R package[28].

Results

Validation of the cell type origin of hematopoietic and non-hematopoietic samples

Various hematological malignancies of different origins and their healthy non-malignant counterparts as well as various cell types isolated or cultured from non-hematopoietic tissues were collected for gene expression profiling by Illumina HT12.0 microarrays to enable high-throughput analysis and selection of targets with relevant expression profiles for immunotherapy of hematological malignancies. The majority of hematopoietic cell types have been included directly after isolation by flow cytometry based on expression of specific surface markers. The genes for isolation markers CD19, CD3, CD14 and CD34 showed restricted expression to B cells, T cells, monocytes and HSC, respectively, thereby confirming the origin of hematopoietic cell samples (data not shown). All cell types from healthy non-hematopoietic tissues were included after short-term incubation or culture under specific conditions to eliminate contaminating peripheral blood cells. These cell types were checked and negative for expression of hematopoietic marker genes, indicating that contamination with peripheral blood cells was below the detection limit (data not shown). In addition, we generated expression profiles for various known cell type-associated genes to confirm the origin of non-hematopoietic cell samples in our dataset. In Figure 1A, expression of cell type-specific or -associated genes are shown for hepatocytes, melanocytes, fibroblasts and keratinocytes. Expression profiles for cell type-associated genes for PTEC, HUVEC and PBEC (lung) are depicted in Figure S1. In addition, profiles for genes that are expressed in the gut are shown as well as profiles for genes with more specific expression in the small intestine. For bile duct epithelial cells, cell type-associated genes with significant probe fluorescence could not be identified and cornea epithelial and cornea stroma cells were shown to share significant gene expression with keratinocytes and fibroblasts, respectively (Figure 1).

For *in vitro* modified hematopoietic cells, we checked whether the induced cell types properly differentiated from their original cell type based on expression of a number of pre-defined genes. DC cultured from monocytes with GM-CSF and IL-4 were checked for down-regulation of the monocyte-specific *CD14* gene and up-regulation of DC-specific genes (Figure 1B, left panel). Full DC maturation was confirmed by induced gene expression of known maturation markers and down-regulated expression of markers for immature DC (Figure 1B, right panel). The combination of these markers allows for quality control and two DC samples were excluded from the dataset for no or incomplete maturation (Figure 1B).

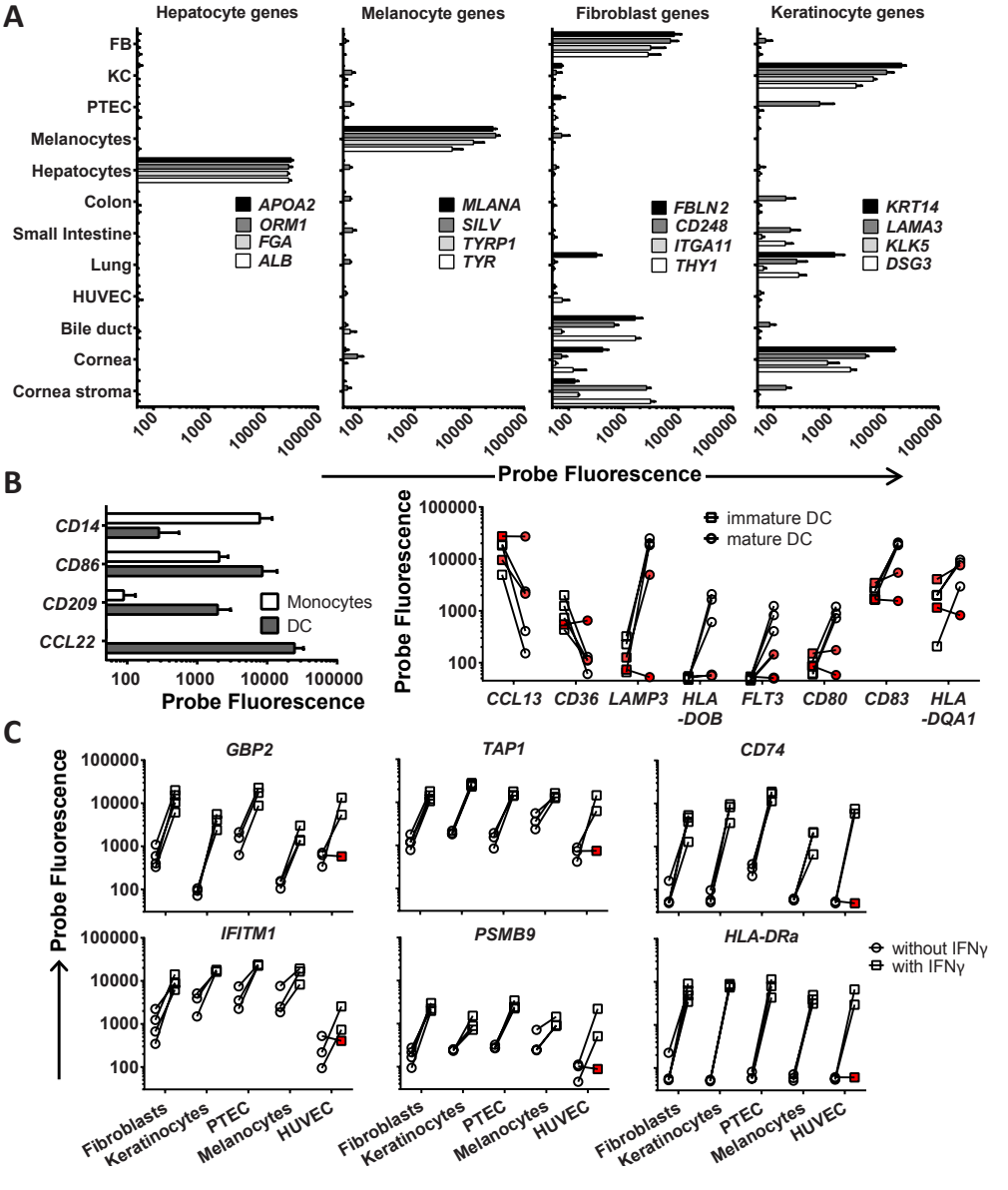

Figure 1: Validation of the cell type origin of (non-)hematopoietic samples

Probe fluorescence as measured by microarray gene expression analysis is depicted on the x-axis in logarithmic scale. (A) Gene expression for various cell type-associated genes as determined by microarray gene expression analysis is shown. Hepatocyte-specific expression is shown for *APOA2*, *ORM1*, *FGA* and *ALB* and melanocyte-specific expression is shown for *MLANA*, *SILV*, *TYRP1* and *TYR*. Fibroblasts-associated expression as defined by detectable expression in fibroblasts as well as a limited number of other non-hematopoietic cell types is shown for *FBLN2*, *CD248*, *ITGA11* and *THY1* and keratinocyte-associated expression is demonstrated for *KRT14*, *LAMA3*, *KLK5* and *DSG3*. Fibroblasts, FB; keratinocytes, KC. (B) Gene expression for monocytes and dendritic cells (DC) is shown (left graph) as well as for immature and mature DC (right graph). Down-regulation of *CD14* and up-regulation of *CD86*, *CD209* and *CCL22* is shown for DC (filled bars) cultured from monocytes (open bars) with GM-CSF and IL-4 (left graph). To validate maturation of DC, down-regulation of markers for immature DC (*CCL13* and *CD36*) and up-regulation of markers for mature DC (*LAMP3*, *HLA-DOB*, *FLT3*, *CD80*, *CD83* and *HLA-DQA1*) was checked (right graph). Immature DC (imDC) are depicted by squares and mature DC (matDC) are indicated by

Macrophages (MΦ) were generated from isolated monocytes by culturing with GM-CSF (type I MΦ) or M-CSF (type II MΦ). Differentiation to macrophages was confirmed by induced expression of *MMP9*[29] and *SPP1*[30] and expression of *CCL2*[31] and *CD163*[32] was stronger in type II than in type I MΦ (data not shown).

To evaluate the role of inflammation on gene expression in non-hematopoietic cells, we cultured various non-hematopoietic cell types (fibroblasts, keratinocytes, PTEC, melanocytes and HUVEC) in the presence of IFN-γ. The effect of IFN-γ was checked by measuring expression of interferon-inducible genes as well as genes involved in HLA-class I and II processing and presentation (Figure 1C). All samples showed strong up-regulation of these genes after IFN-γ treatment, except for one HUVEC sample (HUVEC #3), which was excluded from the dataset.

As additional unbiased method for cell type validation, we performed hierarchical clustering for the complete panel of healthy (non-)hematopoietic samples based on expression profiling of all genes (Figure S2). In this analysis, hematopoietic cell types were distinguished from non-hematopoietic cell types and samples with the same cell type origin clustered based on shared gene expression profiles. This further validated the cell type origin of the (non-)hematopoietic cell samples in the microarray dataset and confirmed lack of detectable contamination of non-hematopoietic cell samples with peripheral blood cells.

Inclusion of hematological malignancies of different origins

All malignant hematopoietic cell types were categorized according to the WHO classification standards and analyzed for cytogenetic abnormalities and, if applicable, for morphology and immune phenotype (Table 1 and complex karyotypes in Table S1). A wide variety of samples were included to obtain a broad repertoire of hematological malignancies. Malignant cell populations were isolated by flow cytometry based on expression of specific surface markers. Gene expression for these surface markers is depicted in Figure S3. In addition to primary hematological malignancies, we included tumor cell lines K562, T2, AML-193, THP-1, Daudi, Raji, Jurkat and HeLa.

circles. Red symbols indicate samples which have been excluded from the dataset for incomplete maturation. (C) Various non-hematopoietic cell types (fibroblasts, keratinocytes, PTEC, melanocytes and HUVEC) were cultured in the presence of IFN-γ (100 IU/ml) for 4 days to mimic inflammation. Expression of various genes that are known to be induced by IFN-γ is shown (*GBP2*, *IFITM1*), including genes that are involved in HLA processing and presentation (*TAP1*, *CD74*, *PSMB9* and *HLA-DRA*). Circles represent samples cultured without IFN-γ, while squares indicate samples after IFN-γ treatment. Red symbols indicate samples which have been excluded from the dataset for incomplete maturation.

Table 1: Characteristics of leukemic cells selected for microarray gene expression analysis

Sample[a]	Origin[b]	WHO classification[c]	Other genetic abnormalities[d]
AML 2467 (CD33/CD14)	PB	Acute myeloid leukemia with inv(16) (p13.1q22); *CBFB-MYH11*	trisomy 8, trisomy 14, trisomy 21
AML 1310 (CD33/CD14)	PB	Acute myeloid leukemia with inv(16) (p13.1q22); *CBFB-MYH11*	-
AML 3097 (CD33)	BM	Acute promyelocytic leukemia with t(15;17) (q22;q12); *PML-RARA*	***CEBPA*** polymorphism (6bp insertion)[e]
AML 2179 (CD33)	PB	Acute promyelocytic leukemia with t(15;17) (q22;q12); *PML-RARA*	-
AML 1591 (CD33)	PB	Acute promyelocytic leukemia with t(15;17) (q22;q12); *PML-RARA*	***FLT3***-ITD positive
AML 1466 (CD33/CD14)	BM	Acute myeloid leukemia with t(9;11) (p22q23); *MLLT3-MLL*	-
AML 4781 (CD33/CD14)	PB	Acute myeloid leukemia with inv(3) (q21q26.2); *RPN1-EVI1*	***EVI1*** overexpression, monosomy 7, del (7) (q21); complex[f]
AML 587 (CD33)	BM	Acute myeloid leukemia with mutated *NPM1*	***FLT3***-ITD positive
AML 2536 (CD33)	BM	Acute myeloid leukemia with mutated *NPM1*	-
AML 4443 (CD33)	PB	Acute myeloid leukemia with mutated *NPM1*	***FLT3***-ITD positive
AML 6395 (CD33)	PB	Acute myeloid leukemia with mutated *NPM1*	-
AML 3370 (CD33)	PB	Acute myeloid leukemia with mutated *NPM1*	-
AML 5205 (CD33/CD14)	PB	Acute myeloid leukemia with mutated *NPM1*	***FLT3***-ITD positive
AML 3590 (CD33)	PB	t-AML	-
AML 3714 (CD33)	BM	AML-NOS, with minimal differentiation	complex[f]
AML 5596 (CD33)	BM	AML-NOS, without maturation	-
AML 3778 (CD33)	PB	AML-NOS, without maturation	complex[f]
AML 3870 (CD33)	BM	AML-NOS, with maturation	trisomy 8
AML 6283 (CD33)	BM	AML-NOS, with maturation	***FLT3***-ITD positive
AML 1143 (CD33)	PB	AML-NOS, acute monoblastic leukemia	-
AML 3009 (CD33)	BM	AML-NOS, acute monoblastic leukemia	***FLT3***-ITD positive
AML 5074 (CD33/CD14)	PB	AML-NOS, acute monoblastic leukemia	complex[f]
Sample	**Origin**	**WHO classification**	**Other genetic abnormalities**
ALL 2391 (CD19)	BM	B Lymphoblastic leukemia NOS	trisomy 5
ALL 2872 (CD19)	BM	B Lymphoblastic leukemia NOS	-
ALL 1299 (CD19)	BM	B Lymphoblastic leukemia NOS	del(6) (q21q23), del(Y)
ALL 3281 (CD19)	PB	B Lymphoblastic leukemia NOS	-
ALL 5903 (CD19)	BM	B Lymphoblastic leukemia with t(9;22) (q34;q11.2); ***BCR-ABL1*** p190	complex[f]
ALL 3639 (CD19)	BM	B Lymphoblastic leukemia with t(9;22) (q34;q11.2); ***BCR-ABL1*** p190	trisomy 5, trisomy 8
ALL 2375 (CD19)	BM	B Lymphoblastic leukemia with t(4;11) (q21;q23); ***MLL*** rearranged	-
ALL 1833 (CD19)	PB	B Lymphoblastic leukemia with t(11;19) (q23;p13.3); ***MLL*** rearranged	-
ALL 3655 (CD19)	BM	B Lymphoblastic leukemia with hyperdiploidy	complex[f]
Sample	**Origin**	**WHO classification**	**Other genetic abnormalities**
CML 3471 (CD34)[g]	BM	Chronic myelogenous leukemia, *BCR-ABL1* positive	del (9q); complex[f]
CML 5036 (CD34)[h]	PB	Chronic myelogenous leukemia, *BCR-ABL1* positive	t(2;9;22) (p13;q34;q11)
CML 3087 (CD34)[h]	BM	Chronic myelogenous leukemia, *BCR-ABL1* positive	del (Xp), del (17q); complex[f]
CML 4779 (CD34)[h]	BM	Chronic myelogenous leukemia, *BCR-ABL1* positive	-
CML 1303 (CD34)[h]	BM	Chronic myelogenous leukemia, *BCR-ABL1* positive	-

Table 1: continued

Sample	Origin	WHO classification	Genetic abnormalities[i]			
			Trisomy 12	13q14.3	*ATM*	*p53*
CLL 1695 (CD19/CD5)	BM	Chronic lymphocytic leukemia	absent	del/del[j]	del	normal
CLL 4725 (CD19/CD5)[f]	BM	Chronic lymphocytic leukemia	absent	del	normal	del
CLL 5535 (CD19/CD5)	PB	Chronic lymphocytic leukemia	absent	del	normal	normal
CLL 6242 (CD19/CD5)	PB	Chronic lymphocytic leukemia	absent	normal	normal	del
CLL 2159 (CD19/CD5)	PB	Chronic lymphocytic leukemia	absent	del/del[j]	normal	normal

Sample	Origin	WHO classification	Genetic abnormalities[i]						
			Hyper-diploidy	numeric abnorm	chr1	13q14	p53	IgH re-arrangements	t(14;16) (q32;q23)
MM 5987 (CD38)[f]	BM	Plasma cell myeloma	hyper-diploid	+9, +15	+1q	del	normal	t(4;14)(p16;q32)	absent
MM 5744 (CD38)[f]	BM	Plasma cell myeloma	diploid	absent	+1q	del	normal	t(4;14)(p16;q32)	absent
MM 6622 (CD38)	BM	Plasma cell myeloma	diploid	absent	normal	normal	normal	normal	absent
MM 4298 (CD38)	BM	Plasma cell myeloma	diploid	-15	normal	del	del	t(4;14)(p16;q32)	absent
MM 5019 (CD38)[f]	BM	Plasma cell myeloma	diploid	absent	normal	del	normal	t(11;14)(q13;q32)	absent

[a] Markers for flow cytometric isolation of malignant cells are indicated between brackets. AML cells have been isolated by expression of CD33 (CD33) or a combination of CD33 and CD14 (CD33/CD14) in which CD33 expressing AML cells positive or negative for monocyte lineage differentiation marker CD14 have been selected as two separate cell populations. CLL cells have been selected for co-expression of CD19 and CD5. ALL, CML and MM cells have been isolated by expression of CD19, CD34 and CD38, respectively.

[b] Origin of sample either peripheral blood (PB) or bone marrow (BM) mononuclear cells.

[c] WHO classification as described by Swerdlow et al, 2008.

[d] Other abnormalities include numerical abnormalities, *CEBPA* mutations, *FLT3*-ITD, or *EVI1* overexpression.

[e] Partial del(6q?) in fraction of the cells

[f] Complex karyotypes are depicted in Supplementary Table 1.

[g] CML in blast crisis.

[h] CML in chronic phase.

[i] Genetic abnormalities as detected by FISH for CLL or MM.

[j] del/del; homozygous deletion.

Validation of microarray gene expression analysis by quantitative RT-PCR

For all 39,426 probes as included in HT12.0 microarray versions 3 and 4, we determined the maximum probe fluorescence as measured in any of the 166 (non-)hematopoietic cell samples in the dataset. Maximum probe fluorescence showed great variability, ranging from log 5.6 to log 15.2. No or low fluorescence can be the consequence of poor probe quality or absence or low expression of the gene transcript in the dataset, while high probe fluorescence indicates that the gene transcript is strongly expressed. To investigate whether gene expression patterns can be accurately and reliably established with our microarray dataset, we validated microarray gene expression data by q-PCR for 24 genes that were selected for different maximum probe fluorescence values.

For 53 samples, which were selected based on wide variability in gene expression throughout the 24 genes, cDNA was generated from the same mRNA source as used for microarray gene expression analysis and gene expression was measured by q-PCR. The complete set of samples, genes, probes and Taqman assays are depicted in Tables S2 and S3. Using a quadratic prediction model, the correlation

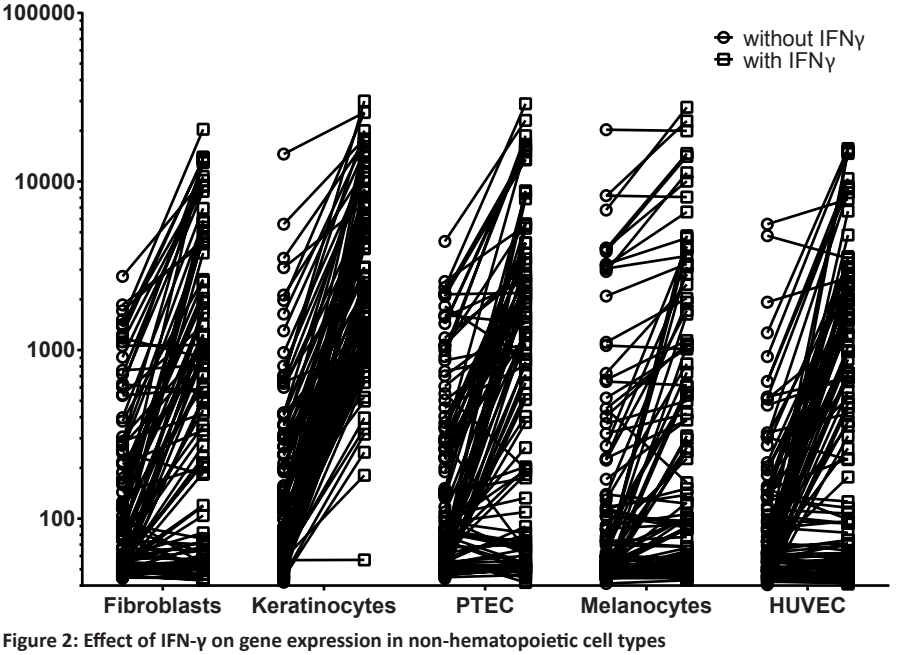

Figure 2: Effect of IFN-γ on gene expression in non-hematopoietic cell types

Microarray gene expression analysis was performed on fibroblasts, keratinocytes, PTEC, melanocytes and HUVEC cultured in the presence of IFN-γ and probe fluorescence was compared with the same cell samples cultured in the absence of IFN-γ. All probes that were >10-fold up-regulated after IFN-γ treatment in one or more cell types are depicted. Probe fluorescence is shown on the y-axis in logarithmic scale. Circles show gene expression in the absence of IFN-γ, while squares indicate expression in the presence of IFN-γ. For each cell type, the number of probes that are >10-fold up-regulated by IFN-γ is shown.

between microarray and q-PCR expression data was determined by calculating the coefficient of determination (R^2). The average correlation for the entire set of 24 genes was strong (corrected $R^2 = 0.868$). Correlation plots for separate genes are depicted in Figure S4. In Table 2, individual R^2 values are depicted as well as the maximum probe fluorescence as measured by microarray gene expression analysis in the sample set for q-PCR validation. Table 2 shows that $R^2 > 0.67$, which indicates that the variability in gene expression in more than two third of the samples fits between microarray and q-PCR analysis, was measured for all 11 genes (100%) with a maximum probe fluorescence > log 11, whereas for the remaining 13 genes with maximum probe fluorescence < log 11, only 3 genes (23%) showed $R^2 > 0.67$.

In conclusion, our data show that gene expression patterns can be accurately established with our microarray dataset for transcripts with a maximum probe fluorescence > log 11, while q-PCR analysis is recommended if the transcript of interest has a maximum probe fluorescence < log 11. If maximum probe fluorescence is < log 11, less detailed qualitative analysis can still be performed, but quantitative analysis by microarray gene expression is not possible.

The effect of inflammation on gene expression in non-hematopoietic cell types

To evaluate gene expression in non-hematopoietic cell types under inflammatory conditions, we performed microarray gene expression analysis on fibroblasts, keratinocytes, PTEC, melanocytes and HUVEC cultured in the presence of IFN-γ and compared probe fluorescence with the same samples that were cultured in the absence of cytokines. In total, 9 probes were >10-fold induced by IFN-γ in all 5 non-hematopoietic cell types. These probes were specific for interferon-inducible genes (*GBP2*) as well as genes involved in HLA-class II processing and presentation (*CD74*, *HLA-DMA*, *HLA-DPA1*, *HLA-DRA*, *HLA-DRB4* and *LOC649143*). In addition, 106 probes were > 10-fold up-regulated in at least one non-hematopoietic cell type (Figure 2 and Table S4). Up-regulated gene expression by IFN-γ was detected for 32, 83, 35, 11 and 40 probes in fibroblasts, keratinocytes, PTEC, melanocytes and HUVEC, respectively, while expression levels in the absence of IFN-γ were similar between these non-hematopoietic cell types.

To determine whether gene expression patterns are different between cell types cultured with a cocktail of inflammatory cytokines as compared to IFN-γ alone, we performed microarray gene expression analysis on fibroblast samples that we cultured in the presence of culture supernatant from an activated CD4 T-cell clone in which high levels of IFN-γ, IL-13, TNF-α and IL-2 were detected. Table

Table 2: R^2 values for regression analysis between microarray and q-PCR[a]

Gene[b]	Probe 1[c]	Probe 2[c]	Maximum expression in dataset[d]			R^2
			Probe 1	Probe 2	Probe average[e]	
HLA-DRA	ILMN_1689655	ILMN_2157441	15.03	14.61	14.82	**0.925[f]**
TAP1	ILMN_1751079		14.78			**0.759**
COL1A1	ILMN_1701308		14.75			**0.948**
CD14	ILMN_1740015	ILMN_2396444	13.20	14.80	14.00	**0.732**
ELANE	ILMN_1706635		13.87			**0.783**
CD34	ILMN_1732799	ILMN_2341229	13.59	13.54	13.57	**0.944**
CD19	ILMN_1782704		13.49			**0.985**
PRTN3	ILMN_1753584		13.16			**0.867**
CD33	ILMN_1747622		11.66			**0.834**
KRT8	ILMN_1753584		11.55			**0.974**
P2RX5	ILMN_1677793		11.09			**0.679**
MOB3A	ILMN_1721344		10.88			0.326
POLE	ILMN_1728199		10.76			0.409
C19orf48	ILMN_1759184	ILMN_2383484	11.34	10.11	10.73	0.266
HMHA1	ILMN_1811392		10.11			**0.779**
CLYBL	ILMN_1663538		9.30			0.487
ROR1	ILMN_1655904		9.20			**0.938**
COIL	ILMN_1688034		8.65			-0.001
MS4A1[g]	ILMN_1776939		8.62			0.320
PFAS	ILMN_1755862		8.61			0.216
PTPRC[h]	ILMN_2340217	ILMN_1653652	8.07	8.78	8.43	0.347
APOBEC3B	ILMN_2219466		8.23			0.652
TTK	ILMN_1788166		8.09			0.545
WT1	ILMN_1802174		8.00			**0.856**

[a] R2 values for individual genes were calculated from the regression model. [b] Official gene symbols are depicted for genes as included in the q-PCR validation set. [c] Illumina probe IDs as measured in the microarray database. [d] Maximum probe fluorescence as measured by microarray gene expression analysis in the sample set for q-PCR validation. [e] Average of maximum probe fluorescence is given for genes with more than 1 probe. [f] R^2 >0.667 are bold. [g] MS4A1 is also known as CD20. [h] PTPRC is also known as CD45.

3 shows all separate probes (n=47) for genes that are >10-fold up-regulated by IFN-γ or T-cell supernatant. The data show that 46 out of 47 probes were at least 5-fold up-regulated under both conditions, indicating that IFN-γ can be used as single agent to induce an inflammatory gene expression signature.

Gene expression profiles of immunotherapeutic targets for hematological malignancies

Minor histocompatibility antigens with hematopoiesis-restricted expression are relevant targets to selectively induce anti-tumor reactivity after alloSCT. Only a limited number of minor histocompatibility antigens have been reported

to be hematopoiesis-restricted. To evaluate expression of these antigens in our microarray dataset of malignant and healthy hematopoietic and non-hematopoietic cell types, we generated gene expression profiles for the known therapeutic minor histocompatibility antigens HA-1 (*HMHA1*)[33,34], LB-ARHGDIB-1R (*ARHGDIB*)[35,36] and LB-ITGB2-1 (*ITGB2*)[37]. Figure 3A shows that maximum probe fluorescence was < log 11 for *HMHA1*, while values > log 11 were measured for *ARHGDIB* and *ITGB2*. Despite low probe fluorescence, *HMHA1* was accurately measured by microarray gene expression analysis as illustrated by strong association with q-PCR data (Table 2; $R^2 = 0.779$). The data also show that expression of *HMHA1* and *ARHGDIB* was restricted or predominant in all or the majority of hematopoietic cells, while expression of *ITGB2* was specific for certain hematopoietic lineages. No expression of *HMHA1* could be measured in any of the non-hematopoietic cell types even when cultured with IFN-γ, while *ARHGDIB* and *ITGB2* showed intermediate and low expression in HUVEC and fibroblasts, respectively. In conclusion, microarray analysis confirmed restricted or predominant gene expression in hematopoietic cells for therapeutic minor histocompatibility antigens.

In addition to minor histocompatibility antigens, surface antigens with restricted expression on hematopoietic lineages or malignancies are relevant targets for therapeutic antibodies or CAR T-cell therapy. We therefore explored our microarray dataset to evaluate gene expression for surface antigens with known expression on B cells (*CD19* and *CD79B*) or B-cell malignancies (*ROR1*). Figure 3B shows that maximum probe fluorescence was > log 11 for *CD19* and *CD79B*, while values < log 11 were observed for *ROR1*. Despite low probe fluorescence, *ROR1* microarray data were reliable as confirmed by q-PCR data ($R^2 = 0.938$, Table 2). Furthermore, the data show that *CD19* was highly expressed in healthy B cells, ALL and CLL, while no expression was detected in any other (non-) hematopoietic cell type. *ROR1* demonstrated overexpression in CLL, while expression of this gene was not detectable in healthy B cells. However, ***ROR1*** expression was also found in biliary epithelial cells and to variable extents in skin fibroblasts. Finally, expression of *CD79B* was most pronounced in the B-cell lineage, but expression was also found in a variety of other (non-)hematopoietic cell types. Thus, restricted or predominant expression in (malignant) B cells could be confirmed by microarray gene expression analysis for surface antigens with known B-cell specific expression.

In conclusion, the data show that our microarray gene expression dataset as collected for (malignant) hematopoietic cell samples and non-hematopoietic cell types cultured under steady state and inflammatory conditions provides a high-throughput platform for detailed analysis and selection of candidate targets with hematopoiesis (lineage)-restricted expression for immunotherapy of hematological malignancies.

Table 3: Gene expression in skin fibroblasts as induced by IFN-γ and T-cell supernatant

Probe ID[a]	Gene[b]	Fibroblasts		Fibroblasts + IFN-γ		Fold Increase[d]
		AVG[c]	SD[c]	AVG	SD	
ILMN_1705247	*ACSL5*	71,48	18,18	915,69	4,61	12,81
ILMN_1756862	*APOL3*	127,45	50,12	1744,54	88,76	13,69
ILMN_1720048	*CCL2*	405,52	320,65	566,98	379,69	1,40
ILMN_2098126	*CCL5*	56,56	5,03	87,02	7,13	1,54
ILMN_1773352	*CCL5*	55,04	4,49	70,60	14,72	1,28
ILMN_1772964	*CCL8*	79,79	26,74	654,98	396,22	8,21
ILMN_1736567	*CD74*	105,73	53,25	4540,97	791,32	42,95
ILMN_2379644	*CD74*	77,73	31,38	1627,96	282,95	20,94
ILMN_1761464	*CD74*	51,45	1,29	730,79	41,60	14,20
ILMN_2047511	*CENTA1*	187,61	62,18	1916,52	1491,98	10,22
ILMN_1791759	*CXCL10*	51,04	4,63	178,24	64,32	3,49
ILMN_1745356	*CXCL9*	48,55	4,44	303,32	131,99	6,25
ILMN_2388547	*EPSTI1*	124,13	41,46	1691,41	606,22	13,63
ILMN_1701114	*GBP1*	183,62	52,59	2569,15	182,46	13,99
ILMN_2148785	*GBP1*	143,83	37,33	1191,59	6,56	8,28
ILMN_1774077	*GBP2*	745,66	345,68	17626,86	2385,66	23,64
ILMN_1771385	*GBP4*	48,49	2,67	903,78	21,36	18,64
ILMN_2114568	*GBP5*	56,21	4,33	1124,80	148,70	20,01
ILMN_1803945	*HCP5*	91,78	15,97	892,47	51,92	9,72
ILMN_1778401	*HLA-B*	1305,90	484,58	9930,80	649,29	7,60
ILMN_1695311	*HLA-DMA*	542,10	87,50	7641,55	2580,39	14,10
ILMN_1761733	*HLA-DMB*	89,92	32,72	2127,14	1065,96	23,66
ILMN_1659075	*HLA-DOA*	51,01	4,51	897,08	186,07	17,59
ILMN_1772218	*HLA-DPA1*	160,29	7,45	3916,33	585,53	24,43
ILMN_1808405	*HLA-DQA1*	59,19	9,86	887,82	661,25	15,00
ILMN_1689655	*HLA-DRA*	176,76	126,36	12566,25	3920,68	71,09
ILMN_2157441	*HLA-DRA*	138,34	86,70	5530,45	687,54	39,98
ILMN_1715169	*HLA-DRB1*	49,64	3,33	302,36	253,61	6,09
ILMN_1752592	*HLA-DRB4*	97,08	25,57	3135,67	1486,29	32,30
ILMN_1697499	*HLA-DRB5*	73,82	26,82	826,23	777,15	11,19
ILMN_2066060	*HLA-DRB6*	56,77	0,82	317,56	109,15	5,59
ILMN_2066066	*HLA-DRB6*	52,33	1,69	192,74	48,32	3,68
ILMN_1723912	*IFI44L*	63,42	5,51	1192,97	174,91	18,81
ILMN_2347798	*IFI6*	212,00	45,36	2234,49	782,87	10,54
ILMN_1739428	*IFIT2*	148,34	6,69	2190,73	666,22	14,77
ILMN_1701789	*IFIT3*	309,27	24,42	5293,10	106,34	17,11

Table 3: continued

Probe ID[a]	Gene[b]	Fibroblasts		Fibroblasts + T-sup[e]		Fold Increase[d]
		AVG[c]	SD[c]	AVG	SD	
ILMN_1705247	*ACSL5*	57,07	5,64	410,79	21,92	7,20
ILMN_1756862	*APOL3*	126,02	3,27	1215,58	198,99	9,65
ILMN_1720048	*CCL2*	146,88	58,76	3739,10	578,67	25,46
ILMN_2098126	*CCL5*	80,04	4,21	1448,07	17,78	18,09
ILMN_1773352	*CCL5*	52,54	0,90	564,89	13,32	10,75
ILMN_1772964	*CCL8*	76,86	23,08	1092,76	27,37	14,22
ILMN_1736567	*CD74*	59,62	4,58	6697,04	438,61	112,33
ILMN_2379644	*CD74*	46,04	4,27	3008,86	137,93	65,35
ILMN_1761464	*CD74*	45,18	2,03	518,30	79,50	11,47
ILMN_2047511	*CENTA1*	94,46	27,37	664,84	489,58	7,04
ILMN_1791759	*CXCL10*	54,72	1,54	1600,24	844,80	29,24
ILMN_1745356	*CXCL9*	41,91	1,69	5149,88	3359,40	122,89
ILMN_2388547	*EPSTI1*	165,03	48,22	2084,78	643,31	12,63
ILMN_1701114	*GBP1*	182,31	43,53	3793,63	414,77	20,81
ILMN_2148785	*GBP1*	274,42	56,92	5802,20	1534,56	21,14
ILMN_1774077	*GBP2*	582,62	90,58	7100,17	300,24	12,19
ILMN_1771385	*GBP4*	57,47	0,85	1439,61	406,66	25,05
ILMN_2114568	*GBP5*	48,52	1,19	1189,30	25,32	24,51
ILMN_1803945	*HCP5*	71,62	1,81	936,66	97,71	13,08
ILMN_1778401	*HLA-B*	1354,92	495,95	15916,89	2069,86	11,75
ILMN_1695311	*HLA-DMA*	355,31	31,05	3309,74	1393,47	9,32
ILMN_1761733	*HLA-DMB*	66,70	10,93	930,50	471,41	13,95
ILMN_1659075	*HLA-DOA*	51,14	1,29	312,10	118,38	6,10
ILMN_1772218	*HLA-DPA1*	119,74	3,57	2708,72	724,98	22,62
ILMN_1808405	*HLA-DQA1*	41,27	0,96	870,79	606,77	21,10
ILMN_1689655	*HLA-DRA*	93,09	0,69	4449,93	1823,37	47,80
ILMN_2157441	*HLA-DRA*	62,36	1,05	5817,44	2067,78	93,29
ILMN_1715169	*HLA-DRB1*	51,16	0,40	880,52	833,29	17,21
ILMN_1752592	*HLA-DRB4*	59,02	1,21	2467,91	384,34	41,81
ILMN_1697499	*HLA-DRB5*	48,12	0,54	1122,44	1073,92	23,32
ILMN_2066060	*HLA-DRB6*	60,67	1,64	812,22	438,83	13,39
ILMN_2066066	*HLA-DRB6*	48,40	2,49	988,46	215,83	20,42
ILMN_1723912	*IFI44L*	64,62	10,67	1230,95	168,61	19,05
ILMN_2347798	*IFI6*	664,54	215,55	12733,61	8737,71	19,16
ILMN_1739428	*IFIT2*	333,39	47,93	2205,74	1097,87	6,62
ILMN_1701789	*IFIT3*	248,64	35,15	2465,82	954,09	9,92

Table 3: continued

Probe ID[a]	Gene[b]	Fibroblasts		Fibroblasts + IFN-γ		Fold Increase[d]
		AVG[c]	SD[c]	AVG	SD	
ILMN_1664543	*IFIT3*	61,94	6,84	500,90	52,90	8,09
ILMN_2334296	*IL18BP*	124,90	13,66	3132,98	608,04	25,08
ILMN_2368530	*IL32*	54,42	6,19	149,61	4,61	2,75
ILMN_1656310	*INDO*	48,99	9,14	523,11	154,06	10,68
ILMN_1708375	*IRF1*	498,42	212,95	2664,97	295,19	5,35
ILMN_1662358	*MX1*	198,75	6,86	10822,34	4316,73	54,45
ILMN_1701613	*RARRES3*	291,17	134,16	9431,88	2494,20	32,39
ILMN_1751079	*TAP1*	1184,40	16,21	13220,08	1203,62	11,16
ILMN_1678841	*UBD*	49,97	2,18	76,70	15,87	1,53
ILMN_1727271	*WARS*	1219,84	167,93	18566,63	8233,61	15,22
ILMN_2337655	*WARS*	1267,64	209,92	13887,52	4384,17	10,96

Table 3: continued

Probe ID[a]	Gene[b]	Fibroblasts		Fibroblasts + T-sup[e]		Fold Increase[d]
		AVG[c]	SD[c]	AVG	SD	
ILMN_1664543	*IFIT3*	111,53	4,69	1162,56	556,31	10,42
ILMN_2334296	*IL18BP*	68,50	2,03	2266,51	1379,17	33,09
ILMN_2368530	*IL32*	109,67	4,68	1873,74	978,51	17,09
ILMN_1656310	*INDO*	45,64	0,65	5685,52	4062,65	124,58
ILMN_1708375	*IRF1*	277,69	29,54	4185,18	822,05	15,07
ILMN_1662358	*MX1*	671,64	353,82	6055,89	2475,95	9,02
ILMN_1701613	*RARRES3*	190,98	15,69	4008,61	1773,14	20,99
ILMN_1751079	*TAP1*	824,61	168,64	6181,11	527,53	7,50
ILMN_1678841	*UBD*	52,95	1,42	1077,09	664,73	20,34
ILMN_1727271	*WARS*	364,88	11,13	7669,97	593,84	21,02
ILMN_2337655	*WARS*	508,79	30,61	11333,68	2227,47	22,28

[a] Illumina probe IDs as included in the microarray database.

[b] Official gene symbols are depicted for genes that are >10-fold up-regulated by IFN-γ, T-cell supernatant or both.

[c] AVG and SD are the average and standard deviation of probe fluorescence as measured in different fibroblast samples, respectively.

[d] Fold increase was calculated from the average probe fluorescence as measured in fibroblasts after pre-treatment with IFN-γ or T-cell supernatant divided by the average probe fluorescence in the corresponding fibroblast samples cultured without cytokines. Values in bold indicate >10-fold upregulated gene expression by IFN-γ, T-cell supernatant or both.

[e] T-sup; T-cell supernatant harvested from an activated CD4 T-cell clone containing high levels of inflammatory cytokines.

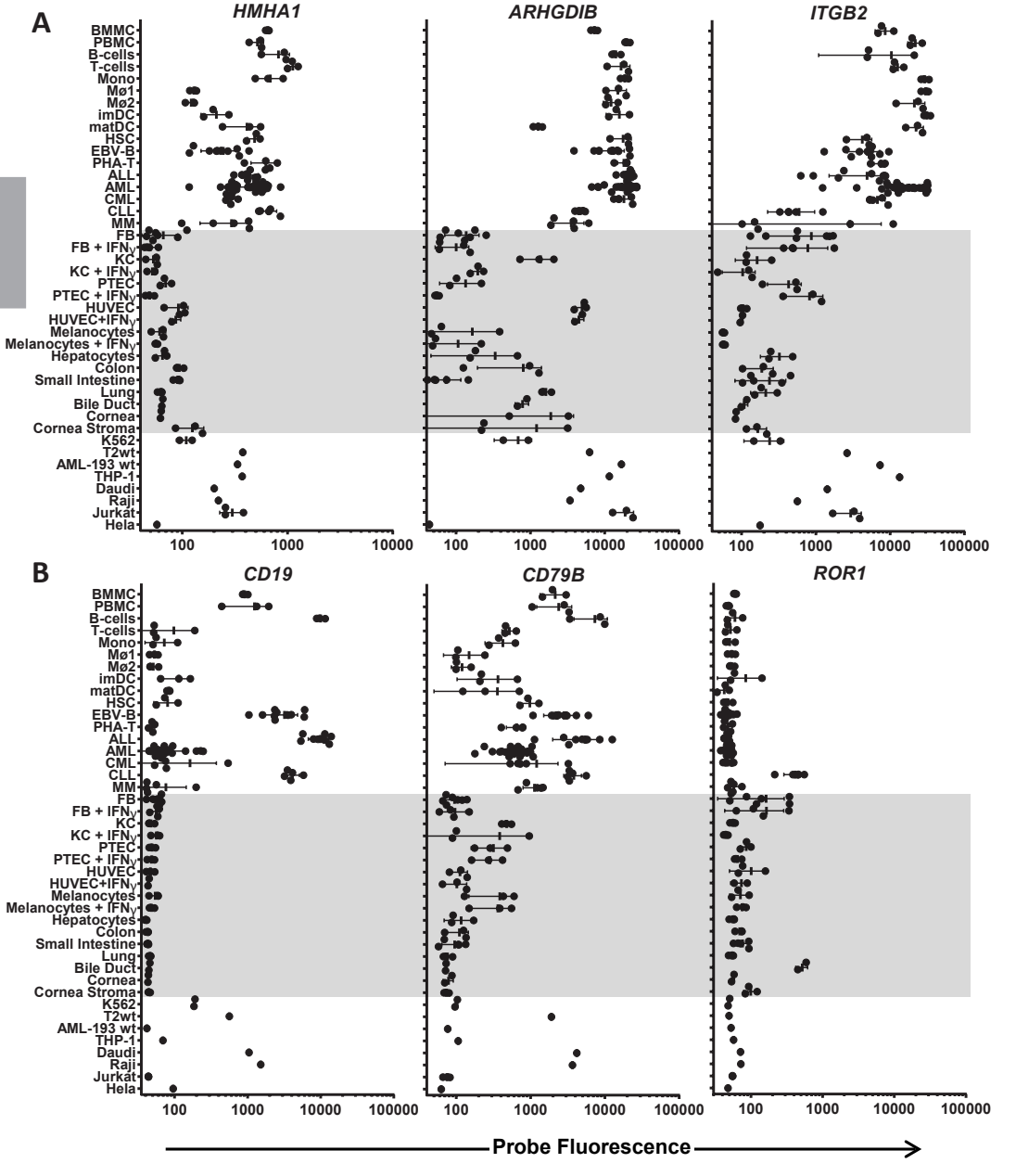

Figure 3: Gene expression profiles for potential targets for immunotherapy of hematological malignancies.

Gene expression profiles were generated for hematopoiesis-restricted minor histocompatibility antigens and B-cell specific surface antigens as potential targets for immunotherapy of hematological malignancies. (A) Gene expression profiles for minor histocompatibility antigens HA-1 (*HMHA1*), LB-ARGHDIB-1R (*ARHGDIB*) and LB-ITGB2-1 (*ITGB2*).

(B) Gene expression profiles for B-cell specific antigens *CD19*, *CD79B* and *ROR1*. Probe fluorescence intensity is shown on the x-axis in logarithmic scale. On the y-axis malignant and healthy (non-)hematopoietic cell types as included in the microarray dataset are shown. Each dot represents a different sample and the mean and standard deviation of gene expression is shown for each cell type.

Discussion

In this study, we performed microarray gene expression analysis on malignant and healthy hematopoietic cells and various non-hematopoietic cell types cultured under steady state and inflammatory conditions. Quality control was performed to confirm cell-type origin of the samples and to exclude peripheral blood contamination of non-hematopoietic samples. Validation of gene expression was performed by quantitative RT-PCR and an inflammatory gene signature was established by comparing gene expression between different non-hematopoietic cells after pre-treatment with IFN-γ. Furthermore, we demonstrated the value of the microarray dataset to generate gene expression profiles for potential targets for immunotherapy of hematological malignancies.

Validation of the Illumina HT12 microarray gene expression dataset by q-PCR analysis demonstrated a strong correlation between both platforms with an overall corrected R^2 of 0.868. However, maximum probe fluorescence as measured in any cell type of the dataset varied significantly. No or low fluorescence can be the consequence of poor probe quality or absence or low expression of the gene transcript in the dataset, while high probe fluorescence indicates that the gene transcript is strongly expressed. Strong correlation between q-PCR and microarray data with $R^2 > 0.667$ was obtained for all probes with maximum fluorescence > log 11. Of the 28,280 probes (20,215 when selecting probes for unique genes) for designated NM transcripts on Illumina HT12 chips, fluorescence > log 11 was measured for 4301 probes (15%), 3787 (19%) after selection of probes for unique genes. Provided that ~50% of all genes as present in the human genome are expressed in differentiated cell types[38], expression profiles can be determined with high accuracy for ~40% of genes. For probes with maximum fluorescence < log 11, qualitative analysis can still be performed, but q-PCR studies are recommended for quantitative gene expression analysis.

To evaluate up-regulated gene expression under inflammatory conditions, we cultured various non-hematopoietic cell types in the presence of IFN-γ and compared gene expression to the same cells cultured in the absence of cytokines. In total 106 probes were >10-fold up-regulated in at least one non-hematopoietic cell type with melanocytes being less sensitive to IFN-γ pre-treatment (n=11 probes) than keratinocytes (n=83 probes). To determine whether IFN-γ can be used as single agent to mimic inflammation, we also cultured fibroblasts in the presence of T-cell culture supernatant containing high levels of inflammatory cytokines (IFN-γ, IL-13, TNF-α and IL-2). There was great overlap between genes up-regulated by IFN-γ and T-cell culture supernatant, illustrating that IFN-γ as single compound can create an inflammatory gene signature. As such, gene

expression analysis of samples cultured with IFN-γ can be used to estimate toxicity of immunotherapeutic targets against non-hematopoietic cells under inflammatory conditions.

In our microarray dataset, contamination of non-hematopoietic cells with peripheral blood cells was excluded to allow identification and selection of genes with hematopoietic (lineage)-restricted expression, which may encode relevant targets for immunotherapy of hematological malignancies. To evaluate the value of our microarray dataset to analyze and select potential targets for immunotherapy of hematological malignancies, we generated gene expression profiles for hematopoiesis-restricted minor histocompatibility antigens that are recognized by specific T cells in the context of HLA. Microarray analysis confirmed restricted or predominant expression of these antigens in hematopoietic cells, but *ARHGDIB* and *ITGB2* also showed intermediate and low expression in endothelial cells and fibroblasts, respectively. Since actual antigen presentation by HLA is not measured by microarray gene expression analysis, additional experiments are required to further evaluate potential toxicity against non-hematopoietic cell types with detectable expression of the gene of interest. For *ARHGDIB* and *ITGB2*, we measured T-cell reactivity against endothelial cells and fibroblasts, but did not find any evidence for toxicity[35,37]. In addition to minor histocompatibility antigens, we generated gene expression profiles for surface antigens with known B-cell specific expression that can be targeted independent of HLA by CAR-based immunotherapy. Microarray analysis confirmed restricted or predominant expression of these antigens in (malignant) B cells. However, *CD79B* was also expressed in a variety of other (non-)hematopoietic cell types, which was supported by Jahn et al.[39], who demonstrated that intracellular CD79B peptides are presented by HLA and recognized by specific T cells on other cell types than B cells. Since actual surface expression is not measured by microarray gene expression analysis, additional experiments are required to evaluate whether CD79B is an appropriate target for CAR-based therapy. For *ROR1*, microarray data confirmed overexpression in CLL as compared to healthy B cells, supporting its relevance as therapeutic target. *ROR1* expression was also found in biliary epithelial cells and to variable extents in skin fibroblasts, but no evidence has been found that gene expression in these cell types leads to detectable surface expression as illustrated by the safety of CAR-based therapy targeting ROR1 in nonhuman primates[40,41].

In summary, we performed microarray gene expression analysis on hematological malignancies of different origins, healthy hematopoietic cells and various (IFN-γ pre-treated) non-hematopoietic cell types and demonstrate that our microarray gene expression database allows detailed analysis and selection of candidate targets with hematopoietic (lineage-)restricted expression for immunotherapy

of hematological cancers.

Acknowledgments

We would like to thank Dagmar Bouwer for performing q-PCR experiments and Sabrina Veld and Guido de Roo for flow cytometric cell sorting.

Supplemental Methods

Isolation and culture of healthy hematopoietic cells

Bone marrow and peripheral blood mononuclear cells (BMMC and PBMC) were isolated by Ficoll-Isopaque separation and cryopreserved. B cells, T cells and monocytes were purified from PBMC by fluorescence-activated cell sorting on a FACS-ARIAIII (BD Biosciences) after staining with monoclonal antibodies (BD Biosciences) for CD19, CD3 and CD14, respectively. Hematopoietic stem cells (HSC) were isolated from G-CSF mobilized peripheral blood by flow cytometric sorting for CD34 surface expression. Immature DC (imDC) were generated by culturing isolated monocytes in medium with 10% human serum (HS) supplemented with 100 ng/mL GM-CSF (Novartis) and 500 IU/mL IL-4 (Schering-Plough) for 5 days. Mature DC (matDC) were generated by culturing imDC for 2 days with 100 ng/mL GM-CSF, 10 ng/mL TNF-α (Cellgenix), 10 ng/mL IL-1β (Cellgenix), 10 ng/mL IL-6 (Cellgenix), 1 μg/mL prostaglandin E2 (Sigma-Aldrich) and 500 IU/mL IFN-γ (Boehringer Ingelheim). Isolated monocytes were also incubated for 7 days in medium with 10% HS supplemented with 5 ng/ml GM-CSF or 5 ng/ml M-CSF (Chiron) to culture M1 and M2 macrophages (MΦ), respectively. EBV-transformed B-cell lines (EBV-LCL) and PHA-stimulated T-cell lines (PHA-T) were generated from PBMC as previously described[1,2].

Isolation and culture of malignant hematopoietic cells

Flow cytometric analyses for malignant cells were performed on a FACS-Calibur and cell sorting on a FACS-AriaIII after staining with monoclonal antibodies (all BD Biosciences). Acute lymphoblastic leukemia (ALL) cells were isolated from samples with >85% leukemic blasts (range 85-98%) using antibodies for CD19. Chronic lymphoblastic leukemia (CLL) cells were purified from samples with >90% malignant cells using antibodies for CD19 and CD5. Chronic myeloid leukemia (CML) cells were isolated using antibodies for CD34 from samples with >5% CD34-positive cells. Multiple myeloma cells were sorted from samples with >30% plasma cells (range 30-95%) using antibodies for CD38. Acute myeloid leukemia (AML) cells were sorted from samples with >20% leukemic blasts (range 22%-95%) as single cell populations or as two separate cell populations expressing CD33 in the absence or presence of CD14 (CD14neg or CD14pos, respectively).

Isolation and culture of non-hematopoietic cells

Fibroblasts and keratinocytes were cultured from skin-biopsies as previously

described[1]. PTEC were provided by C. van Kooten (Dept. of Nephrology, LUMC) after isolation from pre-transplant biopsies or from kidneys not suitable for transplantation and culturing in serum-free DMEM/HAM-F12 (Bio-Whittaker, Walkersville, MD) supplemented with antibiotics and insulin, transferrin, selenium, triiodothyronine, epidermal growth factor and hydrocortisone as described earlier[3]. Skin melanocytes were provided by C. Out (Dept. of Dermatology, LUMC) and cultured in F10 supplemented medium (Invitrogen) from surgically removed nevi obtained after informed consent from patients with the atypical nevus syndrome or healthy individuals[4]. PBEC were provided by P.S. Hiemstra (Dept. of Pulmonology, LUMC) and were isolated from macroscopically normal, resected lung tissue from anonymized patients undergoing surgery for lung cancer. Cells were expanded by culture under submerged conditions, and mucociliary differentiation was achieved by culture at the air-liquid interface5. HUVEC were provided by H.C. de Boer (Dept. of Nephrology, LUMC) and were isolated from umbilical cords according to Jaffe et al.6 using a cannula sized to fit the vein. HUVEC were cultured in EGM-2 medium supplemented with the EGM-2 bullet kit (Lonza BioWhittaker, Basel, Switzerland) and refreshed every 3 days.

Cornea stroma and epithelial cells were provided by M.J. Jager (Dept. of Ophthalmology, LUMC) and cultured as previously described[7]. In short, corneal epithelial cells were harvested by cutting the cornea into four equal quadrants, washing the corneal pieces three times in PBS, and incubating the tissue overnight at 4°C in dispase II (Roche Applied Science, Mannheim, Germany). The corneal epithelium was manually separated as a sheet from the underlying tissue, centrifuged, and incubated in trypsin (TrypLE Select, Life Technologies Europe BV, Bleiswijk, the Netherlands) for 10-15 minutes. Single cell suspensions were cultured in CnT-20 medium (Bio-connect BV, Huissen, the Netherlands) with 1% penicillin/streptomycin. The cornea was cut into small parts of about 1 x 1 mm to isolate cornea stromal cells. The corneal parts were placed in a 0.1% collagenase type II solution (Life Technologies Europe BV) and incubated overnight at 37°C. The obtained cell solution was cultured in DMEM/HAM F12 medium with stable glutamin (Biochrom AG, Berlin, Germany), supplemented with 5% fetal calf serum and 1% penicillin/streptomycin.

Hepatocytes were provided by E. Schmelzer (McGowan Institute for Regenerative Medicine, University of Pittsburgh, USA). Hepatocytes were plated on collagen I-coated culture plates in William's Medium E with glutamax, antibiotics, insulin, transferrin, selenium and hydrocortisone. Medium was renewed daily and hepatocytes were collected at day 2 after two washes with PBS. Colon and small intestinal epithelial cells were provided by R.G. Vries and H. Clevers (Hubrecht Institute for Developmental Biology and Stem Cell Research, University Medical Centre Utrecht, Utrecht, The Netherlands) and cultured as described previously[8].

Bile duct epithelial cells (SC-5100, passage 4) were purchased from ScienCell (Carlsbad, CA, USA) and cultured according to manufacturer's instructions.

Fibroblasts, keratinocytes, PTEC, melanocytes and HUVEC were also cultured in the presence of IFN-γ (100 IU/ml) for 4 days to mimic an inflammatory environment. Additionally, two fibroblast samples were cultured with a T-cell culture supernatant for 4 days. This supernatant was collected from a CD4 T-cell clone that was stimulated with leukemic-antigen presenting cells[9] and contained high levels of IFN-γ (3100 pg/ml), IL-13 (500 pg/ml), TNF-α (700 pg/ml) and IL-2 (600 pg/ml) as measured by multi-cytokine ELISA.

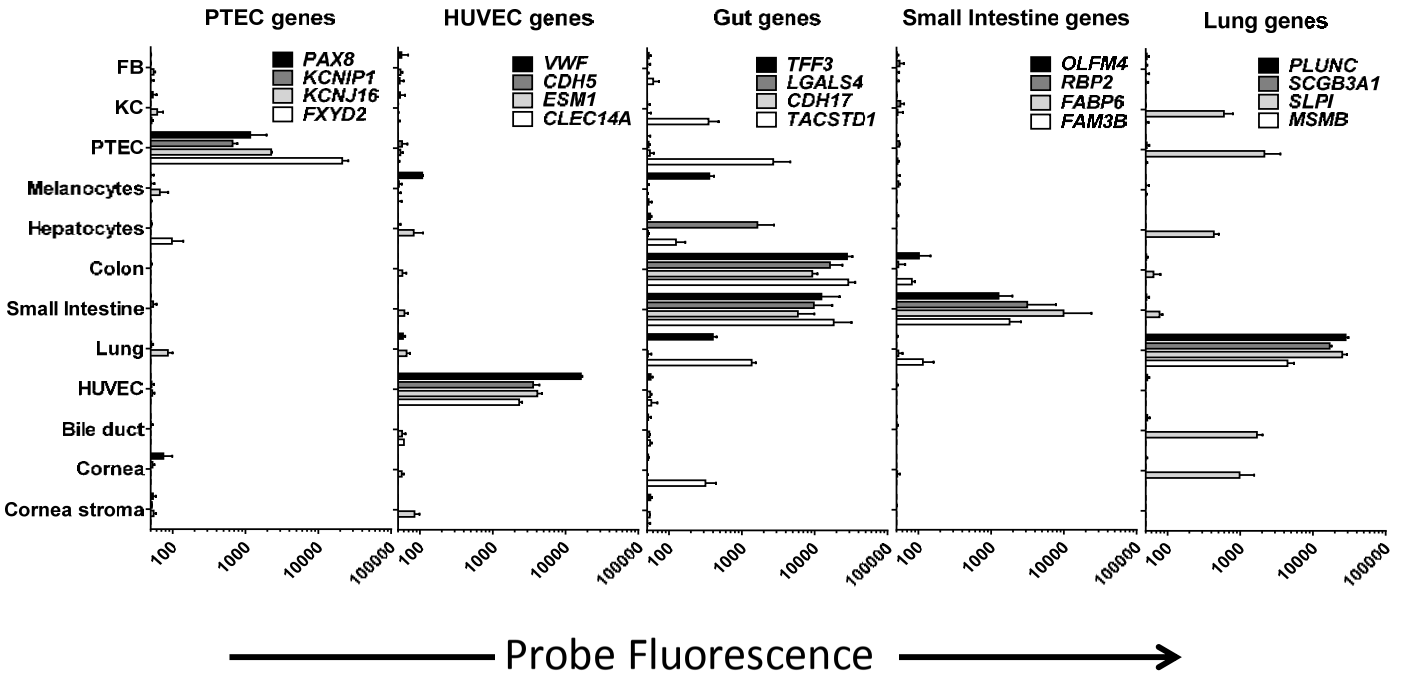

Figure S1: Validation of the cell type origin of non-hematopoietic samples

Gene expression for cell type-specific genes as determined by microarray gene expression is shown. PTEC-specific expression is shown for *PAX8*, *KCNIP1*, *KCNJ16* and *FXYD2*; HUVEC-specific expression is shown for *VWF*, *CDH5*, *ESM1* and *CLEC14A*; small intestine-specific expression is shown for *OLFM4*, *RBP2*, *FABP6* and *FAM3B*. Gut-associated expression as defined by detectable expression in gut (both colon and small intestine) as well as a limited number of other non-hematopoietic cell types is shown for *TFF3*, *LGALS4*, *CDH17* and *TACSTD1* and lung-associated expression is demonstrated for *PLUNC*, *SCGB3A1*, *SLPI* and *MSMB*. Probe fluorescence as measured by microarray gene expression analysis is indicated on the x-axis in logarithmic scale.

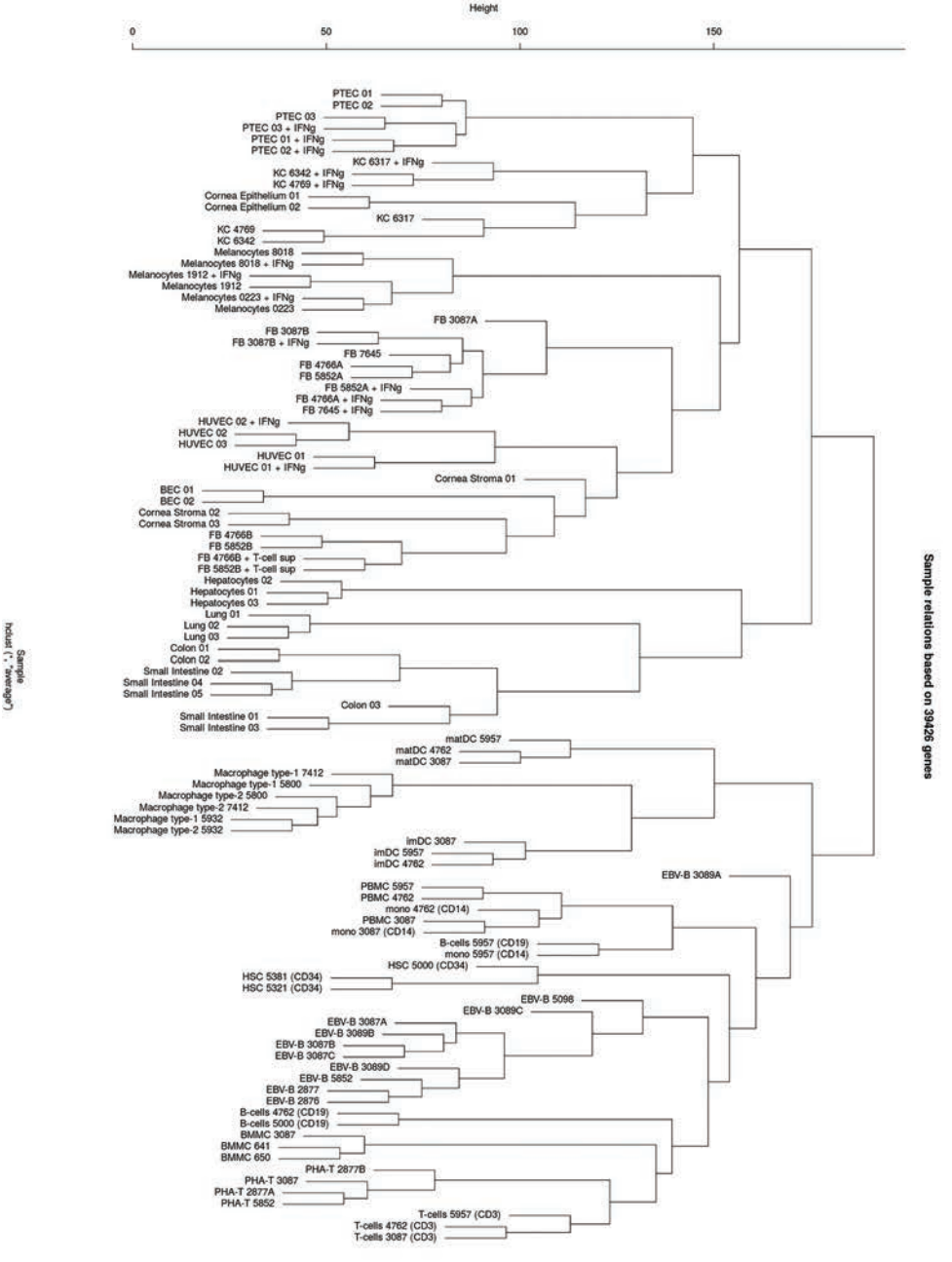

Figure S2: Clustering analysis of hematopoietic and non-hematopoietic cell types

Hierarchical clustering analysis was performed on all healthy hematopoietic and non-hematopoietic cell types as included in the dataset based on microarray expression profiling of all genes. Hematopoietic cell types were accurately distinguished from non-hematopoietic cell types.

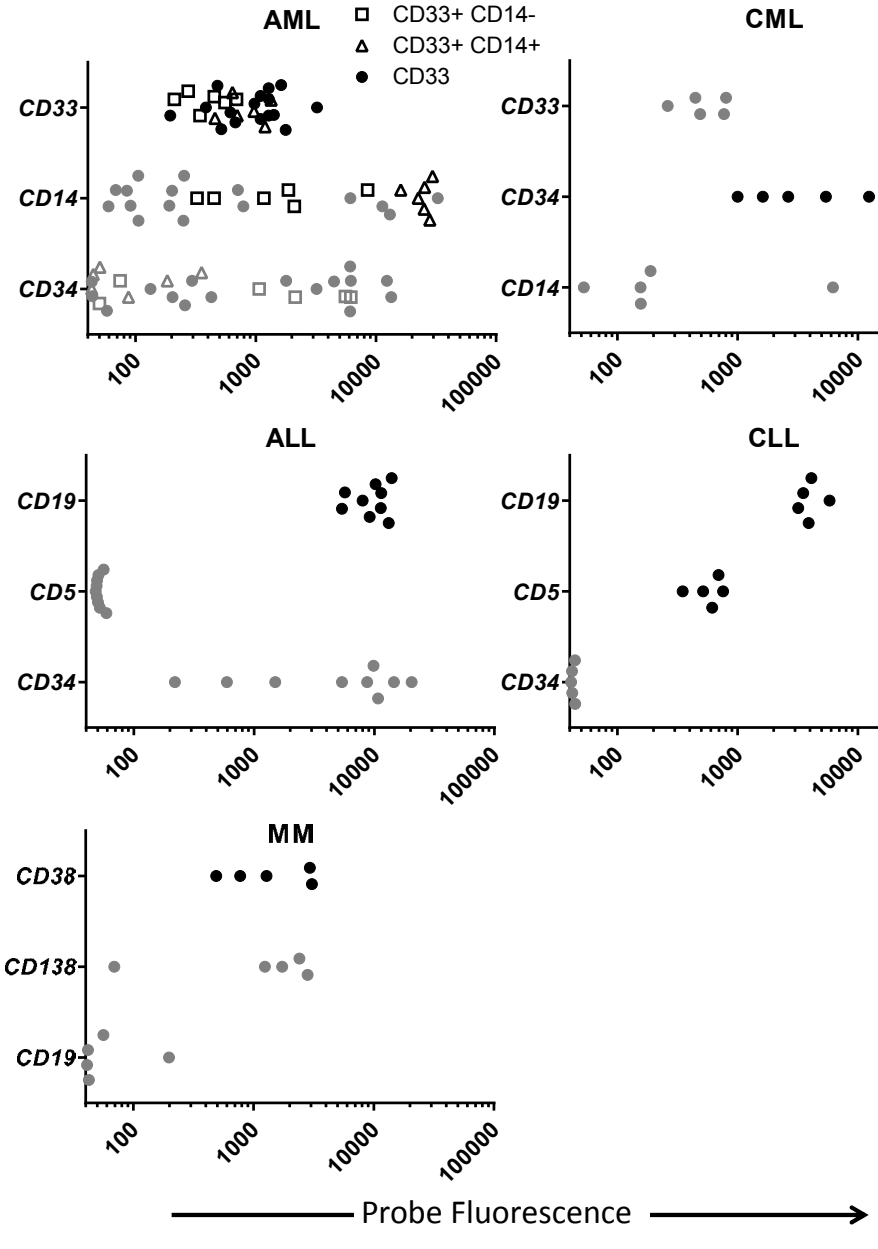

Figure S3: Gene expression for differentiation markers on cell populations isolated from malignant hematopoietic samples

Gene expression for differentiation markers on cell populations isolated from AML, CML, ALL, CLL and MM samples is shown. Black symbols indicate gene expression for surface markers that were used for isolation of malignant cell populations, while gray symbols indicate gene expression for other differentiation markers on isolated cell populations. From AML samples, cell populations were isolated by surface expression of CD33 only (filled circles) or by CD33 in combination with CD14 (open triangles and open squares represent CD33 positive cell populations that are positive or negative for CD14, respectively). Probe fluorescence is indicated on the x-axis in logarithmic scale.

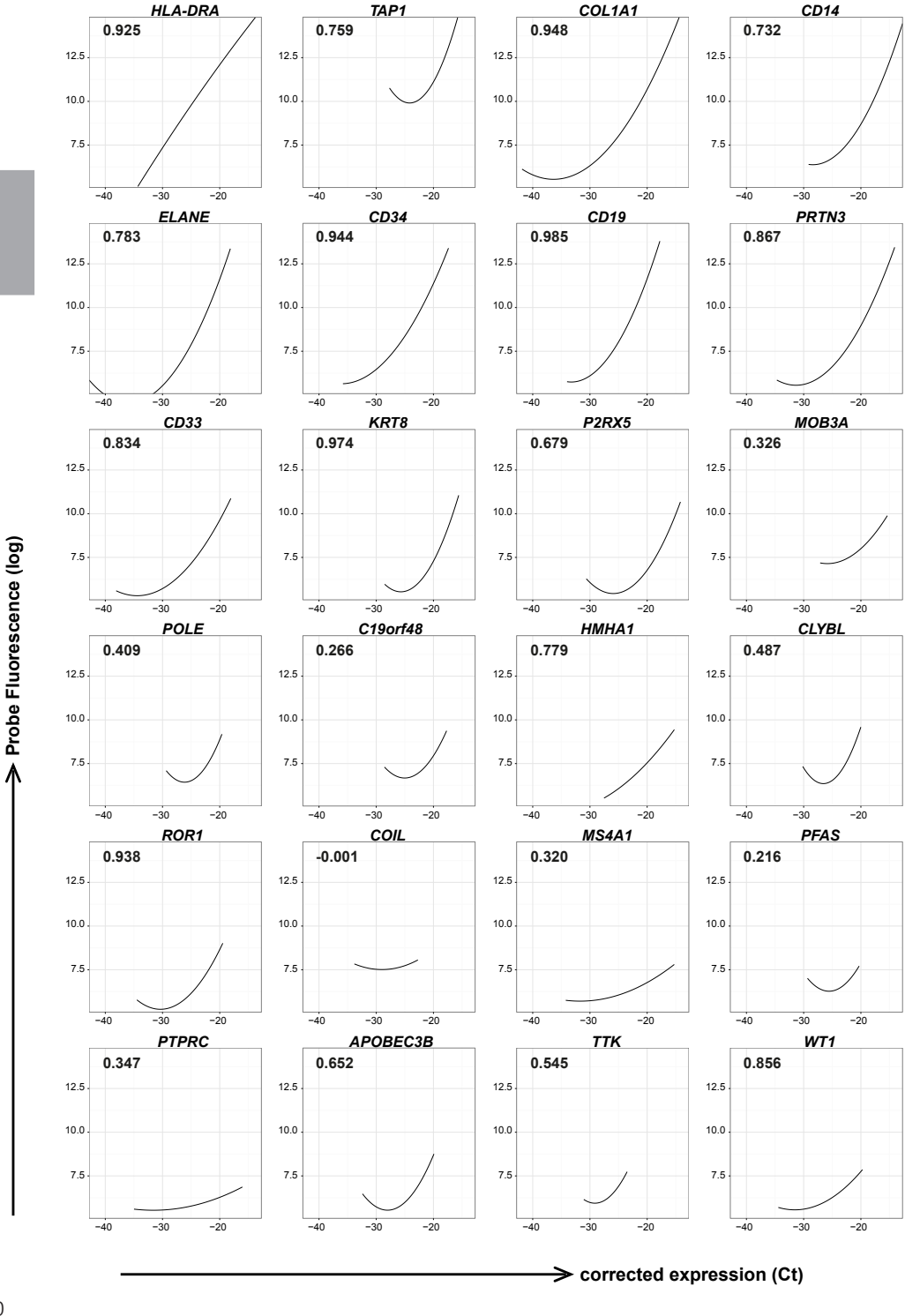
HLA-DRA
0.925
TAP1
0.759
COL1A1
0.948
CD14
0.732
ELANE
0.783
CD34
0.944
CD19
0.985
PRTN3
0.867
CD33
0.834
KRT8
0.974
P2RX5
0.679
MOB3A
0.326
POLE
0.409
C19orf48
0.266
HMHA1
0.779
CLYBL
0.487
ROR1
0.938
COIL
-0.001
MS4A1
0.320
PFAS
0.216
PTPRC
0.347
APOBEC3B
0.652
TTK
0.545
WT1
0.856
12.5
10.0
7.5
−40
−30
−20
Probe Fluorescence (log)
corrected expression (Ct)

Table S1: Complex karyotypes of leukemic cells selected for microarray gene expression analysis

Sample[a]	Complex karyotype[b]
AML 4781 (CD33/CD14)	46,XY,inv(3)(q21q26),del(7)(q21),-17,der(19)t(17;19)(q2?2;q13)[cp6]/46~47,XY,del(2)(p21),-3,del(3)(q23),+6,-7,del(11)(p1?3),add(12)(p11),inv(15)(q?13q?23),+ring,+mar[cp11]/ 46,XY[4]
AML 3714 (CD33)	45-46, XX, ?inv (3) (p?q?),-4, add (5) (q1?2), der (9) t(4;9) (q21;q34), ?dic (11;?) (p1?2;?), add (12) (p13), der (12) add (12) (p?) del (12) (q22), add (14) (q13),-17, del (17) (q21), +1-2mar [19] / 46, XX [1]
AML 3778 (CD33)	47, XX, +8, del (12) (p13) [5] / 47, idem, i (17) (q10) [7] / 47, XX, +add (8) (q24), del (12) (p13), i (17) (q10) [2]
AML 5074 (CD33/CD14)	47, XY, +3 [3] / 48, idem, +20 [2] / 46, XY, t(10;16) (q21;p13) [3]
ALL 5903 (CD19)	46, XX, t(9;22) (q34;q11) [6] / 45, XX,-7, t(9;22) (q34;q11), add (14) (p11) [2] / 46, XX [7]
ALL 3655 (CD19)	85-88, XX, +1,-3,-4,-5,-6,-7,-7,-8,-9,-9,-10, +11, +12,-13,-14,-15,-15,-16, -17,-17,-18. +6-14mar, inc [cp16] / 46, XX [1]
CML 3471 (CD34)	46, XY, t(9;22) (q34;q11) .ish der(9) t(9;22) del(9) (q34q34) (ABL-, WCP22+), der(22) t(9;22) (BCR+, ABL+, WCP22+) [19] /46, XY [1]
CML 3087 (CD34)	46, XX, t(9;22) (q34;q11) [10]/46, X, del(X) (p11.?4), t(9;22) (q34;q11) [13]/46, X, del(X) (p11.?4), t(9;22) (q34;q11), del(17) (q11.2q21) [5]/46, XX [1]
CLL 4725 (CD19/CD5)	45, XY,-10, ?der (17;22) (q10;q10), +mar [5] / 45, XY,-10, ?der (17;18) (q10;q10), +mar [cp3] / 46, XY [2] / 44-46, XY, +1-2 mar [cp5]
MM 5987 (CD38)	46-47, X,-Y, del(1) (p13), +6, del(6) (q1?6), del(8) (p1?2),-11,-12,-12,-13, add(14) (p11), +2-4mar [cp2]
MM 5744 (CD38)	43, X-X, der(2) t(1;2) (q11;q37),-10,-13,-14, +mar [2] / 46,XX [7]
MM 5019 (CD38)	40-43, XY, del (1) (p13), add (6) (q21), add (8) (q24), add (9) (q34), add (12) (p11),-13, der (14) t(11;14) (q13;q32),-16, add (18) (q23), der (19) del (19) (p13) del (19) (q13),-21,-22 [cp16] / 46, XY [4]

[a] Markers for flow cytometric isolation of malignant cells are indicated between brackets. AML cells have been isolated by expression of CD33 (CD33) or a combination of CD33 and CD14 (CD33/CD14) in which CD33 expressing AML cells positive or negative for monocyte lineage differentiation marker CD14 have been selected as two separate cell populations. CLL cells have been selected for co-expression of CD19 and CD5. ALL, CML and MM cells have been isolated by expression of CD19, CD34 and CD38, respectively. [b] Complex karyotypes are depicted for unstimulated and/or stimulated cells.

Figure S4: Correlation plots for q-PCR and microarray data

Plots depicting regression models are given for each gene separately. q-PCR values are given on the x-axis and microarray probe fluorescence on the y-axis. For the purpose of graphical representation Cp values were normalized according to reference genes prior to fitting the regression model. Individual R2 values derived from the model are depicted in the left upper corner of each plot. Genes are shown in order of maximum probe fluorescence as measured in any cell type of the dataset as selected for q-PCR validation starting with genes with highest maximum probe fluorescence. Each dot represents the mean corrected q-PCR value of duplicate measurements and the probe fluorescence intensity as measured by microarray gene expression analysis. Q-PCR measurements were corrected for expression of reference genes (*HMBS*, *ACTB* and *GAPDH*) in the corresponding sample.

Table S2: Assays and probe IDs for genes included for validation by q-PCR

Set[a]	Genes[b]	Taqman assay[c]	Probe 1[d]	Probe 2	Probe 3
1	*PRTN3*	Hs01597752_m1	ILMN_1753584		
1	*ELANE*	Hs00975994_g1	ILMN_1706635		
1	*CD33*	Hs01076281_m1	ILMN_1747622		
1	*CD34*	Hs00990732_m1	ILMN_1732799	ILMN_2341229	
1	*TAP1*	Hs00388675_m1	ILMN_1751079		
1	*CD14*	Hs02621496_s1	ILMN_1740015	ILMN_2396444	
1	*HLA-DRA*	Hs00219575_m1	ILMN_1689655	ILMN_2157441	
1	*PTPRC*	Hs04189704_m1	ILMN_2340217	ILMN_1653652	
1	*HMHA1*	Hs00943375_m1	ILMN_1811392		
1	*COL1A1*	Hs00164004_m1	ILMN_1701308		
1	*CD19*	Hs01047410_g1	ILMN_1782704		
1	*KRT8*	Hs02339474_g1	ILMN_1753584		
2	*APOBEC3B*	Hs00358981_m1	ILMN_2219466		
2	*C19orf48*	Hs01066105_m1	ILMN_1759184	ILMN_2383484	
2	*CLYBL*	Hs00370518_m1	ILMN_1663538		
2	*COIL*	Hs00982300_m1	ILMN_1688034		
2	*MOB3A*	Hs00926925_m1	ILMN_1721344		
2	*MS4A1*	Hs00544819_m1	ILMN_1776939		
2	*P2RX5*	Hs01112471_m1	ILMN_1677793		
2	*PFAS*	Hs00389822_m1	ILMN_1755862		
2	*POLE*	Hs00173030_m1	ILMN_1728199		
2	*ROR1*	Hs00938677_m1	ILMN_1655904		
2	*TTK*	Hs01009870_m1	ILMN_1788166		
2	*WT1*	Hs01103751_m1	ILMN_1802174		
ref[e]	*HMBS*	Hs00609293_g1	ILMN_1685954	ILMN_1726306	
ref[e]	*ACTB*	Hs99999903_m1	ILMN_1777296	ILMN_2038777	ILMN_2152131
ref[e]	*GAPDH*	Hs99999905_m1	ILMN_1343295	ILMN_1802252	ILMN_2038778

[a] Set indicates in which q-PCR validation sample set the gene was included. [b] Official gene symbols are depicted for genes included in the q-PCR validation set. [c] Predesigned Taqman gene expression assays were obtained from Thermo Fisher Scientific. [d] Illumina probe IDs as included in the microarray database. [e] Ref indicates genes that are used as reference genes for q-PCR.

Table S3: RNA samples used for validation by q-PCR

Number	RNA samples[a]	Used in set[b]
1	ALL 2375 (CD19)	1 & 2
2	ALL 2391 (CD19)	1
3	ALL 1833 (CD19)	1 & 2
4	ALL 1299 (CD19)	2
5	ALL 3281 (CD19)	2
6	AML 3714 (CD33)	1 & 2
7	AML 2467 (CD33/CD14pos)	1
8	AML 1310 (CD33/CD14pos)	1
9	AML 1310 (CD33/CD14neg)	1 & 2
10	CML 2195 (CD34)	1
11	CML 5036 (CD34)	1
12	CLL 4725 (CD19/CD5)	2
13	CLL 2159 (CD19/CD5)	2
14	MM 5987 (CD38)	2
15	MM 5744 (CD38)	2
16	PBMC 5957	1
17	PBMC 4762	1
18	B-cells 5957 (CD19)	1 & 2
19	B-cells 4762 (CD19)	1 & 2
20	T-cells 3087 (CD3)	1
21	HSC 5381 (CD34)	1 & 2
22	HSC 5321 (CD34)	1 & 2
23	Mono 5957 (CD14)	1 & 2
24	Mono 4762 (CD14)	1
25	Mono 3087 (CD14)	2
26	matDC 5957	1 & 2
27	matDC 4762	1
28	matDC 3087	2
29	Cornea Stroma 02	1
30	Cornea Stroma 03	1
31	BEC 01	1
32	BEC 02	1
33	FB 5852A	1 & 2
34	FB 7645	1
35	FB 3087B	2
36	FB 5852A + IFN-γ	1 & 2
37	FB 7645 + IFN-γ	1
38	FB 3087B + IFN-γ	2
39	KC 6317	1 & 2
40	KC 6342	1 & 2
41	KC 6317 + IFN-γ	1
42	KC 6342 + IFN-γ	1
43	EBV-B 3089A	2
44	EBV-B 3089C	2
45	EBV-B 2876	2
46	EBV-B 5852	2
47	EBV-B 3087A	2
48	Colon 02	2
49	Colon 03	2
50	BEC 01	2
51	BEC 02	2
52	Hepatocytes 01	2
53	Hepatocytes 02	2

[a] RNA samples for q-PCR were the same as used for microarray gene expression analysis and were stored at-80°C. [b] Used in set indicates in which q-PCR validation set the samples were included.

Table S4: Effect of IFN-γ on gene expression in non-hematopoietic cell types

Probe ID[a]	Gene[b]	FB[c]		FB + IFN-γ[d]		KC[e]		KC + IFN-γ[f]	
		AVG[m]	SD[m]	AVG[n]	SD	AVG	SD	AVG	SD
ILMN_2329927	ABCG1	48.84	0.1	49.90	5.8	81.75	21.1	**1035.69**	252.9
ILMN_1763666	ALDH3B2	49.61	0.1	46.71	2.6	189.23	44.3	**5453.54**	1219.8
ILMN_2363880	ALDH3B2	54.16	0.2	52.95	2.7	72.33	11.1	**962.44**	427.3
ILMN_1692332	ALOX12B	51.75	0.1	51.18	3.6	54.84	5.8	**933.92**	134.3
ILMN_1756862	APOL3	159.03	0.6	**1947.70**	459.5	49.63	6.4	**640.93**	208.9
ILMN_1762284	ASPRV1	58.08	0.0	57.51	5.0	53.05	2.2	**1152.97**	459.9
ILMN_1723480	BST2	115.21	1.0	602.93	306.3	67.15	14.4	**898.60**	138.7
ILMN_1677198	C1R	1852.86	1.2	4264.54	2880.8	156.71	67.2	1299.28	248.7
ILMN_1764109	C1R	1709.28	1.4	4510.50	3015.5	111.55	66.5	**1211.92**	247.7
ILMN_1781626	C1S	2733.16	0.6	10171.05	3994.1	113.80	22.5	846.83	313.2
ILMN_1773352	CCL5	54.39	0.2	73.26	20.2	54.55	1.3	**2737.69**	1472.4
ILMN_2098126	CCL5	57.79	0.2	72.36	18.0	61.30	8.7	**1980.55**	706.8
ILMN_1736567	CD74	77.09	0.8	**3767.31**	1778.8	68.31	25.1	**7122.15**	3193.4
ILMN_2379644	CD74	61.66	0.6	**1642.13**	898.2	53.63	3.4	**2318.52**	842.6
ILMN_1761464	CD74	47.12	0.2	**985.43**	776.3	49.35	6.0	**2704.66**	1553.0
ILMN_1712522	CEACAM6	45.48	0.1	43.42	4.6	48.79	7.1	**985.71**	977.1
ILMN_1774287	CFB	304.78	0.9	1014.58	450.3	128.66	14.3	**5047.12**	1322.1
ILMN_1803838	CNFN	93.28	0.3	75.92	21.3	196.52	45.6	**8871.86**	1546.6
ILMN_1803452	CRCT1	61.52	0.2	55.13	2.0	119.52	57.9	**4816.55**	2047.1
ILMN_1697733	CST6	103.71	1.2	53.76	10.2	99.92	46.5	**2001.80**	1302.7
ILMN_1698666	CST6	79.79	0.8	50.15	3.7	127.88	74.4	**1807.84**	1407.5
ILMN_1654072	CX3CL1	49.39	0.1	56.89	4.3	134.20	47.6	**2110.01**	827.4
ILMN_1791759	CXCL10	50.13	0.1	187.09	128.1	136.35	96.2	**17124.49**	8744.2
ILMN_1745356	CXCL9	54.28	0.2	214.43	158.3	41.93	6.0	**4979.47**	4668.8
ILMN_1686573	DEFB1	51.22	0.1	52.32	5.9	633.89	236.4	**10526.60**	6622.4
ILMN_1684308	DEFB103B	55.06	0.2	53.17	4.1	63.96	13.8	**7264.68**	7549.3
ILMN_1714587	DEFB103B	50.71	0.1	49.86	2.7	53.23	4.7	**2182.45**	1939.4
ILMN_1733998	DHRS9	52.63	0.1	53.11	9.8	79.20	10.4	**2211.26**	2488.2
ILMN_1769201	ELF3	47.54	0.1	49.41	4.0	63.21	9.5	**739.08**	506.2
ILMN_1671600	EPS8L1	49.09	0.2	46.40	4.6	83.61	24.7	**879.20**	406.4
ILMN_2388547	EPSTI1	113.74	0.7	**1647.95**	506.8	317.50	175.0	2245.49	275.1
ILMN_1701114	GBP1	173.11	0.4	**2023.51**	706.8	150.79	84.2	1135.13	297.1
ILMN_2148785	GBP1	125.72	0.4	1239.64	132.5	116.18	39.8	497.33	118.5
ILMN_1774077	GBP2	603.04	0.8	**12958.95**	5995.9	89.61	17.4	**3991.82**	1595.7
ILMN_1771385	GBP4	48.66	0.2	**725.83**	211.4	51.44	4.5	**902.42**	195.9
ILMN_2114568	GBP5	55.38	0.1	**892.66**	507.3	60.87	24.8	**1138.56**	226.2
ILMN_2188862	GDF15	1059.99	0.4	1072.21	600.2	198.91	159.0	**3104.88**	2204.0
ILMN_1803945	HCP5	77.79	0.4	**958.35**	460.8	656.35	301.3	3072.55	1779.9
ILMN_1758623	HIST1H2BD	210.09	0.3	334.05	105.0	295.16	103.9	**4056.45**	2697.8
ILMN_1651496	HIST1H2BD	287.15	0.3	420.55	176.9	409.24	193.7	**5452.04**	3516.2
ILMN_1778401	HLA-B	907.11	0.9	**9361.50**	1594.6	1635.81	252.0	**17150.88**	6003.9
ILMN_1695311	HLA-DMA	396.45	0.8	**6931.34**	2366.2	236.17	111.9	**4290.23**	960.5
ILMN_1761733	HLA-DMB	65.93	0.7	**1780.86**	967.1	56.33	12.8	**2044.10**	785.5
ILMN_1659075	HLA-DOA	50.75	0.1	**1231.98**	741.6	44.49	8.9	247.60	138.4
ILMN_1772218	HLA-DPA1	116.29	0.8	**5347.41**	3408.7	45.00	1.4	**5898.30**	3368.2
ILMN_1808405	HLA-DQA1	55.12	0.2	**1200.68**	1121.2	43.22	2.7	**1594.54**	1138.9
ILMN_2157441	HLA-DRA	96.33	1.0	**5896.75**	2407.4	50.73	2.2	**8090.95**	751.2
ILMN_1689655	HLA-DRA	120.13	1.2	**13994.52**	4867.1	51.71	3.1	**16149.33**	6775.5
ILMN_1715169	HLA-DRB1	52.87	0.3	272.20	263.5	45.56	5.0	316.79	227.4
ILMN_1752592	HLA-DRB4	80.20	0.5	**4722.43**	3240.0	63.89	14.3	**9081.97**	10653.3
ILMN_1697499	HLA-DRB5	61.78	0.5	439.61	775.9	48.06	3.4	**1972.46**	2024.2
ILMN_2066066	HLA-DRB6	52.99	0.1	231.58	66.0	56.97	10.1	396.13	36.8
ILMN_2186806	HLA-F	216.76	0.6	815.38	143.3	364.69	75.9	2206.76	533.1
ILMN_2130441	HLA-H	1416.17	0.6	9505.64	1554.9	2118.79	133.5	11458.84	1271.5
ILMN_2316236	HOPX	45.94	0.1	42.92	5.1	138.08	76.0	**2507.79**	432.2
ILMN_2058782	IFI27	632.45	0.9	**8740.06**	8071.3	14560.92	9119.4	25672.22	808.3
ILMN_1723912	IFI44L	88.38	0.7	**1204.84**	453.2	420.66	327.9	1397.99	544.1
ILMN_1739428	IFIT2	164.99	0.2	**2214.68**	576.0	212.66	88.9	**2151.56**	1623.0
ILMN_1701789	IFIT3	277.23	0.5	**5719.26**	1860.9	600.17	448.6	5257.17	2311.6

Table S4: continued

PTEC[g]		PTEC + IFN-γ[h]		MEL[i]		MEL + IFN-γ[j]		HUVEC[k]		HUVEC + IFN-γ[l]	
AVG	SD	AVG	SD	AVG	SD	AVG	SD	AVG	SD	AVG	SD
50.06	1.6	54.51	6.9	44.59	2.0	48.09	4.9	150.05	21.7	98.93	16.9
46.83	3.6	50.84	4.3	43.76	4.3	48.32	4.6	38.85	0.2	41.77	0.5
54.65	2.4	55.87	2.2	56.12	5.5	58.23	4.1	45.37	4.2	41.72	3.1
52.97	2.3	51.53	4.0	48.58	2.3	48.44	0.9	45.34	1.1	40.87	4.1
75.73	10.1	404.24	81.3	45.81	1.2	59.00	14.6	194.68	160.5	1638.69	590.1
55.18	4.3	60.09	5.6	72.56	7.9	68.28	5.4	49.69	1.0	49.94	1.1
702.79	229.8	1569.08	273.2	227.37	96.1	384.41	129.3	511.90	506.5	1248.34	1181.2
264.47	256.3	1632.03	596.7	56.32	12.4	101.82	30.5	52.36	5.5	**987.57**	259.9
232.46	200.7	1218.73	332.8	62.81	6.4	101.00	32.1	58.07	1.2	**733.80**	113.5
225.07	179.0	**2447.75**	1696.2	54.04	4.2	86.21	17.2	63.89	3.8	**1524.57**	649.4
60.95	11.7	182.60	56.6	91.06	16.9	106.04	69.7	60.86	0.4	58.66	2.9
73.48	26.5	263.78	109.3	114.04	35.4	150.66	83.7	88.92	3.4	82.33	5.3
301.65	91.9	**15682.34**	3869.4	58.57	2.8	**1633.06**	845.3	50.41	3.5	**6673.13**	1222.4
133.58	56.4	**4314.29**	716.8	44.68	5.7	**560.01**	220.9	44.12	1.2	**2848.28**	1142.9
69.99	14.4	**1939.27**	899.9	44.81	7.4	249.88	77.0	40.52	2.3	309.32	151.4
67.23	29.2	70.09	36.1	41.14	3.3	43.02	4.0	46.19	1.3	44.51	2.8
189.58	66.8	1658.66	530.1	54.19	4.3	61.49	7.3	83.75	22.2	353.69	164.0
81.94	2.7	66.44	2.5	109.86	12.3	92.76	20.6	72.91	13.3	64.48	14.4
47.39	0.7	51.37	2.4	50.83	6.0	50.52	6.5	55.02	0.4	54.00	4.0
143.03	58.2	174.10	100.7	49.59	2.9	48.88	4.0	55.37	2.6	55.20	6.3
138.67	40.1	202.76	100.5	45.67	1.9	44.24	4.7	44.30	0.3	45.73	1.2
403.92	166.7	2121.91	962.7	51.93	3.4	50.39	1.7	133.02	43.4	649.37	600.8
54.74	10.1	**2037.19**	1558.5	53.98	10.1	87.52	21.7	69.02	0.6	**15285.57**	16284.2
48.87	4.8	**507.69**	571.4	50.43	2.1	89.30	29.9	44.66	1.0	**14988.97**	19786.6
1816.05	1946.7	883.34	565.2	45.94	8.1	45.16	5.3	47.79	2.7	53.22	1.9
49.21	2.3	54.45	4.7	52.69	4.5	49.26	2.8	58.58	0.7	52.89	1.0
46.29	2.5	50.05	2.4	45.53	1.2	46.63	2.2	46.71	2.9	47.94	3.2
78.67	25.3	54.43	7.6	49.61	2.9	50.49	2.9	64.24	1.4	74.75	2.5
867.37	122.3	1078.05	154.1	56.94	6.1	56.35	0.9	56.94	2.6	61.41	1.1
95.58	29.4	82.11	24.3	114.34	29.4	88.67	16.7	104.74	63.1	93.78	52.4
350.78	64.1	3297.06	297.7	366.54	214.8	498.67	112.1	85.62	20.6	**993.58**	415.0
200.54	44.8	**2493.85**	1102.2	128.84	95.6	827.20	273.8	134.26	62.1	**3115.13**	2505.9
109.20	44.3	**1258.73**	406.2	78.70	31.8	538.87	248.4	150.13	42.2	**3480.33**	2692.5
1435.90	760.5	**16358.86**	7106.1	135.98	28.5	**1920.36**	953.9	518.73	260.1	**9395.13**	5650.8
71.79	15.3	**2237.92**	305.7	50.86	5.2	124.59	67.2	72.91	11.6	**2401.53**	308.5
46.33	3.7	**5276.27**	789.8	44.24	1.1	50.40	6.7	44.09	2.1	**2017.36**	1414.2
2550.20	2171.0	5469.76	2321.4	726.40	235.3	2450.76	2072.3	4771.94	1280.1	3503.67	216.0
254.44	65.1	2029.85	535.5	449.64	451.6	1056.99	905.8	48.92	0.9	**569.00**	235.4
94.68	15.9	109.31	33.9	649.55	153.6	617.30	34.9	61.36	1.3	62.48	9.3
103.39	4.6	132.37	46.8	1063.49	169.2	1013.49	66.1	68.91	5.1	70.99	16.6
2165.09	1430.9	14946.59	964.3	2928.13	2434.1	11274.35	2700.4	305.69	119.6	**8580.11**	3072.6
296.47	53.2	**4341.77**	2171.5	268.77	72.6	**4124.57**	415.3	118.99	46.0	**2158.77**	2130.0
1072.82	206.4	3251.26	1203.6	62.33	20.3	**737.00**	40.8	63.16	5.6	**1047.80**	845.0
46.69	1.5	**852.73**	754.7	46.01	2.5	251.80	72.0	51.47	6.1	376.36	230.0
67.18	6.3	**3476.02**	2001.4	226.50	192.2	**2819.46**	1753.3	55.11	6.1	**1527.72**	1152.5
44.10	1.9	**1238.75**	960.5	43.13	6.5	309.54	147.8	41.21	1.4	**455.84**	448.5
64.95	14.3	**7896.86**	3547.8	59.93	10.1	**3979.94**	923.2	54.50	1.6	**4817.07**	2652.6
69.65	14.1	**8802.78**	5386.2	55.33	8.7	**4770.78**	1192.5	72.54	6.4	**3582.60**	2716.6
53.89	3.2	**638.04**	41.7	47.29	5.5	297.85	212.7	54.96	0.2	57.51	1.1
61.87	5.8	**2789.86**	483.3	59.24	1.3	**3116.55**	2734.7	62.92	4.3	**2740.59**	2753.1
47.41	3.7	**2414.16**	1278.0	45.96	6.1	**1061.59**	908.5	46.57	2.8	48.44	4.4
56.42	1.2	371.08	101.0	55.20	7.1	264.19	36.0	49.87	5.4	**702.18**	568.2
371.17	245.1	2035.55	946.4	519.52	295.8	1016.74	572.3	194.52	72.4	**1946.75**	103.7
2174.33	1698.4	13557.52	3087.1	4030.01	3242.4	10037.66	5575.5	651.59	351.7	**9103.70**	171.5
58.52	3.8	41.71	1.0	48.73	4.7	44.02	3.5	147.44	91.6	226.15	173.8
229.73	293.4	**2802.31**	1266.4	8251.50	9949.4	8078.30	4960.9	5575.76	389.9	7839.86	5570.8
254.71	135.9	**3737.78**	296.1	2091.36	981.5	3245.26	692.0	131.47	37.5	**1500.45**	753.1
224.64	112.9	2156.26	265.6	1110.65	480.2	2026.69	486.0	61.63	0.6	176.29	27.0
339.85	126.6	**4337.01**	354.1	3155.73	1894.5	6597.25	2651.4	60.53	6.3	**732.62**	220.4

Table S4: continued

Probe ID[a]	Gene[b]	FB[c]		FB + IFN-γ[d]		KC[e]		KC + IFN-γ[f]	
		AVG[m]	SD[m]	AVG[n]	SD	AVG	SD	AVG	SD
ILMN_1801246	IFITM1	1117.55	1.2	9494.69	3342.8	3503.69	1844.2	17076.49	837.7
ILMN_2334296	IL18BP	121.12	0.1	**4541.91**	2733.1	73.80	19.9	**1258.71**	223.4
ILMN_1804901	IL1F5	49.36	0.2	52.07	7.8	72.91	6.4	**888.23**	86.5
ILMN_2368530	IL32	57.32	0.2	210.39	74.3	74.24	6.8	**1227.70**	225.6
ILMN_1778010	IL32	78.33	0.2	356.41	214.5	79.44	17.2	**1033.18**	452.3
ILMN_1656310	INDO	45.82	0.3	**525.29**	132.5	59.43	15.1	340.77	266.9
ILMN_1708375	IRF1	378.04	0.8	2621.77	246.6	196.84	19.1	**4635.05**	2186.4
ILMN_1695924	KLK11	53.19	0.2	50.59	4.5	802.88	179.3	**10005.51**	2019.0
ILMN_1745570	KLK7	55.77	0.2	64.67	8.1	1300.40	728.1	**15106.71**	6679.6
ILMN_1791545	KRT23	74.38	0.1	70.16	13.3	124.39	42.6	**2088.33**	1200.5
ILMN_1705814	KRT80	77.66	0.5	48.93	5.6	87.15	29.0	**7107.21**	2982.1
ILMN_2170814	LAMP3	55.19	0.4	119.83	127.9	76.10	21.9	**1048.95**	275.9
ILMN_1808220	LCE3E	66.39	0.3	64.63	14.8	56.19	7.2	**802.66**	396.4
ILMN_1659688	LGALS3BP	544.76	0.8	1396.51	911.7	644.97	299.3	1007.35	384.4
ILMN_2412214	LGALS9	67.59	0.4	314.35	196.5	56.63	5.6	56.83	5.9
ILMN_2332964	LGMN	627.24	0.5	560.58	70.3	424.37	80.7	**5382.45**	2008.1
ILMN_1815895	LOC649143	48.16	0.1	**496.09**	411.0	46.77	4.4	**995.65**	242.8
ILMN_1722670	LYNX1	48.19	0.2	46.55	5.1	54.21	8.6	**842.70**	443.5
ILMN_1718033	LYPD5	44.27	0.1	61.20	16.9	106.35	13.0	**1951.04**	1216.2
ILMN_2388484	MAP2	59.78	0.3	82.31	24.2	98.60	18.6	**1171.85**	722.7
ILMN_1801610	METRNL	536.69	0.3	591.33	251.6	63.46	4.9	**694.96**	345.5
ILMN_2371911	MUC1	143.36	0.6	202.42	53.2	74.92	21.0	**1000.48**	263.6
ILMN_1662358	MX1	718.26	1.9	**10730.74**	7371.9	5578.05	4398.0	17909.55	2646.0
ILMN_1713397	NCCRP1	50.95	0.2	53.63	2.8	105.54	46.3	**2133.37**	612.5
ILMN_1674063	OAS2	253.92	0.6	**4329.48**	1836.7	3083.40	1274.9	7362.87	2188.3
ILMN_1693192	PI3	48.98	0.1	44.36	1.9	965.35	557.7	**11419.86**	2677.6
ILMN_1815023	PIM1	1176.16	1.1	901.48	359.0	354.74	45.6	**4939.44**	2578.8
ILMN_2376108	PSMB9	187.57	0.7	**2542.10**	516.9	243.36	9.9	1042.49	419.2
ILMN_1800091	RARRES1	52.02	0.2	118.93	82.1	48.70	2.1	**1661.48**	1005.2
ILMN_1701613	RARRES3	286.89	0.7	**12942.20**	5804.9	128.36	21.7	**8772.33**	2324.2
ILMN_1683179	RRAD	86.19	0.6	63.27	2.1	69.76	9.0	**1201.41**	880.7
ILMN_1801216	S100P	51.84	0.3	104.19	117.8	58.75	11.5	**12726.25**	1851.0
ILMN_1712759	SBSN	244.46	1.0	182.80	167.6	300.96	100.3	**14248.09**	3514.4
ILMN_1740917	SCNN1B	52.96	0.1	55.99	6.6	62.13	5.3	**696.83**	247.9
ILMN_2114720	SLPI	51.63	0.2	50.64	4.5	597.01	197.4	**6506.51**	739.5
ILMN_1716591	SPRR1A	38.85	0.2	42.92	9.3	266.78	200.3	**6084.44**	5091.9
ILMN_2191967	SPRR2D	44.58	0.2	44.37	2.3	420.01	416.6	**13954.08**	12217.5
ILMN_1810835	SPRR3	50.74	0.1	50.81	2.4	85.75	37.2	**5981.57**	7827.6
ILMN_1727589	SULT2B1	51.65	0.0	51.75	5.2	85.03	13.7	**1457.46**	235.2
ILMN_1751079	TAP1	1236.54	0.5	**13773.11**	3210.4	1972.73	192.8	**25648.96**	2364.5
ILMN_1770922	TMEM45A	758.53	0.2	813.31	134.5	269.60	62.2	**2767.81**	917.2
ILMN_1758418	TNFSF13B	74.69	0.4	697.88	321.1	57.43	1.9	180.66	74.8
ILMN_1678841	UBD	49.53	0.1	68.58	16.1	50.81	13.0	**1960.63**	804.8
ILMN_1727271	WARS	1514.53	0.5	**20408.54**	7452.5	689.49	104.2	**30022.06**	501.3
ILMN_2337655	WARS	1370.47	0.3	13355.12	3647.9	708.45	93.3	**20061.52**	3727.7
ILMN_2079042	WFDC5	47.16	0.1	46.81	1.6	144.72	22.5	**1549.36**	417.2
ILMN_1742618	XAF1	271.66	0.4	890.16	340.1	212.41	108.6	524.67	213.1

Table S4: continued

PTEC[g]		PTEC + IFN-γ[h]		MEL[i]		MEL + IFN-γ[j]		HUVEC[k]		HUVEC + IFN-γ[l]	
AVG	SD	AVG	SD	AVG	SD	AVG	SD	AVG	SD	AVG	SD
4407.33	2726.6	23031.44	893.8	3985.89	3134.6	14673.66	5747.0	155.79	87.8	**1637.90**	1283.6
145.65	38.5	**8542.26**	2796.2	85.65	4.7	541.61	280.5	272.38	157.1	**3289.94**	212.3
49.05	2.4	54.00	2.2	52.98	4.0	55.31	3.1	42.38	3.4	41.52	2.2
608.33	531.3	1470.46	1547.2	51.85	6.1	52.15	10.6	1922.19	1012.3	2679.37	1611.7
454.47	337.1	815.64	698.4	53.89	3.4	51.30	0.8	526.22	456.5	686.87	601.3
59.23	14.7	**1360.05**	819.0	49.24	4.0	86.92	18.1	44.89	0.2	**2549.94**	1035.2
1053.01	505.7	5612.52	2483.5	221.94	84.3	1715.14	649.4	214.73	193.6	**2441.88**	179.7
47.30	4.5	50.59	3.4	49.22	4.6	47.91	4.3	55.29	5.9	50.29	3.1
84.20	49.4	68.63	11.9	56.67	3.9	56.57	9.1	48.37	2.7	47.63	1.7
85.89	26.6	64.48	6.9	104.50	12.7	88.69	16.1	47.56	1.6	47.43	4.3
551.53	267.0	197.97	88.2	50.82	3.3	48.89	2.5	303.35	22.4	223.93	1.7
53.25	9.0	**549.14**	145.3	48.29	4.8	64.23	12.4	323.06	26.2	419.63	22.6
53.53	9.7	65.71	12.2	60.13	6.0	58.36	3.6	51.24	2.6	51.57	4.3
1181.26	513.3	2832.00	660.7	3228.87	1842.7	4620.85	2686.5	45.16	1.2	**480.59**	92.3
67.32	6.6	198.68	59.5	87.12	27.7	92.45	39.4	94.55	34.4	**975.77**	235.6
505.11	46.6	1106.87	235.8	319.24	47.5	419.66	67.4	470.90	38.3	681.96	106.8
46.62	3.8	**714.91**	792.5	47.59	1.4	**604.77**	769.9	58.81	2.1	**880.51**	810.9
46.51	6.0	49.77	9.9	48.51	2.7	50.88	6.9	46.05	2.2	47.37	0.7
55.10	3.4	89.77	13.3	52.32	5.2	66.97	15.7	56.74	7.3	70.75	3.8
58.57	6.7	79.79	3.2	47.16	1.8	53.15	3.2	113.04	27.6	107.14	8.1
62.40	7.5	74.02	12.3	117.07	24.8	138.34	14.0	131.82	14.2	115.86	13.4
1568.28	1073.0	2580.89	1351.5	73.54	7.5	77.76	8.5	49.12	2.2	60.31	16.0
2081.13	1510.0	13433.93	4637.0	20289.26	6972.0	19984.79	6859.6	309.04	70.4	2534.77	893.0
100.53	41.2	61.27	4.9	447.73	398.4	163.58	124.6	44.15	0.6	46.92	0.4
117.20	106.3	**1897.39**	368.1	3043.40	1688.0	3615.51	1555.6	202.56	89.1	1208.07	194.9
283.62	195.0	65.43	10.3	50.67	3.8	48.72	2.4	43.94	2.9	42.29	0.7
747.24	343.8	943.70	416.6	102.64	21.6	96.69	19.9	87.08	32.5	96.57	23.4
288.94	29.2	2723.48	655.0	403.61	274.2	1086.98	313.4	78.08	47.5	**1358.51**	1202.1
89.68	18.2	193.27	89.9	55.11	6.2	58.95	2.3	62.65	6.4	69.09	10.6
2348.77	337.8	**28950.28**	602.9	171.05	44.9	383.49	106.1	62.17	22.9	**1809.49**	1367.0
1611.67	1019.4	1444.14	481.5	45.99	4.5	47.28	3.5	56.15	1.7	53.73	0.5
85.61	34.5	72.25	29.3	49.15	4.8	43.18	1.8	42.09	2.0	41.94	1.5
51.16	3.9	47.55	3.8	53.46	2.9	51.97	3.7	42.26	0.9	44.32	2.9
48.70	3.7	55.12	5.0	54.35	1.6	52.32	2.7	50.34	3.9	51.08	1.6
2139.08	1426.8	2184.73	951.3	49.57	2.3	44.48	1.3	42.82	3.4	43.37	0.4
54.15	20.9	44.65	8.6	48.47	6.0	45.33	11.2	97.59	11.8	93.50	15.3
44.87	3.5	46.25	4.0	44.24	4.0	44.30	1.6	57.09	1.7	52.51	3.3
49.48	1.7	52.13	5.5	52.04	5.8	55.10	2.4	46.01	2.2	42.43	0.2
53.49	7.5	52.54	3.6	69.51	16.2	68.01	8.1	44.97	3.0	48.06	4.8
1434.62	544.7	**15504.01**	1948.7	3833.53	1618.3	14098.87	1982.3	654.16	334.6	**10409.28**	5849.2
73.13	27.7	53.04	3.3	139.19	49.0	122.61	33.8	137.64	90.3	126.11	71.7
65.40	12.7	**819.94**	7.5	75.92	16.8	226.77	79.1	60.31	3.9	260.83	9.5
150.86	117.1	**5551.24**	826.5	47.89	2.2	100.32	33.1	73.61	16.0	**1967.35**	291.8
913.46	79.7	**18692.93**	2211.8	6765.34	1591.4	27572.74	1562.6	914.36	61.8	**14680.06**	11560.4
996.92	110.2	**16604.77**	3358.1	8180.00	4406.7	22874.17	4982.5	1265.00	190.3	**15696.13**	8662.5
73.51	50.8	49.54	5.7	46.09	5.5	48.74	5.9	52.45	0.1	49.06	0.8
86.31	40.4	**1080.09**	306.0	666.42	19.6	1138.79	305.8	180.92	132.4	518.87	198.4

[a] Illumina probe IDs as included in the microarray database. [b] Official gene symbols are depicted for genes that are >10-fold up-regulated by IFN-γ in at least one non-hematopoietic cell type. [c] Fibroblasts (FB) cultured without IFN-γ. [d] Fibroblasts (FB) cultured with 100 IU/ml IFN-γ for 4 days. [e] Keratinocytes (KC) cultured without IFN-γ. [f] Keratinocytes (KC) cultured with 100 IU/ml IFN-γ for 4 days. [g] Proximal tubular epithelial cells (PTEC) cultured without IFN-γ. [h] Proximal tubular epithelial cells (PTEC) cultured with 100 IU/ml IFN-γ for 4 days. [i] Melanocytes (MEL) cultured without IFN-γ. [j] Melanocytes (MEL) cultured with 100 IU/ml IFN-γ for 4 days. [k] Human umbilical vein endothelial cells (HUVEC) cultured without IFN-γ. [l] Human umbilical vein endothelial cells (HUVEC) cultured with 100 IU/ml IFN-γ for 4 days. [m] AVG and SD are the average and standard deviation of probe fluorescence as measured within the sample group, respectively. [n] Values in grey and bold indicate that the average probe fluorescence as measured in the sample group after culturing with IFN-γ is >10-fold higher than the fluorescence measured in the same samples cultured in the absence of cytokines.

Reference list

1. Horowitz MM, Gale RP, Sondel PM, et al. Graft-versus-leukemia reactions after bone marrow transplantation. Blood. 1990;75(3):555-562.
2. Maus MV, Grupp SA, Porter DL, June CH. Antibody-modified T cells: CARs take the front seat for hematologic malignancies. Blood. 2014;123(17):2625-2635.
3. Lamers CHJ, Sleijfer S, van Steenbergen S, et al. Treatment of Metastatic Renal Cell Carcinoma With CAIX CAR-engineered T cells: Clinical Evaluation and Management of On-target Toxicity. Mol Ther. 2013;21(4):904-912.
4. Morgan RA, Chinnasamy N, Abate-Daga D, et al. Cancer regression and neurological toxicity following anti-MAGE-A3 TCR gene therapy. J Immunother. 2013;36(2):133-151.
5. Ferrara JL, Levine JE, Reddy P, Holler E. Graft-versus-host disease. Lancet. 2009;373(9674):1550-1561.
6. Jensen MC, Riddell SR. Designing chimeric antigen receptors to effectively and safely target tumors. Current Opinion in Immunology. 2015;33:9-15.
7. Bleakley M, Riddell SR. Exploiting T cells specific for human minor histocompatibility antigens for therapy of leukemia. Immunol Cell Biol. 2011;89(3):396-407.
8. Spierings E. Minor histocompatibility antigens: past, present, and future. Tissue Antigens. 2014;84(4):374-360.
9. Warren EH, Zhang XC, Li S, et al. Effect of MHC and non-MHC donor/recipient genetic disparity on the outcome of allogeneic HCT. Blood. 2012;120(14):2796-2806.
10. Zilberberg J, Feinman R, Korngold R. Strategies for the identification of T cell-recognized tumor antigens in hematological malignancies for improved graft-versus-tumor responses after allogeneic blood and marrow transplantation. Biol Blood Marrow Transplant. 2015;21(6):1000-1007.
11. Griffioen M, van Bergen CAM, Falkenburg JHF. Autosomal minor histocompatibility antigens; How genetic variants create diversity in immune targets. Frontiers in Immunology. 2016;7.
12. Edgar R, Domrachev M, Lash AE. Gene Expression Omnibus: NCBI gene expression and hybridization array data repository. Nucleic Acids Res. 2002;30(1):207-210.
13. Barrett T, Wilhite SE, Ledoux P, et al. NCBI GEO: archive for functional genomics data sets--update. Nucleic Acids Res. 2013;41(Database issue):D991-995.
14. Rhodes DR, Yu J, Shanker K, et al. ONCOMINE: A Cancer Microarray Database and Integrated Data-Mining Platform. Neoplasia (New York, NY). 2004;6(1):1-6.
15. Su AI, Wiltshire T, Batalov S, et al. A gene atlas of the mouse and human protein-encoding transcriptomes. Proceedings of the National Academy of Sciences of the United States of America. 2004;101(16):6062-6067.
16. Kilpinen S, Autio R, Ojala K, et al. Systematic bioinformatic analysis of expression levels of 17,330 human genes across 9,783 samples from 175 types of healthy and pathological tissues. Genome Biology. 2008;9(9):R139-R139.
17. Maude SL, Frey N, Shaw PA, et al. Chimeric antigen receptor T cells for sustained remissions in leukemia. N Engl J Med. 2014;371(16):1507-1517.
18. Reddy P, Ferrara JL. Immunobiology of acute graft-versus-host disease. Blood Rev. 2003;17(4):187-194.
19. Stevanovic S, van Bergen CA, van Luxemburg-Heijs SA, et al. HLA-class II upregulation during viral infection leads to HLA-DP directed Graft-versus-Host Disease after CD4+ donor lymphocyte infusion. Blood. 2013.
20. Griffioen M, Honders MW, van der Meijden ED, et al. Identification of 4 novel HLA-B*40:01 restricted minor histocompatibility antigens and their potential as targets for graft-versus-leukemia reactivity. Haematologica. 2012;97(8):1196-1204.

21. Stumpf AN, van der Meijden ED, van Bergen CA, Willemze R, Falkenburg JH, Griffioen M. Identification of 4 new HLA-DR-restricted minor histocompatibility antigens as hematopoietic targets in antitumor immunity. Blood. 2009;114(17):3684-3692.

22. Swerdlow SH, Cancer IAfRo, Organization WH. WHO Classification of Tumours of Haematopoietic and Lymphoid Tissues (ed 4th). Lyon: International Agency for Research on Cancer Press; 2008.

23. Wouters BJ, Lowenberg B, Erpelinck-Verschueren CA, van Putten WL, Valk PJ, Delwel R. Double CEBPA mutations, but not single CEBPA mutations, define a subgroup of acute myeloid leukemia with a distinctive gene expression profile that is uniquely associated with a favorable outcome. Blood. 2009;113(13):3088-3091.

24. Groschel S, Lugthart S, Schlenk RF, et al. High EVI1 expression predicts outcome in younger adult patients with acute myeloid leukemia and is associated with distinct cytogenetic abnormalities. J Clin Oncol. 2010;28(12):2101-2107.

25. Barjesteh van Waalwijk van Doorn-Khosrovani S, Erpelinck C, van Putten WLJ, et al. High EVI1 expression predicts poor survival in acute myeloid leukemia: a study of 319 de novo AML patients. Blood. 2002;101(3):837-845.

26. Team RC. R: A Language and environment for statistical computing. Vienna, Austria: R Foundation for Statistical Computing; 2013.

27. Lin SM, Du P, Huber W, Kibbe WA. Model-based variance-stabilizing transformation for Illumina microarray data. Nucleic Acids Res. 2008;36(2):e11.

28. Du P, Kibbe WA, Lin SM. lumi: a pipeline for processing Illumina microarray. Bioinformatics. 2008;24(13):1547-1548.

29. Lepidi S, Kenagy RD, Raines EW, et al. MMP9 production by human monocyte-derived macrophages is decreased on polymerized type I collagen. Journal of Vascular Surgery. 2001;34(6):1111-1118.

30. White FJ, Burghardt RC, Hu J, Joyce MM, Spencer TE, Johnson GA. Secreted phosphoprotein 1 (osteopontin) is expressed by stromal macrophages in cyclic and pregnant endometrium of mice, but is induced by estrogen in luminal epithelium during conceptus attachment for implantation. Reproduction. 2006;132(6):919-929.

31. Sierra-Filardi E, Nieto C, Domínguez-Soto Á, et al. CCL2 Shapes Macrophage Polarization by GM-CSF and M-CSF: Identification of CCL2/CCR2-Dependent Gene Expression Profile. The Journal of Immunology. 2014;192(8):3858-3867.

32. Buechler C, Ritter M, Orsó E, Langmann T, Klucken J, Schmitz G. Regulation of scavenger receptor CD163 expression in human monocytes and macrophages by pro- and antiinflammatory stimuli. Journal of Leukocyte Biology. 2000;67(1):97-103.

33. den Haan JM, Meadows LM, Wang W, et al. The minor histocompatibility antigen HA-1: a diallelic gene with a single amino acid polymorphism. Science. 1998;279(5353):1054-1057.

34. Wilke M, Dolstra H, Maas F, et al. Quantification of the HA-1 gene product at the RNA level; relevance for immunotherapy of hematological malignancies. Hematol J. 2003;4(5):315-320.

35. Pont MJ, Hobo W, Honders MW, et al. LB-ARHGDIB-1R as a novel minor histocompatibility antigen for therapeutic application. Haematologica. 2015;100(10):e419-422.

36. Van Bergen CAM, Rutten CE, Van Der Meijden ED, et al. High-throughput characterization of 10 new minor histocompatibility antigens by whole genome association scanning. Cancer Res. 2010;70(22):9073-9083.

37. Pont MJ, van der Lee DI, Van Der Meijden ED, et al. Integrated whole genome and transcriptome analysis identified a therapeutic minor histocompatibility antigen in a splice variant of ITGB2. Clin Cancer Res. 2016.

38. Jongeneel CV, Delorenzi M, Iseli C, et al. An atlas of human gene expression from massively parallel signature

sequencing (MPSS). Genome Research. 2005;15(7):1007-1014.

39. Jahn L, Hombrink P, Hassan C, et al. Therapeutic targeting of the BCR-associated protein CD79b in a TCR-based approach is hampered by aberrant expression of CD79b. Blood. 2015;125(6):949-958.

40. Berger C, Sommermeyer D, Hudecek M, et al. Safety of targeting ROR1 in primates with chimeric antigen receptor-modified T cells. Cancer Immunol Res. 2015;3(2):206-216.

41. Hudecek M, Schmitt TM, Baskar S, et al. The B-cell tumor-associated antigen ROR1 can be targeted with T cells modified to express a ROR1-specific chimeric antigen receptor. Blood. 2010;116(22):4532-4541.

Supplemental Reference list

1. Griffioen M, Honders MW, van der Meijden ED, et al. Identification of 4 novel HLA-B*40:01 restricted minor histocompatibility antigens and their potential as targets for graft-versus-leukemia reactivity. Haematologica. 2012;97(8):1196-1204.
2. Stumpf AN, van der Meijden ED, van Bergen CA, Willemze R, Falkenburg JH, Griffioen M. Identification of 4 new HLA-DR-restricted minor histocompatibility antigens as hematopoietic targets in antitumor immunity. Blood. 2009;114(17):3684-3692.
3. van Kooten C, Gerritsma JS, Paape ME, van Es LA, Banchereau J, Daha MR. Possible role for CD40-CD40L in the regulation of interstitial infiltration in the kidney. Kidney Int. 1997;51(3):711-721.
4. Gao L, van Nieuwpoort FA, Out-Luiting JJ, et al. Genome-Wide Analysis of Gene and Protein Expression of Dysplastic Naevus Cells. Journal of Skin Cancer. 2012;2012:13.
5. Amatngalim GD, van Wijck Y, de Mooij-Eijk Y, et al. Basal cells contribute to innate immunity of the airway epithelium through production of the antimicrobial protein RNase 7. J Immunol. 2015;194(7):3340-3350.
6. Jaffe EA, Nachman RL, Becker CG, Minick CR. Culture of human endothelial cells derived from umbilical veins. Identification by morphologic and immunologic criteria. J Clin Invest. 1973;52(11):2745-2756.
7. van Essen TH, van Zijl L, Possemiers T, et al. Biocompatibility of a fish scale-derived artificial cornea: Cytotoxicity, cellular adhesion and phenotype, and in vivo immunogenicity. Biomaterials. 2016;81:36-45.
8. Sato T, Stange DE, Ferrante M, et al. Long-term expansion of epithelial organoids from human colon, adenoma, adenocarcinoma, and Barrett's epithelium. Gastroenterology. 2011;141(5):1762-1772.
9. Stevanovic S, Nijmeijer BA, van Schie ML, et al. Donor T Cells Administered Over HLA Class II Barriers Mediate Antitumor Immunity without Broad Off-Target Toxicity in a NOD/Scid Mouse Model of Acute Leukemia. Biol Blood Marrow Transplant. 2013;19(6):867-875.

3

Haematologica 2013

LB-ARHGDIB-1R AS NOVEL MINOR HISTOCOMPATIBILITY ANTIGEN FOR THERAPEUTIC APPLICATION

Margot J. Pont[1], Willemijn Hobo[2], Maria W. Honders[1], Simone A.P. van Luxemburg-Heijs[1], Michel G.D. Kester[1], Annemarie M. van Oeveren-Rietdijk[3], Nicolaas Schaap[4], Hetty C. de Boer[3], Cornelis A.M. van Bergen[1], Harry Dolstra[2], J.H.Frederik Falkenburg[1] and Marieke Griffioen[1].

[1] Department of Hematology, Leiden University Medical Center, Leiden, the Netherlands

[2] Department of Laboratory Medicine, Radboud University Medical Center, Nijmegen, the Netherlands

[3] Department of Nephrology and the Einthoven Laboratory for Experimental Vascular Medicine, Leiden University Medical Center, Leiden, The Netherlands

[4] Department of Hematology, Radboud University Medical Center, Nijmegen, the Netherlands

3

Letter to the Editor

In HLA-matched allogeneic hematopoietic stem cell transplantation, donor T cells can mediate graft-versus-leukemia/lymphoma (GvL) reactivity and graft-versus-host disease (GvHD) by recognition of minor histocompatibility antigens (MiHA)[1-4]. Only a minority of MiHA shows hematopoiesis-restricted expression, and donor T cells for these MiHA may induce beneficial GvL reactivity without GvHD. The number of well-characterized MiHA with therapeutic relevance based on hematopoiesis-restricted expression remains limited and only 25% and 40% of recipients transplanted with sibling and unrelated donors, respectively, are eligible for therapies targeting known hematopoietic MiHA[3,4]. Therefore, to increase efficacy and applicability of cellular therapy for selective GvL induction, more hematopoiesis-restricted MiHA with balanced population frequencies in common HLA molecules must be identified. Here, we investigated the therapeutic significance of a MiHA encoded by *ARHGDIB*[5]. We demonstrated hematopoiesis-restricted gene expression with the exception of intermediate mRNA expression in endothelial cells and showed that T cells recognized LB-ARHGDIB-1R presented by HLA-B*07:02 on primary leukemic cells, but not on (IFN-γ treated) fibroblasts (FB) and keratinocytes (KC). To evaluate potential toxicity against endothelial cells, we tested T-cell recognition of LB-ARHGDIB-1R on human umbilical vein endothelial cells (HUVEC) and found only limited reactivity under inflammatory conditions. Furthermore, we demonstrated *in vivo* targeting of LB-ARHGDIB-1R in 8 out of 10 patients who were screened for post-transplant specific T-cell responses. In one patient with relapsed lymphoma, high T-cell frequencies were induced after donor lymphocyte infusion (DLI) coinciding with long-lasting anti-lymphoma immunity without GvHD. Our data thus support the relevance of LB-ARHGDIB-1R as therapeutic target with potential to induce selective GvL reactivity.

We previously demonstrated that CD8 T cells specific for a MiHA (LB-ARHGDIB-1R) encoded by the *ARHGDIB* gene were induced in a patient with myelodysplastic syndrome who responded to DLI after HLA-matched alloSCT[5]. LB-ARHGDIB-1R is translated from the normal *ARHGDIB* transcript (NM_001175) in an alternative reading frame. Since *ARHGDIB* has been described to be expressed in hematopoietic cells[6,7], we investigated the therapeutic value of LB-ARHGDIB-1R to stimulate GvL reactivity after alloSCT without GvHD. We first examined *ARHGDIB* expression by microarray gene expression analysis using Illumina HT-12 v3/4 BeadChips[8] and compared gene expression between (malignant) hematopoietic and non-hematopoietic cells, which were cultured in the absence or presence of IFN-γ to mimic inflammation. *ARHGDIB* showed strong overexpression in the majority of (malignant) hematopoietic *versus* (IFN-γ pre-treated) non-hematopoietic cells. The *ARHGDIB* expression profile

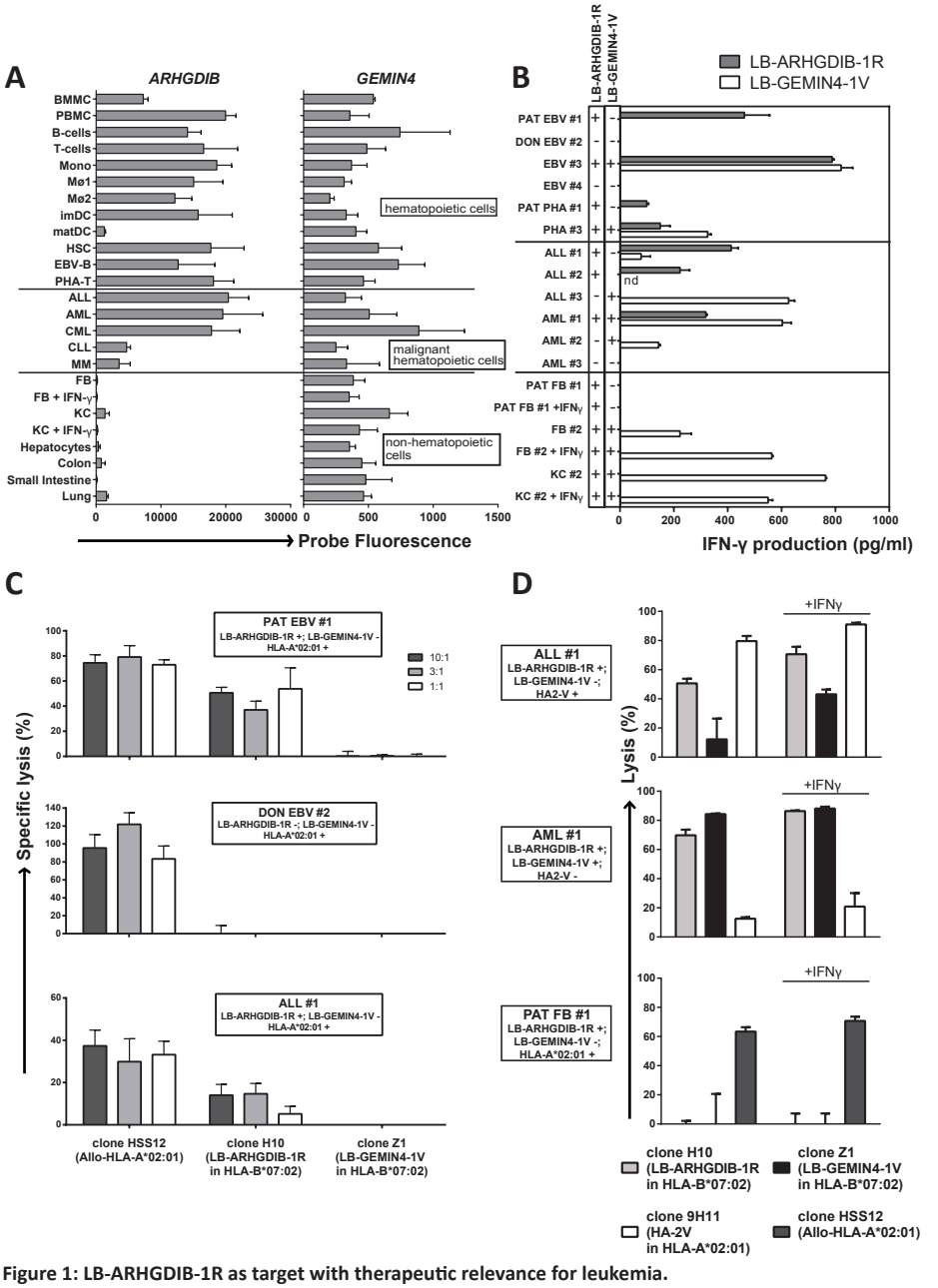

Figure 1: LB-ARHGDIB-1R as target with therapeutic relevance for leukemia.

(A) Expression profiles for *ARHGDIB* and *GEMIN4* as determined by microarray gene expression analysis. *GEMIN4* has been selected as representative gene for MiHA with ubiquitous expression on (non-) hematopoietic cells[5]. Indicated is the probe fluorescence as measured on Illumina Human HT-12 v3/4 BeadChips[8]. Hematopoietic cells included bone marrow and peripheral blood mononuclear cells (BMMC and PBMC), B cells, T cells, monocytes (Mono), macrophages type I and II (MØ1 and MØ2), (im)mature DC (imDC and matDC), hematopoietic stem cells (HSC), EBV-B and PHA-T cells. Malignant hematopoietic cells included acute lymphoblastic leukemia (ALL), acute myeloid leukemia (AML), chronic myeloid leukemia (CML), chronic lymphocytic leukemia (CLL) and multiple myeloma (MM). Non-hematopoietic cells included fibroblasts (FB) and keratinocytes (KC) cultured from skin biopsies in the absence or presence of IFN-γ and hepatocytes, colon and small intestine epithelial cells and lung epithelial cells.

was comparable to the strictly hematopoietic *HMHA1* and *MYO1G* (Figure 1A and data not shown).

Next, we investigated T-cell recognition of different leukemic samples and both primary FB and KC cultured from skin biopsies in the absence or presence of IFN-γ. Samples were collected from patients and healthy individuals after approval by the Leiden or Radboud UMC Institutional Review Board and informed consent according to the Declaration of Helsinki. Recognition of (non-)hematopoietic cell types by LB-ARHGDIB-1R specific T cells was measured by IFN-γ ELISA after overnight co-incubation. The data confirmed hematopoiesis-restricted T-cell recognition of LB-ARHGDIB-1R in HLA-B*07:02 on all MiHA-positive leukemic cells, but not on (IFN-γ pre-treated) FB and KC (Figure 1B). T cells for LB-ARHGDIB-1R were also shown to recognize healthy hematopoietic cell types, including EBV-B, PHA-T and dendritic cells (Figure 1B and data not shown), indicating that alternative translation of LB-ARHGDIB-1R is not restricted to malignant cells. T cells for LB-ARHGDIB-1R also showed specific lysis of patient, but not donor, EBV-B cells and specific lysis of a leukemic sample (ALL #1) in a 10 h ^{51}Cr-release assay (Figure 1C). Lysis of other ALL and AML samples was not detected by ^{51}Cr-release, but could be measured after 48 h co-incubation in a flow cytometry-based cytotoxicity assay, while (IFN-γ pre-treated) patient FB were not lysed (Figure 1D and data not shown). The data showed that T cells for LB-ARHGDIB-1R can specifically lyse hematological malignancies of different origins.

In addition to hematopoietic cells, *ARHGDIB* can also be expressed in endothelial

B-D) Recognition and lysis of (non-)hematopoietic cells as mediated by T cells for LB-ARHGDIB-1R (clone H10)[5]. All samples were positive for HLA-B*07:02. Cell types included EBV-B and PHA-T cells from patient (PAT EBV #1 and PHA #1) or donor (DON EBV #2) origin or from third party individuals (EBV #3, EBV #4 and PHA #3) as well as primary ALL (ALL #1-3) and AML (AML #1-3) samples. One representative example of two independent experiments is shown.

(B) Recognition of LB-ARHGDIB-1R in HLA-B*07:02 as expressed on (malignant) hematopoietic cells, but not on (IFN-γ pre-treated) FB and KC. Malignant cells were isolated by flow cytometry cell sorting based on CD19 (ALL) or CD33 (AML) expression. T cells for LB-GEMIN4-1V (clone Z1) were included as positive control. Genotyping results (+ or -) for the SNPs encoding LB-ARHGDIB-1R (filled bars) and LB-GEMIN4-1V (gray bars) are shown. Mean release of IFN-γ of duplicate wells as measured by ELISA after overnight co-incubation of T cells and stimulator cells at a ratio of 1:6 is depicted.

(C) Cytolysis of primary leukemic blasts as mediated by T cells for LB-ARHGDIB-1R in a ^{51}Cr-release assay. Target cells ($1x10^3$) labeled with $Na_2{}^{51}CrO_4$ (Perkin Elmer, Waltham, MA, USA) were co-incubated with T cells for 10 hours (h) at effector:target ratios of 10:1, 3:1 and 1:1. Mean specific lysis of triplicate wells is shown for patient and donor EBV-B (upper and middle graphs, respectively) and ALL #1 expressing LB-ARHGDIB-1R and HLA-B*07:02 (lower graph). Patient and donor EBV-B and ALL #1 were positive for HLA-A*02:01 and negative for LB-GEMIN4-1V. Allo-HLA-A*02:01 reactive T cells (clone HSS12) and T cells for LB-GEMIN4-1V were included as controls.

(D) Cytolysis of primary leukemic blasts and patient FB as mediated by T cells for LB-ARHGDIB-1R in a 48 h flow cytometry-based cytotoxicity assay. T cells ($2.5x10^4$) were labeled with PKH67 (Sigma-Aldrich, St. Louis, MO, USA) and co-incubated for 48 h with AML or ALL samples or FB cultured from a skin biopsy of the patient in the absence or presence of IFN-γ ($1x10^4$). After co-incubation, cultures were stained with CD33-APC (AML), CD19-PE (ALL) or CD90-PE (FB). Sytox blue was added to gate on viable cells and flow count fluorospheres (Beckman Coulter, Brea, CA, USA) were added to calculate specific lysis. T cells recognizing HA-2 in HLA-A*02:01 (clone 9H11), T cells for LB-GEMIN4-1V and allo-HLA-A*02:01 reactive T cells were included as controls. Mean lysis of triplicate wells is depicted.

cells[9]. We therefore addressed potential toxicity and measured T-cell reactivity against endothelial cells. We confirmed intermediate *ARHGDIB* gene expression in HUVEC under both steady-state and inflammatory conditions by microarray gene expression analysis (Figure S1A, upper panel). Increased *ARHGDIB* mRNA expression in HUVEC as compared to FB was also detectable by q-PCR (see supplemental methods) (Figure S1A, lower panel). To investigate whether gene expression in HUVEC can lead to T-cell recognition, we measured reactivity against two LB-ARHGDIB-1R positive HUVEC samples by IFN-γ ELISA. T cells for LB-ARHGDIB-1R were only capable of recognizing one HUVEC sample (#2) after IFN-γ pre-treatment, which is known to up-regulate HLA, co-stimulatory and adhesion molecules and to increase the antigen processing and presentation capacity (Figure S1B)[10,11]. However, recognition of HUVEC #2 was low compared to EBV-B cells and (IFN-γ pre-treated) HUVEC #1 was not or hardly recognized by specific T cells. Altogether, we demonstrate that *ARHGDIB* gene expression in HUVEC leads to low surface presentation of LB-ARHGDIB-1R that trigger only minimal T-cell reactivity under inflammatory conditions. Our results thus support the value of LB-ARHGDIB-1R as target for T-cell therapy to selectively augment GvL reactivity after alloSCT with a limited risk for GvHD.

Finally, we determined the *in vivo* immunogenicity of LB-ARHGDIB-1R and investigated its relevance as T-cell target in clinical responses after alloSCT. The population frequency of LB-ARHGDIB-1R in Caucasians is 77% (www.hapmap.org), resulting in a disparity rate in which a LB-ARHGDIB-1R positive patient is transplanted with a negative donor of 18%. HLA-B*07:02 is expressed in approximately 20% of Caucasians[12]. In our cohort of 93 HLA-B*07:02 patient-donor pairs, 14 LB-ARHGDIB-1R positive patients were transplanted with a MiHA-negative donor and samples at relevant time points were available for 10 patients. PBMC were stained with APC- and PE-conjugated HLA-B*07:02 tetramers containing LB-ARHGDIB-1R directly *ex vivo* as well as after 7 days of *in vitro* peptide stimulation as previously described[13]. PBMC obtained after alloSCT (and DLI) were analyzed for tetramer positive T cells, and LB-ARHGDIB-1R specific T cells were detected in 4 patients *ex vivo* (Figure 2A) and in 4 additional patients after *in vitro* peptide stimulation (Figure 2B), resulting in 8 of 10 patients (80%) in total.

All patients were treated with partial T-cell depleted alloSCT followed by at least 4 months of immunosuppression with cyclosporin A as GvHD prophylaxis. Six of 10 patients received DLI after alloSCT (Table S1). In 3 of 6 patients treated with DLI, tetramer positive T cells were detected *ex vivo* at frequencies between 0.06-0.92%. Five patients received prophylactic DLI, and a clinical response against (malignant) hematopoietic cells of patient origin could therefore not be monitored. Patient 5 with relapsed follicular lymphoma, which was confirmed

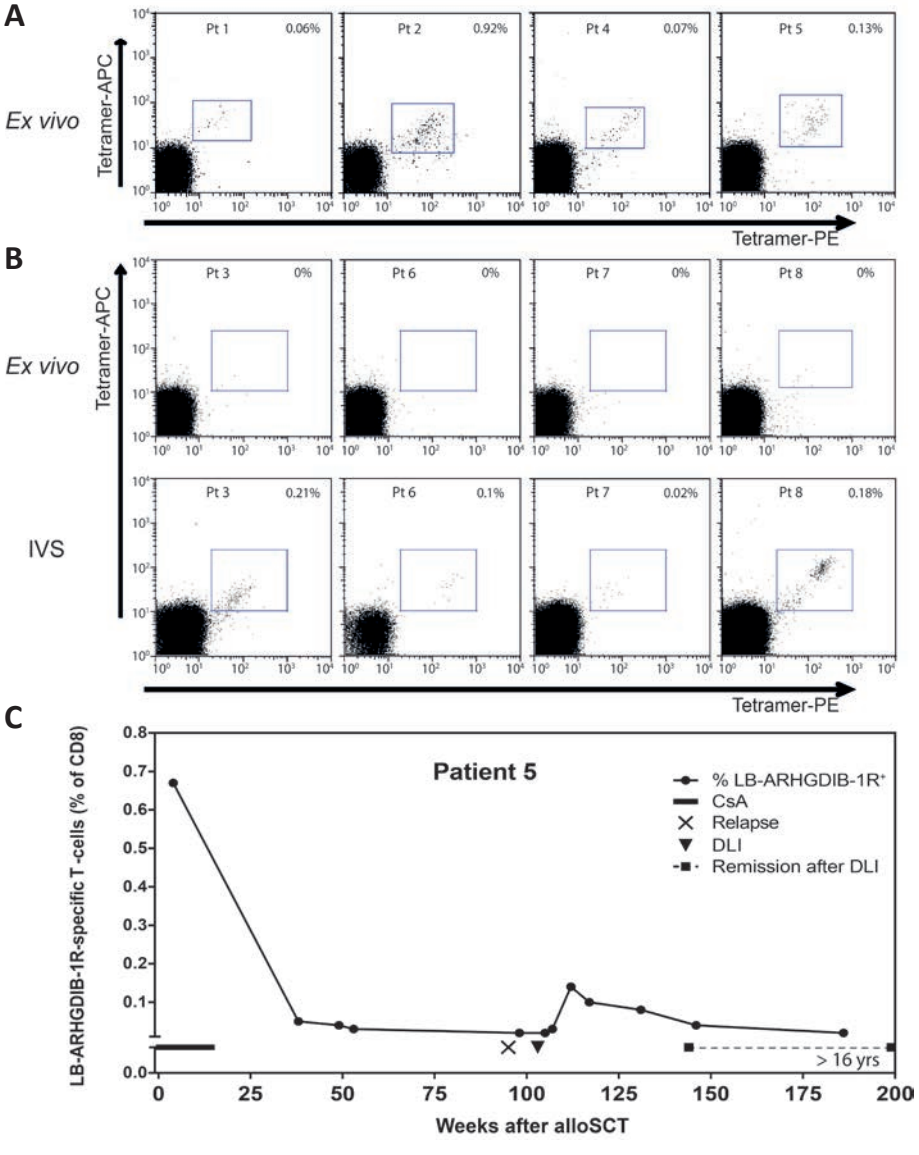

Figure 2: LB-ARHGDIB-1R as immunogenic target with relevance for GvL reactivity.

PBMC from 10 LB-ARHGDIB-1R and HLA-B*07:02 positive patients transplanted with HLA-matched negative donors were screened for LB-ARHGDIB-1R specific CD8 T cells directly *ex vivo* as well as after one week of *in vitro* peptide stimulation (IVS)[13].

(A) Patients with detectable LB-ARHGDIB-1R tetramer positive T cells *ex vivo*. Numbers indicate the percentage of CD8 T cells that are positive for both LB-ARHGDIB-1R tetramers (PE and APC) in the Sytox blue^{neg}, CD8^{pos}, CD4^{neg}, CD14^{neg}, CD16^{neg}, and CD19^{neg} T-cell population.

(B) Dot plots of patients with detectable LB-ARHGDIB-1R tetramer positive T cells after *in vitro* peptide stimulation: day 0 (upper panels) and day 7 (lower panels). Numbers indicate the percentage of CD8 T cells that are positive for both LB-ARHGDIB-1R tetramers (PE and APC).

(C) *Ex vivo* frequencies of LB-ARHGDIB-1R specific T cells and clinical response in patient 5 who was treated with DLI in the absence of additional (chemo) therapy for relapsed lymphoma after partial T-cell depleted alloSCT.

by lymph node biopsy, received therapeutic DLI that in the absence of additional (chemo-)therapy induced a long-lasting complete remission (>16 yrs) without any signs of GvHD. T cells for LB-ARHGDIB-1R were measured in 3 patients with GvHD after DLI (patients 2, 6 and 7). These T cells were detectable *ex vivo* (0.92%) in patient 2 and after *in vitro* stimulation in the other two patients. Although it cannot be excluded that T cells for LB-ARHGDIB-1R may have contributed to GvHD in these patients, we consider it more likely that T cells with other specificities mediated GvHD, since we previously demonstrated that often a variety of MiHA are targeted in patients with GvHD[5,14] and that the majority of these MiHA are ubiquitously expressed on (non-)hematopoietic tissues. This is further supported by the observation that T cells for LB-ARHGDIB-1R were also measured *ex vivo* (0.13%) in patient 5. Induction of tetramer positive T cells in this patient two months after DLI coincided with long-lasting GvL reactivity without GvHD. Dynamic analysis of LB-ARHGDIB-1R tetramer positive T cells in this patient demonstrated high frequencies not only after DLI, but also within the first weeks after alloSCT during immunosuppression with cyclosporin A (Figure 2C). Although the long-lasting GvL response in patient 5 suggests that LB-ARHGDIB-1R specific T cells are capable of mediating strong anti-tumor immunity, T cells with other specificities than LB-ARHGDIB-1R may also be involved in the therapeutic effect of DLI. Systemic toxicity as a result of vascular damage has not been observed in any of the patients with circulating LB-ARHGDIB-1R specific T cells. Thus, clinical observations support the therapeutic value of LB-ARHGDIB-1R and do not show evidence for specific attack of endothelial cells as might be suggested based on detectable *ARHGDIB* gene expression and low T-cell recognition of endothelial cells *in vitro*.

In conclusion, our data support the relevance of LB-ARHGDIB-1R as highly immunogenic and hematopoiesis-restricted MiHA with potential to shift the delicate balance between GvL reactivity and GvHD in favor of desired anti-tumor reactivity. At the Radboud UMC, we started a clinical trial in which transplanted patients are vaccinated with donor DC loaded with mRNA and included *ARHGDIB* as one of the transcripts for hematopoiesis-restricted MiHA (Dutch Trial Registry #NTR4128). Future clinical data will therefore show definite evidence whether T cells for LB-ARHGDIB-1R are capable of inducing selective GvL responses. In addition to hematopoietic cells, *ARHGDIB* has been reported to be expressed in several solid tumors correlating with advanced tumor stage and metastatic potential[15]. As such, LB-ARHGDIB-1R may have broad value as target for T-cell therapy to treat hematological malignancies and solid tumors after alloSCT.

Acknowledgments

The authors would like to thank Cynthia Kramer (Radboud UMC) for tetramer analyses and cell culture, and Martijn Dane (Department of Nephrology and the Einthoven Laboratory of Experimental Vascular Medicine, Leiden University Medical Center, Leiden, The Netherlands) for isolation of HUVEC.

Supplemental methods:

Cell samples and culture

Human umbilical vein endothelial cells (HUVEC) were isolated from umbilical cords according to Jaffe et al.[1] using a cannula sized to fit the vein. HUVEC were cultured up to passage 4 in EGM-2 medium supplemented with the EGM-2 bullet kit (Lonza BioWhittaker, Basel, Switzerland) and refreshed every 3 days. Fibroblasts (FB), keratinocytes (KC) and HUVEC were cultured in the absence or presence of 200 IU/ml IFN-γ (Boehringer-Ingelheim, Ingelheim am Rhein, Germany) for 3 days. Retroviral transduction of the HLA-B*07:02 restriction allele was performed as described previously[2].

Quantitative RT-PCR

Expression of *ARHGDIB* mRNA was measured by quantitative real-time PCR using Taqman Universal Master Mix II, without UNG and Taqman gene expression assays for *ARHGDIB* (Hs00171288_m1) and normalized as a ratio of *GAPDH* (Hs99999905_m1) expression (all from Applied Biosystems, Life Technologies, Carlsbad, CA, USA). Amplifications were started with 10 minutes at 95°C, followed by 50 cycles of 15 seconds for denaturing at 95°C, 30 seconds of annealing at 60°C, and 30 seconds extension at again 60°C.

Figure S1: LB-ARHGDIB-1R as target with potential toxicity for endothelial cells

(A) *ARHGDIB* gene expression in FB and HUVEC relative to EBV-B cells by microarray gene expression analysis (upper panel) and quantitative RT-PCR (q-PCR; lower panel). FB and HUVEC were cultured in the absence or presence of IFN-γ. Gene expression by q-PCR was corrected for *GAPDH* expression.

(B) Reactivity of LB-ARHGDIB-1R specific T cells (clone H10) against HUVEC by IFN-γ ELISA. LB-ARHGDIB-1R positive HUVEC #1 and #2 were retrovirally transduced with HLA-B*07:02 (B7td) and cultured in the absence (upper panel) or presence (lower panel) of IFN-γ. LB-ARHGDIB-1R negative HUVEC #3 expressing HLA-B*07:02 endogenously (B7pos) and after retroviral introduction (B7td) were included as negative controls. T-cell reactivity was also measured against EBV-B cells and FB of patient origin expressing HLA-B*07:02 endogenously (PAT EBV and FB) as well as EBV-B cells and FB from patient HDV expressing HLA-B*07:02 after retroviral transduction (HDV EBV-B7td and FB-B7td). EBV-B cells of donor origin (DON EBV) and EBV-B cells from LB-ARHGDIB-1R negative patient MAE expressing HLA-B*07:02 after retroviral transduction (MAE EBV-B7td) were included as negative controls. In addition to LB-ARHGDIB-1R specific T cells (clone H10), T cells for LB-GEMIN4-1V (clone Z1) and allo-HLA-A*02:01 (clone HSS12) were included. Genotyping results (+ or-) for SNPs encoding LB-ARHGDIB-1R (filled bars), LB-GEMIN4-1V (grey bars) and HLA-A*02:01 (open bars) are shown. Mean release of IFN-γ of duplicate wells is shown.

(C) LB-ARHGDIB-1R negative MAE EBV-B7td as well as LB-ARHGDIB-1R positive HDV FB-B7td and HUVEC #2-B7td were cultured in the absence of IFN-γ and pulsed with exogenous LB-ARHGDIB-1R at titrated peptide concentrations. These cells were subsequently compared for their capacity to stimulate T cells for LB-ARHGDIB-1R (clone H10) by IFN-γ ELISA (left panel). In addition, LB-ARHGDIB-1R negative HUVEC #3 B7pos and B7td were cultured in the absence of IFN-γ and compared for their stimulatory capacity (middle panel) as well as LB-ARHGDIB-1R positive HUVEC #2 B7td cultured in the absence or presence of IFN-γ (right panel). Mean release of IFN-γ of duplicate wells is shown.

(D) HLA-B*07:02 surface expression on EBV-B, FB and HUVEC B7pos or B7td by flow cytometry. FB and HUVEC were cultured in the presence of IFN-γ and stained with a PE-labeled antibody against HLA-B*07:02 (clone BB7.1). HLA-B*07:02 surface expression is shown by dark grey histograms. Light grey histograms represent non-stained EBV-B, FB and HUVEC and open histograms indicate antibody staining of EBV-B, FB and HUVEC that are negative for HLA-B*07:02.

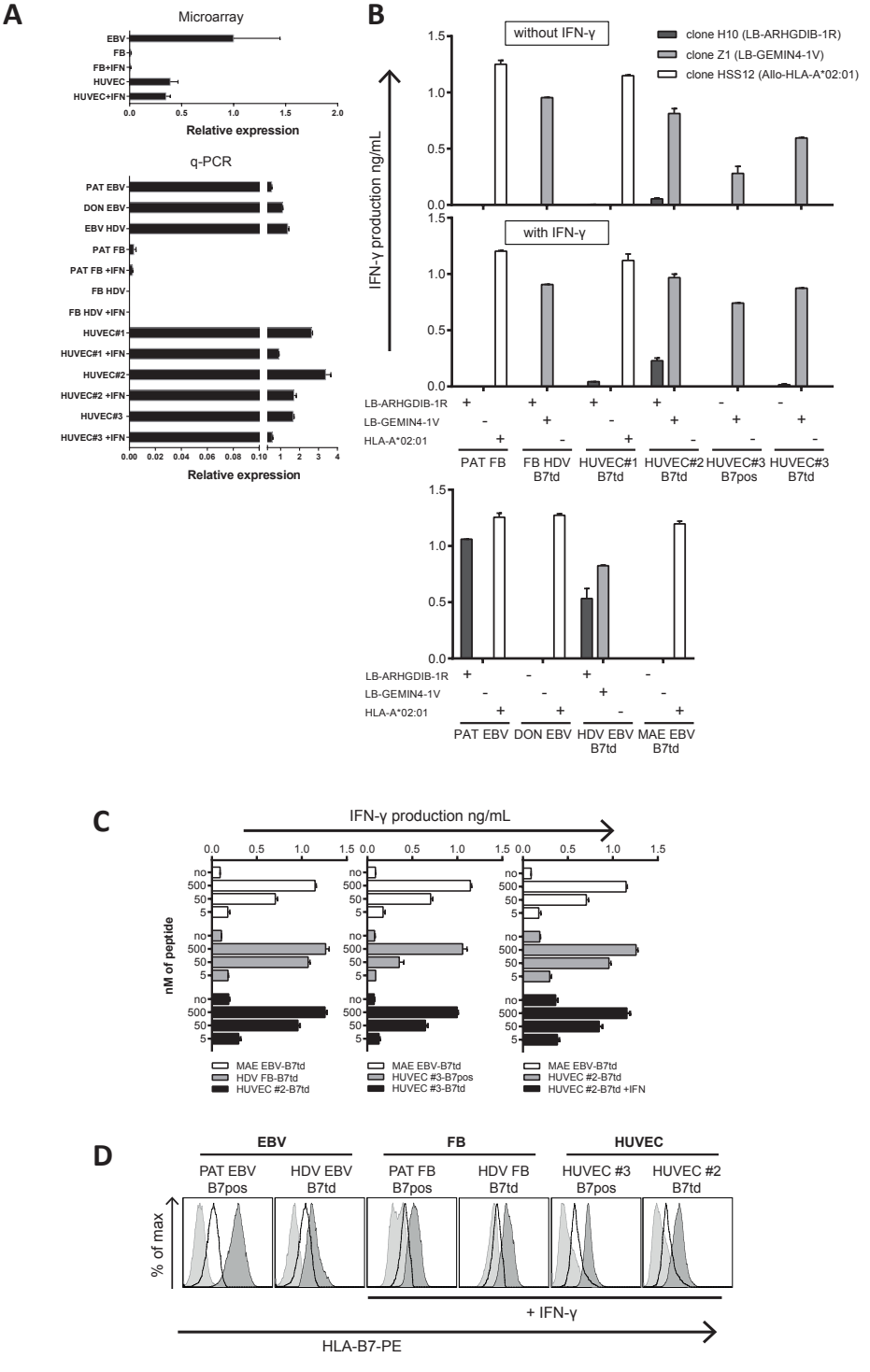
A
Microarray
EBV
FB
FB+IFN
HUVEC
HUVEC+IFN
Relative expression
q-PCR
PAT EBV
DON EBV
EBV HDV
PAT FB
PAT FB +IFN
FB HDV
FB HDV +IFN
HUVEC#1
HUVEC#1 +IFN
HUVEC#2
HUVEC#2 +IFN
HUVEC#3
HUVEC#3 +IFN
Relative expression
B
without IFN-γ
with IFN-γ
clone H10 (LB-ARHGDIB-1R)
clone Z1 (LB-GEMIN4-1V)
clone HSS12 (Allo-HLA-A*02:01)
IFN-γ production ng/mL
LB-ARHGDIB-1R
LB-GEMIN4-1V
HLA-A*02:01
PAT FB
FB HDV B7td
HUVEC#1 B7td
HUVEC#2 B7td
HUVEC#3 B7pos
HUVEC#3 B7td
PAT EBV
DON EBV
HDV EBV B7td
MAE EBV B7td
C
IFN-γ production ng/mL
nM of peptide
MAE EBV-B7td
HDV FB-B7td
HUVEC #2-B7td
HUVEC #3-B7pos
HUVEC #3-B7td
HUVEC #2-B7td +IFN
D
EBV
FB
HUVEC
PAT EBV B7pos
HDV EBV B7td
PAT FB B7pos
HDV FB B7td
HUVEC #3 B7pos
HUVEC #2 B7td
% of max
+ IFN-γ
HLA-B7-PE

Supplemental results:

To investigate whether gene expression in HUVEC leads to surface presentation of LB-ARHGDIB-1R at levels that can be recognized by specific T cells, we cultured LB-ARHGDIB-1R positive HUVEC #1 and #2 and measured T-cell recognition by IFN-γ ELISA after retroviral introduction of the HLA-B*07:02 restriction allele. Figure S1B shows that T cells for LB-ARHGDIB-1R were only capable of recognizing HUVEC #2 after IFN-γ pre-treatment, which is known to enforce high expression of HLA, co-stimulatory and adhesion molecules as well as molecules involved in antigen processing and presentation[3, 4]. However, recognition of HUVEC #2 was low as compared to EBV-B cells and (IFN-γ pre-treated) HUVEC #1 was not or hardly recognized by specific T cells. Peptide-loaded control experiments (Figure S1C) illustrated that HLA-B*07:02 surface expression on HUVEC was sufficient to mediate strong T-cell reactivity, which is in line with detection of these surface molecules by flow cytometry (Figure S1D). Altogether, the data demonstrate that *ARHGDIB* gene expression in HUVEC leads to low surface presentation of LB-ARHGDIB-1R at levels that trigger only minimal T-cell reactivity under inflammatory conditions. Our results thus support the value of LB-ARHGDIB-1R as target for T-cell therapy to selectively augment GvL reactivity after alloSCT with a limited risk for GvHD.

Table S1: Clinical data patients

patient	sex	diagnosis[a]	sample[b]	T cell response		acute GvHD after SCT (<100 days)[c]	chronic GvHD after SCT (>100 days)[d]	relapse after SCT	DLI after SCT[e]	GvHD after DLI[f]	total FU (years)	disease status
				ex vivo	*in vitro* stimulation							
1	F	AML-M2	6 m post-DLI	0.06%	0.09%	grade I (at d15)	no	no	prophylactic DLI (at 8 m)	no	10.0	remission
2	M	AML-M1	1 m post-DLI	0.92%	9.19%	no	no	no	prophylactic DLI (at 6 m)	grade II (at d46)	9.6	remission
3	F	AML-M2	3 m post-SCT	<0.01%	0.21%	no	limited (at d132)	no	no	-	6.4	remission
4	M	AML-M1	6 m post-SCT	0.07%	0.64%	grade I (at d23)	extensive (at d125)	no	no	-	13.0	remission
5	F	FL grade 2	2 m post-DLI	0.13%	1.31%	no	no	yes (at 22 m)	therapeutic DLI (at 24 m)	no	19.6	remission
6	F	AML-M5	6 m post-DLI	<0.01%	0.10%	no	no	no	prophylactic DLI (at 4 m)	extensive (at d372)	2.5	deceased due to GVHD
7	M	pro-B ALL	2 m post-DLI	<0.01%	0.02%	no	no	no	prophylactic DLI (at 6 m)	grade IV (at d69)	13.0	remission
8	F	AML	52 m post-DLI	<0.01%	0.18%	no	no	no	prophylactic DLI (at 8 m)	no	7.1	remission
9	F	AML-M2	3 m post-SCT	no	no	grade I (at d13)	no	no	no	-	18	remission
10	M	CLL	2 m post-SCT	no	no	grade III (at d26)	limited (at d149)	no	no	-	6.3	remission

[a] Diagnosis according to WHO classification. AML: acute myeloid leukemia; FL: follicular lymphoma; ALL: acute lymphoblastic leukemia, CLL: chronic lymphocytic leukemia, MDS: myelodysplastic syndrome.

[b] Peripheral blood samples for T-cell analysis have been collected at different time points after SCT or DLI. Time points are indicated in months (m) post-SCT or post-DLI.

[c] Acute GvHD was graded according to the criteria of Przepiorka et al. (Bone Marrow Transplant 1995). The time of diagnosis is indicated in days (d) after SCT.

[d] Chronic GvHD was classified according to the revised Seattle criteria of Lee et al. (Biol. Blood Marrow Transplant 2003). The time of diagnosis is indicated in days (d) after SCT.

[e] DLI was administered to prevent (prophylactic) or treat (therapeutic) relapse of the disease. The time of DLI is indicated in months (m) after SCT.

[f] GvHD was graded as in [c] (acute) or in [d] (chronic) The time of diagnosis is indicated in days (d) after DLI.

Reference list

1. Kolb HJ. Graft-versus-leukemia effects of transplantation and donor lymphocytes. Blood. 2008;112(12):4371-4383.
2. Bleakley M, Riddell SR. Exploiting T cells specific for human minor histocompatibility antigens for therapy of leukemia. Immunol Cell Biol. 2011;89(3):396-407.
3. Warren EH, Zhang XC, Li S, et al. Effect of MHC and non-MHC donor/recipient genetic disparity on the outcome of allogeneic HCT. Blood. 2012;120(14):2796-2806.
4. Spierings E, Hendriks M, Absi L, et al. Phenotype frequencies of autosomal minor histocompatibility antigens display significant differences among populations. PLoS Genet. 2007;3(6):e103.
5. Van Bergen CAM, Rutten CE, Van Der Meijden ED, et al. High-throughput characterization of 10 new minor histocompatibility antigens by whole genome association scanning. Cancer Res. 2010;70(22):9073-9083.
6. Lelias JM, Adra CN, Wulf GM, et al. cDNA cloning of a human mRNA preferentially expressed in hematopoietic cells and with homology to a GDP-dissociation inhibitor for the rho GTP-binding proteins. Proc Natl Acad Sci U S A. 1993;90(4):1479-1483.
7. Scherle P, Behrens T, Staudt LM. Ly-GDI, a GDP-dissociation inhibitor of the RhoA GTP-binding protein, is expressed preferentially in lymphocytes. Proc Natl Acad Sci U S A. 1993;90(16):7568-7572.
8. Kremer AN, van der Meijden ED, Honders MW, et al. Endogenous HLA class II epitopes that are immunogenic in vivo show distinct behavior toward HLA-DM and its natural inhibitor HLA-DO. Blood. 2012;120(16):3246-3255.
9. Theodorescu D, Sapinoso LM, Conaway MR, Oxford G, Hampton GM, Frierson HF, Jr. Reduced expression of metastasis suppressor RhoGDI2 is associated with decreased survival for patients with bladder cancer. Clin Cancer Res. 2004;10(11):3800-3806.
10. Fu H, Kishore M, Gittens B, et al. Self-recognition of the endothelium enables regulatory T-cell trafficking and defines the kinetics of immune regulation. Nat Commun. 2014;5:3436.
11. Ma W, Lehner PJ, Cresswell P, Pober JS, Johnson DR. Interferon-gamma rapidly increases peptide transporter (TAP) subunit expression and peptide transport capacity in endothelial cells. J Biol Chem. 1997;272(26):16585-16590.
12. Gonzalez-Galarza FF, Christmas S, Middleton D, Jones AR. Allele frequency net: a database and online repository for immune gene frequencies in worldwide populations. Nucleic Acids Res. 2011;39:D913-919.
13. Hobo W, Broen K, van der Velden WJ, et al. Association of disparities in known minor histocompatibility antigens with relapse-free survival and graft-versus-host disease after allogeneic stem cell transplantation. Biol Blood Marrow Transplant. 2013;19(2):274-282.
14. Griffioen M, Honders MW, van der Meijden ED, et al. Identification of 4 novel HLA-B*40:01 restricted minor histocompatibility antigens and their potential as targets for graft-versus-leukemia reactivity. Haematologica. 2012;97(8):1196-1204.
15. Cho HJ, Baek KE, Yoo J. RhoGDI2 as a therapeutic target in cancer. Expert Opinion on Therapeutic Targets. 2010;14(1):67-75.

Supplemental Reference list:

1. Jaffe EA, Nachman RL, Becker CG, Minick CR. Culture of human endothelial cells derived from umbilical veins. Identification by morphologic and immunologic criteria. J Clin Invest. 1973;52(11):2745-2756.
2. Heemskerk MH, Hoogeboom M, de Paus RA, et al. Redirection of antileukemic reactivity of peripheral T lymphocytes using gene transfer of minor histocompatibility antigen HA-2-specific T-cell receptor complexes expressing a conserved alpha joining region. Blood. 2003;102(10):3530-3540.
3. Fu H, Kishore M, Gittens B, et al. Self-recognition of the endothelium enables regulatory T-cell trafficking and defines the kinetics of immune regulation. Nat Commun. 2014;5:3436.
4. Ma W, Lehner PJ, Cresswell P, Pober JS, Johnson DR. Interferon-gamma rapidly increases peptide transporter (TAP) subunit expression and peptide transport capacity in endothelial cells. J Biol Chem. 1997;272(26):16585-1

4

To be submitted

MINOR HISTOCOMPATIBILITY ANTIGEN LB-TTK-1D IS ENCODED BY AN ALTERNATIVE TRANSCRIPT THAT IS DEGRADED BY NONSENSE MEDIATED DECAY

Margot J. Pont*[1], R. Oostvogels*[2], C.A.M. van Bergen[1], E.M. van der Meijden[1], H. Lokhorst[3], J.H.F. Falkenburg[1], T. Mutis[3], M. Griffioen[1], R.M. Spaapen[4]

[1] Department of Hematology, Leiden University Medical Center, Leiden, the Netherlands

[2] Department of Hematology, University Medical Center Utrecht, Utrecht, the Netherlands

[3] Department of Hematology, VU University Medical Center, Amsterdam, the Netherlands

[4] Department of Immunopathology, Sanquin Research and Landsteiner Laboratory, Amsterdam, the Netherlands

** both authors contributed equally.*

The identification of minor histocompatibility antigens (minor H Ag) is an important step towards understanding their immunobiology and therapeutic application. Specific induction of cytotoxic T-cell responses against hematopoiesis-restricted minor H Ags may represent an effective immunotherapy for hematological malignancies after allogeneic stem cell transplantation. Recently, we developed a novel identification strategy based on the 1000 Genomes Project and we now utilized a variation of this approach for identification of minor H Ag LB-TTK-1D, which could not be identified with previous whole genome association scanning studies. Using an 'inferred correlation' analysis based on the results of a previously executed whole genome association scanning analysis, we identified rs240226 to be the encoding genetic variation for this minor H Ag. Strikingly, this SNP is located in an alternative transcript of the gene *TTK*, containing a premature termination codon in the fourth of its five exons. This premature termination codon targets the transcript for nonsense mediated decay (NMD), leading to rapid degradation of the mRNA. This is the first identification of an endogenous T-cell epitope that is translated from an NMD transcript. Importantly, our T cells fail to recognize the majority of tumor cells that are positive for the minor H Ag, underscoring potential pitfalls of targeting NMD-derived epitopes as immunotherapeutic approach. Our finding can be useful for prospective minor H Ag identification studies and provides novel insights in the biology behind the source of transcripts producing antigenic epitopes in effective immune responses.

Introduction

Allogeneic stem cell transplantation (alloSCT) followed by donor lymphocyte infusion (DLI) is a potentially curative treatment for hematological malignancies. The therapeutic, so-called graft-versus-tumor (GvT) effect of alloSCT and DLI is mainly mediated by allo-reactive donor T cells recognizing minor histocompatibility antigens (minor H Ag) on the remaining tumor cells. Minor H Ags are immunogenic peptides, resulting from natural genetic variations, presented by HLA on recipient cells that can be recognized by alloreactive T-cells[1]. As minor H Ags are "non-self" to the transplanted immune system, donor T cells are capable of inducing potent responses against the malignant cells of the patient, while the new donor derived- and thus minor H Ag negative - cells are spared[2,3].

Clinical outcome in patients treated with alloSCT and DLI may, however, be threatened by the development of Graft-versus-Host disease (GvHD), which is caused by donor T cells recognizing minor H Ags on healthy tissues. Immunotherapy in which hematopoietic cell lineage restricted minor H Ags are specifically targeted may therefore provide or stimulate antitumor immunity without the risk for GvHD. For this purpose, the identification of hematopoiesis specific minor H Ags has been the focus of intensive research over the past decades, resulting in the development of increasingly efficient identification strategies[4,5]. Since natural genetic variation constitutes the basis of minor H Ags, genome-wide genetic correlation analyses whereby an association between the minor H Ag phenotype and the genotypes of the same individuals is sought, appears a highly efficient minor H Ag identification strategy[6]. Recently, we improved the genome-wide correlation analysis based identification strategies by implementing data of the 1000 Genomes Project (1000GP)[7,8]. We now used these data to pinpoint the encoding genetic variation of a minor H Ag for which we previously identified strongly correlating non-coding SNPs using the so-called whole genome association scanning (WGAs) analysis, but were unable to exactly identify the encoding variation[6]. This strategy led to identification of the new minor H Ag LB-TTK-1D, which is encoded by a SNP in the intron of the primary *TTK* transcript, but translated as non-synonymous coding variant in an alternative transcript that is degraded by nonsense-mediated decay (NMD)[9,10]. The discovery of this minor H Ag provides the first endogenous evidence that NMD transcripts can serve as a source of antigenic peptides. This finding improves our understanding of the biology behind epitope generation in effective immune responses[11,12].

Materials and Methods

Cell samples, culture conditions and isolation of T-cell clones

The CD8 minor H Ag-specific cytotoxic T-cell (CTL) clones 10-4 and 10-5, designated as clone type H4, recognizing LB-TTK-1D were generated as described previously[6]. In short, T cells were isolated from a patient with myelodysplastic syndrome (patient 5852) who converted to 100% donor chimerism after treatment with alloSCT and DLI. T-cell clones were generated by single cell sorting of HLA-DR CD8 positive cells by flow cytometry. T cells were cultured in IMDM supplemented with 5% FBS, 5% human serum, interleukin 2 (100 IU/mL), and re-stimulated every 14 days with irradiated allogeneic peripheral blood mononuclear cells (PBMC) and phytohemagglutinin (0.8 μg/mL, Murex Biotec Limited). PBMC and bone marrow mononuclear cells (BMMC) were obtained from patients and healthy individuals after approval by the Leiden UMC Institutional Review Board and informed consent according to the Declaration of Helsinki. Mononuclear cells were isolated by Ficoll-Isopaque separation and cryopreserved. Fibroblasts (FB), keratinocytes (KC), EBV-transformed B (EBV-LCL) cells, CD40L cultured B cells, PHA-T blasts and allo-HLA-A*02:01 reactive T cells (clone HSS12)[13] were cultured as described previously[14,15]. FB and KC were cultured in the absence or presence of 200 IU/ml IFN-γ (Boehringer Ingelheim, Alkmaar, the Netherlands) for 3 days.

Whole Genome Association scanning

Clone 10-5 was tested for recognition of 80 SNP-genotyped EBV-LCLs by IFN-γ ELISA. T-cell recognition was investigated for association with 1.1M SNPs by WGAs using Fisher's exact test as described previously[6].

1000 Genomes Project correlation analysis

We retrieved the genotypes for the highest associating SNP as identified by WGAs (rs608962) of 50 Caucasian (CEU) individuals from the 1000GP[16]. The probable minor H Ag phenotype for each of those individuals was inferred from these data and used to calculate which other SNPs on chromosome 6 (where rs608962 is located) correlated with the minor H Ag in the 50 Caucasian individuals using our previously described algorithm in R[8]. The top correlating SNPs were further analyzed for translational consequences using Ensembl (https://www.ensembl.org). Peptide HLA-binding predictions were made using the NetMHC 3.2 server[17].

Tetramer staining

Cryopreserved PBMC from patient 5852 obtained after alloSCT 6 weeks before (148 days after alloSCT) and 6 and 7 weeks after DLI (231 and 237 days after alloSCT) were thawed and stained with PE-conjugated UV-exchange tetramers containing LB-TTK-1D and APC-conjugated tetramers containing LB-ERAP1-1R. Tetramers were constructed as described previously[18,19]. Acquisition was performed on a FACS Calibur analyzer (BD) using CellQuest software and analyzed using FlowJo (Tree Star, Ashland, OR).

T-cell reactivity assays

Stimulator cells (5-15 × 10^3 cells/well) and T cells (2 × 10^3 cells/well) were co-incubated overnight in 384-wells plates (Greiner Bio-One, Frickenhausen, Germany). IFN-γ release was measured by ELISA (Sanquin, Amsterdam, The Netherlands). To identify the antigenic epitope, peptides were synthesized, dissolved in DMSO and pulsed at titrated concentrations in IMDM on EBV-LCLs from the stem cell donor. After 2h of pulsing at 37°C, T cells were added, and IFN-γ production in the supernatant was measured after overnight co-incubation by IFN-γ ELISA. T-cell recognition of healthy and malignant cells, which included PHA-blasts, CD40L cultured B cells, dendritic cells, FB, KC and leukemic cells of different origins (ALL, AML, CLL and CML), as well as of donor EBV-LCLs either transduced with TTK-007 construct or a mock vector was tested in a similar manner.

Quantitative RT-PCR and Sanger Sequencing

For quantitative RT-PCR and sequencing analysis, total RNA was isolated using the RNAqueous Micro-Kit and Small Scale Kit (Ambion, Life Technologies) for a maximum of 0.5 × 10^6 and 10 × 10^6 cells, respectively, following manufacturer's instructions. cDNA was synthesized from total RNA using Moloney murine leukemia virus reverse transcriptase (Invitrogen). For q-PCR, *TTK* expression was measured on the Roche Lightcycler 480 using Fast Start TaqDNA Polymerase (both Roche) and EvaGreen (Biotium, Hayward, CA) with forward primer 5'-ACCTTACTGATGAACTAAGCTTGAA-3' and reverse primer 5'-TCCCGAGTTATCTGTAGTATCAGC-3' for the full-length *TTK* transcript and forward primer 5'-ACTTTGAATGGTGTCTGGCACA-3' and reverse primer 5'-CTCTGGGTTGTTTGCCATCAT-3' for the alternative *TTK* transcript. Expression was normalized to the *HMBS* reference gene. For Sanger Sequencing of the alternative transcript, we performed two sequential rounds of PCR on cDNA of patient EBV-LCLs using two primer sets each containing one primer

that was specific for the alternative (and not the full-length) transcript. In the first round, forward primer 1 5'-ATGGAATCCGAGGATTTAAGTG-3' and reverse primer 1 5'-TGTGCCAGACACCATTCAAAG-3' as well as forward primer 2 5'-ACTTTGAATGGTGTCTGGCACA-3' and reverse primer 2 5'-GTAGTCACGTGCATCATCTG-3' were used to produce two bands, which were combined to one fragment in a second round of amplification using forward primer 1 and reverse primer 2. The alternative *TTK* transcript was confirmed by Sanger sequencing in both directions.

Minigene cloning and transduction

A construct for the alternative *TTK* transcript containing exon 1-5 was cloned into a pLZRS vector containing a truncated ΔNGFR marker gene linked by an IRES. The construct was cloned from patient 5852 cDNA (homozygous for the minor H Ag encoding SNP) using a two-step PCR with forward primer 1 5'-CGCGGATCCACCATGGAATCCGAGGATTTAAGTG-3' and reverse primer 1 5'-TGTGCCAGACACCATTCAAAG-3' as well as forward primer 2 5'-ACTTTGAATGGTGTCTGGCACA-3' and reverse primer 2 5'-TATATACTCGAGGTAGTCACGTGCATCATCTG-3' in the first round to produce two bands, which were combined to one fragment in a second round of amplification using forward primer 1 and reverse primer 2. Fragments were digested with BamHI and XhoI for cloning and the transcript construct was confirmed by Sanger Sequencing. Retroviral supernatant was obtained by transfecting wild-type Φnx-A packaging cells as previously described[20] with the exception that the Fugene HD transfection kit (Roche) was used. Viral supernatant was used for transduction on plates coated with recombinant human fibronectin CH 296 (Takara Shuzo).

Results

Selection and analysis of T-cell clones for a novel minor H Ag

We previously isolated several T-cell clones, designated clone type H4, specific for a single minor H Ag from a patient after alloSCT and DLI[6]. In total 14 clones using 2 different TCRBV recognized a minor H Ag with a population frequency of 50% in HLA-A*02:01. To identify the polymorphic epitope that is recognized by clone type H4, T-cell recognition was tested against a panel of EBV-LCLs that are genotyped for 1.1×10^6 SNPs by the 1M Illumina array (Figure 1A). WGAs was performed by calculating the correlation between T-cell recognition and the genotypes of those SNPs. We identified 13 SNPs that associated with $p < 3.0 \times 10^{-16}$, of which the strongest associating SNP rs608962 had a *p*-value of 3.64×10^{-20} (Figure 1B). These SNPs were all located in introns of the *TTK* gene (SNP rs608962 in intron 20) or in other regions located outside coding exons, and were therefore unlikely to be responsible for generation of the minor H Ag. Sanger sequencing of the primary transcript of *TTK* did not identify differences between patient and stem cell donor (data not shown). Thus, the minor H Ag recognized by the H4 clones could not be identified by WGAs using genotypes for 1.1×10^6 SNPs.

Extended correlation analysis using 1000 Genome Project genotype data

With the development of novel identification strategies using whole genome data[8], we initiated a second attempt to identify the minor H Ag recognized by the H4 clones. Therefore, in an "inferred correlation" analysis, we sought strong correlations between these noncoding SNPs and coding SNPs present in the databases of 1000 GP. Because these so-called haplotype blocks may differ per ethnic population and because the original WGAs was based on minor H Ag phenotypes of Dutch individuals, we selected 50 individuals of European descent within the 1000GP for this extended correlation analysis.

For these 50 individuals, the strongest associating SNP as identified by WGAs (rs608962) was investigated for association with each SNP on chromosome 6 within the 1000GP by a Fisher's exact test. This analysis yielded 93 fully correlating SNPs (Figure 2A, B), of which only SNP rs240226 is translated as non-synonymous coding variant in an alternative *TTK* transcript, encoding a glutamic acid (E) to aspartic acid (D) change. Based on NetMHC HLA-peptide binding predictions[17], we hypothesized that epitope RLH**D**GRVFV was the most likely candidate to be recognized by clone type H4 with RLH**E**GRVFV being the allelic

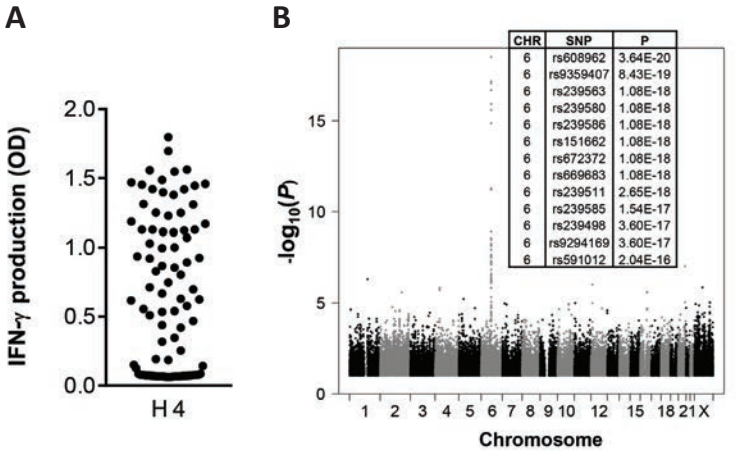

Figure 1. Identification of associating SNPs in the *TTK* gene by whole genome association scanning

(A) Recognition of a panel of 80 EBV-LCLs genotyped for 1.1M SNPs was measured for T-cell clone type H4. Each symbol indicates IFN-γ production as measured by ELISA after overnight co-incubation.

(B) Whole genome association results for clone type H4 (minus logarithm of the p-value of each SNP is plotted, each dot represents a single SNP). SNPs are grouped by their location on chromosomes (x-axis). SNPs with a p-value <10-1 are displayed. All SNPs associating with a p-value < 10-15 are shown in the inserted table with their individual p-values. The strongest associating SNP rs608962 is located in intron 20 of the *TTK* gene.

variant. Indeed, T-cell experiments confirmed that RLHDGRVFV is the minor H Ag (LB-TTK-1D) as it was potently recognized by clone type H4 with picomolar affinity, while the allelic variant (E-variant) was not recognized. The two different TCRs for LB-TTK-1D represented by clone 10-4 (TRBV19) and clone 10-5 (TRBV3-1) showed similar peptide affinity (Figure 2C).

T cells for LB-TTK-1D were detectable after DLI

Next, we investigated the *in vivo* frequency of T cells for LB-TTK-1D as compared to minor H Ag LB-ERAP1-1R, which was identified as dominant target in the same patient after DLI[6]. PBMC obtained 6 weeks before DLI and 6 and 7 weeks after DLI were stained with tetramers for LB-TTK-1D and LB-ERAP1-1R. Both LB-TTK-1D and LB-ERAP1-1R specific T cells were detected 6 weeks after DLI (0.08% and 0.14% of total lymphocytes, respectively) and further increased at week 7 (0.25% and 0.58%, respectively), while absent prior to DLI (Figure 3). This indicates that a polyclonal T-cell response was induced, which was partially directed at LB-TTK-1D and coincided with conversion to full donor chimerism.

Presentation of LB-TTK-1D on (non-)hematopoietic cell types

To determine the tissue specificity of LB-TTK-1D, we tested T-cell recognition of different cell types of (non-)hematopoietic origin. Patient EBV-LCL and

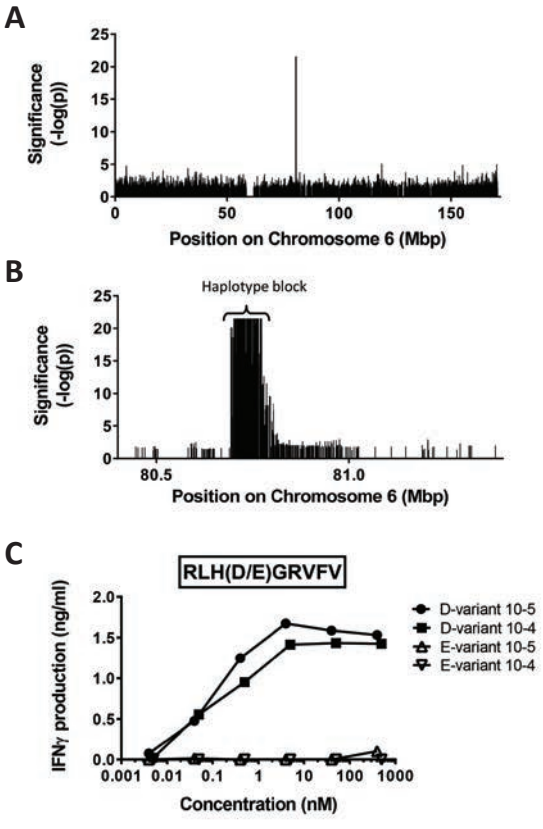

Figure 2. Identification of LB-TTK-1D by 1000 Genome Project association analysis

(A) Histogram showing p-values for all SNPs on chromosome 6 from the 1000 Genomes Project in an extended association analysis with SNP rs608962 for 50 European individuals (minus logarithm of the p-value of each SNP is plotted). Each bar represents a single SNP. Only SNPs with $p < 0.05$ are shown and ordered by location on chromosome 6 on the x-axis.

(B) Zoom view of the significant area on chromosome 6, showing a clear haplotype block with 93 SNPs that fully correlate.

(C) Identification of the HLA-A*02:01 restricted epitope as recognized by T-cell clone 10-4 and 10-5. Peptides RLH(D/E)GRVFV, which were both predicted to bind to HLA-A*02:01 by NetMHC with a binding affinity <50 nM were titrated on donor EBV-LCLs and co-incubated with T-cell clones 10-4 and 10-5. T-cell recognition after overnight co-incubation was measured by IFN-γ ELISA.

PHA-T cells were strongly recognized by clone type H4, while donor EBV-LCL and PHA-T cells remained negative (Figure 4A). The T cells also recognized CD40 activated B cells and mature dendritic cells from HLA-A*02:01 and minor H Ag positive individuals, but failed to react with peripheral blood and bone marrow mononuclear cells as well as immature dendritic cells. Of the non-hematopoietic cells tested, T-cell reactivity against patient fibroblasts (FB) as well as FB from third party minor H Ag positive individuals was measured and recognition increased after pre-treatment with IFN-γ. Keratinocytes, however, remained negative even when cultured under inflammatory conditions (Figure 4B). We then selected primary leukemia samples of different origins and an ALL-cell line based on SNP status and expression of HLA-A*02:01. One CML sample was strongly recognized, but all other leukemic samples were negative, despite strong recognition by the allo-HLA-A*02:01 control clone (Figure 4C). Pre-treatment with IFN-γ did not induce T-cell recognition as tested for one CML sample (data not shown). In summary, LB-TTK-1D specific T cells recognized cell types of hematopoietic (EBV-LCL, PHA-T cells, mature dendritic cells and CD40L cultured B cells) as well as non-hematopoietic (FB) origin, but showed reactivity

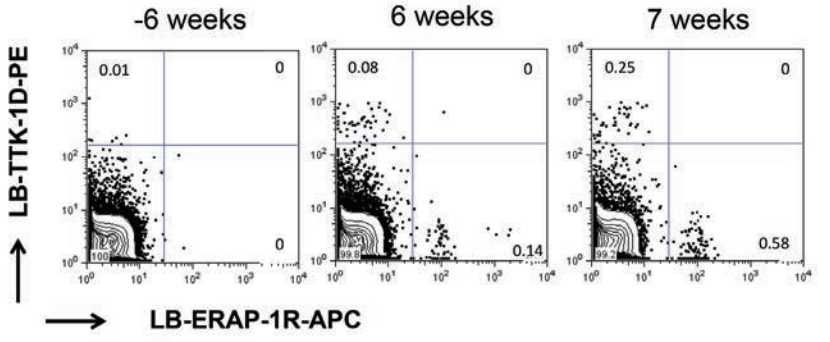

Figure 3. Detection of LB-TTK-1D specific T cells after DLI

PBMC from patient 5852 before (-6 weeks) and 6 and 7 weeks after DLI were thawed and stained with PE-labeled HLA-peptide UV-exchange tetramers for LB-TTK-1D and APC-labeled HLA-peptide tetramers for LB-ERAP-1R. Numbers indicate the percentage of cells that are positive for the specific tetramer within the lymphocyte gate.

against only one CML sample, indicating a specific recognition profile that is not restricted to (malignant) hematopoietic cells and depends on other factors than presence of the HLA-A*02:01 restricted minor H Ag.

LB-TTK-1D is encoded within an NMD transcript.

Minor H Ag LB-TTK-1D is generated by SNP rs240226 in intron 2-3 of the main *TTK* transcript, of which specific sequences are retained as alternative exon 3 in a transcript annotated as TTK-007 in Ensembl (Figure 5A). To establish whether minor H Ag LB-TTK-1D is derived from alternative transcript TTK-007, we cloned TTK-007 from patient cDNA (homozygous for SNP rs240226) and retrovirally introduced this construct into donor EBV-LCL. LB-TTK-1D specific T cells recognized donor EBV-LCL upon retroviral transduction with the construct (Figure 5B), confirming processing and presentation of LB-TTK-1D as minor H Ag from transcript TTK-007.

Interestingly, TTK-007 contains a premature termination codon (PTC) in exon 4, which renders this transcript susceptible for nonsense mediated decay (NMD). To confirm endogenous presence of this NMD transcript, we performed a PCR-strategy to specifically amplify this transcript followed by Sanger sequencing (illustrated in Figure 5A). This analysis confirmed the presence of NMD transcript TTK-007 in cDNA of patient EBV-LCL.

NMD transcripts are rapidly degraded through a surveillance mechanism to prevent the formation of aberrant dysfunctional proteins[9,10]. To investigate whether the specific recognition profile of clone 10-5 as shown in Figure 4 could be explained by cell type-specific differences in expression of the TTK-

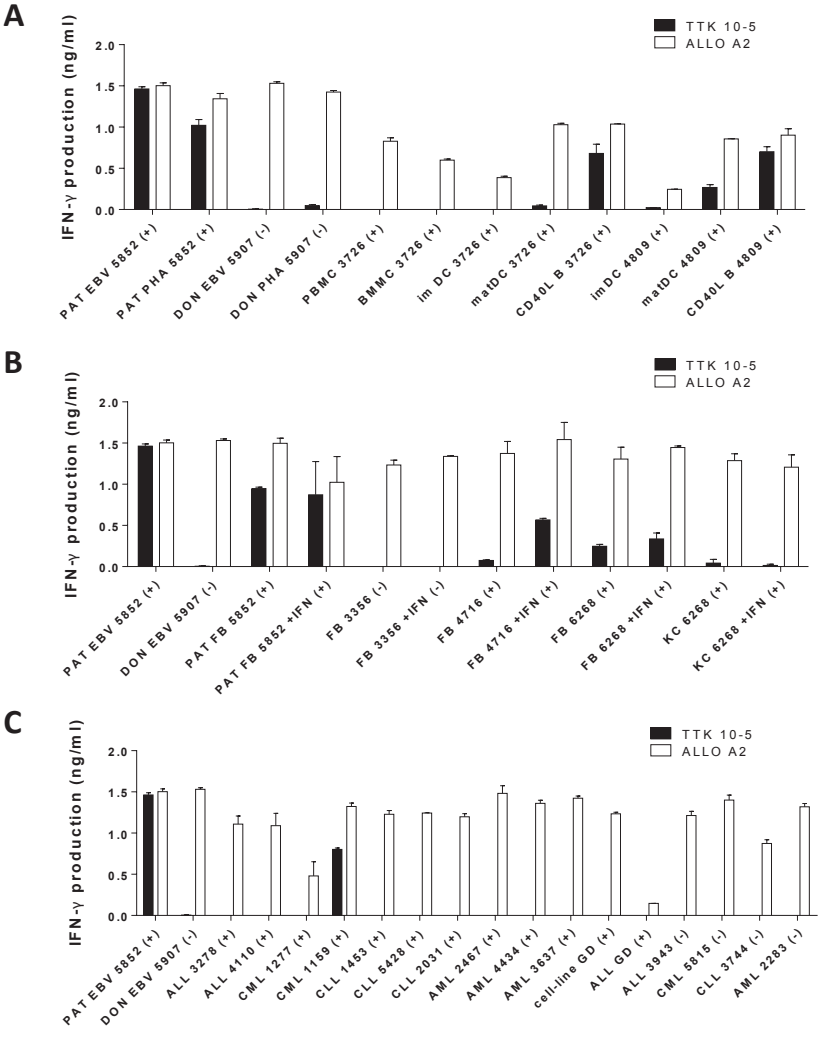

Figure 4. T-cell recognition of LB-TTK-1D on (non-)hematopoietic cell types

Reactivity of clone 10-5 (filled bars) measured by IFN-γ ELISA against healthy hematopoietic (A) and non-hematopoietic (B) cells as well as malignant hematopoietic cells (C) of different origins. The allo-HLA-A*02:01 reactive T-cell clone HSS12[13] was included as positive control (white bars). All samples were HLA-A*02:01 positive and presence or absence of the LB-TTK-1D genotype is indicated by + or -.

(A) Hematopoietic samples included patient and donor EBV-B and PHA T cells as well as PBMC, BMMC, immature and mature dendritic cells and B cells cultured on CD40L expressing cells from third party LB-TTK-1D positive healthy donors.

(B) Non-hematopoietic samples included patient fibroblasts (FB) as well as FB from third party LB-TTK-1D positive donors that were cultured in the absence or presence of IFN-γ. Of one of these donors, skin-derived keratinocytes were also included. Patient and donor EBV-LCLs as well as LB-TTK-1D negative FB were included as controls.

(C) Malignant hematopoietic cells of different origins included ALL, CLL, AML and CML samples as well as an ALL cell line (cell-line GD) and its primary sample (ALL GD). Patient and donor EBV-LCLs and LB-TTK-1D negative samples were included as controls.

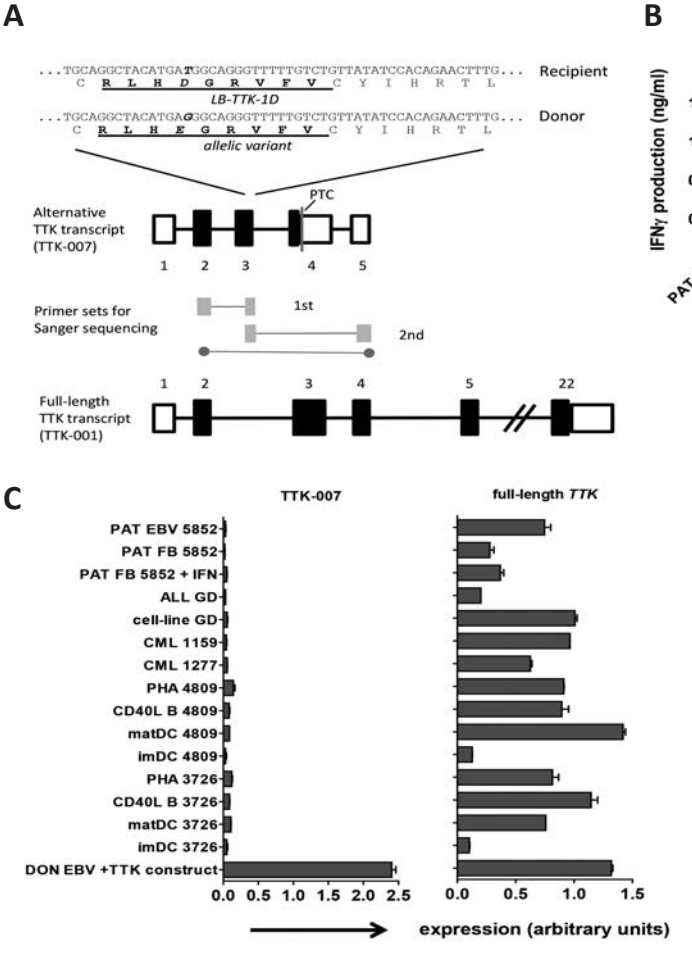

Figure 5: LB-TTK-1D is encoded by alternative transcript TTK-007

(A) Both full-length and alternative *TTK* transcripts are depicted. Coding (filled rectangles) and non-coding (white rectangles) regions of the transcripts are shown as well as intronic sequences that are spliced out to form the mature transcript (black lines) and primer binding sites used for Sanger sequencing. A detailed view of the intron 2-3 sequence that is retained as exon 3 in alternative transcript TTK-007 is inserted. SNP rs240662 encodes an amino acid change from E in donor to D in recipient cells, resulting in RLHDGRVFV as minor H antigen LB-TTK-1D recognized by clones type H4.

(B) Reactivity of clone 10-5 (filled bars) measured by IFN-γ ELISA against patient and donor EBV-LCLs and donor EBV-LCL retrovirally transduced with mock or the TTK-007 minigene. The allo-HLA-A*02:01 reactive T-cell clone HSS1213 was included as positive control (white bars).

(C) Expression of the full-length (right panel) and alternative (left panel) transcripts of *TTK* as measured by quantitative RT-PCR are shown. Expression was measured for healthy and malignant hematopoietic cell types as well as ALL cell line GD. Patient FB cultured in the absence or presence of IFN-γ were also included. All samples were positive for SNP rs240226. Donor EBV-LCL transduced with the TTK-007 construct were included as positive control for the transcript specific q-PCR. Expression of the full-length and alternative *TTK* transcript is shown after correction for expression of the PBGD reference gene in arbitrary units.

007 transcript, we designed a transcript-specific q-PCR with primers that were validated using the TTK-007 construct and measured expression of the alternative NMD as well as full-length *TTK* transcripts in cDNA produced for the same (non-)hematopoietic cell types as selected for T-cell recognition. In all cell types tested, expression of the NMD transcript was low and barely detectable as compared to the full-length *TTK* transcript (Figure 5C), suggesting that the TTK-007 mRNA is rapidly degraded as expected for an NMD transcript. Strikingly, expression levels of the NMD transcript were in a similar range in different cell types in and did not associate with T-cell recognition as shown in Figure 4. These data indicate that the specific recognition profile of clone 10-5 cannot be explained by expression of TTK-007, suggesting that other factors are involved in cell type specific surface presentation of LB-TTK-1D. Altogether, LB-TTK-1D is derived from an alternative TTK protein whose mRNA is a template for NMD, indicating that antigenic epitopes in effective immune responses can be produced by alternative transcripts that are barely detectable.

Discussion

In this paper we report the identification of a new minor H Ag that is derived from a short alternative protein encoded by an NMD targeted transcript. LB-TTK-1D was identified by combining conventional WGAs with a 1000GP-based analysis. For the HLA-A*02:01 restricted minor H Ag recognized by T-cell clones of type H4, WGAs revealed a number of highly correlating SNPs located within or in close proximity of the *TTK* gene on chromosome 6, but identification of the antigenic epitope failed. We therefore hypothesized that the true encoding variation was absent in the 1.1M SNPs as measured by the Illumina array, but might be included in the comprehensive data of the 1000GP. Since no experimental data for individuals included in the 1000GP were available, we performed an *in silico* analysis in which the most significant hit as identified by WGAs was investigated for association with all genetic variations as present on chromosome 6 in the 1000GP. This 'inferred correlation' led to identification of rs240226 as the minor H Ag encoding SNP with peptide RLHDGRVFV as the recognized epitope, confirming the power of 1000GP based identification strategies.

SNP rs240226 was found to be located in an intron region of the main *TTK* transcript that is retained as unique exon in alternative transcript TTK-007. As TTK-007 contains a PTC, it will be subjected to the surveillance mechanism of NMD leading to rapid mRNA degradation. Despite its low expression, we confirmed the presence of the NMD transcript in EBV-LCLs, and demonstrated that the transcript is sufficiently expressed for efficient induction of T cells *in vivo* and T-cell recognition of LB-TTK-1D on various (non-)hematopoietic cells *in vitro*. Recognition of LB-TTK-1D on EBV-LCL was partly abolished by proteasome inhibitor bortezomib (data not shown), indicating that the antigenic peptide is processed via the canonical route of the ubiquitin-proteasome system. Remarkably, T-cell recognition of LB-TTK-1D on different cell types of (non-) hematopoietic origin did not correlate with expression of the TTK-007 NMD transcript. This may be explained by a discrepancy between mRNA levels of the TTK-007 NMD-transcript and protein expression or turnover[21]. Alternatively, peptide source-independent differences in antigen processing may be responsible for this finding, such as variations in TAP expression or proteasome activity between tested cells.

Over the past years there has been much debate about the intracellular location and timing of NMD and how much protein is actually produced by NMD transcripts[22,23]. Evidence from *in vitro* data using model antigens accumulates, stating that NMD transcripts lead to newly-synthesized but dysfunctional proteins that are rapidly degraded via the ubiquitin-proteasome pathway, also defined as a subgroup of defective ribosomal products (DRiPs). These DRiPs are

presumably generated in the pioneering rounds of translation, and artificial DRiPs encoded by NMD transcripts have been shown to produce significant amounts of peptides for MHC class I presentation[9,12,24]. However, the endogenous contribution of these DRiPs relative to stable mature proteins to the total pool of antigenic peptides remains unclear[11,12,22,25].

Our data now demonstrate for the first time that endogenous NMD transcripts can function as a relevant source for antigenic peptides. Epitopes originating from DRiPs have been proposed to provide useful target antigens for antitumor immunotherapy[9,26-28]. It is expected that the repertoire of antigenic peptides on tumor cells will be increased upon inhibition of the rapid degradation process of NMD. This is supported by the finding that specific inhibition of NMD resulted in production of neoantigens and induction of specific immune responses, leading to tumor rejection *in vivo*[28]. Strikingly, in our experiments only one of eleven HLA-A*02:01 and LB-TTK-1D positive leukemic cell samples was recognized by our endogenous DRiP recognizing T-cell clone 10-5, while expression levels of the NMD transcript were comparable according to q-PCR, suggesting that targeting DRiP-derived peptides may not necessarily be a powerful anti-tumor strategy.

Taken together, the strategy behind the discovery of this new minor H Ag is relevant for future epitope identification studies. More importantly, the finding that this endogenous antigen is encoded by an NMD transcript and only occasionally expressed on tumor cells provides novel insights in the specificity and potential risks of DRiP-directed immunotherapeutic applications.

Acknowledgments

The authors would like to thank Michel Kester for the production of tetramers.

Reference list

1. Goulmy E. Human minor histocompatibility antigens: new concepts for marrow transplantation and adoptive immunotherapy. Immunol Rev. 1997;157:125-140.
2. Mutis T, Goulmy E. Targeting alloreactive T cells to hematopoietic system specific minor histocompatibility antigens for cellular immunotherapy of hematological malignancies after stem cell transplantation. Ann Hematol. 2002;81 Suppl 2:S38-39.
3. Falkenburg JH, van de Corput L, Marijt EW, Willemze R. Minor histocompatibility antigens in human stem cell transplantation. Exp Hematol. 2003;31(9):743-751.
4. Zilberberg J, Feinman R, Korngold R. Strategies for the identification of T cell-recognized tumor antigens in hematological malignancies for improved graft-versus-tumor responses after allogeneic blood and marrow transplantation. Biol Blood Marrow Transplant. 2015;21(6):1000-1007.
5. Bleakley M, Riddell SR. Exploiting T cells specific for human minor histocompatibility antigens for therapy of leukemia. Immunol Cell Biol. 2011;89(3):396-407.
6. Van Bergen CAM, Rutten CE, Van Der Meijden ED, et al. High-throughput characterization of 10 new minor histocompatibility antigens by whole genome association scanning. Cancer Res. 2010;70(22):9073-9083.
7. Spaapen RM, de Kort RA, van den Oudenalder K, et al. Rapid identification of clinical relevant minor histocompatibility antigens via genome-wide zygosity-genotype correlation analysis. Clin Cancer Res. 2009;15(23):7137-7143.
8. Oostvogels R, Lokhorst HM, Minnema MC, et al. Identification of minor histocompatibility antigens based on the 1000 Genomes Project. Haematologica. 2014;99(12):1854-1859.
9. Chang YF, Imam JS, Wilkinson MF. The nonsense-mediated decay RNA surveillance pathway. Annu Rev Biochem. 2007;76:51-74.
10. Rebbapragada I, Lykke-Andersen J. Execution of nonsense-mediated mRNA decay: what defines a substrate? Curr Opin Cell Biol. 2009;21(3):394-402.
11. Anton LC, Yewdell JW. Translating DRiPs: MHC class I immunosurveillance of pathogens and tumors. J Leukoc Biol. 2014;95(4):551-562.
12. Apcher S, Daskalogianni C, Lejeune F, et al. Major source of antigenic peptides for the MHC class I pathway is produced during the pioneer round of mRNA translation. Proc Natl Acad Sci U S A. 2011;108(28):11572-11577.
13. Amir AL, van der Steen DM, Hagedoorn RS, et al. Allo-HLA-reactive T cells inducing graft-versus-host disease are single peptide specific. Blood. 2011;118(26):6733-6742.
14. Griffioen M, Honders MW, van der Meijden ED, et al. Identification of 4 novel HLA-B*40:01 restricted minor histocompatibility antigens and their potential as targets for graft-versus-leukemia reactivity. Haematologica. 2012;97(8):1196-1204.
15. Jahn L, Hombrink P, Hassan C, et al. Therapeutic targeting of the BCR-associated protein CD79b in a TCR-based approach is hampered by aberrant expression of CD79b. Blood. 2015;125(6):949-958.
16. Genomes Project C, Abecasis GR, Auton A, et al. An integrated map of genetic variation from 1,092 human genomes. Nature. 2012;491(7422):56-65.
17. Lundegaard C, Lund O, Nielsen M. Prediction of epitopes using neural network based methods. J Immunol Methods. 2011;374(1-2):26-34.
18. Burrows SR, Kienzle N, Winterhalter A, Bharadwaj M, Altman JD, Brooks A. Peptide-MHC class I tetrameric complexes display exquisite ligand specificity. J Immunol. 2000;165(11):6229-6234.
19. Rodenko B, Toebes M, Hadrup SR, et al. Generation of peptide-MHC class I complexes through UV-mediated ligand exchange. Nat Protoc. 2006;1(3):1120-1132.

20. Griffioen M, van Egmond HM, Barnby-Porritt H, et al. Genetic engineering of virus-specific T cells with T-cell receptors recognizing minor histocompatibility antigens for clinical application. Haematologica. 2008;93(10):1535-1543.

21. de Klerk E, t Hoen PA. Alternative mRNA transcription, processing, and translation: insights from RNA sequencing. Trends Genet. 2015;31(3):128-139.

22. Rock KL, Farfan-Arribas DJ, Colbert JD, Goldberg AL. Re-examining class-I presentation and the DRiP hypothesis. Trends Immunol. 2014;35(4):144-152.

23. Apcher S, Daskalogianni C, Fahraeus R. Pioneer translation products as an alternative source for MHC-I antigenic peptides. Mol Immunol. 2015.

24. Durand S, Lykke-Andersen J. Nonsense-mediated mRNA decay occurs during eIF4F-dependent translation in human cells. Nat Struct Mol Biol. 2013;20(6):702-709.

25. Yewdell JW, Anton LC, Bennink JR. Defective ribosomal products (DRiPs): a major source of antigenic peptides for MHC class I molecules? J Immunol. 1996;157(5):1823-1826.

26. Williams DS, Bird MJ, Jorissen RN, et al. Nonsense mediated decay resistant mutations are a source of expressed mutant proteins in colon cancer cell lines with microsatellite instability. PLoS One. 2010;5(12):e16012.

27. Kim WK, Park M, Kim YJ, et al. Identification and selective degradation of neopeptide-containing truncated mutant proteins in the tumors with high microsatellite instability. Clin Cancer Res. 2013;19(13):3369-3382.

28. Pastor F, Kolonias D, Giangrande PH, Gilboa E. Induction of tumour immunity by targeted inhibition of nonsense-mediated mRNA decay. Nature. 2010;465(7295):227-230.

5

Clinical Cancer Research 2016

INTEGRATED WHOLE GENOME AND TRANSCRIPTOME ANALYSIS IDENTIFIED A THERAPEUTIC MINOR HISTOCOMPATIBILITY ANTIGEN IN A SPLICE VARIANT OF *ITGB2*

Margot J. Pont[1], D.I. van der Lee[1], E.D. van der Meijden[1], C.A.M. van Bergen[1], M.G.D. Kester[1], M.W. Honders[1], M. Vermaat[2], M. Eefting[1], E.W. Marijt[1], S.M. Kielbasa[3], P.A.C. 't Hoen[2], J.H.F. Falkenburg[1] and M. Griffioen[1]

[1] Department of Hematology, Leiden University Medical Center, Leiden, the Netherlands;

[2] Department of Human Genetics, Leiden University Medical Center, Leiden, the Netherlands;

[3] Department of Medical Statistics and Bioinformatics, Leiden University Medical Center, Leiden, the Netherlands

Translational relevance

Hematopoiesis-restricted minor histocompatibility antigens (MiHA) are relevant targets for immunotherapy, since donor T cells for these antigens stimulate anti-tumor immunity after HLA-matched allogeneic hematopoietic stem cell transplantation (alloSCT) without undesired side effects. We here identified LB-ITGB2-1 as hematopoiesis-restricted MiHA that is presented on leukemic cells, but not on non-hematopoietic cells, by a new approach in which whole genome and transcriptome analysis are combined. In this approach, RNA-sequence data were analyzed and LB-ITGB2-1 was shown to be encoded by an alternative transcript in which intron sequences are retained. Our data show that (1) LB-ITGB2-1 is a relevant antigen to stimulate donor T cells after alloSCT by vaccination or adoptive transfer and (2) RNA-sequence analysis is a valuable tool to identify immune targets that are encoded by alternative transcripts and created by genetic variants.

Purpose: In HLA-matched allogeneic hematopoietic stem cell transplantation (alloSCT), donor T cells recognizing minor histocompatibility antigens (MiHA) can mediate desired anti-tumor immunity as well as undesired side effects. MiHA with hematopoiesis-restricted expression are relevant targets to augment anti-tumor immunity after alloSCT without side effects. To identify therapeutic MiHA, we analyzed the *in vivo* immune response in a patient with strong anti-tumor immunity after alloSCT.

Experimental design: T-cell clones recognizing patient, but not donor, hematopoietic cells were selected for MiHA discovery by whole genome association scanning. RNA-sequence data from the GEUVADIS project were analyzed to investigate alternative transcripts and expression patterns were determined by microarray analysis and q-PCR. T-cell reactivity was measured by cytokine release and cytotoxicity.

Results: T-cell clones were isolated for two HLA-B*15:01-restricted MiHA. LB-GLE1-1V is encoded by a non-synonymous single nucleotide polymorphism (SNP) in exon 6 of *GLE1*. For the other MiHA, an associating SNP in intron 3 of *ITGB2* was found, but no SNP disparity was present in the normal gene transcript between patient and donor. RNA-sequence analysis identified an alternative *ITGB2* transcript containing part of intron 3. Q-PCR demonstrated that this transcript is restricted to hematopoietic cells and SNP positive individuals. *In silico* translation revealed LB-ITGB2-1 as HLA-B*15:01-binding peptide, which was validated as hematopoietic MiHA by T-cell experiments.

Conclusions: Whole genome and transcriptome analysis identified LB-ITGB2-1 as MiHA encoded by an alternative transcript. Our data support the therapeutic relevance of LB-ITGB2-1 and illustrate the value of RNA-sequence analysis for discovery of immune targets encoded by alternative transcripts.

Introduction

Patients with hematological malignancies can be successfully treated with allogeneic hematopoietic stem cell transplantation (alloSCT)[1]. Unfortunately, the desired anti-tumor effect often coincides with undesired side effects against healthy tissues, a complication known as Graft-versus-Host Disease (GvHD)[2]. In HLA-matched alloSCT, donor-derived T cells recognize polymorphic peptides presented by HLA molecules on patient cells. These polymorphic peptides or so-called minor histocompatibility antigens (MiHA) are not expressed on donor cells due to differences in single nucleotide polymorphisms (SNPs) between patient and donor. Donor T cells recognizing MiHA with ubiquitous expression on (non-)hematopoietic tissues induce not only the desired anti-tumor or Graft-versus-Leukemia (GvL) effect, but also undesired GvHD[3]. T-cell depletion of the stem cell graft significantly reduces the incidence and severity of GvHD, but it also diminishes the GvL effect. Therefore, to preserve GvL reactivity, donor T cells are administered after alloSCT as donor lymphocyte infusion (DLI)[2,4]. The development of GvL reactivity after DLI can be accelerated by co-administration of interferon-α (IFN-α)[5,6]. Analysis of the diversity and tissue distribution of MiHA targeted in T-cell responses after alloSCT (and DLI) provides insight into the immunobiology of GvL reactivity and GvHD. Moreover, MiHA with restricted expression on cells of the hematopoietic lineage are relevant targets for T-cell therapy to stimulate GvL reactivity after alloSCT without GvHD, since donor T cells for these MiHA will eliminate all patient hematopoietic cells, including the malignant cells, while sparing healthy hematopoiesis of donor origin.

Since 2009, MiHA discovery accelerated due to development of whole genome association scanning (WGAs). In WGAs as exploited in our laboratory, association between T-cell recognition and SNP genotype is investigated for a panel of 80 EBV-B cell lines, which have been genotyped for 1.1×10^6 SNPs[7-14]. Associating SNPs as identified by WGAs may directly encode MiHA or serve as genetic markers for antigen-encoding SNPs that are in linkage disequilibrium with associating SNPs, but which have not been captured by the array. In general, MiHA can be easily identified by WGAs if one or more associating SNPs are present in coding gene regions. However, antigen discovery is more difficult if associating SNPs are found in genomic regions that are unknown to code for protein. In a number of cases, we sequenced the primary gene transcript as derived from the associating genomic region, but failed to determine any SNP disparity between patient and donor, suggesting that the MiHA may be encoded by an alternative transcript. MiHA encoded by alternative transcripts have previously been reported for ACC-6[15] and ZAPHIR[16]. Although MiHA discovery may become more efficient when EBV-B cell lines are used which have been sequenced for their entire genome to increase SNP coverage[17], WGAs identifies a genomic region and MiHA encoded

by alternative transcripts from these regions may remain difficult to discover.

In this study, we explored whether RNA-sequence data as available in the GEUVADIS project[18,19] can be used to identify MiHA encoded by alternative transcripts. With the rapid advances in sequence technology, the GEUVADIS consortium set out to combine whole genome and transcriptome data and sequenced all mRNA expressed in 462 EBV-B cell lines from the 1000 Genomes Project (1000GP)[20]. We analyzed RNA-sequence data to unravel alternative transcripts from *ITGB2* located in a genomic region that has been identified by WGAs for a T-cell clone recognizing an HLA-B*15:01-restricted MiHA. Our data showed the successful discovery of LB-ITGB2-1 as MiHA encoded by an alternative *ITGB2* transcript by RNA-sequence analysis. We showed that the alternative *ITGB2* transcript is hematopoiesis-restricted and specifically expressed in SNP-positive individuals. Moreover, T-cell experiments demonstrated specific recognition and lysis of malignant (and healthy) hematopoietic cells, but no reactivity against skin-derived fibroblasts. As such, our data support the therapeutic relevance of LB-ITGB2-1 as hematopoiesis-restricted MiHA to augment GvL reactivity after alloSCT without GvHD.

Materials and Methods

Patient

Patient 6940 (HLA-A*01:01; A*02:01, B*07:02, B*15:01, C*04:01, C*07:02) is a female patient with chronic myeloid leukemia (CML) in blast crisis, who was transplanted with a T-cell depleted stem cell graft from her HLA-matched brother (donor 7034). She developed a cytogenetic relapse 5.5 months after alloSCT for which she was successfully treated with DLI and IFN-α. GvL reactivity after DLI was accompanied with acute GvHD grade II of the skin that evolved into chronic GvHD.

Cell samples and culture

Peripheral blood, bone marrow and skin biopsies were obtained from patient 6940, donor 7034 and third party individuals after approval by the LUMC Institutional Review Board and informed consent according to the Declaration of Helsinki. Peripheral blood and bone marrow mononuclear cells (PBMC and BMMC) were isolated by Ficoll-Isopaque separation and cryopreserved. Fibroblasts (FB), EBV-B cells and T cells were cultured as described previously[9,10]. In house generated EBV-B cell lines were authenticated using short-tandem repeat profiling upon freezing of stock vials. FB were cultured in the absence or presence of 200 IU/ml IFN-γ (Boehringer Ingelheim, Alkmaar, The Netherlands) for 4 days. Patient CML cells in blast crisis in a PBMC sample obtained at diagnosis prior to alloSCT were *in vitro* modified into professional antigen-presenting cells (CML-APC) as described previously[21].

Isolation of T-cell clones

T cells were isolated from patient PBMC obtained 9 weeks after DLI using the MACS pan T isolation kit according to manufacturer's instructions (Miltenyi Biotec, Bergisch Gladbach, Germany). CML-APC and CD3 T cells were co-incubated for 48h at a 1:10 stimulator: responder ratio. Cultures were stained with CD8-FITC and CD137-APC monoclonal antibodies and activated CD137-positive CD8 T cells were single cell-sorted by flow cytometry. Isolated T cells were stimulated with irradiated feeders, phytohemagglutinin and IL-2 as previously described[9]. Growing T-cell clones were analyzed for reactivity and restimulated every 14 days as described above.

T-cell reactivity assays

Stimulator cells (5-15x10^3 cells/well) and T cells (2x10^3 cells/well) were co-incubated overnight in 384-wells plates (Greiner Bio-One, Frickenhausen, Germany). IFN-γ release was measured by ELISA (Sanquin, Amsterdam, The Netherlands). In chromium release assays, target cells (1x10^3 cells/well) were labeled for 1h at 37°C with 100μCi (3.7MBq) $Na_2{}^{51}CrO_4$ and co-incubated with T cells for 10h at a 10:1 effector-target ratio. Specific lysis was calculated as previously described[10].

Whole Genome Association scanning

SNP-genotyped EBV-B cell lines (n=71) were transduced with an LZRS retroviral vector[22] encoding HLA-B*15:01. Mean transduction efficiency was 24% (range 12-34%) and T-cell recognition was measured by IFN-γ ELISA. WGAs was performed as described previously[9].

RNA-sequence analysis

EBV-B cell lines for which RNA-sequence data (.bam files) are available in the GEUVADIS project[18,19] were selected for SNP genotype (+/+, +/- and -/-) from the 1000 Genomes Project[20]. For each SNP (rs760462 and rs9945924), two representative individuals per genotype were selected and bigwig files containing RNA-sequence coverage and mapping and split coordinates of individual sequence reads in the region of interest for these EBV-B cell lines were uploaded to the UCSC genome browser[23].

Prediction of HLA binding peptides

Transcript sequences were translated in forward reading frames and protein sequences were fed into the NetMHC algorithm[24,25] to search for peptides with predicted binding to HLA class I alleles. Peptides were synthesized, dissolved in DMSO and tested for T-cell recognition by IFN-γ ELISA[9].

Microarray gene expression and q-PCR analysis

Malignant and healthy hematopoietic cells and untreated as well as IFN-γ pretreated non-hematopoietic cells of different origins were processed and hybridized on Human HT-12 v3/4 Expression BeadChips (Illumina, San Diego, CA, USA) as described previously[26]. The data have been deposited in NCBI's Gene Expression Omnibus[27] and are accessible through GEO Series

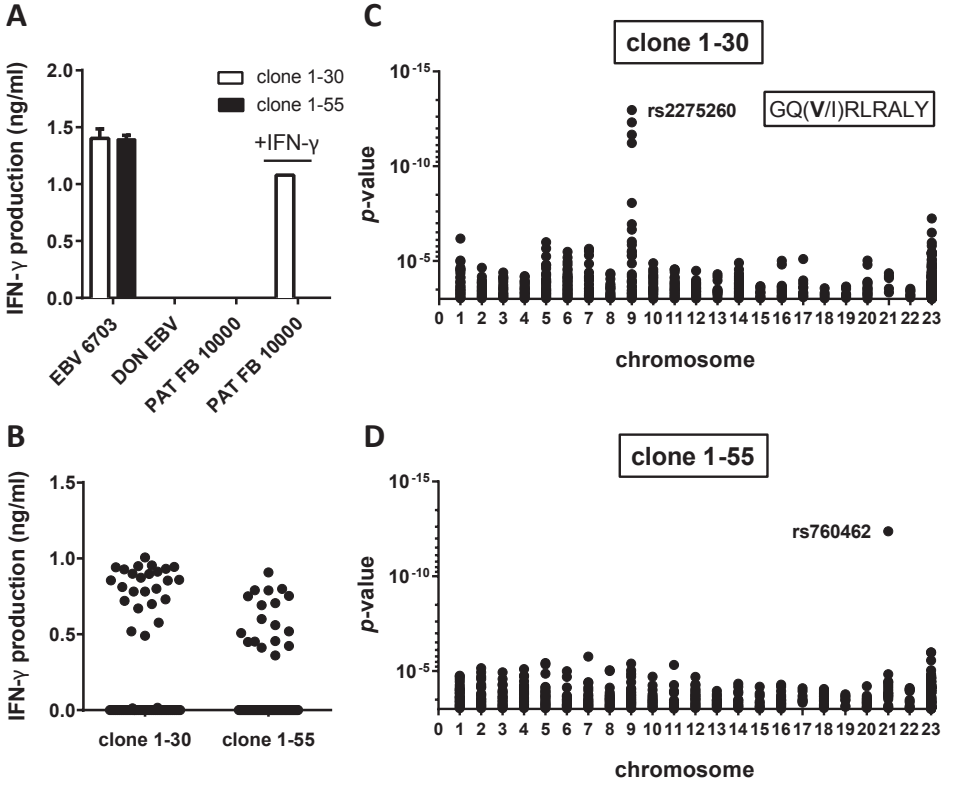

Figure 1: T-cell clones 1-30 and 1-55 recognize HLA-B*15:01-restricted minor histocompatibility antigens

(A) Reactivity of T-cell clones 1-30 (open bars) and 1-55 (filled bars) was measured against patient FB, which were cultured in the absence or presence of IFN-γ, and against HLA-B*15:01 positive, MiHA-positive and -negative EBV-B cells (third party EBV 6703 and DON EBV, respectively). T-cell reactivity was measured by IFN-γ ELISA after overnight co-incubation.

(B) Recognition of a panel of 71 SNP-genotyped EBV-B cell lines after retroviral transduction with HLA-B*15:01 was measured for T-cell clones 1-30 and 1-55. Each symbol represents IFN-γ production as measured by ELISA after overnight co-incubation of the T-cell clone with each individual EBV-B cell line.

(C-D) Association was measured between T-cell recognition of 71 EBV-B cell lines transduced with HLA-B*15:01 and each of the $1.1x10^6$ SNPs as measured by the Illumina 1M array. SNPs are grouped by their location on chromosomes (x-axis). SNPs with p-value $<10^{-3}$ are displayed.

(C) Whole genome association scanning results for clone 1-30 are depicted. Strong association was found for SNP rs2275260 (p=$1.08x10^{-13}$) located in exon 6 of the *GLE1* gene, which encodes an amino acid change in a peptide with strong predicted binding to HLA-B*15:01 by NetMHC: GQ(**V**/I)RLRALY.

(D) Whole genome association scanning results for clone 1-55 are depicted. Strong association was found for SNP rs760462 (p=$4.26x10^{-13}$) located in intron 3 of the *ITGB2* gene.

accession number GSE76340 (http://www.ncbi.nlm.nih.gov/geo/query/acc.cgi?acc=GSE76340). For quantitative RT-PCR, RNA isolation, cDNA synthesis and q-PCR were performed as described previously[28]. *ITGB2* expression was measured using forward primer 5'-CTCTCTCAGGAGTGCACGAA-3' and reverse primer 5'-CCCTGTGAAGTTCAGCTTCTG-3' for the normal *ITGB2* transcript and forward primer 5'-CAGCAGCTGCCGGGAATG-3' and reverse primer 5'-CTCAGTCCGAGGACAGACGG-3' for the alternative *ITGB2* transcript. Expression was normalized for expression of the *HMBS* reference gene.

Colony Forming Assay

Bone marrow or peripheral blood samples from patients with CML were pre-incubated with irradiated (35 Gy) T-cell clones at E:T ratios of 3:1. After overnight co-inucbation, single cell suspensions ($2x10^4$ target cells) were seeded in 30-mm culture dishes containing IMDM with methylcellulose and growth factors (GM-CSF, stem cell factor, IL-3, erythropoietin and other supplements (MethoCult H4434, STEMCELL technologies SARL, Grenoble, France). As controls, single cell suspensions and irradiated T cells at E:T ratios of 3:1 were seeded without pre-incubation. After 14 days of culture, colony forming units for granulocyte/macrophage (CFU-GM, CFU-G, CFU-M) and erythroid (CFU-E, BFU-E) lineages were enumerated as well as colony forming units containing early progenitors that differentiated to granulocyte/macrophage/erythroid lineages.

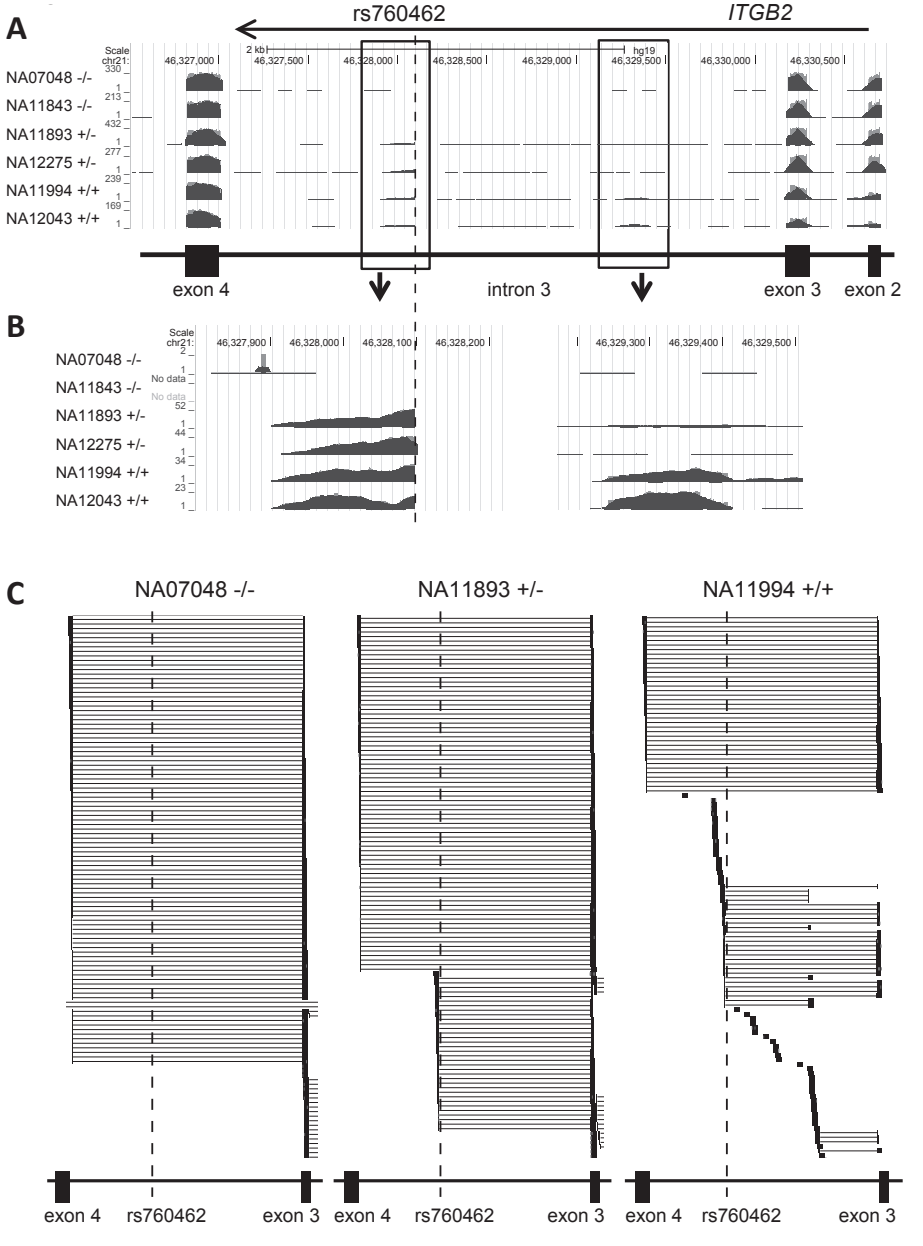

Figure 2: Discovery of an alternative *ITGB2* gene transcript by whole transcriptome analysis

ITGB2 is located on chromosome 21q22.3 and is encoded on the reverse strand. Graphs (A-C) are screenshots from the UCSC genome browser at http://genome.ucsc.edu. Exons are indicated by black rectangles. The genomic location of associating SNP rs760462 as identified by WGAs is indicated by the vertical dotted lines.

(A) RNA-sequence reads aligning with exon 2 to 4 of the *ITGB2* gene in the human HG19 reference genome are shown for 6 individuals representing different genotype groups for associating SNP rs760462 (+/+, +/- and-/-). The y-axis indicates the total number of RNA-sequence reads aligning with the indicated *ITGB2* gene region as summarized peaks. Substantial numbers of RNA-sequence reads aligned with exon regions of the *ITGB2* gene in all 6 individuals irrespective of genotyping for SNP rs760462.

(B) Enlarged view with the y-axis adjusted to a lower range of RNA-sequence reads is shown for two regions

Results

Isolation of T-cell clones for HLA-B*15:01-restricted MiHA

To identify MiHA that are targeted in effective GvL responses, CD8 T-cell clones were isolated from a patient with CML in blast crisis who entered into complete remission upon treatment with DLI after HLA-matched alloSCT. Development of anti-tumor immunity after DLI was accompanied with grade II skin GvHD. CD3 T cells isolated from patient PBMC after DLI were stimulated with a patient CML sample obtained at diagnosis prior to alloSCT. This sample consisted of a heterogeneous population, containing 63% mature myelocytes, 17% immature CD34-negative cells and 17% immature CD34-positive cells. To enhance antigen-presentation by the stimulator cells, patient CML cells were modified *in vitro* into professional APC (CML-APC). After 48h of stimulation, CD8 T cells were single cell sorted by flow cytometry based on expression of activation marker CD137. Growing CD8 T-cell clones (n=112) were tested for reactivity against patient CML-APC, donor EBV-B, donor EBV-B pulsed with a mix of known MiHA peptides and patient FB, which were cultured in the absence or presence of IFN-γ to mimic the inflammatory environment of the early post-transplantation period. T-cell clones recognizing known MiHA peptides were specific for LB-ADIR-1F[29] and LRH-1[30]. T-cell clones 1-30 and 1-55 recognized unknown MiHA.

T-cell clones 1-30 and 1-55 both showed strong reactivity against patient CML-APC (data not shown) as well as EBV-B cells from an HLA-B*15:01 third party individual, but not against donor EBV-B (Figure 1A). In contrast to clone 1-30 that strongly recognized patient FB after pretreatment with IFN-γ, T-cell clone 1-55 lacked reactivity against (IFN-γ pretreated) FB. To identify the epitopes that are recognized by clones 1-30 and 1-55, WGAs was performed to investigate association between T-cell recognition and all individual SNPs as measured by the array (Figure 1B)[9]. For clone 1-30, WGAs identified 4 SNPs that associated with T-cell recognition of HLA-B*15:01-transduced EBV-B cells with the same

in intron 3 that are transcriptionally active, as indicated by black rectangles in (A). The intron 3 region located upstream (right panel) of associating SNP rs760462 was transcribed in individuals who were +/+ for this SNP, but not in individuals who were -/- for this SNP. Since this region is not transcribed in +/- individuals, we concluded that this region is unlikely to encode the MiHA. In contrast, the intron 3 region located downstream of associating SNP rs760462 (left panel) was transcribed in both +/- and +/+ individuals, but not in-/- individuals, and we therefore analyzed this region in more detail.

(C) Single RNA-sequence reads aligning within the gene region spanning exon 3 to exon 4 of *ITGB2* in the human HG19 reference genome are shown for 3 individuals representing different SNP genotypes (+/+, +/- and-/-). RNA-sequence reads that aligned with continuous 75bp sequences that do not cross exon boundaries (exon reads) were excluded from the analysis. All other RNA-sequence reads, which included intron reads and split reads, are shown. Split reads are indicated by two boxes connected with a horizontal line and are the result of distinct genomic sequences that are joined in a transcript due to splicing. All split reads in -/- individuals contained exon 3 connected to exon 4, indicating expression of the normal *ITGB2* gene transcript. In addition to split reads for the normal gene transcript, split reads in which exon 3 was connected to intron 3 sequences located downstream of the associating SNP were measured in +/- and +/+ individuals. These data indicate that in addition to the normal gene transcript, an alternative *ITGB2* transcript in which part of intron 3 is retained is expressed in individuals who are positive for associating SNP rs760462.

p-value of $1.08x10^{-13}$ (Figure 1C). These 4 SNPs were located in a genomic region on chromosome 9 comprising the *GLE1* gene. One non-synonymous SNP (rs2275260) in exon 6 encoded an amino acid change in the GLE1 protein. Patient and donor peptides GQ(V/I)RLRALY with predicted binding to HLA-B*15:01 by NetMHC[24,25] were identified and the V-variant (LB-GLE1-1V) was recognized by clone 1-30.

For clone 1-55, WGAs identified a single SNP on chromosome 21 with a *p*-value of $4.26x10^{-13}$ (Figure 1D). This SNP rs760462 A/G (A; recognized allele) is located in intron 3 (region between exon 3 and exon 4) of the *ITGB2* gene. Sanger sequencing of the normal *ITGB2* transcript did not detect any SNP differences between patient and donor. In addition, intron sequences comprising rs760462 were translated *in silico* in different reading frames, but no peptide with predicted binding to HLA-B*15:01 was found (data not shown).

Whole transcriptome analysis enabled discovery of a MiHA encoded by an alternative *ITGB2* gene transcript.

Since no SNP differences were found between patient and donor in the normal *ITGB2* transcript, we explored the possibility that the MiHA as recognized by clone 1-55 may be encoded by an alternative transcript. RNA-sequence data were analyzed as online available in the GEUVADIS project[18,19] for 462 EBV-B cell lines for which corresponding whole genome sequences are available in the 1000GP. Based on SNP genotypes, EBV-B cell lines were selected from individuals who were homozygous positive (A/A; +/+), heterozygous (A/G; +/-) or homozygous negative (G/G;-/-) for associating SNP rs760462. For 6 individuals, RNA-sequence reads were aligned with the *ITGB2* gene in the human HG19 reference genome. Figure 2A depicts transcriptional activity summarized as RNA-sequence read coverage surrounding SNP rs760462. Significant numbers of reads aligned with exon regions in the *ITGB2* gene, but also two regions in intron 3 were transcribed. The intron region located upstream of associating SNP rs760462 (Figure 2B, right) was transcriptionally active in individuals who were +/+, but not in individuals who were +/- or-/- for this SNP. Since this region was not transcribed in +/- individuals, we considered it unlikely that this region

Table 1: predicted peptides for ITGB2

Frame	Length (aa)	Peptide	Logscore	Affinity	Bind Level
2	9	GQAPGGNYL	0.545	136	WB
2	10	GQAGFFPSPF	0.735	17	SB
2	11	EQGGQAPGGNY	0.435	451	WB
2	11	LGQAGFFPSPF	0.613	65	WB

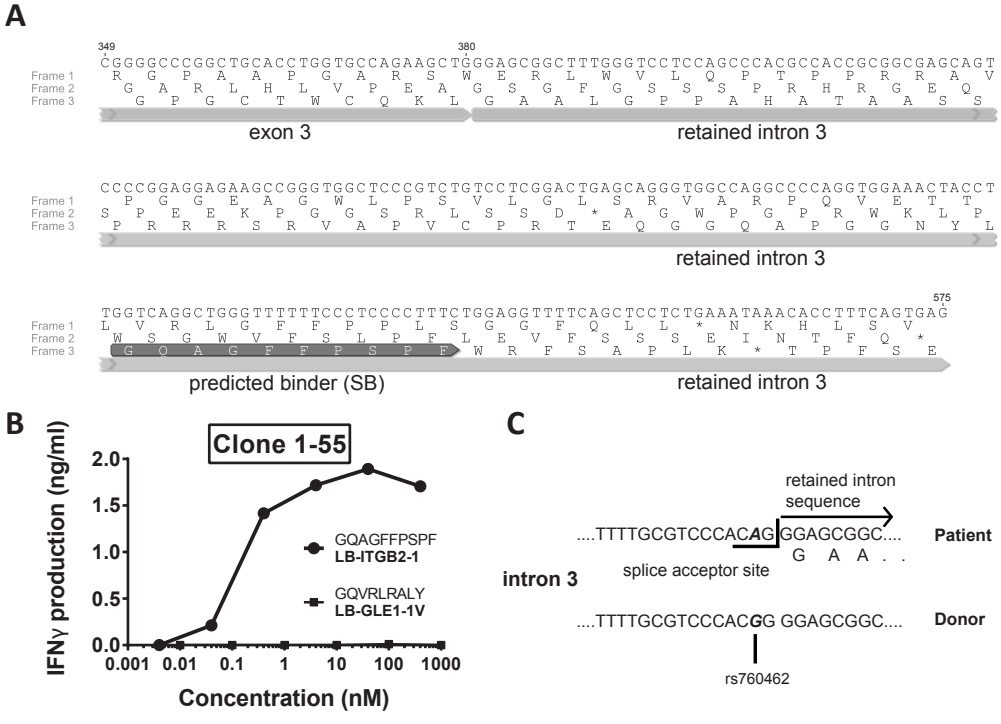

Figure 3: Discovery of a MiHA that is encoded by the alternative *ITGB2* gene transcript

(A) The exact sequence composition of the alternative *ITGB2* transcript in which exon 3 is connected to a region in intron 3 located downstream from associating SNP rs760462 was deduced from split read analysis as shown in Figure 2C. The alternative transcript was translated and a peptide with strong predicted binding (SB) to HLA-B*15:01 as revealed by NetMHC is depicted by the dark gray bar. Sequences are depicted using Geneious (version 7.1.5 created by Biomatters, available from http://www.geneious.com/)

(B) Identification of the HLA-B*15:01-restricted epitope as recognized by T-cell clone 1-55. Peptide GQAGFFPSPF, which has been identified as peptide with strong predicted binding to HLA-B*15:01 by NetMHC, was titrated on donor EBV-B cells and co-incubated with T-cell clone 1-55. T-cell recognition after overnight co-incubation was measured by IFN-γ ELISA.

(C) Intron 3 sequences of *ITGB2* for patient and donor including rs760462 (in bold) are depicted. SNP rs760462 likely creates a splice acceptor site (C**A**G), resulting in retention of intron sequences located 2 nucleotides downstream from the SNP in patient, but not donor.

encoded the MiHA. In contrast, the intron 3 region downstream from rs760462 was transcribed in both +/- and +/+, but not in-/- individuals (Figure 2B, left) and we therefore investigated this region in more detail.

To determine the sequence composition of the alternative transcript, we evaluated alignments of split reads in the region that spanned exon 3 to exon 4 (Figure 2C). Split reads are the result of distinct genomic sequences that are joined in a transcript due to splicing. In-/- individuals, all split reads contained exon 3 connected to exon 4, indicating expression of the normal *ITGB2* transcript. In contrast, in +/- and +/+ individuals, split reads for the normal *ITGB2* transcript were found as well as split reads in which exon 3 was connected to intron 3 sequences located two nucleotides downstream from the associating

SNP. These data demonstrate expression of an alternative *ITGB2* gene transcript in which part of intron 3 is retained. Expression of the alternative transcript was restricted to SNP-positive individuals, likely due to rs760462 introducing a cryptic splice acceptor site.

Next, we translated the alternative *ITGB2* transcript *in silico* (Figure 3A) and protein sequences starting from exon 3 were fed into the NetMHC algorithm[24,25] to identify peptides with predicted binding to HLA-B*15:01. Four peptides were identified (Table 1) including one 10-mer peptide with strong predicted binding to HLA-B*15:01. T-cell experiments confirmed that GQAGFFPSPF is the MiHA (LB-ITGB2-1) that is recognized by clone 1-55 with picomolar affinity (Figure 3B). In conclusion, RNA-sequence analysis revealed an alternative *ITGB2* transcript in which associating SNP rs760462 generates a splice acceptor site, thereby creating a transcript in which part of intron 3 is retained (Figure 3C). This alternative transcript encoded the MiHA recognized by T-cell clone 1-55. As such, whole transcriptome analysis enabled discovery of LB-ITGB2-1 as MiHA encoded by an alternative *ITGB2* transcript.

Whole transcriptome analysis also allows discovery of antigens generated by exon skipping

To explore the value of RNA-sequence analysis for identification of antigens beyond LB-ITGB2-1, we analyzed RNA-sequence data for ACC-6, an HLA-B*40:01-restricted MiHA encoded by an *HMSD* splice variant[15]. Expression of ACC-6 is associated with SNP rs9945924 in intron 2 of *HMSD* located 5 bp downstream of exon 2. We selected EBV-B cell lines from GEUVADIS and compared *HMSD* gene transcription between individuals with different genotypes for the associating SNP (+/+, +/- and -/-). In contrast to *ITGB2*, no transcriptional activity was found outside exon regions of *HMSD* (Figure S1A). Furthermore, we noticed that exon 2 was not transcribed in +/+ individuals, while transcription was clearly detectable in -/- and +/- individuals, indicating that SNP rs9945924 is associated with exon 2 skipping. Split read analysis revealed that only the full-length *HMSD* transcript was expressed in -/- individuals, whereas both the full-length transcript as well as an alternative transcript in which exon 1 was connected to exon 3 were detectable in +/- individuals (Figure S1B). In +/+ individuals, only the alternative transcript was expressed in which exon 2 is skipped. *In silico* translation of the full-length and alternative *HMSD* transcripts revealed that exon 2 skipping deleted the ATG start site, thereby producing a shorter protein in an alternative reading frame (Figure S2). We searched the alternative protein for peptides with predicted binding to HLA-B*40:01 and identified 8 peptides (Table S1), including ACC-6 epitope MEIFIEVFSHF[15], in which M is encoded by the first start codon in the alternative transcript. These data demonstrate that RNA-sequence analysis

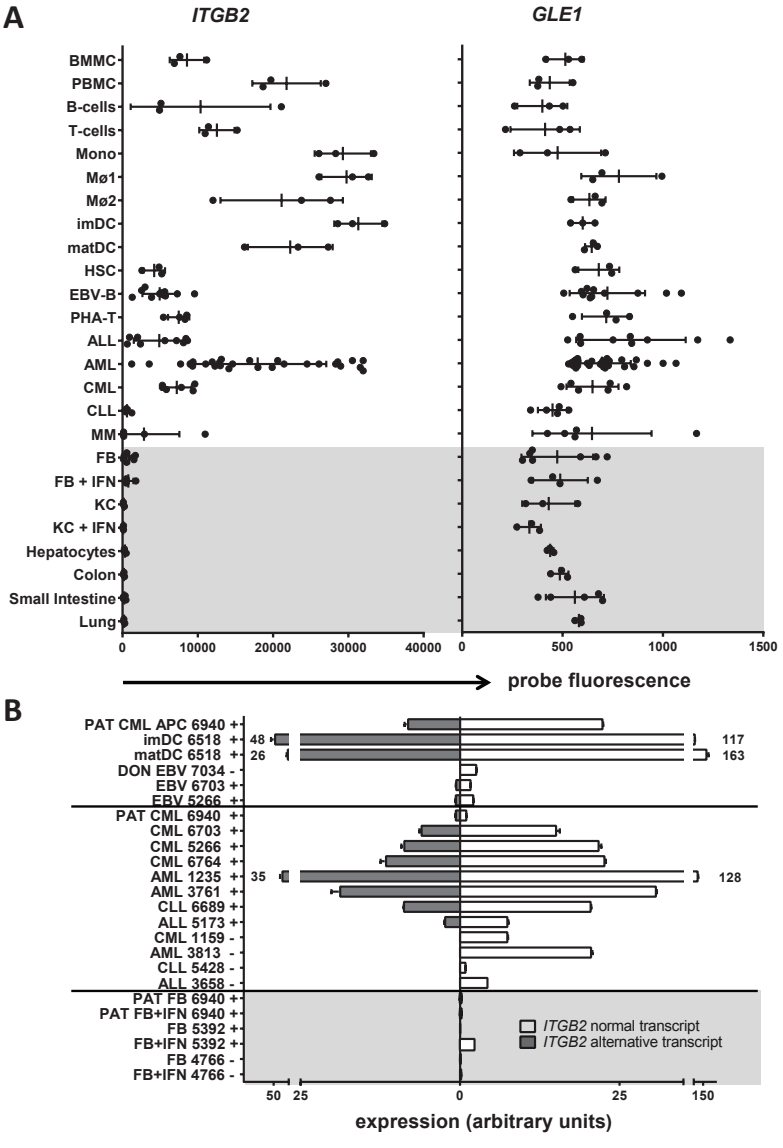

Figure 4: Expression of the alternative *ITGB2* transcript is hematopoiesis-restricted

(A) Expression of *ITGB2* and *GLE1* as determined by microarray gene expression analysis. *GLE1* is broadly expressed, whereas expression of *ITGB2* is hematopoiesis-restricted. Indicated is the probe fluorescence as measured on Illumina Human HT-12 v3/4 BeadChips. Hematopoietic cells included bone marrow and peripheral blood mononuclear cells (BMMC and PBMC), B cells, T cells, monocytes (Mono), macrophages type I and II (MØ1 and MØ2), (im)mature DC (imDC and matDC), hematopoietic stem cells (CD34 HSC), EBV-B and PHA-T cells. Malignant hematopoietic cells included acute lymphoblastic leukemia (CD19 ALL), acute myeloid leukemia (CD33 AML), chronic myeloid leukemia (CD34 CML), chronic lymphocytic leukemia (CD5 CD19 CLL) and multiple myeloma (CD138 MM), which were sorted by flow cytometry based on the indicated markers. Non-hematopoietic cells as indicated by the shaded panel included skin FB and KC which were cultured in the absence or presence of IFN-γ, hepatocytes, colon and small intestine epithelial cells and lung epithelial cells.

(B) Expression of normal and alternative *ITGB2* transcripts as measured by quantitative RT-PCR in various cell types. Malignant hematopoietic samples included unselected PBMC or BMMC samples obtained at diagnosis with >30% malignant cells. Genotyping results (+ or -) for LB-ITGB2-1 associating SNP rs760462 are depicted. Expression of the normal (open bars) and alternative (filled bars) *ITGB2* transcripts is shown after correction for expression of the *HMBS* reference gene in arbitrary units.

also allows discovery of antigens encoded by alternative transcripts that are generated by exon skipping.

T cells for LB-ITGB2-1 were detected after DLI

Next, we investigated the *in vivo* immunodominance of LB-ITGB2-1 during GvL reactivity and compared the T-cell frequency for LB-ITGB2-1 at 9 weeks after DLI with other MiHA that were targeted in patient 6940 (LB-ADIR-1F, LRH-1 and LB-GLE1-1V). Tetramer analysis in Figure S3 shows that T cells for LB-ADIR-1F (0.46%), LRH-1 (0.35%), LB-ITGB2-1 (0.14%) and LB-GLE1-1V (0.08%) are involved in the immune response after DLI. T-cell frequencies prior to DLI were absent or significantly lower for all MiHA, indicating induction and expansion of a polyclonal T-cell response targeting multiple MiHA during GvL reactivity.

Expression of the alternative *ITGB2* transcript is hematopoiesis-restricted

Since T-cell clone 1-55 recognized patient CML-APC, but failed to react with FB (Figure 1A), and expression of *ITGB2* has been reported to be hematopoiesis-restricted[31], we investigated whether T cells for LB-ITGB2-1 could contribute to GvL responses. Microarray gene expression analysis[26] confirmed that the normal *ITGB2* transcript was expressed in malignant and healthy hematopoietic cells, but not in non-hematopoietic cells from organs that are often targeted in GvHD

Figure 5: T cells for LB-ITGB2-1 showed specific recognition and lysis of primary leukemic cells

(A) Reactivity of T-cell clones 1-55 (left panel) and 1-30 (middle panel) was measured against CML-APC and FB cultured in the absence or presence of IFN-γ of patient 6940 as well as patient PBMC obtained at diagnosis (PAT CML) and samples from other HLA-B*15:01 patients suffering from CML or AML who were positive for SNP rs760462 (LB-ITGB2-1) or rs2275260 (LB-GLE1-1V). Donor EBV-B cells and third party HLA-B*15:01 individuals negative for one or both SNPs were included as controls. The allo-HLA-A*02:01 reactive T-cell clone HSS1238 (right panel) was included as a control clone. Genotyping results (+ or-) for LB-ITGB2-1 (left panel), LB-GLE1-1V (middle panel) and HLA-A*02:01 (right panel) are indicated for the selected samples. Mean release of IFN-γ of duplicate wells as measured by IFN-γ ELISA after overnight co-incubation of T cells and stimulator cells is depicted.

(B) Lysis of patient CML-APC as well as other primary leukemic samples from HLA-B*15:01 patients who were positive for SNP rs760462 (LB-ITGB2-1) was measured in a 10h chromium-release assay. Clone 1-30 (LB-GLE1-1V), clone HSS12 (allo-HLA-A*02:01) and clone FK47 (HA-1H)39 were included as controls. Genotyping results (+ or-) for LB-ITGB2-1 (upper left panel), LB-GLE1-1V (upper right panel), HLA-A*02:01 (lower left panel) and HA-1H (lower right panel) are shown. Mean specific lysis of triplicate wells is depicted.

(C) Lysis of CML progenitor cells from patient 6940 (PAT CML 6940) and patient 1159 (CML 1159) in a colony forming assay. Peripheral blood or bone marrow samples were pre-incubated overnight in the absence or presence of T cells at an E:T ratio of 3:1. After overnight co-incubation, single cell suspensions were seeded and colony forming units were enumerated for the granulocyte/macrophage (CFU-GM, CFU-G, CFU-M) and erythroid (CFU-E, BFU-E) lineages as well as for mixed granulocyte/macrophage/erythroid lineages. Indicated are the number of CFU for the LB-ITGB2-1 specific T-cell clone 1-55, the HA-1H specific T-cell clone FK47 and the HLA-A*02:01 specific alloreactive T-cell clone HSS12. Patient 6940 is positive for LB-ITGB2-1 and HLA-A*02:01, but negative for HA-1H. Patient 1159 is positive for HLA-A*02:01, but negative for LB-ITGB2-1 and HA-1H. O/n indicates overnight co-incubation.

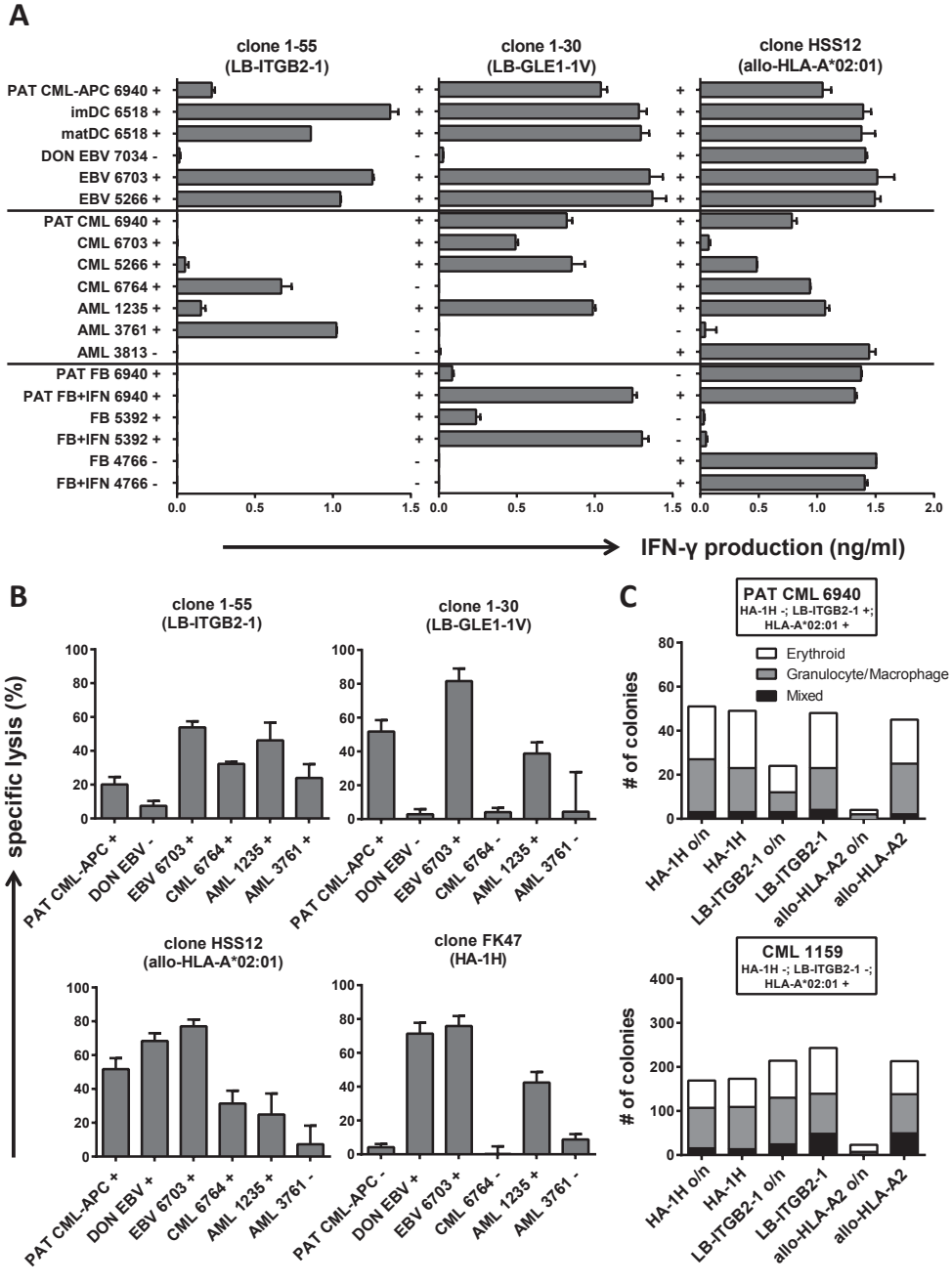
A
clone 1-55 (LB-ITGB2-1)
clone 1-30 (LB-GLE1-1V)
clone HSS12 (allo-HLA-A*02:01)
PAT CML-APC 6940 +
imDC 6518 +
matDC 6518 +
DON EBV 7034 -
EBV 6703 +
EBV 5266 +
PAT CML 6940 +
CML 6703 +
CML 5266 +
CML 6764 +
AML 1235 +
AML 3761 +
AML 3813 -
PAT FB 6940 +
PAT FB+IFN 6940 +
FB 5392 +
FB+IFN 5392 +
FB 4766 -
FB+IFN 4766 -
IFN-γ production (ng/ml)
B
clone 1-55 (LB-ITGB2-1)
clone 1-30 (LB-GLE1-1V)
clone HSS12 (allo-HLA-A*02:01)
clone FK47 (HA-1H)
specific lysis (%)
C
PAT CML 6940
HA-1H -; LB-ITGB2-1 +; HLA-A*02:01 +
CML 1159
HA-1H -; LB-ITGB2-1 -; HLA-A*02:01 +
Erythroid
Granulocyte/Macrophage
Mixed
# of colonies
HA-1H o/n
HA-1H
LB-ITGB2-1 o/n
LB-ITGB2-1
allo-HLA-A2 o/n
allo-HLA-A2

(skin, liver, gut, lung) (Figure 4A). In contrast, the *GLE1* gene, which encodes the MiHA recognized by clone 1-30, was ubiquitously expressed in (non-) hematopoietic tissues.

Since LB-ITGB2-1 is encoded by a splice variant, we investigated the tissue distribution of this alternative transcript and compared expression with the normal transcript by quantitative RT-PCR. In line with RNA-sequence data (Figure 2), the alternative transcript was only detected in SNP rs764062-positive individuals, while the normal transcript was measured in all individuals irrespective of SNP genotype (Figure 4B). In all hematopoietic samples from SNP-positive individuals, expression of the *ITGB2* splice variant followed the same pattern as the normal transcript. Moreover, both normal and alternative transcripts were undetectable in non-hematopoietic (IFN-γ pretreated) FB, indicating that these gene products are regulated by the same hematopoiesis-restricted transcriptional control elements.

T cells for LB-ITGB2-1 showed specific recognition and lysis of primary leukemic cells

To investigate whether LB-ITGB2-1 has therapeutic potential, we selected leukemic cells of different origins and compared T-cell recognition of these samples as measured by IFN-γ ELISA with FB cultured in the absence or presence of IFN-γ. Figure 5A shows that clone 1-55 recognized patient CML-APC as well as EBV-B cells and (im)mature DC from HLA-B*15:01 individuals who were positive for SNP rs760462 (left panel). EBV-B cells were strongly recognized by clone 1-55, while *ITGB2* gene expression was low (Figure 4B), which can be explained by high surface expression of HLA class I, costimulatory and adhesion molecules as well as other molecules involved in intracellular antigen processing and presentation. In addition, various CML and AML samples from SNP-positive patients were recognized, while the T-cell clone failed to recognize (IFN-γ pretreated) patient FB as well as FB from another SNP-positive individual. Clone 1-55 also failed to recognize patient CML cells obtained at diagnosis and CML cells from another SNP-positive patient. Both CML samples expressed low levels of the alternative *ITGB2* transcript by quantitative RT-PCR (Figure 4B). One AML sample (AML 1235) was only moderately recognized by clone 1-55, while the *ITGB2* gene was highly expressed, which can be due to suboptimal expression of HLA class I or other accessory molecules in antigen processing and presentation.

Furthermore, we showed that T cells for LB-ITGB2-1 mediated specific lysis of primary leukemic cells in a 10h chromium-release assay (Figure 5B, left upper panel). T-cell clone 1-55 mediated specific lysis of patient CML-APC, whereas donor EBV-B cells were not lysed. In addition, EBV-B cells as well as AML and

CML samples from other SNP-positive individuals were lysed.

To investigate the capacity of LB-ITGB2-1 specific T cells to recognize primary AML cells directly *ex vivo*, we performed a flow cytometry experiment in which we measured upregulation of activation marker CD137 on LB-ITGB2-1 tetramer-positive T cells as circulating in peripheral blood after DLI. The data showed significant upregulation of CD137 on T-cell clone 1-55 after 36h of stimulation with unmanipulated AML cells that were positive for LB-ITGB2-1 and HLA-B*15:01 as compared to HLA-B*15:01 positive AML cells that were negative for LB-ITGB2-1 (Figure S4). However, numbers of LB-ITGB2-1 tetramer-positive T cells in peripheral blood were too low to draw firm conclusions.

Finally, we performed a colony forming assay to investigate the capacity of LB-ITGB2-1 specific T cells to kill the malignant hematopoietic progenitor cells as present in peripheral blood from our patient with CML at diagnosis. After overnight co-incubation of CML precursor cells with clone 1-55, a 50% reduction was measured in number of colonies differentiated into the granulocyte/macrophage (CFU-GM, CFU-G and CFU-M) or erythroid (CFU-E and BFU-E) lineage as well as in number of colonies from more early progenitor cells containing a mixture of cells differentiated into granulocyte/macrophage/erythroid lineages (Figure 5C). No decrease in number of colonies was observed when the sample was co-incubated with a negative control T-cell clone for HA-1H and no decrease in number of colonies was measured when clone 1-55 was co-incubated with a bone marrow sample from another patient with CML who was negative for LB-ITGB2-1 (CML 1159). In conclusion, the data demonstrated that LB-ITGB2-1 specific T cells are capable of mediating specific cytolysis of malignant hematopoietic (progenitor) cells, further supporting the therapeutic value of LB-ITGB2-1 as target for immunotherapy to induce GvL reactivity after alloSCT without GvHD.

Discussion

In this study, we identified two HLA-B*15:01-restricted MiHA targeted by CD8 T cells in a CML patient who reached complete remission after alloSCT and DLI. T cells for these MiHA showed strong recognition of patient CML-APC, but different reactivity against patient FB. Whereas clone 1-30 strongly recognized patient FB after pretreatment with IFN-γ, clone 1-55 consistently failed to recognize (IFN-γ pretreated) FB. We performed WGAs and identified SNP rs2275260 in the *GLE1* gene that encodes LB-GLE1-1V, the MiHA recognized by clone 1-30. For clone 1-55, associating SNP rs760462 in intron 3 of the *ITGB2* gene was found, but no SNP disparity could be detected in the normal *ITGB2* transcript between patient and donor. We here demonstrated that RNA-sequence analysis enabled discovery of LB-ITGB2-1 as MiHA encoded by an alternative transcript. LB-GLE1-1V and LB-ITGB2-1 have population frequencies of 35% and 21% in Caucasians (www.hapmap.org), resulting in disparity rates of 24% and 23%, respectively. LB-GLE1-1V and LB-ITGB2-1 are the first MiHA presented by HLA-B*15:01, which is expressed in approximately 7% of Caucasians[32]. As such, these MiHA may contribute to broaden immunotherapy to treat patients with hematological malignancies after alloSCT.

Since no SNP disparity was found in the normal *ITGB2* transcript, we investigated whether an alternative transcript could encode the MiHA. Alternative transcripts have previously been reported to encode ACC-6[15] and ZAPHIR[16]. ACC-6 is a MiHA that has been identified by screening a cDNA library, whereas ZAPHIR has been discovered by WGAs followed by cloning and screening transcript variants as detected by PCR. For *ITGB2*, we failed to detect splice variants by PCR using different primers. Retrospectively, this failure can be explained by absence of the forward or reverse primer binding site in the alternative *ITGB2* transcript. We therefore investigated *ITGB2* gene transcription by RNA-sequence analysis. In the GEUVADIS project, RNA-sequencing has been performed for EBV-B cell lines for which also whole genome data are available in the 1000GP, allowing us to select samples for the associating SNP as identified by WGAs. We demonstrated that associating SNP rs760462 functions as splice acceptor site, thereby creating an alternative transcript in which part of intron 3 is retained that encodes LB-ITGB2-1. We also demonstrated that antigens encoded by alternative transcripts that are generated by exon skipping can be elucidated by RNA-sequence analysis. As such, RNA-sequence analysis is a powerful tool to identify MiHA, but its value will extend beyond the field of alloSCT, since neoantigens and other immune targets may also be encoded by alternative transcripts.

In human melanoma and small cell lung carcinoma, tumor-specific mutations can create neoantigens. Neoantigens resemble minor histocompatibility antigens in that peptides are presented by HLA surface molecules and recognized by specific T cells[33]. The chance that neoantigens are targeted after antibody or T-cell therapy is dependent on mutational load and tumors with <1 mutations per Mb coding DNA have been proposed to present neoantigens only occasionally. This prediction, however, is based on the presence of tumor-specific mutations in coding exons leading to single amino acid changes in the normal protein reading frame, whereas alternative splicing, a mechanism that is frequently deregulated in cancer[34,35], has not been taken into consideration. However, when tumor-specific mutations in pre-mRNA sequences, spliceosomal components or regulatory factors lead to aberrant splicing, transcript variants can be produced that encode entirely new protein products. By producing these aberrant proteins, alternative splicing may create a repertoire of neoantigens that is larger than expected based on mutational load. Since alternative transcripts can be elucidated by RNA-sequence analysis, this technique may also be relevant to apply to cancer neoantigen discovery.

Since T cells for LB-ITGB2-1 strongly recognized patient CML-APC, but lacked reactivity against patient FB, and *ITGB2* has been reported as gene with hematopoiesis-restricted expression, we investigated whether LB-ITGB2-1 may be a new MiHA with therapeutic relevance. We confirmed hematopoiesis-restricted expression of the normal *ITGB2* transcript by microarray gene expression analysis and demonstrated that the alternative *ITGB2* transcript followed the same pattern of expression by q-PCR (Figure 4). Therapeutic relevance of LB-ITGB2-1 was supported by recognition and lysis of leukemic samples of different origins by specific T cells. Only two CML samples, both expressing low levels of the alternative *ITGB2* transcript, were not recognized. One sample was obtained from our patient at diagnosis prior to alloSCT. This sample mainly consisted of mature myelocytes, which are poor stimulators of an immune response. Previous work in our laboratory demonstrated that leukemic APC can be generated from CD34-positive CML precursor cells as illustrated by detection of *BCR-ABL*[36]. We therefore *in vitro* modified patient CML cells and used CML-APC to stimulate and isolate T cells after DLI. Our data demonstrated that CML-APC expressed increased levels of the alternative *ITGB2* transcript (Figure 4B) and mediated specific T-cell recognition and lysis (Figure 5). Thus, T cells for LB-ITGB2-1 as present in the DLI may have contributed to GvL reactivity *in vivo* by eliminating *BCR-ABL* positive CML precursor cells as detected during cytogenetic relapse after alloSCT. This is further substantiated by the finding that T cells for LB-ITGB2-1 are capable of mediating specific cytolysis of CML progenitor cells in a colony forming assay. Moreover, T cells for LB-ITGB2-1 may have contributed to GvL reactivity by eliminating CML cells with an acquired APC

phenotype *in vivo* either by co-infusion of IFN-α, which is known to accelerate the GvL response[5,6] or indirectly upon cytokine release by T cells with other specificities than LB-ITGB2-1. We previously demonstrated in a NOD/scid mouse model that human CML cells in lymphoid blast crisis can become professional APC after treatment with DLI[37]. In our patient, T cells for three other MiHA than LB-ITGB2-1 were detected after DLI (Figure S3), including LB-GLE1-V, which is strongly recognized on patient CML cells at diagnosis (Figure 5A). As such, T cells for LB-ITGB2-1 may have cooperated with other immune cells in mediating the anti-tumor response. In contrast to patient CML cells at diagnosis, the majority of unmodified leukemic samples were directly recognized and lysed by clone 1-55, suggesting that in most patients, T cells for LB-ITGB2-1 are capable of mediating GvL reactivity independent of whether the leukemic cells become professional APC.

In our patient, GvL reactivity after DLI was accompanied with development of grade II skin GvHD. Since *ITGB2* is not expressed in non-hematopoietic cell types and LB-ITGB2-1 could not be recognized on FB even after treatment with inflammatory cytokines, we consider it more likely that T cells with other specificities than LB-ITGB2-1 as measured in our patient after DLI (Figure S3) mediated or contributed to development of GvHD.

In summary, an integrated strategy of whole genome and transcriptome analysis enabled identification of LB-ITGB2-1 as HLA-B*15:01-restricted MiHA encoded by an alternative transcript. The alternative *ITGB2* transcript was shown to be expressed in leukemic cells of different origins, whereas no expression was found in non-hematopoietic cell types from organs that are often targeted in GvHD. In addition, T cells specifically recognized and lysed leukemic cells of different origins, whereas no reactivity was measured against patient FB. As such, our data demonstrate the discovery of a new hematopoiesis-restricted MiHA with therapeutic value to augment GvL reactivity after alloSCT without GvHD and illustrate the relevance of RNA-sequence analysis to identify immune targets that are encoded by alternative transcripts and created by genetic variants.

Acknowledgments

The authors would like to thank Mireille Toebes and Ton Schumacher for providing HLA-B*15:01 inclusion bodies.

Supplemental methods

Tetramer staining

PBMC from patient 6940 prior to DLI (168 days after alloSCT) and 9 weeks after DLI (232 days after alloSCT) were stained with PE-conjugated HLA-B*15:01 tetramers containing LB-ITGB2-1 (GQAGFFPSPF) or LB-GLE1-1V (GQVRLRALY), PE-conjugated HLA-A*02:01 tetramer containing LB-ADIR-1F[1], or APC-conjugated HLA-B*07:02 tetramer containing LRH-1[2]. Cells were subsequently stained with Alexa Fluor 700-conjugated CD8 (Invitrogen, Life Technologies, Carlsbad, CA, USA) in combination with FITC-conjugated CD4, CD14 and CD19 (BD/Pharmingen, San Diego, CA, USA). Propidium Iodide (PI) was added to exclude dead cells. Tetramer-positive T cells were measured within CD8-positive cells that were negative for CD4, CD14 and CD19. Tetramers were constructed as described previously[3] with minor modifications. Acquisition was performed on a LSRII analyzer (BD, San Jose, CA, USA) using DIVA software.

Ex vivo T-cell activation assay

PBMC from patient 6940 obtained 9 weeks after DLI (232 days after alloSCT) were thawed and CD8 T cells were isolated using the MACS CD8 untouched isolation kit according to manufacturer's instructions (Miltenyi Biotec). Primary AML-M5 samples were depleted of CD8 T cells using CD8 microbeads (Miltenyi Biotec). Peripheral blood CD8 T cells or clone 1-55 ($7x10^4$) were co-incubated for 36 hours with primary AML samples in a 1:1 stimulator:responder ratio. Cultures were stained with LB-ITGB2-1 or LB-ADIR-1F tetramers as described above, followed by staining with Alexa Fluor 700-conjugated CD8 (Invitrogen) and APC-conjugated CD137 in combination with FITC-conjugated CD4, CD14, CD19, CD33 and CD34 (BD/Pharmingen, San Diego, CA, USA). Propidium Iodide (PI) was added to exclude dead cells. Activated T cells that were double positive for CD137 and tetramer were measured within CD8-positive cells that were negative for CD4, CD14, CD19, CD33 and CD34. Acquisition was performed on a LSRII analyzer (BD) and analysis was performed using FlowJo Software (Tree Star, Inc, Ashland, OR, USA).

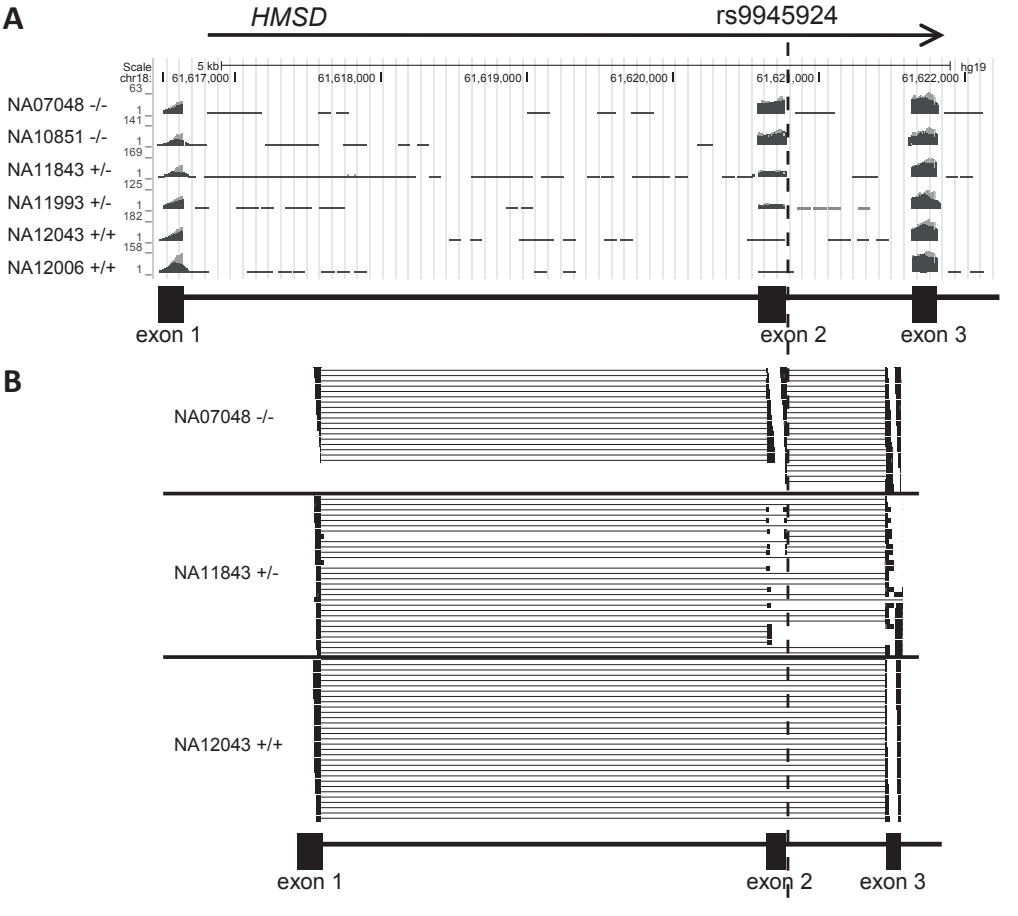

Supplemental Figure 1: RNA-sequence analysis allows discovery of antigens generated by exon skipping.

HMSD is located on chromosome 18q22.1 and is encoded on the forward strand. Graphs (A-B) are screenshots from the UCSC genome browser at http://genome.ucsc.edu. Exons are indicated by black rectangles. The genomic location of SNP rs9945924 is indicated by the vertical dotted line.

(A) RNA-sequence reads aligning with the *HMSD* gene in the HG19 human reference genome are shown as summarized peaks for 6 individuals representing different genotype groups for MiHA associating SNP rs9945924 (+/+, +/- and-/-).

(B) Single RNA-sequence reads aligning with the *HMSD* gene in the HG19 reference genome are shown for 3 individuals with different genotyping for MiHA associating SNP (+/+, +/- and-/-). All exon reads were excluded from this analysis, whereas intron and split reads were retained. Analysis of split reads (indicated by boxes connected with horizontal lines) showed that in-/- individuals, only reads for the full-length *HMSD* transcript (exon 1 connected to exon 2 and exon 2 connected to exon 3) are present. In +/- individuals, split reads for both the full-length as well as an alternative transcript (exon 1 connected to exon 3) are found, whereas only split reads for the alternative transcript were measured in +/+ individuals. These data show expression of an alternative transcript in which exon 2 is skipped in SNP-positive individuals.

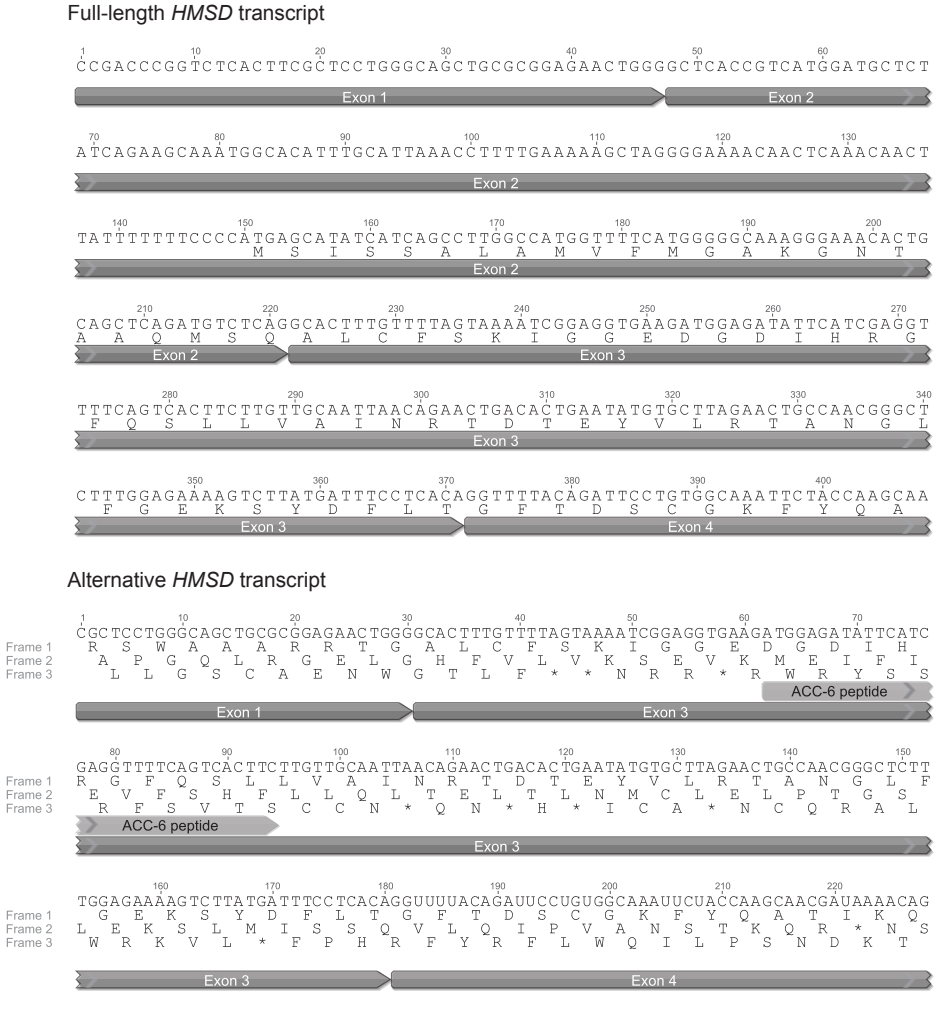

Supplemental Figure 2: Sequence composition of the alternative *HMSD* transcript.

Nucleotide and translated protein sequences as deduced from split read analysis are shown for the full-length and alternative *HMSD* transcripts. The alternative *HMSD* transcript is generated by exon 2 skipping, resulting in a transcript in which exon 1 is connected to exon 3 in which the normal translational start site is deleted. The alternative transcript was translated in three forward reading frames and the known ACC-6 epitope is depicted by the light gray bar. Sequences were depicted in Geneious (version 7.1.5 created by Biomatters, available from http://www.geneious.com/)

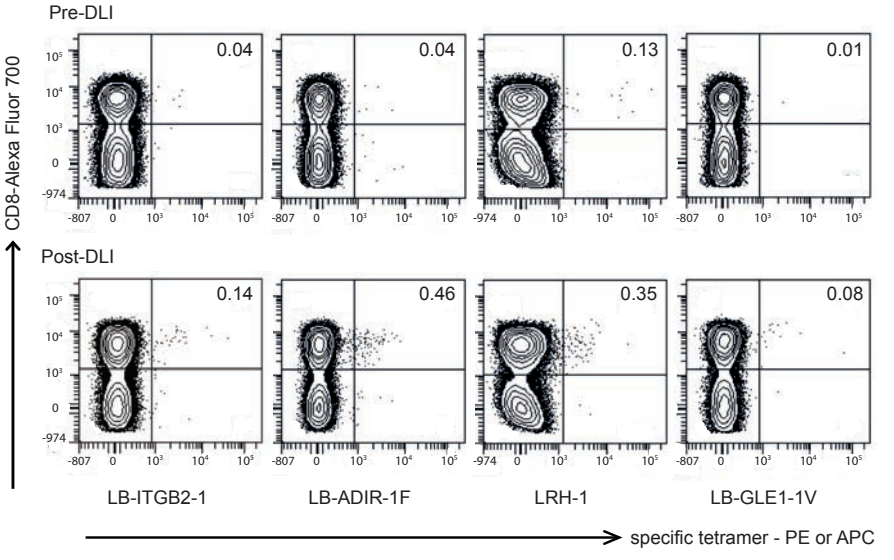

Supplemental Figure 3: T cells for LB-ITGB2-1 are detected after DLI

PBMC from patient 6940 before (upper panels) and 9 weeks after DLI (lower panels) were stained with PE-labeled HLA-tetramers for LB-ITGB2-1, LB-ADIR-1F or LB-GLE1-1V or the APC-labeled tetramer for LRH-1. Tetramer-positive T cells were measured within CD8-positive cells that were negative for CD4, CD14 and CD19. Indicated is the percentage of CD8 cells that are positive for the specific tetramer.

Table S1: predicted peptides for HMSD

Frame	Length (aa)	Peptide	Logscore	Affinity (nM)	Bind Level
2	9	GELGHFVLV	0.739	16	SB
2	9	SEVKMEIFI	0.619	61	WB
2	11	SEVKMEIFIEV	0.603	73	WB
2	11	MEIFIEVFSHF*	0.578	96	WB
2	9	IEVFSHFLL	0.825	6	SB
2	11	IEVFSHFLLQL	0.747	15	SB
2	9	TELTLNMCL	0.621	60	WB
2	11	TELTLNMCLEL	0.672	34	SB

* ACC-6 epitope

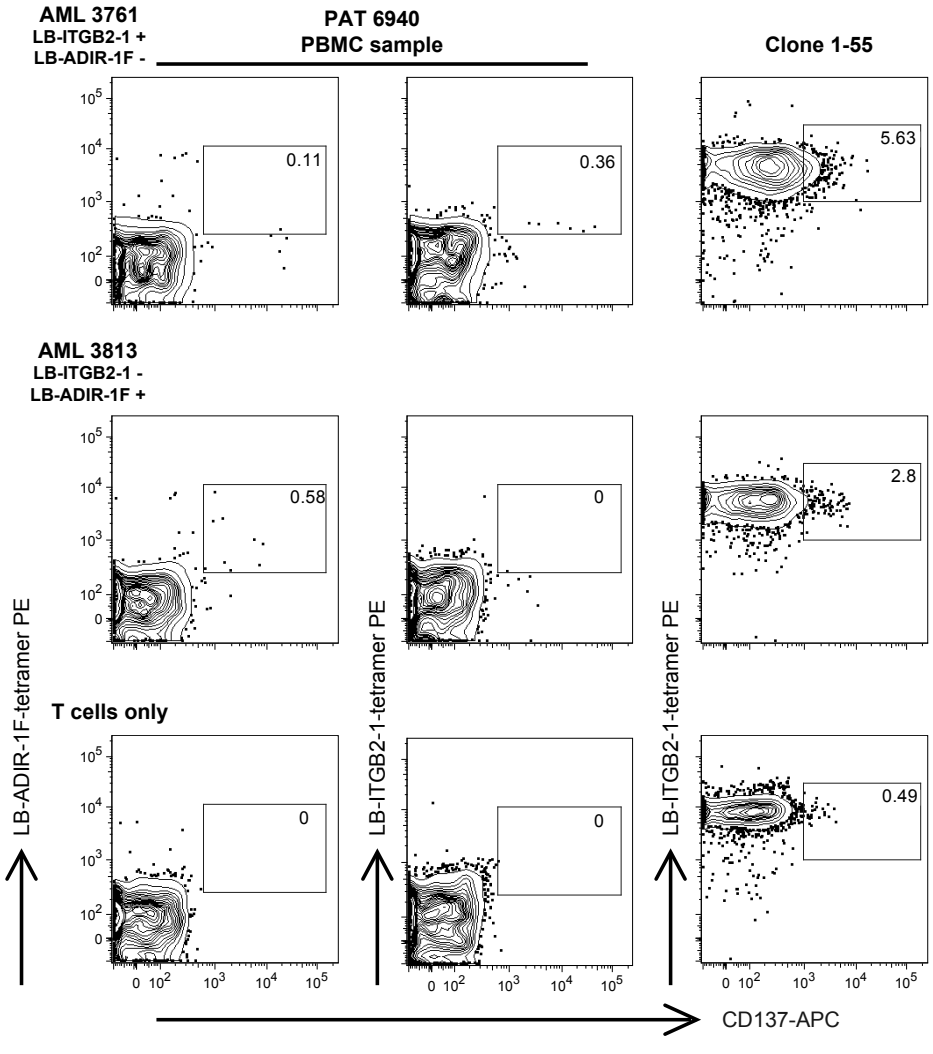

Supplemental Figure 4: *Ex vivo* activation of LB-ITGB2-1 specific T cells

CD8 T cells from PBMC from patient 6940 obtained 9 weeks after DLI (left and middle panels) and clone 1-55 (right panels) were co-incubated with primary AML-M5 samples for 36 hours. Cultures were stained with PE-labeled HLA-tetramers for LB-ITGB2-1 (middle and right panels) or LB-ADIR-1F (left panels) and subsequently with APC-labeled CD137 monoclonal antibody. Activated CD137-tetramer-double positive T cells were measured within CD8-positive cells that were negative for CD4, CD14, CD19, CD33 and CD34. Indicated is the percentage of CD8 cells that are double positive for the specific tetramer and CD137.

Reference list

1. Appelbaum FR. The current status of hematopoietic cell transplantation. Annu Rev Med. 2003;54:491-512.
2. Kolb HJ. Graft-versus-leukemia effects of transplantation and donor lymphocytes. Blood. 2008;112(12):4371-4383.
3. Spierings E. Minor histocompatibility antigens: past, present, and future. Tissue Antigens. 2014;84(4):374-360.
4. Barge RM, Starrenburg CW, Falkenburg JH, Fibbe WE, Marijt EW, Willemze R. Long-term follow-up of myeloablative allogeneic stem cell transplantation using Campath "in the bag" as T-cell depletion: the Leiden experience. Bone Marrow Transplant. 2006;37(12):1129-1134.
5. Eefting M, von dem Borne PA, de Wreede LC, et al. Intentional donor lymphocyte-induced limited acute graft-versus-host disease is essential for long-term survival of relapsed acute myeloid leukemia after allogeneic stem cell transplantation. Haematologica. 2014;99(4):751-758.
6. Posthuma EF, Marijt EW, Barge RM, et al. Alpha-interferon with very-low-dose donor lymphocyte infusion for hematologic or cytogenetic relapse of chronic myeloid leukemia induces rapid and durable complete remissions and is associated with acceptable graft-versus-host disease. Biol Blood Marrow Transplant. 2004;10(3):204-212.
7. Kawase T, Nannya Y, Torikai H, et al. Identification of human minor histocompatibility antigens based on genetic association with highly parallel genotyping of pooled DNA. Blood. 2008;111(6):3286-3294.
8. Bleakley M, Riddell SR. Exploiting T cells specific for human minor histocompatibility antigens for therapy of leukemia. Immunol Cell Biol. 2011;89(3):396-407.
9. Van Bergen CAM, Rutten CE, Van Der Meijden ED, et al. High-throughput characterization of 10 new minor histocompatibility antigens by whole genome association scanning. Cancer Res. 2010;70(22):9073-9083.
10. Griffioen M, Honders MW, van der Meijden ED, et al. Identification of 4 novel HLA-B*40:01 restricted minor histocompatibility antigens and their potential as targets for graft-versus-leukemia reactivity. Haematologica. 2012;97(8):1196-1204.
11. Spaapen RM, de Kort RA, van den Oudenalder K, et al. Rapid identification of clinical relevant minor histocompatibility antigens via genome-wide zygosity-genotype correlation analysis. Clin Cancer Res. 2009;15(23):7137-7143.
12. Spaapen RM, Lokhorst HM, van den Oudenalder K, et al. Toward targeting B cell cancers with CD4+ CTLs: identification of a CD19-encoded minor histocompatibility antigen using a novel genome-wide analysis. J Exp Med. 2008;205(12):2863-2872.
13. Bleakley M, Otterud BE, Richardt JL, et al. Leukemia-associated minor histocompatibility antigen discovery using T-cell clones isolated by in vitro stimulation of naive CD8+ T cells. Blood. 2010;115(23):4923-4933.
14. Warren EH, Fujii N, Akatsuka Y, et al. Therapy of relapsed leukemia after allogeneic hematopoietic cell transplantation with T cells specific for minor histocompatibility antigens. Blood. 2010;115(19):3869-3878.
15. Kawase T, Akatsuka Y, Torikai H, et al. Alternative splicing due to an intronic SNP in HMSD generates a novel minor histocompatibility antigen. Blood. 2007;110(3):1055-1063.
16. Broen K, Levenga H, Vos J, et al. A polymorphism in the splice donor site of ZNF419 results in the novel renal cell carcinoma-associated minor histocompatibility antigen ZAPHIR. PLoS One. 2011;6(6):e21699.
17. Oostvogels R, Lokhorst HM, Minnema MC, et al. Identification of minor histocompatibility antigens based on the 1000 Genomes Project. Haematologica. 2014;99(12):1854-1859.
18. Lappalainen T, Sammeth M, Friedlander MR, et al. Transcriptome and genome sequencing uncovers functional variation in humans. Nature. 2013;501(7468):506-511.

19. t Hoen PA, Friedlander MR, Almlof J, et al. Reproducibility of high-throughput mRNA and small RNA sequencing across laboratories. Nat Biotechnol. 2013;31(11):1015-1022.

20. Genomes Project C, Abecasis GR, Auton A, et al. An integrated map of genetic variation from 1,092 human genomes. Nature. 2012;491(7422):56-65.

21. Jedema I, Meij P, Steeneveld E, et al. Early detection and rapid isolation of leukemia-reactive donor T cells for adoptive transfer using the IFN-gamma secretion assay. Clin Cancer Res. 2007;13(2 Pt 1):636-643.

22. Heemskerk MH, Hoogeboom M, de Paus RA, et al. Redirection of antileukemic reactivity of peripheral T lymphocytes using gene transfer of minor histocompatibility antigen HA-2-specific T-cell receptor complexes expressing a conserved alpha joining region. Blood. 2003;102(10):3530-3540.

23. Kent WJ, Sugnet CW, Furey TS, et al. The human genome browser at UCSC. Genome Res. 2002;12(6):996-1006.

24. Lundegaard C, Lund O, Nielsen M. Accurate approximation method for prediction of class I MHC affinities for peptides of length 8, 10 and 11 using prediction tools trained on 9mers. Bioinformatics. 2008;24(11):1397-1398.

25. Nielsen M, Lundegaard C, Worning P, et al. Reliable prediction of T-cell epitopes using neural networks with novel sequence representations. Protein Sci. 2003;12(5):1007-1017.

26. Kremer AN, van der Meijden ED, Honders MW, et al. Endogenous HLA class II epitopes that are immunogenic in vivo show distinct behavior toward HLA-DM and its natural inhibitor HLA-DO. Blood. 2012;120(16):3246-3255.

27. Edgar R, Domrachev M, Lash AE. Gene Expression Omnibus: NCBI gene expression and hybridization array data repository. Nucleic Acids Res. 2002;30(1):207-210.

28. Jahn L, Hombrink P, Hassan C, et al. Therapeutic targeting of the BCR-associated protein CD79b in a TCR-based approach is hampered by aberrant expression of CD79b. Blood. 2015;125(6):949-958.

29. van Bergen CA, Kester MG, Jedema I, et al. Multiple myeloma-reactive T cells recognize an activation-induced minor histocompatibility antigen encoded by the ATP-dependent interferon-responsive (ADIR) gene. Blood. 2007;109(9):4089-4096.

30. de Rijke B, van Horssen-Zoetbrood A, Beekman JM, et al. A frameshift polymorphism in P2X5 elicits an allogeneic cytotoxic T lymphocyte response associated with remission of chronic myeloid leukemia. J Clin Invest. 2005;115(12):3506-3516.

31. Hickstein DD, Hickey MJ, Collins SJ. Transcriptional regulation of the leukocyte adherence protein beta subunit during human myeloid cell differentiation. J Biol Chem. 1988;263(27):13863-13867.

32. Gonzalez-Galarza FF, Christmas S, Middleton D, Jones AR. Allele frequency net: a database and online repository for immune gene frequencies in worldwide populations. Nucleic Acids Res. 2011;39:D913-919.

33. Schumacher TN, Schreiber RD. Neoantigens in cancer immunotherapy. Science. 2015;348(6230):69-74.

34. Dehm SM. mRNA Splicing Variants: Exploiting Modularity to Outwit Cancer Therapy. Cancer Research. 2013;73(17):5309-5314.

35. Daguenet E, Dujardin G, Valcárcel J. The pathogenicity of splicing defects: mechanistic insights into pre-mRNA processing inform novel therapeutic approaches. EMBO reports. 2015;16(12):1640-1655.

36. Smit WM, Rijnbeek M, van Bergen CA, et al. Generation of dendritic cells expressing bcr-abl from CD34-positive chronic myeloid leukemia precursor cells. Hum Immunol. 1997;53(2):216-223.

37. Stevanovic S, van Schie ML, Griffioen M, Falkenburg JH. HLA-class II disparity is necessary for effective T cell mediated Graft-versus-Leukemia effects in NOD/scid mice engrafted with human acute

lymphoblastic leukemia. Leukemia. 2013;27(4):985-987.

38. Amir AL, van der Steen DM, Hagedoorn RS, et al. Allo-HLA-reactive T cells inducing graft-versus-host disease are single peptide specific. Blood. 2011;118(26):6733-6742.

39. Kloosterboer FM, van Luxemburg-Heijs SAP, Soest RAv, et al. Direct cloning of leukemia-reactive T cells from patients treated with donor lymphocyte infusion shows a relative dominance of hematopoiesis-restricted minor histocompatibility antigen HA-1 and HA-2 specific T cells. Leukemia. 2004;18(4):798-808.

Supplemental Reference list

1. van Bergen CA, Kester MG, Jedema I, et al. Multiple myeloma-reactive T cells recognize an activation-induced minor histocompatibility antigen encoded by the ATP-dependent interferon-responsive (ADIR) gene. Blood. 2007;109(9):4089-4096.

2. de Rijke B, van Horssen-Zoetbrood A, Beekman JM, et al. A frameshift polymorphism in P2X5 elicits an allogeneic cytotoxic T lymphocyte response associated with remission of chronic myeloid leukemia. J Clin Invest. 2005;115(12):3506-3516.

3. Burrows SR, Kienzle N, Winterhalter A, Bharadwaj M, Altman JD, Brooks A. Peptide-MHC class I tetrameric complexes display exquisite ligand specificity. J Immunol. 2000;165(11):6229-6234.

6

SUMMARY AND GENERAL DISCUSSION

Summary

Allogeneic stem cell transplantation (alloSCT) can be a curative treatment for hematological malignancies. However, the desired anti-tumor or Graft-versus-Leukemia (GvL) effect is often accompanied by undesired side effects, a complication known as Graft-versus-Host Disease (GvHD). GvL and GvHD are both caused by donor-derived T cells recognizing alloantigens on patient cells. The main challenge for treatment of hematological malignancies with alloSCT is to evoke an effective GvL response, while limiting the risk of severe GvHD.

One strategy to reduce GvHD is depletion of donor T cells from the stem cell graft. However, T-cell depletion also reduces the anti-tumor effect, and therefore, donor T cells are often administered after alloSCT by donor lymphocyte infusion (DLI) to reinstall GvL reactivity. In HLA-matched alloSCT, alloantigens recognized by donor T cells are polymorphic peptides presented by HLA surface molecules on patient cells, the so-called minor histocompatibility antigens (MiHA). Depending on the tissue distribution of the MiHA that are targeted, donor T cells can mediate GvL in the absence or presence of GvHD. Donor T cells recognizing MiHA on the malignant hematopoietic cells of the patient mediate GvL reactivity, whereas donor T cells recognizing MiHA that are expressed on healthy non-hematopoietic tissues induce GvHD. MiHA with hematopoiesis-restricted expression are relevant targets for immunotherapy, since donor T cells for these MiHA will attack the malignant cells of the patient, while sparing healthy hematopoietic cells of donor origin. In this thesis, *in vivo* immune responses after alloSCT and DLI were analyzed with respect to specificity, diversity, frequency and dynamics of MiHA-specific T cells. This analysis is relevant (1) to provide insight into the immunobiology of GvL and GvHD after alloSCT and (2) to identify MiHA with restricted expression on hematopoietic cells as potential targets for T-cell therapy to stimulate GvL reactivity after alloSCT without GvHD.

MiHA can be identified by strategies in which alloreactive T cells from patients with clinical immune responses after alloSCT are isolated and characterized for their specificity and potential role in GvL and GvHD. In Whole Genome Association scanning (WGAs), T-cell recognition of a panel of test cells is investigated for association with individual SNPs to discover new MiHA. Most MiHA identified thus far are generated by non-synonymous SNPs in primary gene transcripts. However, the frequencies of MiHA encoded by other genetic variations are likely to be underestimated, since polymorphisms in coding regions are generally more easily identified by current discovery techniques. This thesis is focused on efficient characterization of MiHA with potential therapeutic relevance, including MiHA that are encoded or produced by alternative transcripts.

In **chapter 2** we describe a microarray gene expression database in which cell types are included that are often targeted in GvL and GvHD. The dataset was designed to provide a platform for efficient generation of expression profiles. Malignant and healthy hematopoietic cell samples as well as non-hematopoietic cell types cultured under normal and inflammatory conditions were included. Gene expression was investigated by Illumina HT12.0 microarrays and quality control analysis confirmed the cell-type origin of the samples and excluded contamination with peripheral blood cells. Microarray data were validated by quantitative RT-PCR (q-PCR) and a strong correlation in gene expression was observed between both platforms. We also established an inflammatory gene signature by comparing microarray data from different non-hematopoietic cells after pre-treatment with IFN-γ. Furthermore, we demonstrated the value of the microarray dataset to estimate efficacy and toxicity of potential targets for immunotherapy of hematological malignancies and concluded that our microarray database provides a relevant platform to analyze and select candidate antigens with hematopoietic (lineage)-restricted expression as potential targets for immunotherapy of hematological cancers.

In **chapter 3** we characterized LB-ARHGDIB-1R as MiHA with potential therapeutic relevance after alloSCT. Using microarray gene expression analysis as described in **chapter 2**, we demonstrated that expression of *ARHGDIB* is hematopoiesis-restricted with the exception of intermediate mRNA expression in endothelial cells. T-cell recognition experiments confirmed hematopoiesis-restricted expression, since skin-derived fibroblasts and keratinocytes were not recognized even when cultured under inflammatory conditions. Intermediate *ARHGDIB* gene expression in endothelial cells was confirmed by q-PCR, but recognition of endothelial cells by LB-ARHGDIB-1R-specific T cells was limited and only observed under inflammatory conditions. In contrast, recognition of primary leukemic cells was strong and LB-ARHGDIB-1R-specific T cells were capable of mediating specific lysis in long-term cytotoxicity assays. Finally, we investigated the *in vivo* immunogenicity of LB-ARHGDIB-1R and found specific T cells in 8 out of 10 transplanted patients of which 4 responses could be measured directly *ex vivo*. One patient with relapsed Non-Hodgkin's lymphoma showed high T-cell frequencies after DLI, coinciding with induction of long-lasting GvL reactivity without GvHD. The data thus support the relevance of LB-ARHGDIB-1R as therapeutic target with potential to induce selective GvL reactivity after alloSCT.

Although WGAs is an efficient method, MiHA discovery failed for 20-30% of T-cell clones for which associating SNPs were successfully identified by WGAs using a panel of EBV-B cell lines that are genotyped for 1.1M SNPs. For these T-cell clones, associating SNPs were found outside known exons and no SNP

disparities were present in primary gene transcripts. Therefore, in **chapter 4** we adopted an 'inferred correlation' approach using whole genome data from the 1000 Genomes Project and identified LB-TTK-1D as new MiHA. SNP rs240226 was identified as the genetic variation that encodes this MiHA and the SNP was shown to be located in an alternative transcript of the *TTK* gene. In this alternative transcript, which is composed of 5 exons, a premature termination codon is present in exon 4, that targets the transcript to rapid degradation by nonsense mediated decay (NMD). LB-TTK-1D has been identified as first human natural T-cell target that is translated from an endogenous NMD transcript. Expression of the alternative *TTK* transcript was barely detectable as confirmed by q-PCR and LB-TTK-1D-specific T cells were shown to recognize cell types of hematopoietic as well as non-hematopoietic origin. Strikingly, despite low expression of the alternative *TTK* transcript, T cells for LB-TTK-1D showed robust recognition of EBV-LCLs while they failed to recognize the majority of primary leukemic samples, indicating that T-cell recognition also depends on other factors than gene expression and presence of the SNP and HLA-A*02:01 restriction allele. These findings are important for prospective MiHA identification studies and contribute to our understanding of the biology behind epitope generation in effective immune responses.

In **chapter 5**, we implemented whole transcriptome analysis in our WGAs approach and successfully identified LB-ITGB2-1 as MiHA encoded by an alternative transcript. WGAs identified an associating SNP rs760462 in the *ITGB2* gene and subsequent RNA-sequence analysis revealed a region with transcriptional activity in intron 3 directly downstream from the associating SNP. Analysis of single RNA-sequence reads showed that rs760462 introduced a cryptic splice site and created an alternative transcript that is only expressed in MiHA-positive individuals. The immunogenic epitope was translated from the alternative transcript downstream from the SNP. We also demonstrated that RNA-sequence analysis allows discovery of antigens generated by exon skipping as illustrated for ACC-6, which is a MiHA translated from an alternative transcript of *HMSD*. We further analyzed the therapeutic value of LB-ITGB2-1 and found that the tissue distribution of the alternative transcript followed expression of the normal *ITGB2* transcript. Expression of the normal and alternative *ITGB2* transcripts was hematopoiesis-restricted, which was confirmed by lack of T-cell reactivity against fibroblasts even under inflammatory conditions. In contrast, LB-ITGB2-1-specific T cells were clearly capable of mediating specific recognition and cytolysis of malignant hematopoietic (progenitor) cells, further supporting the therapeutic value of LB-ITGB2-1 as target for immunotherapy to induce GvL reactivity after alloSCT without GvHD.

In summary, we efficiently identified and characterized various MiHA that are generated by different mechanisms. Microarray gene expression data were successfully used to estimate the tissue distribution of the MiHA and whole genome and transcriptome data were implemented in the WGAs approach to allow identification of MiHA encoded by alternative transcripts. By combining these strategies, we are now able to efficiently identify a large variety of MiHA, evaluate their role in GvL or GvHD and select hematopoiesis-restricted candidates with potential relevance for immunotherapy after alloSCT.

General discussion

Discovery of minor histocompatibility antigens

Most currently known MiHA have been identified by a forward approach in which T cells isolated from *in vivo* immune responses are used to identify antigens[1]. To focus forward approaches on discovery of MiHA with therapeutic relevance, T cells can be specifically isolated for their reactivity against patient leukemic cells or other hematopoietic cells of patient origin based on surface expression of activation marker CD137 after *in vitro* stimulation. Furthermore, T cells can be screened for their reactivity against patient fibroblasts cultured in the absence or presence of IFN-γ already in the first round of screening to rapidly separate T-cell clones for broadly expressed MiHA from T-cell clones recognizing potential hematopoiesis-restricted MiHA. This strategy has been followed in **chapter 5** and led to successful discovery of LB-ITGB2-1 as new MiHA with potential therapeutic relevance. In reverse strategies, peptides encoded by genes with hematopoiesis-restricted expression are selected to search for specific T cells[2]. Although the reverse strategy allows for more direct identification of hematopoietic MiHA, the method is based on prediction of HLA binding peptides by computer algorithms and often leads to detection of T cells that fail to recognize antigens that are naturally processed and presented on malignant cells[3]. Inclusion of an additional step for selection of peptides that are present in the HLA ligandome of EBV-LCL or leukemic cells improves the efficiency of the reverse strategy to identify antigens that are truly presented on the cell surface[4,5], but decreases the sensitivity of the approach, since not all T-cell epitopes can be detected as eluted peptides in the HLA ligandome by mass spectrometry. Furthermore, in reverse strategies, a number of HLA alleles need to be selected to predict HLA binding by the algorithm and, if pMHC-multimers are needed for T-cell isolation, only HLA alleles can be selected for which these complexes can be produced.

In a reverse strategy that has been followed in our laboratory by Hombrink et al.[3], peptides encoded by the hematopoiesis-restricted *ITGB2* gene were initially selected as candidate targets with therapeutic relevance, but no high avidity T cells for these peptides could be found. In **chapter 5** of this thesis, LB-ITGB2-1 has successfully been identified as new hematopoiesis-restricted MiHA by a forward approach. There are several reasons why discovery of this epitope by the reverse strategy failed. First, LB-ITGB2-1 is presented by HLA-B*15:01, which has not been selected as HLA class I allele in the NetMHC prediction algorithm of the reverse strategy. Second, the MiHA is encoded by an alternative transcript in which intron sequences are retained and only peptide candidates encoded

by exon regions were included in the reverse strategy. Finally, the SNP that is present in the patient and absent in the donor genome functioned as splice acceptor site and created a new transcript. The MiHA was not directly encoded by the SNP, but translated from an intron region that is located downstream from the SNP, while only peptide candidates with polymorphic amino acids that are directly encoded by SNPs were selected in the reverse strategy. As such, the MiHA as identified in this thesis by forward approaches provide relevant insight into which steps of the reverse approach should be improved to make the strategy more efficient.

Whole Genome Association scanning

WGAs is an efficient method for MiHA discovery. In WGAS, T-cell recognition of a panel of test cells is investigated for association with individual SNP genotypes[6-9]. This strategy led to successful discovery of LB-ARHGDIB-1R (**chapter 3**), LB-TTK-1D (**chapter 4**) and LB-ITGB2-1 (**chapter 5**). Although WGAS is an efficient method, MiHA discovery still fails for approximately 20-30% of T-cell clones for which associating SNPs in intron regions have been found, but no SNP disparity is present in the primary gene transcript. These MiHA are likely encoded by alternative transcripts in which intron sequences are retained. In this thesis, we successfully implemented publicly available whole genome and transcriptome data to enable discovery of MiHA encoded by alternative transcripts.

Recently, Oostvogels et al.[10] described the use of whole genome data from the 1000 Genomes Project[11] for identification of a MiHA that could not be elucidated with EBV-LCL that were SNP-genotyped with lower resolution. Publicly available whole genome data can thus successfully be applied to increase the efficiency of MiHA discovery. In **chapter 4**, we followed a similar approach and applied whole genome data from the 1000 Genomes Project in an 'inferred correlation' analysis for identification of LB-TTK-1D. The strongest associating SNP in the 'inferred correlation' is located in an intron region that is included as alternative exon in a transcript splice variant. In contrast to LB-ITGB2-1, the SNP directly encodes the MiHA and the alternative transcript is expressed in both patient and donor cells. Identification of LB-TTK-1D thus illustrates that MiHA discovery is most efficient when WGAs is performed with a panel of test cells of which all SNPs as present in the entire genome are known. Furthermore, in **chapter 5** we investigated whether publicly available RNA-sequence data can be used to elucidate alternative transcripts, thereby facilitating discovery of MiHA that are encoded by intron sequences or other regions located outside known exons. We developed an integrated whole genome and transcriptome analysis method in which WGAs and RNA-sequence data are combined and successfully identified LB-ITGB2-1 as new hematopoiesis-restricted MiHA. A major advantage of RNA-

sequence data is that the exact architecture of the transcript can be revealed and that actual gene sequences are shown that are involved in transcription and splicing. As such, whole genome and transcriptome methods may significantly contribute to discovery of MiHA that are encoded by alternative transcripts, a category of MiHA that has previously been underestimated as compared to MiHA that are encoded by non-synonymous SNPs in primary gene transcripts. Characterization of MiHA that are encoded by alternative transcripts also provides additional insight into mechanisms of transcription, translation and antigen processing and presentation. LB-TTK-1D, for example, is a MiHA encoded by a transcript that is targeted by nonsense mediated RNA decay. As shown in **chapter 4**, the alternative transcript of *TTK* is barely detectable in all cell types tested, but the MiHA is produced in EBV-B cells at levels that are sufficient to be consistently recognized by the T-cell clone, demonstrating that aberrant protein products as translated from alternative transcripts can provide a relevant source of T-cell antigens.

Therapeutic minor histocompatibility antigens

Targeting therapeutic MiHA allows for selective induction of GvL after alloSCT without GvHD. However, only a limited number of MiHA have thus far been reported to be therapeutically relevant. Effective identification and characterization methods have resulted in an increase in known MiHA and the criteria for therapeutic relevance need to be strictly defined to distinguish therapeutic MiHA from other antigens. In this thesis, the following criteria for therapeutic MiHA have been taken into consideration. First, gene expression for therapeutic MiHA should be hematopoiesis-restricted. Second, hematopoiesis-restricted expression of the MiHA should be confirmed by T-cell recognition. Third, MiHA-specific T cells should be capable of mediating specific lysis of primary leukemic cells. Finally, MiHA should be relevant targets for immunotherapy in a substantial number of transplanted patients based on population frequency of the MiHA (optimal frequency between 20-80%) and HLA class I restriction allele (frequency of at least 5%) and presence of donor T cells in the transplanted immune system that are capable of targeting the MiHA. The latter criterion is only required if MiHA-specific T cells in therapeutic strategies need to be induced *in vivo* or isolated from *in vivo* immune responses.

As first step in MiHA characterization, gene expression profiles are determined to select MiHA with hematopoiesis-restricted expression. Microarray and RNA-sequence data allow efficient analysis of gene expression profiles irrespective of HLA type and MiHA status. Although gene expression data from various platforms have become increasingly available over the years through online tools such as Gene Expression Omnibus, the value of these datasets for selection of genes

with hematopoiesis-restricted expression remains limited due to potential contamination of non-hematopoietic tissues with peripheral blood cells and no possibility to investigate gene expression under inflammatory conditions. We therefore performed microarray gene expression analysis as described in **chapter 2** on various cell types involved in GvL and GvHD and cultured specific non-hematopoietic cell types in the absence and presence of IFN-γ to exclude contamination with peripheral blood cells and enable gene expression analysis under inflammatory conditions. We showed that expression of largely the same set of genes is induced by IFN-γ as compared to T-cell culture supernatant in which multiple cytokines including IFN-γ, IL-13, TNF-α and IL-2 were released. As such, we established a gene expression signature for inflammation and demonstrated that IFN-γ can be used as single agent to mimic inflammation.

Disadvantages of microarray data are that reliable gene expression analysis between different cell types requires good probe quality and that quantitative expression analysis between different genes is not possible due to differences in probe quality. Collection of RNA-sequence data from a panel of hematopoietic and non-hematopoietic cell types would be ideal to enable direct comparison of gene expression irrespective of probe quality. RNA-sequence data would also provide the additional advantage to investigate expression of alternative transcripts. As described in **chapter 4**, we developed q-PCR to measure expression of the normal *TTK* transcript, since quality of the microarray probe was poor and did not allow gene expression analysis. This in contrast to the microarray probe for the normal *ITGB2* transcript for which a reliable hematopoiesis-restricted gene expression profile could be established in **chapter 5**. In both chapters, we also developed q-PCR to measure expression of the alternative transcripts that encode LB-TTK-1D and LB-ITGB2-1, illustrating the benefit that RNA-sequence data would provide as high-throughput platform to measure and compare expression of normal and alternative gene transcripts.

The question remains how strict the requirement for hematopoiesis-restricted expression needs to be followed in order to use MiHA as targets for immunotherapy for selective GvL induction. In **chapter 3**, we showed intermediate expression of *ARHGDIB* in endothelial cells, but there was no evidence for systemic toxicity as a result of vascular damage in any of the patients with circulating LB-ARHGDIB-1R-specific T cells, suggesting that MiHA with predominant expression in hematopoietic cells may also be relevant targets for immunotherapy.

As second step, T-cell recognition experiments are performed to confirm hematopoiesis-restricted expression of the MiHA. MiHA will only be selected as candidates with potential therapeutic relevance when their specific T cells are capable of recognizing primary leukemic cells and fail to recognize non-hematopoietic cell types. This approach is limited by the availability of samples that are positive for the relevant MiHA and HLA restriction allele. Skin-derived fibroblasts can be quite easily obtained and cultured and are therefore commonly included as non-hematopoietic targets. In our T-cell recognition experiments, skin fibroblasts are also pre-treated for 4 days with IFN-γ, since we previously noticed that T-cell recognition is often significantly enhanced when skin fibroblasts are cultured under inflammatory conditions[12,13]. This is probably due to stimulated intracellular antigen processing and presentation and increased surface expression of HLA class I, adhesion and co-stimulatory molecules, thereby lowering the threshold for T-cell recognition. This is also illustrated for LB-GLE-1V in **chapter 5**. T cells for this broadly expressed MiHA strongly react with skin fibroblasts after pre-treatment with IFN-γ, whereas they fail to recognize these cells when cultured in the absence of IFN-γ. In **chapter 3** we investigated potential toxicity of LB-ARHGDIB-1R-specific T cells against endothelial cells, since intermediate *ARHGDIB* expression was measured in these cells by microarray expression analysis and q-PCR. The data showed that T cells for LB-ARHGDIB-1R strongly recognized primary leukemic cells of different origin, while T-cell reactivity against human umbilical vein endothelial cells was limited even when cultured under inflammatory conditions. The necessity to measure T-cell recognition of primary leukemic cells and non-hematopoietic cell types is also illustrated by T cells for LB-TTK-1D. Induction of T cells for LB-TTK-1D coincided with GvL reactivity and EBV-LCL are strongly recognized in WGAs, but T cells for LB-TTK-1D failed to recognize the majority of primary leukemic samples in **chapter 4**, while fibroblasts were recognized. This demonstrates that gene expression can be used as first step to distinguish hematopoiesis-restricted MiHA with potential therapeutic relevance from other MiHA that are more broadly expressed, but that T-cell recognition experiments remain required to demonstrate surface presentation of the MiHA on primary leukemic cells and confirm lack of reactivity against non-hematopoietic cells.

As third step cytotoxicity assays are performed to confirm actual lysis of primary leukemic cells by the MiHA-specific T cells. Cytotoxicity assays include 4 hours chromium-release assays, overnight to 48 hours FACS-based survival assays and colony forming assays after overnight co-incubation of hematopoietic progenitor cells with MiHA-specific T cells. We selected all hematopoiesis-restricted MiHA for which T-cell mediated lysis could be detected in any assay as MiHA with potential therapeutic relevance, but noticed significant differences in cytotoxic potential. As described in **chapter 3 and 5**, T cells for LB-ARHGDIB-

1R and LB-ITGB2-1 mediated specific lysis of primary leukemic samples only after long-term co-incubation, whereas T cells for HA-1 were already capable of mediating specific lysis of primary leukemic cells after 4 hours of co-incubation. It is unknown whether this difference in cytolytic capacity between MiHA-specific T cells is entirely mediated by the affinity of the TCR for its peptide-HLA complex or whether also other factors such as expression of adhesion and co-stimulatory or co-inhibitory molecules or T-cell maturation contribute to their capacity to degranulate and release cytotoxic mediators. Therefore, TCR gene transfer experiments in which different MiHA-specific TCRs are introduced into the same virus-specific T cells are relevant to confirm that the affinity of the TCR for the MiHA as presented by HLA class I on primary leukemic cells is sufficiently high to mediate strong specific lysis. The actual contribution of MiHA-specific T cells to the anti-tumor response, however, still requires detailed analysis of the specificity, diversity and frequency of *in vivo* immune responses in GvL and GvHD. This analysis may provide relevant insight whether the requirement for cytotoxic potential of MiHA-specific T cells as measured *in vitro* needs to be more strictly defined.

The fourth step in selection of MiHA with potential therapeutic relevance is to determine their immunogenicity. However, this step is only relevant for therapies in which MiHA-specific T cells are induced *in vivo* or isolated from *in vivo* immune responses after alloSCT. In **chapter 3** we demonstrate that LB-ARHGDIB-1R is immunogenic in 80% of MiHA-disparate patient-donor pairs and is therefore the most immunogenic MiHA identified thus far[14]. Different factors may contribute to *in vivo* immunogenicity, including the number and affinity of different TCRs that are capable of recognizing the MiHA in the naïve repertoire of donor T cells, to which extent the peptide is “foreign” for the donor immune system and the level of surface expression of the MiHA on antigen presenting cells, which is relevant for induction of an effective immune response. More insight into these mechanisms would allow better application of different active and passive forms of immunotherapy for hematological malignancies in which MiHA are used as targets.

Immunobiology of GvL and GvHD

Although *in vivo* immune responses as induced after alloSCT have been analyzed in detail in a number of patients, the exact composition and difference in immune responses in GvL and GvHD is still not fully understood. GvL and GvHD are both mediated by polyclonal T-cell responses in which multiple MiHA are targeted, but frequencies of MiHA-specific T cells in patients with GvHD are higher than in patients without GvHD (van Bergen et al., 2016, submitted). Furthermore, there is no strict separation of GvL and GvHD based on the tissue distribution of MiHA,

since T cells for broadly-expressed and hematopoiesis-restricted MiHA are induced in both patient groups. The MiHA-specificities as described in **chapter 5** of this thesis showed a similar pattern: T cells for hematopoiesis-restricted LRH-1 and LB-ITGB2-1 and T cells for broadly expressed LB-ADIR-1F and LB-GLE1-1V were isolated from the same patient with combined GvL and GvHD after DLI. Since immune responses in GvHD are generally strong, it can be hypothesized that T-cell reactivity against non-hematopoietic tissues needs to exceed a certain threshold in order to develop GvHD. This suggests that for selective induction of GvL, MiHA with predominant expression in hematopoietic cells may also be therapeutically relevant as long as recognition of non-hematopoietic tissues remains below the threshold.

Analysis of the *in vivo* immune response in **chapter 5** also resulted in T-cell isolation for known MiHA, i.e. LRH-1 and LB-ADIR-1F. The finding that T cells for known MiHA are often found in different patients has been described previously[14,15], but is unexpected based on the number of non-synonymous SNPs that two unrelated individuals differ from each other (~10,000) and suggests that the total number of existing MiHA may be restricted and follow rules for immunodominance which cannot be predicted by measuring SNP disparities. It is unknown which factors determine the immunogenicity of an HLA binding peptide. Surface expression of the MiHA on professional APC may be critical, since these cells are known to prime specific T cells in the initiation phase of the immune response. However, the affinity and diversity of TCRs as expressed by T cells in the naïve donor repertoire that are able to react with a specific MiHA is probably also important and may depend on surface expression of the MiHA on the APC. If the total number of existing MiHA is indeed restricted, it can be expected that the majority of MiHA will be identified in the coming years. This would allow composition of a toolbox of pMHC-multimers to measure and follow MiHA-specific T cells in GvL and GvHD in the majority of patients treated with alloSCT (and DLI). Such an analysis would confer significant knowledge to the composition of *in vivo* immune responses in GvL and GvHD and allow analysis and comparison of efficacy and toxicity of different alloSCT treatment modalities. Although processing and presentation of peptides is important, the presence of a specific TCR in the naïve repertoire of donor T cells is probably the most limiting factor for an HLA-binding peptide to become a MiHA that can be recognized by specific T cells. This repertoire of specific TCR on donor T cells is shaped by negative selection as a result of presentation of self-peptides in the thymus. If many self-peptides are highly similar to MiHA, the total number of existing MiHA that can be recognized by specific TCR with high affinity may be more limited than suggested based on genetic disparity. Therefore, actual MiHA-specific T-cell responses instead of SNP disparities need to be measured in order to correlate MiHA with clinical outcome. Thus, characterization of MiHA

in patients with GvL and GvHD can both contribute to increase the repertoire of MiHA that are available for immunotherapy as well as understanding of the immunobiology of GvL and GvHD.

Manipulation of GvL and GvHD

Patients with hematological malignancies can be successfully treated with alloSCT and DLI[16,17]. Unfortunately, there are still patients who do not develop an effective anti-tumor response, emphasizing the need to increase the efficacy of this treatment modality. Moreover, many patients suffer from side effects as a result of damage to healthy organs that are targeted by donor T cells, illustrating that there is also a strong need to reduce toxicity of the treatment while maintaining the GvL effect. An improved balance between GvL and GvHD is relevant to increase quality of life, improve efficacy and broaden applicability of alloSCT as treatment modality for hematological malignancies.

MiHA can be exploited by immunotherapy to selectively induce GvL while limiting the risk of GvHD. Several different strategies are currently explored to augment GvL after alloSCT. These strategies include adoptive transfer of MiHA-specific T cells that are produced or isolated *in vitro* from the naïve donor repertoire or engineered by TCR gene transfer as well as *in vivo* vaccination protocols in which DNA, RNA or peptides are directly administered or used as antigen sources to load antigen-presenting cells. LB-ARHGDIB-1R and LB-ITGB2-1 as described in **chapter 3 and 5**, respectively, can be easily targeted in such approaches when patients are HLA-B*07:02 or B*15:01 positive. Other approaches aim to reduce the risk for GvHD. These approaches include non-specific depletion of alloreactive T cells or specific depletion of T cells for broadly expressed MiHA from the DLI. In most immunotherapies, newly identified MiHA can be easily implemented and may therefore contribute to increase efficacy and reduce toxicity of alloSCT as treatment modality for hematological malignancies.

Vaccination approaches are aimed at *in vivo* priming of immune responses. Peptides, mRNA or DNA can be directly injected or pulsed on professional APC to ensure efficient antigen processing and presentation. However, vaccination often fails to induce an effective anti-tumor response for various reasons. First, numbers of MiHA-specific T cells as present in the transplanted immune system of the donor may be too low. Furthermore, T-cell priming may be suboptimal as a result of low expression of co-activation, adhesion or other accessory molecules on the APC or high expression of co-inhibitory molecules. Finally, antigen doses as injected or loaded on APC by peptides, mRNA or DNA may exceed the amount of antigens that are endogenously processed and presented and lead to induction of T cells with an affinity that is below the threshold for

efficient recognition of leukemic cells and therefore fail to mount an effective anti-tumor response.

Another strategy to augment GvL is adoptive transfer of MiHA-specific T cells that have been isolated from the naïve donor repertoire or from *in vivo* immune responses after alloSCT. These T cells can be transferred directly into the patient after isolation by pMHC-multimers or administered after *in vitro* expansion. The advantage of direct infusion of donor T cells after isolation is that long-term *in vitro* culture, which is known to limit *in vivo* survival and expansion, is not required. Moreover, multiple pMHC complexes for different MiHA can be easily combined. This allows for isolation of T cells for a cocktail of MiHA with different HLA restriction alleles, which may contribute to increase efficacy and reduce the risk for antigen escape variants after treatment. A disadvantage of direct infusion of MiHA-specific T cells after isolation by pMHC-multimers is that numbers of donor T cells in the naïve repertoire are generally low and that their *in vivo* survival and expansion still require proper activation by endogenously processed and presented antigens on professional APC. Moreover, the absence of "help" as provided by other T cells in the DLI may significantly hamper *in vivo* survival and expansion of MiHA-specific T cells after adoptive transfer. As such, the efficacy of this approach may be increased by addition of a small dose of unselected DLI or by boosting the immune response after adoptive transfer by vaccination with MiHA-pulsed professional APC.

TCR gene transfer in which donor T cells are genetically engineered with a high affinity TCR can also be used to augment GvL after alloSCT[18]. By this method, high T-cell frequencies for a desired MiHA can be obtained within a relatively short culture period. The presence of high frequencies of TCR-transduced donor T cells favor adoptive transfer of a relatively low dose of DLI, thereby limiting the risk of GvHD. Alternatively, TCR gene transfer can be performed by introducing the high affinity TCR into virus-specific T-cells[19]. The advantage of virus-specific donor T cells is that they do not induce GvHD when infused early after alloSCT. Another benefit of TCR gene transfer is that high affinity TCRs capable of targeting endogenous MiHA as presented on leukemic cells can be selected. However, a disadvantage of TCR gene transfer is that it bears a risk for off-target toxicity as a result of mixed dimer formation leading to T cells with unknown and potentially unwanted specificities. The risk for off-target toxicity after TCR gene transfer to virus-specific T cells is significantly reduced as compared to unselected DLI due to expression of a more restricted repertoire of endogenous TCRs. Furthermore, mixed dimer formation can be reduced by introducing a disulfide bond which increases stability of the exogenous TCR[18]. Another disadvantage of TCR gene transfer is that a retroviral or lentiviral vector needs to be produced under GMP conditions and that multiple TCRs cannot easily be combined in the same cell

product. As such, TCR gene transfer will probably remain an approach limited to patients with specific MiHA mismatches and HLA restriction alleles.

In addition to strategies that are aimed to augment GvL, approaches can be developed to reduce the risk of GvHD by depleting T cells for broadly expressed MiHA from the DLI. That such an approach can be effective is illustrated by studies in haplo-identical transplantations in which alloreactive T cells are depleted from donor lymphocytes using an anti-CD25 immunotoxin. Administration of this depleted lymphocyte product allows for early immune reconstitution without the use of immune suppressive drugs, since no severe GvHD has been reported[20]. Another approach that aims to deplete alloreactive T cells *in vivo* is administration of cyclophosphamide 48-72 hours after haplo-identical transplantation[21]. However, strategies that aim to deplete alloreactive T cells generally hamper an effective GvL response. Therefore, specific depletion of T cells for broadly expressed MiHA may be a better strategy to reduce GvHD, since T cells for MiHA with predominant or restricted expression to hematopoietic cells are unaffected and remain available in the DLI to induce a selective GvL response. In general, the number of broadly expressed MiHA that are targeted in an *in vivo* immune response after alloSCT is higher than the number of hematopoiesis-restricted MiHA. As such, depletion of donor T cells for one or a limited number of broadly expressed MiHA may already be sufficient to reduce the overall magnitude and skew T-cell reactivity towards the hematopoietic system. T-cell depletion for broadly-expressed MiHA has the additional benefit that the exact antigens that are targeted in the GvL response do not need to be defined. However, for this approach, a number of broadly expressed MiHA with balanced population frequencies in common HLA alleles need to be identified.

Future perspectives

To broaden applicability of alloSCT as treatment modality for hematological malignancies and to ensure improved quality of life, more targeted therapy for selective induction of GvL is required. Although application of immunotherapy in which MiHA are targeted is limited by HLA-restriction and MiHA status, many clinical approaches allow the simultaneous use of multiple MiHA, which may increase the efficacy of therapy and reduce the risk for antigen escape variants. However, to increase the number of patients in which at least one therapeutic MiHA can be targeted, more MiHA in common HLA alleles need to be identified. In this thesis, we describe new methods for efficient discovery of MiHA. Currently, we are composing new panels for WGAs consisting of EBV-LCLs from the Geuvadis project[22,23] for which whole genome and transcriptome data are available. These panels will allow direct association between T-cell phenotype and whole genome data and transcriptional variants and may substantially

accelerate MiHA discovery. Furthermore, RNA-sequence data for leukemic samples and different healthy cell types will become increasingly available in the future and provide important tools for better estimation of MiHA efficacy and toxicity profiles. Large-scale analysis of T-cell responses after HLA-matched alloSCT and DLI using a toolbox of pMHC-multimers for MiHA will provide insight into the specificity, diversity, frequency and dynamics of MiHA-specific T cells in GvL and GvHD. This knowledge can then be implemented to manipulate the DLI in such a way that *in vivo* responses in selective GvL are mimicked.

This thesis is focused on discovery of MiHA as immunotherapeutic targets for T cells, but other types of antigens can also be targeted by cellular immunotherapy to treat patients with hematological malignancies. For example, non-transplanted patients and patients with relapsed leukemia after alloSCT can be treated by chimeric antigen receptor or TCR gene therapy in which non-polymorphic antigens are targeted that are overexpressed in leukemic cells or in specific hematopoietic lineages. These approaches have the advantage that they can be applied in the absence of alloSCT without any risk for GvHD. However, most non-polymorphic target antigens are not exclusively expressed on leukemic cells and these therapies therefore carry a substantial risk for attack of healthy tissues as a result of on-target toxicity. Another approach that has been pioneered in patients with melanoma is T-cell therapy in which neoantigens are targeted. Neoantigens are T-cell epitopes with amino acid changes that are created by tumor-specific mutations. Neoantigens are ideal targets for immunotherapy, since T cells will eradicate tumor cells without toxicity towards healthy cells which do not carry the somatic mutation. However, a major drawback of neoantigens as targets for T-cell therapy is that the mutational profile is different for each patient and that therapies thus require truly personalized medicine. Moreover, it is unknown whether sufficient neoantigens are presented on leukemic cells with low mutational load for effective immunotherapy. Therefore, an attractive approach would be to combine neoantigens with MiHA to increase the number of patient-specific variants that can be targeted by donor T cells. The advantage of MiHA is that they do not need to be restricted to tumor cells but can be hematopoiesis-restricted, because healthy hematopoietic cells are of donor origin and will be spared by the donor-derived immune system. Thus, hematopoiesis-restricted MiHA remain important therapeutic targets to effectively treat hematological malignancies after alloSCT without or with a low risk for GvHD.

Reference list

1. Spierings E. Minor histocompatibility antigens: past, present, and future. Tissue Antigens. 2014;84(4):374-360.
2. Broen K, Greupink-Draaisma A, Woestenenk R, Schaap N, Brickner AG, Dolstra H. Concurrent detection of circulating minor histocompatibility antigen-specific CD8+ T cells in SCT recipients by combinatorial encoding MHC multimers. PLoS One. 2011;6(6):e21266.
3. Hombrink P, Hadrup SR, Bakker A, et al. High-throughput identification of potential minor histocompatibility antigens by MHC tetramer-based screening: feasibility and limitations. PLoS One. 2011;6(8):e22523.
4. Hombrink P, Hassan C, Kester MG, et al. Identification of Biological Relevant Minor Histocompatibility Antigens within the B-lymphocyte-Derived HLA-Ligandome Using a Reverse Immunology Approach. Clin Cancer Res. 2015;21(9):2177-2186.
5. Granados DP, Sriranganadane D, Daouda T, et al. Impact of genomic polymorphisms on the repertoire of human MHC class I-associated peptides. Nat Commun. 2014;5:3600.
6. Van Bergen CAM, Rutten CE, Van Der Meijden ED, et al. High-throughput characterization of 10 new minor histocompatibility antigens by whole genome association scanning. Cancer Res. 2010;70(22):9073-9083.
7. Spaapen RM, Lokhorst HM, van den Oudenalder K, et al. Toward targeting B cell cancers with CD4+ CTLs: identification of a CD19-encoded minor histocompatibility antigen using a novel genome-wide analysis. J Exp Med. 2008;205(12):2863-2872.
8. Kamei M, Nannya Y, Torikai H, et al. HapMap scanning of novel human minor histocompatibility antigens. Blood. 2009;113(21):5041-5048.
9. Kawase T, Nannya Y, Torikai H, et al. Identification of human minor histocompatibility antigens based on genetic association with highly parallel genotyping of pooled DNA. Blood. 2008;111(6):3286-3294.
10. Oostvogels R, Lokhorst HM, Minnema MC, et al. Identification of minor histocompatibility antigens based on the 1000 Genomes Project. Haematologica. 2014;99(12):1854-1859.
11. Genomes Project C, Abecasis GR, Auton A, et al. An integrated map of genetic variation from 1,092 human genomes. Nature. 2012;491(7422):56-65.
12. Griffioen M, Honders MW, van der Meijden ED, et al. Identification of 4 novel HLA-B*40:01 restricted minor histocompatibility antigens and their potential as targets for graft-versus-leukemia reactivity. Haematologica. 2012;97(8):1196-1204.
13. van Bergen CA, Verdegaal EM, Honders MW, et al. Durable remission of renal cell carcinoma in conjuncture with graft versus host disease following allogeneic stem cell transplantation and donor lymphocyte infusion: rule or exception? PLoS One. 2014;9(1):e85198.
14. Hobo W, Broen K, van der Velden WJ, et al. Association of disparities in known minor histocompatibility antigens with relapse-free survival and graft-versus-host disease after allogeneic stem cell transplantation. Biol Blood Marrow Transplant. 2013;19(2):274-282.
15. Marijt WA, Heemskerk MH, Kloosterboer FM, et al. Hematopoiesis-restricted minor histocompatibility antigens HA-1- or HA-2-specific T cells can induce complete remissions of relapsed leukemia. Proc Natl Acad Sci U S A. 2003;100(5):2742-2747.
16. Barge RM, Starrenburg CW, Falkenburg JH, Fibbe WE, Marijt EW, Willemze R. Long-term follow-up of myeloablative allogeneic stem cell transplantation using Campath “in the bag” as T-cell depletion: the Leiden experience. Bone Marrow Transplant. 2006;37(12):1129-1134.
17. Eefting M, von dem Borne PA, de Wreede LC, et al. Intentional donor lymphocyte-induced limited acute graft-versus-host disease is essential for long-term survival of relapsed acute myeloid leukemia after allogeneic stem cell transplantation. Haematologica. 2014;99(4):751-758.

18. van Loenen MM, de Boer R, Hagedoorn RS, van Egmond EH, Falkenburg JH, Heemskerk MH. Optimization of the HA-1-specific T-cell receptor for gene therapy of hematologic malignancies. Haematologica. 2011;96(3):477-481.

19. van Loenen MM, de Boer R, van Liempt E, et al. A Good Manufacturing Practice procedure to engineer donor virus-specific T cells into potent anti-leukemic effector cells. Haematologica. 2014;99(4):759-768.

20. Amrolia PJ, Muccioli-Casadei G, Huls H, et al. Adoptive immunotherapy with allodepleted donor T-cells improves immune reconstitution after haploidentical stem cell transplantation. Blood. 2006;108(6):1797-1808.

21. Ciurea SO, Zhang M-J, Bacigalupo AA, et al. Haploidentical transplant with posttransplant cyclophosphamide vs matched unrelated donor transplant for acute myeloid leukemia. Blood. 2015;126(8):1033-1040.

22. Lappalainen T, Sammeth M, Friedlander MR, et al. Transcriptome and genome sequencing uncovers functional variation in humans. Nature. 2013;501(7468):506-511.

23. t Hoen PA, Friedlander MR, Almlof J, et al. Reproducibility of high-throughput mRNA and small RNA sequencing across laboratories. Nat Biotechnol. 2013;31(11):1015-1022.

&

APPENDICES

NEDERLANDSE SAMENVATTING

DANKWOORD

CURRICULUM VITAE

LIST OF PUBLICATIONS

Het ontdekken van minor histocompatibiliteits antigenen als doelwit structuren voor immuuntherapie

Allogene stamceltransplantatie

Kwaadaardige aandoeningen van de bloedvormende organen kunnen door middel van een allogene stamceltransplantatie (SCT) worden genezen. In allogene SCT wordt het bloedvormend systeem van de patiënt vernietigd en vervangen door een nieuw hematopoietisch systeem van een gezonde donor. Chemotherapie, bestraling en toediening van middelen die het immuunsysteem onderdrukken dienen daarbij als conditionering van de patiënt voorafgaand aan de transplantatie. Het doel van de conditionering is de kwaadaardige cellen te vernietigen en het immuunsysteem van de patiënt te onderdrukken, opdat het donor stamceltransplantaat niet wordt afgestoten en de donor hematopoiese te laten uitgroeien. Hoewel deze conditionering als doel heeft het aantal tumorcellen sterk te verminderen, kan de uitgroei van overlevende maligne cellen leiden tot het terugkeren van de tumor (recidief). Succesvolle behandeling met allogene SCT hangt daarom af van de complete uitroeiing van achtergebleven tumorcellen door het donor immuunsysteem dat met het transplantaat mee geïnfundeerd wordt: de zogenaamde Graft-versus-Leukemie (GvL) reactiviteit. Helaas gaat het gewenste anti-tumor effect vaak gepaard met ongewenste bijwerkingen, ook wel Graft-versus-Host ziekte (GvHD) genoemd. GvHD is een ernstige en mogelijk levensbedreigende complicatie van allogene SCT waarbij, naast de kwaadaardige cellen, ook gezonde weefsels van de patiënt worden aangevallen. Zowel GvL reactiviteit als GvHD worden veroorzaakt door T cellen van donor origine die lichaamsvreemde ofwel allo-antigenen herkennen op patiëntcellen. Het opwekken van effectieve GvL reactiviteit, terwijl het risico op (ernstige) GvHD beperkt blijft, is de grootste uitdaging voor de behandeling van hematologische maligniteiten met allogene SCT.

Donor lymfocyten infusie

Om het risico op GvHD te beperken kunnen donor T cellen uit het transplantaat verwijderd worden. Helaas wordt door deze T-cel depletie ook het gewenste anti-tumor effect tenietgedaan. Om een GvL effect te bewerkstelligen worden donor T cellen vaak op een later moment alsnog gegeven in de vorm van donor lymfocyten infusie (DLI). Doordat de schade ontstaan door de pre-transplantatie conditionering (en het bijbehorende ontstekingsmilieu) grotendeels is hersteld en dus minder patiënt antigenen gepresenteerd worden, is het risico op GvHD na DLI lager. Helaas kan ook DLI nog steeds ernstige bijwerkingen in de vorm van GvHD geven. Het tijdstip waarop de DLI wordt gegeven is van belang: lang

wachten geeft een lager risico op GvHD, maar een grotere kans op het optreden van een recidief in de periode tussen allogene SCT en DLI. Bij patiënten met een agressieve maligniteit met een hoog risico op recidief wordt daarom kort na allogene SCT al DLI gegeven, waardoor de kans op een sterke GvL reactie groot is en het risico op een recidief afneemt. Als de DLI zodanig veranderd kan worden dat het cel-product specifiek de maligne cellen van de patiënt herkent, verhoogt dit de effectiviteit en veiligheid van allogene SCT als behandelmethode voor hematologische maligniteiten en neemt het risico op ernstige GvHD af.

Minor histocompatibiliteits antigenen

Bij allogene SCT met een transplantaat afkomstig van een donor met een volledig identieke humane leukocyten antigen (HLA) typering zorgt genetische variatie – de zogenaamde single nucleotide polymorfismen (SNP) – voor de allo-antigenen die door donor T cellen herkend kunnen worden. Deze allo-antigenen zijn polymorfe peptiden die aan HLA kunnen binden en op patiëntcellen gepresenteerd kunnen worden. De patiënt varianten van polymorfe peptiden kunnen vervolgens als lichaamsvreemd herkend worden door het donor-afkomstige immuunsysteem. Deze antigenen heten ook wel minor transplantatie antigenen (MiHA). Of donor T cellen die MiHA herkennen alleen GvL of ook GvHD veroorzaken hangt af van op welke cellen van de patiënt de MiHA worden gepresenteerd. Donor T cellen specifiek voor een MiHA die op maligne bloedcellen van de patiënt tot expressie komen zorgen voor GvL reactiviteit, terwijl donor T cellen die MiHA op gezonde niet-hematopoietische weefsels herkennen GvHD kunnen induceren. MiHA die specifiek tot expressie komen op cellen van het bloedvormend systeem zijn relevante doelwit structuren voor immuuntherapie, omdat donor T cellen gericht tegen deze MiHA de kwaadaardige cellen van de patiënt zullen aanvallen terwijl gezonde hematopoietische cellen van donor origine gespaard blijven. De toepasbaarheid van MiHA in verschillende patiënten hangt af van hoe vaak de SNP en het HLA-restrictie molecuul in de populatie voorkomen. Om therapieën die MiHA als doelwit structuren gebruiken in het merendeel van de patiënten toe te kunnen passen, zijn daarom meer hematopoietisch-specifieke MiHA in verschillende HLA-allelen nodig.

MiHA kunnen geïdentificeerd worden met behulp van alloreactieve T cellen die uit patiënten met klinische immuunreacties na allogene SCT worden geïsoleerd en gekarakteriseerd op basis van hun specificiteit en mogelijke rol in GvL en GvHD. Om nieuwe MiHA te ontdekken wordt door middel van whole genome association scanning (WGAs) de T-cel herkenning van een panel van testcellen onderzocht op associatie met individuele SNPs. De meeste van de tot nu toe gevonden MiHA worden gegenereerd door SNPs die coderen voor een aminozuurverandering (‘non-synonymous’) in het primaire gen transcript. Omdat polymorfismen

in coderende gebieden in het algemeen makkelijker te identificeren zijn met de huidige MiHA identificatie technieken, wordt de frequentie van MiHA die gecodeerd worden door andere genetische variaties dan non-synonymous SNPs waarschijnlijk onderschat. In dit proefschrift hebben we ons gericht op efficiënte karakterisering van MiHA met mogelijke therapeutische relevantie, waaronder MiHA die gecodeerd worden door alternatieve transcripten.

Dit proefschrift

Om de effectiviteit en veiligheid van allogene SCT als behandelmethode voor hematologische maligniteiten te verhogen, moeten meer MiHA in verschillende HLA-restrictie allelen worden geïdentificeerd. Ondanks het feit dat het ontdekken van MiHA efficiënter is geworden door de implementatie van WGAs, blijven de antigenen voor 20-30% van de T-cel klonen onopgelost. Voor deze T-cel klonen zijn wel vaak associërende SNPs gevonden, maar geen SNP verschillen ('disparity') in het primaire gen transcript. Deze MiHA worden waarschijnlijk gecodeerd door alternatieve transcripten en moeten gekarakteriseerd worden met meer geavanceerde technieken dan WGAs gebaseerd op een panel van EBV-B-cellen waarvoor 1,1 miljoen SNPs getypeerd zijn. MiHA die door alternatieve transcripten gecodeerd worden, zijn hoogstwaarschijnlijk ondervertegenwoordigd in de huidige verzameling van bekende MiHA. Het ontdekken van meer van deze MiHA vormt een belangrijke bijdrage aan het samenstellen van een 'toolbox' van antigenen om T-cel responsen in GvL en GvHD na allogene SCT te kunnen meten en aan het uitbreiden van het repertoire van MiHA met therapeutische relevantie. In dit proefschrift hebben wij de specificiteit, diversiteit, frequentie en dynamiek van MiHA-specifieke T cellen bestudeerd in het kader van *in vivo* immuunreacties na allogene SCT en DLI. De in dit proefschrift beschreven studies geven inzicht in de immuun-biologie van GvL en GvHD na allogene SCT. Daarnaast dragen zij bij aan het identificeren van MiHA met therapeutische relevantie om selectieve GvL reactiviteit te induceren na allogene SCT zonder de complicaties van GvHD.

Met de ontwikkeling van WGAs en het daardoor verhoogde tempo van MiHA identificatie ontstond de behoefte aan een efficiënte en stelselmatige inschatting van de bijbehorende weefseldistributie, omdat die bepalend is voor het optreden van GvL en GvHD. De weefseldistributie kan worden gebruikt om de rol van een MiHA in GvL of GvHD in te schatten om zo MiHA met mogelijke therapeutische relevantie te kunnen onderscheiden van MiHA die breed tot expressie komen op niet-bloedvormende weefsels. De weefseldistributie van MiHA kan worden bepaald door T-cel herkenning te testen, maar dan moeten de celtypes positief zijn voor het MiHA- en HLA-restrictie-allel en de toegang tot niet-hematopoietische weefsels is vaak beperkt. In **hoofdstuk 2** beschrijven we een

microarray genexpressie database, die celtypes bevat die vaak betrokken zijn in GvL reactiviteit en GvHD. De database is ontworpen als platform om op efficiënte wijze gen expressieprofielen van nieuwe antigenen te kunnen genereren. We hebben in de database kwaadaardige en gezonde hematopoietische celtypes opgenomen alsmede niet-hematopoietische celtypes die onder normale en ontstekings-condities gekweekt zijn. Genexpressie is bestudeerd met Illumina HT12.0 microarrays waarmee messenger RNA (mRNA) voor ~39.000 genen per monster gemeten wordt. Op basis van kwaliteitscontroles is de oorsprong van de verschillende celtypes bevestigd en mogelijke verontreiniging met perifere bloedcellen uitgesloten. Validatie van de microarray genexpressie data is gedaan door middel van kwantitatieve RT-PCR (q-PCR) waarbij een sterke correlatie tussen genexpressie met beide technieken werd gevonden. Verder hebben we een specifiek profiel van ontstekings-genen vastgesteld door microarray data van verschillende niet-bloedvormende celtypes onder ontstekingscondities (na kweek met IFN-γ) onderling te vergelijken. Tenslotte hebben we de waarde van de microarray genexpressie database aangetoond door de effectiviteit en toxiciteit in te schatten van mogelijke doelwit structuren voor immuuntherapie van hematologische maligniteiten. We concluderen dat onze microarray database een relevant platform biedt om kandidaat antigenen met bloedcel-specifieke expressie te identificeren als potentiële doelwit structuren voor de behandeling van hematologische maligniteiten met immuuntherapie.

In **hoofdstuk 3** bestuderen we in detail LB-ARHGDIB-1R als een minor transplantatie antigen met mogelijke therapeutische relevantie na allogene SCT. Gebruikmakend van de microarray genexpressie data zoals beschreven in **hoofdstuk 2** laten we zien dat expressie van *ARHGDIB* specifiek is voor bloedvormende cellen, met beperkte mRNA expressie in endotheel cellen als uitzondering. T-cel experimenten bevestigden de bloedcel-specifieke expressie, waarbij fibroblasten en keratinocyten uit de huid niet herkend werden, zelfs niet na kweken onder ontstekingscondities. Met Q-PCR kon inderdaad *ARHGDIB* genexpressie in endotheel cellen worden bevestigd, maar LB-ARHGDIB-1R specifieke T cellen herkenden endotheel cellen slechts in beperkte mate en alleen onder ontstekingscondities. Herkenning van primaire leukemiecellen was daarentegen sterk en T cellen die LB-ARHGDIB-1R herkennen kunnen specifieke celdood veroorzaken in langdurige cytotoxiciteit experimenten. Tenslotte hebben we de *in vivo* immunogeniciteit van LB-ARHGDIB-1R bestudeerd. In 8 van de 10 bestudeerde patiënten vonden we na allogene SCT specifieke T cellen, waarvan in 4 patiënten de frequentie hoog genoeg was om de T cellen direct uit het bloed ('*ex vivo*') te kunnen meten. In een patiënt met gerecidiveerd Non-Hodgkin's lymfoom werden hoge T-cel frequenties gevonden na DLI, op hetzelfde moment als inductie van een langdurige GvL reactie zonder GvHD. Deze data ondersteunen daarom de relevantie van LB-ARHGDIB-1R als therapeutisch

doelwit met de potentie om selectieve GvL te induceren na allogene SCT.

Ondanks dat WGAs een efficiënte methode is, lukt het niet om het precieze antigen te achterhalen voor 20-30% van de T cel klonen. Associatie studies met een panel van EBV-B cellen waarvoor 1,1 miljoen SNPs zijn bepaald, hebben voor deze T-cel klonen associërende SNPs geïdentificeerd buiten de bekende coderende gebieden (exonen) van een gen, terwijl in de primaire gen-transcripten geen SNP disparity kon worden gevonden. In **hoofdstuk 4** hebben we een afgeleide correlatie-strategie gevolgd, waarbij SNP data van het hele genoom uit het 1000 Genomes Project zijn gebruikt om LB-TTK-1D te identificeren als nieuw MiHA. SNP rs240226 werd geïdentificeerd als de genetische variatie die codeert voor het MiHA. Deze SNP bevindt zich in een alternatief transcript van het *TTK* gen waarin een te vroeg of 'prematuur' stop codon aanwezig is dat het transcript doelwit maakt voor snelle afbraak door een proces genaamd nonsense mediated decay (NMD). LB-TTK-1D is het eerste niet-artificiële antigen dat wordt getransleerd van een endogeen NMD transcript in de mens. Het alternatieve *TTK* transcript komt nauwelijks tot expressie volgens q-PCR experimenten en T cellen voor LB-TTK-1D kunnen zowel bloedvormende als niet-bloedvormende celtypes herkennen. Ondanks de extreem lage expressie van het alternatieve *TTK* transcript laten T cellen voor LB-TTK-1D robuuste herkenning van EBV-B cellen zien, terwijl de meerderheid van de primaire leukemie monsters niet herkend wordt. Deze data suggereren dat T-cel herkenning, naast genexpressie en aanwezigheid van de SNP en HLA-restrictie allel, nog afhankelijk is van andere factoren. Deze bevindingen zijn belangrijk voor toekomstige MiHA-identificatie studies en dragen bij aan het begrip hoe antigenen in effectieve immuunreacties ontstaan en de biologie die daaraan ten grondslag ligt.

In **hoofdstuk 5** beschrijven we de implementatie van 'whole transcriptome' analyse in onze WGAs strategie en de succesvolle identificatie van LB-ITGB2-1 als MiHA gecodeerd door een alternatief transcript. Met behulp van WGAs identificeerden we een associërende SNP rs760462 in het *ITGB2* gen en ontdekten vervolgens met behulp van RNA-sequentie analyse een regio met transcriptionele activiteit in intron 3 direct volgend op de associërende SNP. Analyse van losse RNA-sequentie 'reads' laat zien dat SNP rs760462 een nieuwe 'splice'-sequentie introduceert waarmee een alternatief transcript gegenereerd wordt dat alleen tot expressie komt in MiHA positieve individuen. Het immunogene antigen wordt 'downstream' van de SNP van het alternatieve transcript afgeschreven. Verder laten we zien dat RNA-sequentie analyse het mogelijk maakt antigenen te identificeren die gegeneerd worden door transcripten die ontstaan doordat een exon wordt overgeslagen met ACC-6 als voorbeeld. Verder brengen we in kaart in hoeverre LB-ITGB2-1 therapeutische waarde heeft en hebben we gevonden dat de weefseldistributie van het alternatieve transcript hetzelfde patroon volgt

als het normale *ITGB2* transcript. Expressie van het normale en alternatieve *ITGB2* transcript is hematopoiese-specifiek, zoals bevestigd door het gebrek aan T-cel reactiviteit tegen huidfibroblasten, zelfs onder ontstekingscondities. Tenslotte waren LB-ITGB2-1 specifieke T cellen in staat specifieke herkenning en celdood van kwaadaardige hematopoietische (voorloper) cellen te veroorzaken. Dit ondersteunt de therapeutische relevantie van LB-ITGB2-1 als doelwit voor immuuntherapie om GvL reactiviteit te induceren na allogene SCT zonder GvHD.

Samenvattend hebben we verschillende MiHA die door diverse mechanismen gegenereerd worden, efficiënt geïdentificeerd en gekarakteriseerd. Microarray genexpressie data zijn met succes gebruikt om een inschatting te maken van de weefseldistributie van MiHA en whole genome en transcriptome data zijn geïmplementeerd in de WGAs methode om identificatie van MiHA gecodeerd door alternatieve transcripten mogelijk te maken. Door het combineren van deze strategieën, is het nu mogelijk op efficiënte wijze een grote variëteit aan MiHA te identificeren, hun rol in GvL reactiviteit en GvHD te evalueren en hematopoiese-specifieke kandidaat antigenen te selecteren met potentiële waarde voor immuuntherapie na allogene SCT. Door MiHA te gebruiken om selectief GvL reactiviteit te induceren zonder GvHD, kunnen patiënten met kwaadaardige aandoeningen van het bloedvormend systeem effectiever en veiliger behandeld worden met allogene SCT en DLI.

&

Dankwoord

"Als het makkelijk was, zou iedereen het doen" is een spreuk waar ik de afgelopen jaren regelmatig houvast aan heb gehad als dingen niet gingen zoals ik hoopte, maar uiteindelijk kan ik trots terugkijken op een bijzondere periode met als eindresultaat dit proefschrift! Voor mij is het proefschrift maar een beperkte weergave van het gehele promotietraject en daarom wil ik hier graag iedereen bedanken die een bijdrage aan dit proefschrift heeft geleverd, maar daarbovenop een ieder die op welke wijze dan ook betrokken was bij de afgelopen 5 jaar (familie, vrienden, collega's, Cayenne-cordialgenootjes, hockeyteamgenoten, yoga-studenten, etc).

Allereerst wil ik alle (oud-)collega's bedanken van het laboratorium voor Experimentele Hematologie. De sfeer op het lab en de 'brug' tijdens de koffiepauzes en lunch was open en verwelkomend, waarin ik me al snel thuis voelde. De 'verplichte' pauzes hebben me door grote experimenten en lange schrijfdagen heen geholpen en waren erg gezellig.

Veel dank voor alle collega's van kamer 38 en 42 voor het aanhoren van al mijn verhalen of een helpende hand als de proef toch iets te groot uitviel. **Ellie:** jouw celkweek trucs zal ik nooit vergeten. **Kees:** jij hebt me geleerd dat *'ongeveer'* precies genoeg is als je grote hoeveelheden klonen wil screenen. **Sanja en Anita:** de vrijdagochtend besprekingen hebben me vanaf het begin laten meedenken over andermans data; dank voor jullie input en support. Anita, de congressen in Erlangen waren een mooi moment om elkaar te zien. Sanja, ik heb genoten van onze discussies en de congressen in Milaan en Washington waar we een kamer deelden. Ik heb veel geleerd van jouw ervaringen als Post-Doc in de VS. Alle OIOs en kamergenoten van C-7, C-5 en C-2: **Hetty, Matthijs, Pleun, Boris, Floris, Lisa, Peter, Lorenz, Marthe, Aicha en Marjolein:** fijn om je werkplek te delen met mensen die in hetzelfde schuitje zitten. Dank voor de nodige afleiding en hilarische momenten of ontsnappingen als er wat te vieren was. **Gerrie en Karien:** dank voor jullie steun en advies, binnen en buiten het werk. **Sabrina en Guido:** door jullie support is FACSen of sorteren geen probleem en staan er mooie plaatjes in dit proefschrift: onmisbaar voor het werk dat we doen.

Mijn paranimfen, **Willy** en **Edith:** ik ben er trots op dat jullie naast mij willen staan tijdens de verdediging. Samen hebben we lief en leed gedeeld en bergen werk verzet.

Graag wil ik ook mijn familie en vrienden bedanken voor alle steun en belangstelling en natuurlijk de nodige afleiding. **Wendy:** dankjewel voor de 'stoom-afblaas'-drankjes en onuitputtelijke bron van bijbaantjes voor de laatste loodjes. **Lisette:** wij zitten op één lijn en hebben vaak aan een enkel

woord genoeg. Bijzonder om samen toekomstplannen uit te wisselen, met alle uitdagingen die daarbij horen. **Niki:** jouw werkweek motiveerde me om er op het laatst nog een extra schepje bovenop te doen. **Henk** en **Linda:** wat fijn was het om bij jullie in Brielle te kunnen schrijven. Linda, dank voor de stok achter de deur. **Meindert** en **Henk:** heel bijzonder hoe jullie hebben meegeleefd en meegedacht, ook met af en toe een kritische blik. **Tim** en **Olivier:** bijzonder dat jullie ook een tijd in het buitenland zijn geweest, lieve broertjes. Succes met het volgen van jullie eigen pad. **Opapa** en **Omama:** ik ben blij dat ik jullie het afgelopen jaar meer heb kunnen zien. Bedankt voor jullie interesse en liefde.

Mijn **ouders:** jullie wil ik graag bedanken voor jullie onvoorwaardelijke steun, liefde en begrip en de ruimte om mezelf te ontdekken. Na eerst alles 'zelf' te willen doen, vind ik het juist fijn om nu lief en leed met jullie te kunnen delen, ook straks vanuit Seattle.

Lieve **Kris:** bij jou voel ik me veilig. Samen is meer dan 1+1. Dankjewel voor de vrijheid om mijn eigen koers te kiezen en het vertrouwen om de volgende stap samen te nemen.

&

Curriculum vitae

Margot is op 16 november 1986 geboren in Leidschendam en groeide op in Voorschoten. Op het Stedelijk Gymnasium te Leiden deed ze in 2005 eindexamen in het profiel Natuur en Gezondheid. Aansluitend begon ze aan de opleiding Biomedische Wetenschappen in het Leids Universitair Medisch Centrum (LUMC). Na een bachelorstage op de afdeling Klinische Genetica van het LUMC bij dr. Elles Boon, koos ze als eerste masterstage voor de Klinische Oncologie onder begeleiding van dr. Els Verdegaal. Ze was verantwoordelijk voor het programma tijdens het symposium ter gelegenheid van het 25-jarig bestaan van de opleiding Biomedische Wetenschappen in Leiden in 2009. Voor de afsluitende stage en scriptie ging ze naar het 'La Jolla Institute for Allergy and Immunology' in San Diego, California in de Verenigde Staten onder supervisie van dr. Stephen Schoenberger en dr. Ramon Arens. In 2011 behaalde ze haar Master of Science diploma en in april van dat jaar begon ze aan het promotieonderzoek zoals in dit proefschrift beschreven betreffende minor transplantatie antigenen als doelwit structuren voor de behandeling van hematologische maligniteiten, begeleid door dr. Marieke Griffioen en prof. dr. Fred Falkenburg. In 2015 ontving ze de AIO award tijdens de Dutch Tumor Immunology Meeting in juni en een Young Investigator award tijdens de Society of Immunotherapy of Cancer Annual Meeting in november. Tijdens haar promotieonderzoek voltooide ze een yoga-docenten opleiding, startte haar eigen onderneming (beide 2011) en werkte tijdelijk bij de Graduate School Office van het LUMC (2015-2016).

Na de verdediging van het in dit proefschrift beschreven onderzoek, zal ze als post-doc onderzoek doen naar 'chimeric antigen receptor' T cellen in het lab van dr. Stanley Riddell in het "Program in Immunology" van het Fred Hutchinson Cancer Research Center in Seattle, Washington in de Verenigde Staten en zo het onderzoek naar immuuntherapie van kanker voortzetten.

List of Publications

M.J. Pont, W. Hobo, M.W. Honders, S.A.P. van Luxemburg-Heijs, M.G. Kester, A.M. van Oeveren-Rietdijk, N. Schaap, H.C. de Boer, C.A.M. van Bergen, H. Dolstra, J.H.F. Falkenburg, M. Griffioen;
LB-ARHGDIB-1R as a novel minor histocompatibility antigen for therapeutic application;
Haematologica. 2015 Oct;100(10):e419-22.

M.J. Pont, D.I. van der Lee, E.D. van der Meijden, C.A.M. van Bergen, M.G.D. Kester, M.W. Honders, M. Vermaat, M. Eefting, E.W.A. Marijt, S.M. Kielbasa, P.A.C. 't Hoen, J.H.F. Falkenburg, M. Griffioen;
Integrated whole genome and transcriptome analysis identified a therapeutic minor histocompatibility antigen in a splice variant of *ITGB2*;
Clin Cancer Res. 2016 March 10; doi:10.1158/1078-0432.CCR-15-2307

M.J. Pont, M.W. Honders, A.N. Kremer, C. van Kooten, C. Out, P.S. Hiemstra, H.C. de Boer, M.J. Jager, E. Schmelzer, R.G. Vries, A.A. Hinai, W.G. Kroes, R. Monajemi, J.J. Goeman, S. Böhringer, E.W.A. Marijt, J.H.F. Falkenburg, M. Griffioen;
Cell Type Specific Expression Patterns by Microarray Analysis to Evaluate Targets Relevant for Immunotherapy of Hematological Malignancies;
PLOS ONE. 2016 in press

M.J. Pont*, R. Oostvogels*, C.A.M. van Bergen, E.M. van der Meijden, H. Lokhorst, J.H.F. Falkenburg, T. Mutis, M. Griffioen, R.M. Spaapen;
Minor histocompatibility antigen LB-TTK-1D is encoded by an alternative transcript that is degraded by nonsense mediated decay;
to be submitted

*These authors contributed equally.

Publications not in this thesis

P. Hombrink, C. Hassan, M.G.D. Kester, L. Jahn, M.J. Pont, A.H. de Ru, C.A.M. van Bergen, M. Griffioen, J.H.F. Falkenburg, P.A. van Veelen, M.H.M. Heemskerk;
Identification of Biological Relevant Minor Histocompatibility Antigens within the B-lymphocyte-Derived HLA-Ligandome Using a Reverse Immunology Approach.
Clin Cancer Res. 2015 May 1;21(9):2177-86.

A.N. Kremer, E.D. van der Meijden, M.W. Honders, M.J. Pont, J.J. Goeman, J.H.F. Falkenburg, M. Griffioen;
Human leukocyte antigen-DO regulates surface presentation of human leukocyte antigen class II-restricted antigens on B cell malignancies.
Biol Blood Marrow Transplant. 2014 May;20(5):742-7.

J.W. Rutten, E.M. Boon, M.K. Liem, J.G. Dauwerse, M.J. Pont, E. Vollebregt, A.J. Maat-Kievit, H.B. Ginjaar, P. Lakeman, S.G. van Duinen, G.M. Terwindt, S.A. Lesnik Oberstein;
Hypomorphic NOTCH3 alleles do not cause CADASIL in humans.
Hum Mutat. 2013 Nov;34(11):1486-9.